

Summary of FY 1999 Geosciences Research

December 2000



U.S. Department of Energy

Office of Science
Office of Basic Energy Sciences
Division of Engineering and Geosciences
Washington, D.C. 20585

CONTENTS

Contents	ii
Foreword	x
The Geosciences Research Program in the Office of Basic Energy Sciences	xi
PART I: ON-SITE	1
CONTRACTOR: Argonne National Laboratory	1
CATEGORY: Geochemistry.....	1
Mineral-Fluid Interactions: Synchrotron Radiation Studies at the Advanced Photon Source	1
CONTRACTOR: Brookhaven National Laboratory.....	2
CATEGORY: Geology, Geophysics, and Earth Dynamics.....	2
Study of the Microgeometry of Geological Materials Using Synchrotron Computed Microtomography	2
CATEGORY: Geochemistry.....	3
Geochemistry of Organic Sulfur in Marine Sediments.....	3
CONTRACTOR: Lawrence Berkeley National Laboratory.....	5
CATEGORY: Geophysics and Earth Dynamics.....	5
High-Resolution Imaging of Electrical Conductivity Using Low-Frequency Electromagnetic Fields.....	5
Center for Computational Seismology (CCS).....	6
Deformation and Fracture of Poorly Consolidated Media.....	7
Decomposition of Scattering and Intrinsic Attenuation on Rock with Heterogeneous Multiphase Fluids Distributions	8
CATEGORY: Geochemistry.....	9
Integrated Isotopic Studies of Geochemical Processes.....	9
Isotopic and Chemical Composition of Fault Zone Fluids	11
Clay Mineral Surface Geochemistry.....	13
Molecular-level studies of Fe-Al oxyhydroxide coating formation on quartz.....	14
CATEGORY: Hydrogeology.....	15
Geochemical and Isotopic Constraints on Processes in Oil Hydrogeology.....	15
Reactive Chemical Transport in Structured Porous Media: X-ray Microprobe and Micro-XANES Studies.....	16
Unsaturated Fast Flow in Fractured Rock: Testing Film Flow and Aperture Influences.....	17
Colloid Transport in Unsaturated Porous Media and Rock Fractures.....	17
CONTRACTOR: Lawrence Livermore National Laboratory	19
CATEGORY: Geophysics and Earth Dynamics.....	19
Pore Scale Simulations of Rock Deformation, Fracture and Fluid Flow in Three Dimensions.....	19

Three-dimensional Analysis of Seismic Signatures and Characterizations of Fluids and Fractures in Anisotropic Formations	20
Visco-, Thermo-, and Poroelasticity of Rocks and Rock/Fluid Mixtures.....	20
Reactive Solute Transport and Processes of Dissolution and Deposition in Single Fractures in Rock.....	22
The Role of Carbon and Temperature in Determining Electrical Conductivity of Basins, Crust, and Mantle.	23
Water distribution in partially saturated porous materials.....	23
CATEGORY: Geochemistry.....	24
An Experimental Investigation of Mechanisms Controlling Glass Dissolution	24
Mineral Dissolution and Precipitation Kinetics: A Combined Atomic-Scale and Macro-Scale Investigation	25
Collaborative Research: Studies for Surface Exposure Dating in Geomorphology.....	26
Dating depositional surfaces: Applications of <i>in situ</i> Cosmic-ray Exposure Dating	27
Thermodynamic and Transport Properties of Aqueous Geochemical Systems	28
CONTRACTOR: Los Alamos National Laboratory	30
CATEGORY: Geophysics and Earth Dynamics.....	30
Fast 3D Seismic Modeling and Prestack Depth Migration Using Generalized Screen Methods	30
The Role of Carbon and Temperature in Determining Electrical Conductivity of Basins, Crust, and Mantle.	31
Nonlinear Elasticity in Earth Materials.....	31
CATEGORY: Geochemistry.....	32
Uranium-Series Concordance Studies	32
Surface Exposure Dating in Geomorphology	34
Microbial Dissolution of Iron Oxides.....	34
CATEGORY: Solar-Terrestrial Physics	35
Energy Transport in Space Plasma.....	35
The Solar Wind-Magnetospheric Interaction	36
Energetic Particle Acceleration and Transport.....	36
CONTRACTOR: Oak Ridge National Laboratory	38
CATEGORY: Geochemistry.....	38
Thermodynamic Mixing Properties of C-O-H-N Fluids	38
Fundamental Research in the Geochemistry of Geothermal Systems.....	39
Ion Microprobe Studies of Fluid-Rock Interaction	41
Experimental Studies of Fundamental Stable Isotope Exchange Reactions.....	42
Potentiometric Studies of Geochemical Processes	43
Mechanisms and Rates of Isotope Exchange in Mineral-Fluid Systems.....	45
CONTRACTOR: Pacific Northwest Laboratory	46
CATEGORY: Geochemistry.....	46
Local Reactions on Carbonate Surfaces: Structure, Reactivity, and Solution	46
Geometric and Electronic Structure of Oxide Surfaces.....	47
Structure and Reactivity of Iron Oxide and Oxyhydroxide Surfaces and Interfaces	48
Electron Transfer at the Fe(III) Oxide-Microbe Interface	51

CONTRACTOR: Sandia National Laboratories.....	53
CATEGORY: Geophysics and Earth Dynamics.....	53
Effects of fluid flow on inelastic deformation and failure in dilating and compacting rock	53
Inversion of Full Waveform Seismic Data for Shallow Subsurface Properties.....	54
Micromechanical Processes in Porous Geomaterials	55
Resolution and Accuracy of 3-D Electromagnetic Imaging	56
CATEGORY: Geochemistry.....	58
Atomistic Simulations of Clay Minerals and Their Interaction with Hazardous Wastes: Molecular Orbital and Empirical Methods	58
CATEGORY: Hydrology	60
Multi-component Convection in Porous Media and Fractures	60
Laboratory Investigation of Permeability Upscaling.....	61
Two-Phase Immiscible Fluid Flow in Fractured Rock: The Physics of Two-Phase Flow Processes in Single Fractures	62
PART II: OFF-SITE	65
GRANTEE: American Museum Of Natural History	65
Influence of carbon on the electrical properties of crustal rocks.....	65
GRANTEE: Arizona State University.....	66
Reaction Mechanisms of Clay Minerals and Organic Diagenesis: An HRTEM/AEM Study.....	66
Chemical Dynamics of Hydrocarbon Reservoirs Investigated by Secondary Ion Mass Spectrometry	68
GRANTEE: Boston University.....	70
Nonlinear Systems Approach to Understanding the Origin of Geodetic Crustal Strains (Collaborative Research).....	70
GRANTEE: California Institute Of Technology	71
Infrared Spectroscopy and Hydrogen Isotope Geochemistry of Hydrous Silicate Glasses.....	71
Isotope Tracer Studies of Diffusion in Silicates and of Geological Transport Process in Aqueous Systems Using Actinide Elements	72
GRANTEE: University Of California, Berkeley	74
Advective-Diffusive/Dispersive Transport of Chemically Reacting Species in Hydrothermal Systems.....	74
Collaborative Research: Studies for Surface Exposure Dating in Geomorphology.....	76
Microbial Dissolution of Iron Oxides.....	77
GRANTEE: University Of California, Davis	78
The Kinetics of Dissociation of Aluminum-Oxygen Bonds in Aqueous Complexes	78
Thermodynamics of Minerals Stable Near the Earth's Surface.....	80
Electrochemical Measurements of Thermodynamics Properties of Minerals and the Processes of Reconstruction at Mineral Surfaces	81

GRANTEE: University Of California, Los Angeles.....	83
Application of ⁴⁰ Ar/ ³⁹ Ar thermochronometry and ion microprobe stable isotope geochemistry to the evolution of petroleum reservoirs and hydrothermal systems	83
GRANTEE: University Of California, Santa Barbara	85
The Hydrodynamics of Geochemical Mass Transport and Clastic Diagenesis: San Joaquin Basin, California	85
Magma Rheology, Mixing of Rheological Fluids, Molecular Dynamics Simulation, and Lithospheric Dynamics.....	86
GRANTEE: University Of California, Santa Cruz	88
Fast 3-D Modeling and Prestack Depth Migration Using Generalized Screen Methods	88
GRANTEE: The University Of Chicago.....	90
Kinetic isotope fractionation	90
GeoSoilEnviroCARS: A National Resource for Earth, Planetary, Soil and Environmental Science Research at the Advanced Photon Source.....	92
Synchrotron X-ray Microprobe and Microspectroscopy: Technical Development for Advanced Photon Source Research and Low Temperature Geochemistry Applications	94
GRANTEE: The City College Of The City University Of New York.....	95
Particulate Dynamics in Filtration and Granular Flow	95
GRANTEE: University Of Colorado	96
Nonlinear Systems Approach to Understanding the Origin of Geodetic Crustal Strains (Collaborative Research).....	96
Evolution of Rock Fracture Permeability During Shearing	97
Nucleation and Growth Kinetics of Clays and Carbonates on Mineral Substrates	99
Two-Phase Immiscible Fluid Flow in Fractured Rock: The Physics of Two-Phase Flow Processes in Single Fractures	101
Seismic Absorption and Modulus Measurements in Single Cracks and Porous Rocks: Physical and Chemical Effects of Fluids	103
GRANTEE: Colorado School Of Mines	104
Three-Dimensional Analysis of Seismic Signatures and Characterization of Fluids and Fractures in Anisotropic Formations.....	104
GRANTEE: Columbia University.....	106
Rock Varnish Record of Holocene Climate Variations in the Great Basin of Western US	106
GRANTEE: University Of Connecticut.....	107
Geochemical and Isotopic Constraints on Processes in Oil Hydrogeology.....	107
GRANTEE: University Of Delaware.....	109
Development of an Experimental Database and Theories for Prediction of Thermodynamic Properties of Aqueous Electrolytes and Nonelectrolytes of Geochemical Significance at Supercritical Temperatures and Pressures	109

GRANTEE: University Of Florida.....	111
Pore Scale Simulations of Rock Deformation, Fracture, and Fluid Flow in Three Dimensions.....	111
GRANTEE: Georgia Institute Of Technology.....	113
Biomineralization: Organic-Directed Controls on Carbonate Growth Structures and Kinetics Determined by <i>In Situ</i> Atomic Force Microscopy.....	113
GRANTEE: University Of Hawaii.....	115
Growth of Faults, Scaling of Fault Structure, and Hydrologic Implications	115
GRANTEE: Indiana University	116
Basin Nonlinear Dynamics and Self-Organization	116
GRANTEE: The Johns Hopkins University.....	118
The Hydrodynamics of Geochemical Mass Transport and Clastic Diagenesis: San Joaquin Basin, California	118
Predictive Single-site Protonation and Cation Adsorption Modeling.	119
Reaction and Transport of Toxic Metals in Rock-Forming Silicates at 25°C.....	120
GRANTEE: Kent State University.....	122
Microbial Dissolution of Iron Oxides.....	122
GRANTEE: Lehigh University.....	123
Reaction and Transport of Toxic Metals in Rock-Forming Silicates at 25°C.....	123
GRANTEE: University Of Maryland.....	125
Theoretical Studies on Metal Species in Solution and on Mineral Surfaces	125
GRANTEE: Massachusetts Institute Of Technology.....	127
Evolution of Pore Structure and Permeability of Rocks under Hydrothermal Conditions.....	127
GRANTEE: University Of Michigan.....	128
Combined Noble Gas and Stable Isotope Constraints on Nitrogen Gas Sources within Sedimentary Basins	128
GRANTEE: University Of Minnesota, Twin Cities	129
Magma Rheology, Mixing of Rheological Fluids, Molecular Dynamics Simulation, and Lithospheric Dynamics.....	129
GRANTEE: National Academy of Sciences, Board on Earth Sciences and Resources	131
Board on Earth Sciences and Resources and Its Activities.....	131
GRANTEE: University Of Nevada, Reno.....	132
Growth of Faults, Scaling of Fault Structure, and Hydrogeologic Implications.....	132
GRANTEE: New England Research Inc.....	134
The Role of Fracture Intersections in the Flow and Transport Properties of Rock.....	134

GRANTEE: University Of New Mexico.....	136
Continuum and Particle Level Modeling of Concentrated Suspension Flows	136
GRANTEE: New Mexico Institute Of Mining And Technology	137
Investigation of Permeability Upscaling.....	137
GRANTEE: State University Of New York At Stony Brook.....	139
High Precision Radiometric Dating of Sedimentary Materials.....	139
Medial Axis Analysis of Porous Media	140
Surface Chemistry of Pyrite: An Interdisciplinary Approach.....	142
Micromechanics of Failure in Brittle Geomaterials	144
GRANTEE: Northwestern University.....	146
Factors Affecting Shear Strain Localization in Rocks.....	146
GRANTEE: Oklahoma State University	147
Two-Phase Immiscible Fluid Flow in Fractured Rock: The Physics of Two-Phase Flow Processes in Single Fractures	147
GRANTEE: University Of Oklahoma.....	149
Development and Application of a Paleomagnetic/Geochemical Method for Constraining the Timing of Fluid Migration and Other Diagenetic Events.....	149
GRANTEE: The Pennsylvania State University.....	151
Dissolution of Feldspar in the Field and Laboratory	151
GRANTEE: Purdue University.....	152
Mechanical Models of Fault-Related Folding.....	152
Effects of Micro- and Macro-Scale Interfaces on Seismic Wave Propagation in Rock and Soil	153
GRANTEE: Rensselaer Polytechnic Institute.....	154
Transport Phenomena in Fluid-Bearing Rocks	154
GRANTEE: Rice University.....	156
Transition Metal Catalysis in the Generation of Petroleum and Natural Gas.....	156
GRANTEE: Scripps Institution Of Oceanography	158
Joint Inversion of Acoustic and Induction Log Data for Enhanced Resistivity Structure.....	158
GRANTEE: Stanford University	159
Metal Ion Sorption at Oxide Surfaces and Oxide-Water Interfaces: Spectroscopic Studies and Modeling	159
Seismic Signatures of Fluids in Anisotropic Rocks	161
Porous Rocks with Fluids: Seismic and Transport Properties	163
Rock Physics for Seismic and SAR Characterization and Monitoring of Reservoir Fluids and Their Recovery	165
Diffusion of CO ₂ during Hydrate Formation and Dissolution	167

Development of Fracture Networks and Clusters: Their Role in Channelized Flow in Reservoirs and Aquifers.....	168
Coupled Fluid Deformation Effects in Earthquakes and Energy Extraction	170
GRANTEE: Temple University	171
Surface Chemistry of Pyrite: An Interdisciplinary Approach.....	171
GRANTEE: The University Of Tennessee.....	173
Development of Laser-Based Resonance Ionization Techniques for ⁸¹ Kr and ⁸⁵ Kr in the Geosciences, II	173
GRANTEE: Texas A&M University	175
Fluid-Assisted Compaction and Deformation of Reservoir Lithologies	175
GRANTEE: University Of Texas	176
High-Resolution Temporal Variations in Groundwater Chemistry: Tracing the Links Between Climate, Hydrology, and Element Mobility in the Vadose Zone.	176
Integrated 3-D Ground-penetrating Radar, Outcrop, and Borehole Data Applied to Reservoir Characterization and Flow Simulation.....	177
Thermohaline Convection in the Gulf of Mexico Sedimentary Basin, South Texas	178
GRANTEE: Texas Tech University.....	180
Continuum and Particle Level Modeling of Concentrated Suspension Flows	180
GRANTEE: University Of Utah	181
High Resolution Imaging of Electrical Conductivity using Low-Frequency Electromagnetic Fields.....	181
GRANTEE: Utah State University.....	183
Big Hole Drilling Project: Characterization of Fault Zone Properties from <i>In-Situ</i> Analyses.....	183
Growth of Faults and Scaling of Fault Structure.....	184
GRANTEE: Virginia Polytechnic Institute & State University.....	185
Experimental Studies in the System H ₂ O-CH ₄ -“Petroleum”-Salt Using Synthetic Fluid Inclusions	185
GRANTEE: University Of Washington	187
Electromagnetic Imaging of Fluids in the San Andreas Fault	187
GRANTEE: University Of Wisconsin	188
Resolution and Accuracy of 3-D Electromagnetic Imaging	188
Comparative Studies of Physiochemically and Biologically Mediated Reactions at Mineral Surfaces	190
Deformation and Fracture of Poorly Consolidated Media.....	192
Microanalysis of Stable Isotope Ratios in Low Temperature Rocks	194
Pore-Scale Simulations of Rock Deformation, Fracture, and Fluid Flow in Three Dimensions.....	196

GRANTEE: Woods Hole Oceanographic Institution.....	197
Laboratory Constraints on the Stability of Petroleum at Elevated Temperatures: Implications for the Origin of Natural Gas	197
Organic Geochemistry of Outer Continental Margins and Deep-Water Sediments	198
GRANTEE: University Of Wyoming	200
Mineral Dissolution and Precipitation Kinetics: A Combined Atomic-Scale and Macro-Scale Investigation	200
GRANTEE: Yale University	202
A Field Experiment on Plants and Weathering.....	202
Reactive Fluid Flow and Applications to Diagenesis, Mineral Deposits, and Crustal Rocks	203
Subject Index	205
Author Index.....	210
DOE/OBES Geosciences Research: Historical Budget Summary.....	215

Foreword

The Department of Energy supports research in the geosciences in order to provide a sound foundation of fundamental knowledge in those areas of the geosciences that are germane to the Department of Energy's many missions. The Division of Engineering and Geosciences, part of the Office of Basic Energy Sciences of the Office of Energy Research, supports the Geosciences Research Program. The participants in this program include Department of Energy laboratories, academic institutions, and other governmental agencies. These activities are formalized by a contract or grant between the Department of Energy and the organization performing the work, providing funds for salaries, equipment, research materials, and overhead. The summaries in this document, prepared by the investigators, describe the scope of the individual projects. The Geosciences Research Program includes research in the broad areas of geophysics, geochemistry, resource evaluation, hydrogeology and solar-terrestrial interactions, and their subdivisions, including Earth dynamics, properties of Earth materials, rock mechanics, underground imaging, rock-fluid interactions, continental scientific drilling, geochemical transport, solar/atmospheric physics, and modeling, with emphasis on the interdisciplinary areas. All such research is related either directly or indirectly to the Department of Energy's long-range technological needs. Further information on the Geosciences Research Program, including recent program activities and highlights, may be found on the Geosciences Programs home page at: <http://www.sc.doe.gov/production/bes/geo/geohome.html>

The Geosciences Research Program in the Office of Basic Energy Sciences

The Geosciences Research Program is directed by the Department of Energy's (DOE's) Office of Energy Research (OER) through its Office of Basic Energy Sciences (OBES). Activities in the Geosciences Research Program are directed toward building the long-term fundamental knowledge base necessary to provide for energy technologies of the future. Future energy technologies and their individual roles in satisfying the nations energy needs cannot be easily predicted. It is clear, however, that these future energy technologies will involve consumption of energy and mineral resources and generation of technological wastes. The Earth is a source for energy and mineral resources, and is also the host for wastes generated by technological enterprise. Viable energy technologies for the future must contribute to a national energy enterprise that is efficient, economical, and environmentally sound. The Geosciences Research Program emphasizes research leading to fundamental knowledge of the processes that transport, modify, concentrate, and emplace (1) the energy and mineral resources of the Earth and (2) the energy byproducts of man. The Geosciences Research Program is divided into five broad categories:

1. Geophysics and Earth Dynamics.
2. Geochemistry.
3. Energy Resource Recognition, Evaluation, and Utilization.
4. Hydrogeology.
5. Solar-Terrestrial Interactions.

The following outline of current research in these categories is intended to be illustrative. The program evolves with time and progress in these and related fields. Individual research projects supported by this program at DOE laboratories, national laboratories, academic institutions, research centers, and other federal agencies typically have components in more than one of the categories or subcategories listed. In addition, it is common for research activities to involve a high level of collaboration between investigators and different institutions.

1. GEOPHYSICS AND EARTH DYNAMICS

- A. *Large-Scale Earth Dynamics.* Research on the physics of lithospheric dynamics such as plate motion, mountain building, basin development, and regional scale uplift/subsidence and its concomitant effects.
- B. *Evolution of Geologic Structures.* Research on the physical controls and physical effects of the dynamic evolution of geologic structures (*e.g.*, folds, faults, basins, volcanoes) on a local or regional scale.
- C. *Properties of Earth Materials.* Research on physical properties of rocks and minerals determined in the laboratory or in the field (*in situ*), by direct or indirect techniques, and applicable on the spatial and temporal scales of geologic processes.
- D. *Rock Mechanics, Fracture, and Fluid Flow.* Research on the response of rock and rock units to induced stress and the role of fluid flow as a cause and/or effect.

- E. *Underground Imaging*. Research to characterize the layering, mineralogy, lithology, geometry, fracture density, porosity, fluid content, and composition of the lithosphere using geophysical methods.

2. GEOCHEMISTRY

- A. *Thermochemical Properties of Geologic Materials*. Research on the thermodynamic and chemical properties of geologic materials and their kinetic/dynamic interactions.
- B. *Rock-Fluid Interactions*. Research on the chemical and mechanical consequences of rock-fluid interactions and the mass and energy transport controls of such interactions.
- C. *Organic Geochemistry*. Research on naturally occurring carbonaceous and biologically derived substances of geologic and energy importance.
- D. *Geochemical Transport*. Research (both experimental and theoretical) on the geochemical separation, transport, and concentration of materials in the Earth's crust induced by the spatial and temporal dynamics of lithospheric processes leading to a predictive capability.

3. ENERGY RESOURCE RECOGNITION, EVALUATION, AND UTILIZATION

- A. *Resource Definition and Utilization*. Research to develop new and advanced bases for the physicochemical dynamics needed for improved energy and energy-related resource exploration, definition, and use.
- B. *Reservoir Dynamics and Modeling*. Research on the physicochemical dynamics of geothermal and hydrocarbon reservoirs in their natural and perturbed (by production, injection, or reinjection) states.
- C. *Properties and Dynamics of Magma*. Research on the origin, migration, emplacement, and crystallization of natural silicate liquids and their heat energy.
- D. *Continental Scientific Drilling*. Research on the scientific objectives of the OBES Geosciences Research Program using advanced technologies in shallow, intermediate, and deep drilling for Earth observation facilities. Scientific research and advanced drilling technologies development are coordinated by an Interagency Coordinating Group (DOE, the U.S. Geological Survey, and the National Science Foundation) under the aegis of the Interagency Accord on Continental Scientific Drilling.

4. HYDROGEOLOGY

- A. *Fluid Transport Dynamics and Modeling*. Research on the chemical transport and energy/mechanical consequences of fluid interactions and transport, leading to a predictive capability.
- B. *Thermochemical Properties of Energy Materials*. Research on the thermodynamic and chemical properties of materials and their kinetic/dynamic interactions in fluidrock systems.
- C. *Perturbations of Fluid Flow*. Research on the physicochemical dynamics and chemical transport of fluidrock systems in response to mechanical and energy perturbations, leading to a predictive capability.

5. SOLAR-TERRESTRIAL INTERACTIONS

- A. *Magnetospheric Physics*. Research on the fundamental interactions of the solar wind with the terrestrial magnetic field and the Earth's magnetosphere as a model magnetohydrodynamic generator and associated plasma physics research.
- B. *Upper Atmosphere Chemistry and Physics*. Research on thermal, compositional, and electrical phenomena in the upper atmosphere and the interactions induced by solar radiation.
- C. *Solar Radiation and Solar Physics*. Research on the structure and dynamics of the sun and the characteristic interactions of solar radiation with the Earth, including the effects of solar radiation on the climate.

PART I: ON-SITE

CONTRACTOR: Argonne National Laboratory

Argonne, Illinois 60439

CONTRACT: W-31-109-Eng-38

CATEGORY: Geochemistry

PERSON IN CHARGE: N. C. Sturchio

Mineral-Fluid Interactions: Synchrotron Radiation Studies at the Advanced Photon Source

N. C. Sturchio (630-252-3986; Fax: 630-252-7415; Sturchio@anl.gov), P. Fenter, and M. J. Bedzyk (Northwestern University)

Objectives: The objective of this program is to advance the basic understanding of rock-fluid and soil-fluid interactions through experimental studies of atomic-scale processes at mineral-fluid interfaces. This is crucial to establishing the relation between atomic-scale processes and macroscopic geochemical transport in large-scale natural systems.

Project Description: The principal approach is to observe single-crystal mineral surfaces *in situ* during chemically controlled reactions with fluids, using X-ray scattering, standing wave, and absorption techniques with high-brilliance synchrotron radiation. These techniques provide high-resolution atomic-scale structural information that cannot be acquired by any other means. Experiments are being performed on common rock- and soil-forming minerals under conditions representative of geochemical environments near the Earth's surface. Types of reactions being investigated include dissolution-precipitation, adsorption-desorption, and oxidation-reduction.

Results: Progress during the past year included further successful demonstrations of the ability to perform *in situ* X-ray reflectivity, diffraction, and standing-wave studies of reacting mineral surfaces under chemically controlled conditions. During the past year, experiments were conducted to characterize the atomic structure of the orthoclase (001) cleavage plane in contact with aqueous solutions, and to observe changes in this structure as a function of solution composition and time, using X-ray reflectivity measurements. We are focusing on the relaxations of near-surface atoms in orthoclase and the structure of adsorbed water. A study of the dissolution kinetics and structure of orthoclase at low pH was performed. X-ray standing waves and surface X-ray absorption spectroscopy were combined to determine the structure and amount of Rb and Sr adsorbed onto rutile. X-ray standing wave and absorption spectroscopy studies of uranyl adsorption on calcite were performed. Organic acid and protein adsorption on calcite was studied using X-ray reflectivity in collaboration with M. McBride and J. DeYoreo (Lawrence Livermore National Laboratory). Experimental studies of clay mineral growth on muscovite substrates using X-ray reflectivity techniques were continued, in collaboration with K. L. Nagy (University of Colorado).

CONTRACTOR: Brookhaven National Laboratory

Associated Universities, Inc.
Upton, Long Island, New York 11973

CATEGORY: Geology, Geophysics, and Earth Dynamics

CONTRACT: DE-AC02-98CH10886

PERSON IN CHARGE: K. W. Jones

Study of the Microgeometry of Geological Materials Using Synchrotron Computed Microtomography

K. W. Jones (631-344-4588; Fax: 631-344-5271; kwj@bnl.gov), and H. Feng (631-344-2081; Fax: 631-344-5271; hfeng@sun2.bnl.gov)

Objectives: The objective of this project is to gain improved knowledge of the properties and behavior of geological materials on a grain-size scale. Measurements are made to determine: 1) the microgeometry of typical rock types, 2) changes in the microgeometry of the rocks as a function of applied pressure, 3) fluid-flow paths through the rocks, 4) changes in rock composition caused by fluid-rock interactions, and 5) determination of fracture structures and growth as a function of pressure.

Project Description: Experimental data are obtained using the technique of synchrotron computed microtomography. Intense x-ray beams from the Brookhaven National Synchrotron Light Source pass through the sample and strike an area scintillation detector. Light from the scintillator is detected with a charge-coupled device and stored for later analysis. The tomographic volume is found by analyzing a series of the two-dimensional views obtained as the sample is rotated around an axis normal to the x-ray beam. The maximum number of voxels in the final volume is about 10^{10} . The minimum voxel size is about 3 μm on an edge. Other x-ray techniques are also being applied to selected samples. These techniques include microbeam x-ray fluorescence, high-resolution x-ray microscopy, and Fourier Transform Infrared Spectroscopy (FTIR).

Results: Experimental investigations of sandstones, limestones, and carbonates were carried out during FY 1999. These investigations included further measurements on the native sandstones from the Vosges, Darley Dale from Yorkshire, and Berea sandstone from Indiana. Investigations of changes in the microstructure as a function of applied pressures as high as 300 MPa were carried out. In addition, samples prepared to simulate conditions found in perforation of well casings with an explosive charge were investigated. The hope is to characterize the changes in the specimen caused by the perforating explosion and to relate these mechanical changes to those caused by pressures applied under carefully controlled laboratory conditions. Fluid flow in sandstones was also investigated through measurement of Wood's metal-filled 5% porosity Berea sandstone. The percolation front was clearly observed in one partially filled sample. The initial study of type I deep-sea spherules begun in FY 1997 was carried on in FY 1998 with over 20 particles being examined. Several specimens from hydrothermal vents were measured. Qualitative comparison with measurements made using a commercial scanner showed the effectiveness of the synchrotron instrumentation in defining structures on the micrometer size scale. Several sediment samples were investigated with the aim of obtaining data for comparison with theoretical predictions. In addition, experiments were carried out on sediments using high-resolution x-ray microscopy (0.1-micrometer resolution), microbeam x-ray fluorescence (10-micrometer resolution),

and Fourier Transform Infrared Spectroscopy (15-micrometer resolution) to obtain supplemental information on surfaces and contaminants. Analysis of measurements on Vosges sandstone and limestone was completed and analysis of other results is in progress.

CATEGORY: Geochemistry

CONTRACT: DE-AC02-76CH00016

PERSON IN CHARGE: A. Vairavamurthy

Geochemistry of Organic Sulfur in Marine Sediments

M. A. Vairavamurthy (631-344-5337; Fax: 516-344-7905; vmurthy@bnl.gov)

Objectives: The overall objective of this study is to gain a fuller understanding of the geochemical role of the sulfur system in transforming sedimentary organic matter from organized structures typical of biopolymers (*e.g.*, proteins and carbohydrates) to heterogeneous sedimentary geopolymers, such as humic substances and kerogen. A major emphasis is placed on understanding the abiotic mechanisms of sulfur incorporation into organic matter and its influence in the preservation of organic matter in marine sediments.

Program Description: Sulfur is believed to be involved in preserving organic matter in sediments, in converting this organic matter to petroleum and in controlling the timing of petroleum generation from a source rock. A fundamental geochemical issue is the mechanism of incorporation of sulfur into sedimentary organic matter. Although it is accepted that H₂S and its partial oxidation products (such as polysulfide ions) are involved, there is controversy about its molecular mechanism, and the active species involved. This project, which is aimed at understanding the formation and transformation of sedimentary organic sulfur during early diagenesis, has four major components: (1) studies of sulfur speciation in sediments, (2) mechanistic studies of organic sulfur formation, (3) mechanistic studies of the pathways of transformation of organic sulfur compounds in sediments, and (4) development of analytical methods. The suite of complementary spectroscopic and chromatographic techniques used (particularly synchrotron-radiation-based XANES spectroscopy for sulfur speciation and liquid chromatography combined with mass spectrometry, LC-MS) give detailed structural information on sulfur and its associated organic moieties.

Results: To better understand the natural mechanisms of organic sulfur formation under anaerobic conditions, we investigated the chemical composition of dissolved organic matter from the Upper Mystic Lake, Boston, Massachusetts, a stratified lake with highly reducing stagnant bottom waters with intense sulfate reduction. This lake provides an ideal setting to understand how organic matter transforms when conditions change from oxic to anoxic, along with high levels of H₂S production. There is much evidence to suggest that such anaerobic conditions were prevalent in ancient oceans and that they enhanced the preservation of organic matter.

The XANES analysis clearly showed a distinct shift in sulfur speciation from oxidized forms dominated with sulfonates in oxic waters, to predominantly reduced sulfur forms in anoxic waters comprising mono-di-and polysulfidic sulfur. Concomitant with these changes in speciation, the relative sulfur content also increased. Moreover, the molecular weight of the diagenetically formed humic macromolecules increased with increasing depth, supporting the view of increasing macromolecular

complexity of the geological molecules with the progression of diagenesis. In combination, these results suggest that sulfur cross-linking is an important step in forming humic polymers under anoxic sulfide-rich conditions, and hence in preserving organic matter.

Mass spectrometric analysis of the isolated compounds show a group of molecules in the bottom waters containing silicon in addition to sulfur. The molecules ranged from a molecular weight of 600 up to 2000. The silicon is probably interspersed in the backbone of the molecule with repeating units of $-(\text{OSi}(\text{CH}_3)_2)_n$ and $-(\text{SC}(\text{CH}_3)_2)_n$. These results present the first evidence for the formation of silicon- and sulfur-containing polymers under anaerobic conditions.

CONTRACTOR: Lawrence Berkeley National Laboratory

University of California
Berkeley, CA

CONTRACT: DE-AC03-76F00098

CATEGORY: Geophysics and Earth Dynamics

Person in Charge: S. Benson

High-Resolution Imaging of Electrical Conductivity Using Low-Frequency Electromagnetic Fields

K.H. Lee (510-486-7468; Fax: 510-486-5686; khlee@lbl.gov), H.F. Morrison, and A. Becker

Objectives: The objective is to develop numerical and field techniques for high-resolution imaging of electrical conductivity using magnetotelluric (MT) and controlled-source electromagnetic (CSEM) methods. Applications of high-resolution conductivity imaging include the mapping of groundwater, resource exploration and reservoir characterization, subsurface processes monitoring, and general geological mapping of the crust of the Earth.

Project description: Many fundamental questions relating to resolution, depth of exploration, required bandwidth in frequency and spatial sampling rate remain to be answered. To resolve some of these questions four main tasks have been selected in this project; 1) improvement of the q-domain imaging method using the wavefield transform and tomographic inversion, 2) development of an approximate analysis and imaging method using Born inversion, 3) development of a rapid and practical 3-D inversion scheme, and 4) development of a borehole time-domain EM system. Some of these tasks are driven by the pressing need to interpret an increasing amount of field data available to us. The data may be in the frequency domain, but can only be interpreted properly if and when tasks 2 and 3 become successful. Also, the evident success of the q-domain tomographic imaging process strongly argues for the development of a suitable wideband borehole system (task 4).

Results: An approximate imaging scheme for mapping cross-hole electrical conductivity using nonlinear traveltimes tomography has been developed (Lee *et al.*, 1999). Data used are arrival time estimates based on an approximate wavefield transform of frequency-domain EM field. In this study, a ray series expansion has been used to obtain approximate wavefield in the transformed domain. If reflected and refracted energy is weak compared to that of direct wave, picking of the arrival time may be reduced to estimating the coefficients of the leading term in the ray series expansion. This simplification is valid when the conductivity contrast is small. An adaptive simulated annealing scheme is used to estimate the coefficients of ray series. For a whole space, exact traveltimes can be extracted using only 4 frequency data. Nonlinear traveltimes tomography using thus extracted traveltimes shows a reasonable image of the conductivity structure between boreholes.

Development of the non-linear Born inversion for mapping 3-D conductivity structures has been completed. One of the highlights of the method is that the evaluation of integral of the product of Green's function and scattering current is carried out in the wavenumber domain, thereby greatly accelerating the computational speed. The inversion algorithm has been used to analyze EM data

obtained from the saline water injection experiment conducted at the Richmond Field Station of the University of California at Berkeley.

Center for Computational Seismology (CCS)

T.V. McEvilly (510-486-7316; Fax: 510-486-5686; tvmcevilly@lbl.gov), E.L. Majer and L.R. Johnson)

Objectives: The Center for Computational Seismology (CCS) serves as the core data processing, computation and visualization facility for seismology-related research at LBNL. As such, it will be integral to our critical efforts in mapping the distribution and migration of fluids in the subsurface, a problem requiring new approaches in seismic waveform inversion techniques that can take into account the presence and effects of diffracted waves. A wide range of research projects relies upon CCS resources for development and application of methods for characterization, process definition, and process monitoring in the rock-fluid-thermochemical subsurface environment. Pursuing an objective of providing modern tools for seismological research, the Center is designed and operated to provide a focused environment for research in modern computational seismology by scientists whose efforts at any time may be distributed among diverse research projects. A large number of varied, separately funded research projects, from many different sponsors, rely upon this resource for intellectual exchange as well as computational needs. Ph.D. theses and journal publications reveal a spectrum of effort from the most fundamental theoretical studies to field applications at all scales.

Project Description: CCS provides a specially equipped and staffed computational facility to support and advance a wide-ranging program of seismological research. Beyond computers, work stations, seismic processing packages and visualization capabilities, it is a physical facility in which scientists pursuing individual research interact with other scientists and technical support staff in a multidisciplinary intellectual environment. CCS supports research in the general areas of wave propagation, geophysical inverse methods, earthquake and explosion source theory, seismic imaging, borehole geophysics, four-dimensional process monitoring and visualization technology.

Results: Results from the diverse seismological program at CCS are best demonstrated in the CCS research output. Major accomplishments flow largely from the breadth of research support provided by CCS, and the cross-fertilization between applications and fundamental studies. Significant recent results involve successful imaging of contaminant flow zones in fractured basalt, development of borehole orbital vibrator technology and promising results in CO₂ monitoring with borehole imaging methodology.

Findings for a facility and scientific environment such as that provided by CCS must be defined in the context of the multidisciplinary research base that is supported there, rather than project-specific accomplishments (those appear in other sections of this report). It is fair to attribute a large part of the scientific reputation in seismology at LBNL to the CCS environment.

Deformation and Fracture of Poorly Consolidated Media

L. R. Myer (510-486-6456; Fax: 510-486-5686; myer@lbl.gov), K.T.Nihei (510-486-5349; Fax 510-486-5686; KTNihei@lbl.gov), and B. C. Haimson (Univ. of Wisconsin)

Objectives: What distinguishes a well-consolidated granular rock from a unconsolidated granular soil, *e.g.*, sand, is the presence of strong inter-grain cohesion and frictional sliding resulting from reduced porosity. Although the mechanical properties of these two limits among granular materials have been a focus of extensive research for the past decades, the intermediate case of weakly-consolidated soil and its behavioral transition from soil to rock is not well-understood yet. This research investigates the effects of porosity and mechanical properties of grain contact such as cohesion and frictional coefficient on the strength and failure mode of poorly consolidated granular rocks.

Earlier investigations revealed that in weakly cemented porous granular materials, the lack of dilatational forces at the grain scale can lead to the development of an unusual thin slit-like failure feature (Figure 1) around a borehole. In contrast to the typical borehole breakout resulting from KI-mode (opening mode) fractures propagating perpendicular to the direction of local tensile stress, this type of failure feature develops in the direction perpendicular to the local compressional stress and therefore is called an "anti-KI" fracture. Understanding fundamental microprocesses associated with these features is important for design of stable boreholes in weakly cemented rock. Whereas a typical borehole breakout achieves a stable geometry for a given material strength and *in situ* stress state, observations imply that these features extend indefinitely. It also appears that they may form even if only a small, unsupported area is present, such as at a perforation. In this research, a series of laboratory experiments has been performed to understand the effect of grain shape, cementation, and the mechanical removal of debonded grains upon the failure mode of a weakly cemented granular medium.

Project description: Model specimens for weakly consolidated sandstone were fabricated from clean silica sand and glass beads. After testing a variety of binding materials, sodium silicate solution was chosen to cement the grains. Since this material tends to dissolve in water, future experiments involving pore fluid will be conducted with non-aqueous fluid such as highly concentrated alcohol. Laboratory uniaxial compression tests were performed on thin rectangular bricks (8 inches tall, 4 inches wide, and 1.1 inches thick) of artificial sandstones made of glass beads and silica sand. Each brick contained a single small diameter hole as an analogue of a two-dimensional borehole. Beads and natural sand were used (sieved to have grain diameters between 150 μm to 212 μm) so the effect of grain shape on the failure behavior of the specimens could be studied. Varying amounts of sodium silicate solution were used as a binder to achieve a range of cohesive strength between grains. The bricks were loaded vertically in the direction perpendicular to the borehole, and the development of compaction zones and fractures around the hole were observed. Following these experiments, fracture toughness tests will be performed to determine the cohesive strength and triaxial tests to determine the frictional strength of the granular media. Concurrently with the laboratory experiments, 2D and 3D numerical models based on discrete element method (DEM) will be developed to simulate the behavior of weakly consolidated and cemented materials.

Results: For glass bead specimens, the characteristic "anti-KI" fracture formed regardless of the amount of sodium silicate binder. In contrast, for silica sand specimens, "dog-ear" shaped compaction/shear zones formed in the direction perpendicular to the axial load. However, if the debonded grains were removed from the failure zone using compressed air flow, the fracture similar to the glass-bead specimens developed. In a silica sand specimen with very strong intergranular cohesion, fractures propagating parallel to the direction of compressional stress were observed (classical borehole breakout

failure). These fractures penetrated through individual sand grains, indicating that the dilation due to failed grains allowed the transmission of local compressional stress driving the fractures in this direction. These results indicate the importance of grain removal in determining the failure mode a weakly cemented porous granular rock. Rock characteristics such as high porosity, round grains, and the existence of a mechanical force that dislodges the grains from the fracture tip can assist in the development of the anti-KI borehole failure. It is likely that this mode of failure can occur even within relatively competent sandstones if liquid flow (water, drilling fluid, *etc.*) can remove sand grains in a manner similar to the compressed air used in this study.

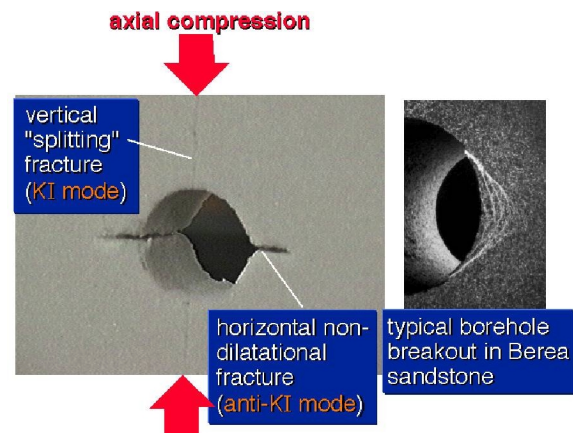


Figure. Anti-KI mode fracture formed around a borehole within a synthetic sandstone. This failure feature is markedly different from the classical borehole breakout with fractures developing parallel to the local compressional stress field.

For the triaxial strength tests, the fabrication of a test cell that houses a 1.25-inch diameter and 3.75 inch tall core has been completed. Using this cell, volumetric change of the sample during compression can be measured by the amount of confining fluid expelled out of the cell while maintaining a constant confining pressure. As for the numerical code, the first part of the code that provides the initial packing geometry of the granular medium by simulating the deposition of spherical grains under gravity was completed (both in 2D and 3D). It has been observed that this type of low-energy deposition procedure results relatively low packing densities (approximately 50% porosity in 3D). To obtain a more realistic packing geometry of the grains, subsequent consolidation of the system is required.

Decomposition of Scattering and Intrinsic Attenuation on Rock with Heterogeneous Multiphase Fluids Distributions

K.T.Nihei (510-486-5349; Fax: 510-486-5686; KTNihei@lbl.gov) L.R.Myer (510-486-6456; Fax: 510-486-5686; LRMyer@lbl.gov)

Objectives: The overall focus of this project is a fundamental investigation of scattering and intrinsic attenuation of seismic waves in rock with heterogeneous distributions of fluids and gas. This research represents a departure from past rock physics studies on seismic attenuation in that the emphasis here is not a detailed study of a specific attenuation mechanism, but rather to investigate theoretical and laboratory methods for obtaining separate estimates of scattering and intrinsic attenuation in rock with heterogeneous pore fluid distributions. It is anticipated that methods for obtaining separate estimates of intrinsic and scattering attenuation may lead to higher resolution methods for monitoring the movement of fluids in the subsurface.

This project combines laboratory, numerical, and theoretical studies to the investigation of scattering and intrinsic attenuation in rock with heterogeneous fluid distributions. The objectives of this project are threefold: (1) to adapt and further refine methods for decomposing scattering and intrinsic attenuation in rock with heterogeneous multiphase fluids, (2) to apply these methods to laboratory seismic measurements in porous rock with heterogeneous fluid distributions and compare these results

with direct laboratory measurements, and (3) to examine a new method for focusing seismic waves in heterogeneous media using time reversal mirrors. These objectives are addressed in three tasks to be performed over a period of three years.

Project Description: In this project, laboratory, theoretical, and numerical studies are combined to investigate methods for estimating scattering and intrinsic attenuation in rock with heterogeneous distributions of gas and fluid. The focus is on sandstone and carbonates under conditions in which the relative saturation of miscible and immiscible liquids (*e.g.*, water and oil) and gas (*e.g.*, CO₂) vary. Decomposition of the attenuation will be conducted to compare the contributions from scattering and intrinsic attenuation and related to the characteristics of introduced heterogeneity obtained from X-ray CT images. Numerical and theoretical models will be performed to help interpret the results of the laboratory experiments and to investigate the effect of both attenuation mechanisms on the characteristics of the waves. Laboratory and numerical studies of wave focusing on selected heterogeneities using elastic time reversal mirrors will also be investigated. The effects of intrinsic attenuation on the time reversal focusing process and methods for correcting for intrinsic attenuation will be examined.

Results: Work to date consists primarily of experimental design and set-up, and numerical code development. Bar resonance and pulse transmission systems capable of operating in the 1-50 kHz frequency range has been assembled, and calibrated on aluminum and plexiglass bars.

The first series of experiments to investigate Q-intrinsic and Q-scattering are currently being set up in the lab. These tests will examine the differences in Q estimates obtained from resonance and pulse propagation tests on aluminum bars with scatterers in the form of a circumferential notch and a parallel array of cylindrical holes. The next series of tests will utilize the same scatter geometries, but located in a plexiglass bar. In support of these tests, we are currently modifying our cylindrical codes for resonance and bar propagation to include attenuation resulting from viscoelasticity.

CATEGORY: Geochemistry

Person in Charge: S. M. Benson

Integrated Isotopic Studies of Geochemical Processes

D. J. DePaolo (510-486-4975, 510-643-5064, Fax: 510-642-9520, depaolo@socrates.berkeley.edu or djdepaolo@lbl.gov) and B. M. Kennedy (510-486-6451, Fax: 510-486-5496; bmkennedy@lbl.gov)

Objectives: Combine high-precision measurements of isotopic ratios in natural materials with mathematical models to understand the spatial and time scales of geochemical processes of interest for energy management.

Project Description: Current effort is concentrated on Sr, Ca, O, C, He, Ne, Ar, Xe, Pb, and Nd isotopic ratios, and on problems of mass transport in fluid-rock systems, interpretation of past global climatic change, crustal magmatic and tectonic processes, and Quaternary geochronological methods. A mathematical basis for the application of isotopic measurements of fluids and rocks to the field-scale

parameterization of hydrological systems is a major effort of the Center. Modeling is accompanied by systematic measurements of relatively simple natural systems, and by improved sampling and measuring techniques. Emphasis in development is on microsampling of geological materials, on high-precision measurement of the small amounts of recovered material, and on rapid, automated low-blank chemical separation of trace elements. Other efforts of the Center are aimed at geochemical techniques for dating and correlation of sedimentary and volcanic rocks, and for understanding the timescales and mechanisms of crustal processes such as extensional faulting, mountain building, and volcanism. All efforts are aimed at improved characterization of natural rock and fluid systems.

Results: (1) Geochemical transport in fractured rock systems generally cannot be adequately modeled using a simple porous medium formulation. The fracture system must be considered separately from the intervening matrix blocks. This situation presents complications for interpreting isotopic data on fluids at field scales, but also offers opportunities for using isotopic data to learn more about the fracture-matrix interaction, and about fracture spacing in subsurface systems. An analytical formulation has been derived that describes isotopic effects for parallel fractures separated by porous rock "matrix" containing stagnant fluid. The behavior of a steady-state system is dependent on the ratio of the diffusive reaction length (L_e) to the fracture spacing. Different chemical elements can be affected to differing degrees depending on their solubility and diffusivity in the fluid phase, and on the reaction rates in the system. The model can be applied to geothermal systems to estimate the average spacing of fluid-carrying fractures, and in general, to evaluate the limits of applicability of single-porosity models.

(2) Current understanding of the extent and rates of past global climate change is based heavily on isotopic records retrieved from glacial ice in Antarctica and Greenland. How isotopic ratios should be converted to paleotemperature estimates is still uncertain. To address this issue we developed a relatively simple model of meridional water vapor transport, which uses meteorologic characteristics of the Earth. This model extends the description of advective transport via Rayleigh models by adding transport by eddy-processes and recharge to the atmosphere by evaporation. The model allows us to investigate how these factors and others control the relationships between location, temperature and isotopic composition. A significant result is that the model shows that the modern spatial relationship between $\delta^{18}\text{O}$ and mean annual temperature cannot be used to infer past temperature from ice core $\delta^{18}\text{O}$ and other isotopic proxy records. In general, at low latitudes the $\delta^{18}\text{O}$ of precipitation is largely buffered by evaporation from the oceans, and this buffering extends to about $\pm 50^\circ$ latitude north and south. The $\delta^{18}\text{O}$ of precipitation near the poles therefore records only the difference in temperature between the poles and 50° latitude. The absolute temperature change can be significantly larger.

(3) The fate of volatiles entrained in subducted sediments and mantle lithosphere, particularly green house gases such as CO_2 and CH_4 , is relatively unknown but important for establishing global carbon budgets for longer time scales. We have initiated a study of noble gas abundances and isotopic compositions in back arc volcanic systems to evaluate the feasibility of using noble gases to study the fate of other important volatile species during the subduction process. In the initial phase of this study we measured noble gas isotopes and abundances in olivine separates from ash samples associated with recent explosive basaltic eruptions in the back arc volcanic systems of Nicaragua. Air-like isotopic compositions combined with Xe/Ar ratios varying from $\sim 2.5 - 11.7$ times air suggest that a significant amount of gas associated with sediments is carried deep into subduction zones.

(4) We have measured Sr-Nd-Pb-He-Ar isotopic values for Mauna Loa (ML) lavas from the Hawaii Scientific Drilling Project (HSDP) Pilot Hole to complete the isotopic coverage of the sampled section. These new data, in combination with those existing for ML and Mauna Kea (MK), provide two

“continuous” ~200 kyr records of the isotopic evolution of Hawaii’s two largest volcanoes. These records allow us to evaluate the structure of the Hawaiian plume.

(5) To compliment our past and ongoing monitoring of gas discharging from Mammoth Mountain, Long Valley Caldera, we have measured helium isotope ratios in olivines from basalts erupted over the last 3.2 million years. Our goal was to better understand the relationship between helium isotopic ratios currently measured in gas being discharged from Mammoth Mountain and those found in the magma systems. We found a spatial pattern in the helium isotopic composition of the different basalt flows. Basalts along the edges of the caldera, ranging in age from 3.2 million years to less than 100,000 years, have relatively uniform helium isotopic ratios (5.8 - 6.2 R_a). Whereas, the westernmost basalts in the area, which are outside the Long Valley caldera, have much lower helium isotope ratios (4.6 - 5.2 R_a). Since the ages of these two groups of basalts overlap, it appears they are derived from two different magmatic systems. During the recent period (1989 to the present) of earthquake activity beneath Mammoth Mountain, the helium isotopic composition in gasses from the summit fumarole increased significantly to 6-7 times air. The similarity between this ratio and those in the caldera-rim basalts indicates that the magmatic system sampled by the discharged gasses at Mammoth Mountain is probably the one responsible for generation of the small-scale basalt flows. The fact that gasses presently being discharged from Mammoth Mountain are associated with recent seismic unrest beneath Mammoth Mountain and have helium ratios similar to the caldera-rim basalts has important implications for volcanic hazard evaluation.

(6) To examine the mechanisms utilized by the lichen *Stereocaulon volcanii* to take up copper from recent Hawaiian basalts, X-ray absorption spectra (XAS) were collected using beamline 10.3.2 at the Advanced Light Source. These analyses showed that the lichens transport the copper as copper oxalate through the inner algal layer. Further, small grains (~<1 μm in diameter) of copper metal with significant cobalt were found in the regions of the lichens containing the highest copper concentrations. This suggests that the lichens are reducing the copper to avoid toxic concentrations of organo-metallic complexes.

(7) A series of experiments were performed to examine the biochemical processes affecting carbon isotopic fractionation caused by bacterial oxidation of methane. Methane-oxidizing bacteria in soils play a key role in the cycling of methane, an important greenhouse gas. Carbon isotope measurements of methane potentially represent a valuable tool for studying this process in nature. However, previously published studies have reported significantly different fractionation effects. The results of our experiments demonstrated that the magnitude of fractionation is a function of the concentration of active organisms. These findings indicate that carbon isotope measurements of methane in soils can be used to track levels of methane-oxidation in the soils.

Isotopic and Chemical Composition of Fault Zone Fluids

B. M. Kennedy (510-486-6451; Fax: 510-486-5496; bmkennedy@lbl.gov) and E. Pili, (Departement Analyse et Surveillance de l'Environnement, F-91680 Bruyeres-le-Chatel, France.)

Objectives: The San Andreas Fault (SAF) is weak in an absolute sense and relative to adjacent plate interiors. Near lithostatic fault zone fluid pressures are thought to play a critical role in fault weakening and the discriminating factor between fluid-pressure based models of fault weakening is the origin of the fault zone fluids. The isotopic and chemical compositions of fluids associated with the SAF system are being measured to identify fluid source and flow rates through the fault system.

Project Description: Explanations for SAF weakness invoke either low friction fault zone materials or super-hydrostatic fluid pressures within the fault zone. However, heat flow and stress orientation data have not been reconciled with laboratory friction coefficient measurements on fault gouge materials, so that elevated fluid pressures are the preferred explanation. Models invoking high fluid pressures are similar but rely on different fluid sources. During the earthquake cycle fault zone fluid pressure increases to near lithostatic values and induces rupture. Dilation accompanies rupture, locally lowering the fault zone fluid pressures and the cycle begins again. Crustal fluids, connate or meteoric, may be drawn into the fault zone in response to fault rupture and become trapped by mineral reactions; the high fluid pressures required to weaken the fault are reestablished by compaction of the sealed fault-zone materials. In this model, the base of the seismogenic zone, defined by the brittle-ductile transition, is treated as an impermeable boundary. In an alternative model, fault-weakening fluid pressures are generated by a high flux of deep crustal or mantle fluids that are continually supplied to the seismogenic zone from the ductile lower crust at super-hydrostatic pressure. To investigate fluid source and influence on SAF dynamics, we conducted a chemical and helium isotopic study of groundwater associated with the SAF and companion faults. We found that the groundwater contained elevated $^3\text{He}/^4\text{He}$ ratios, thus providing evidence for a geopressed mantle fluid source (Kennedy *et al.*, 1997, *Science*, 278, 1278-1281).

It is likely that mantle helium is associated with other more abundant mantle volatiles, certainly CO_2 and perhaps water. However, using estimated mantle $\text{CO}_2/{}^3\text{He}$ ratios, the vertical CO_2 flux inferred from the helium isotopic data is low and appears inadequate, by at least an order of magnitude, to re-establish fault-weakening fluid pressures on the relevant time scale. Apparently, an additional source of fluid (water, CO_2 , *etc.*) is required. Also, it is not clear if the springs and wells sampled in this study tapped fluids directly from a fault zone or from the adjacent crust. If the fluids are directly from the fault zone, then the observation that mantle helium is mixed with fluids from the adjacent crust, as indicated by dissolved solids and water isotopes, implies that elements of both models are important. Since weakness is generated by high fluid pressures in the fault zone relative to surrounding crust, infiltration of crustal fluids into the fault zone requires episodic reversals of the fluid pressure gradient.

To address these two issues, we initiated a program to sample and analyze rocks and minerals associated with the fault zones and surrounding country rocks. These samples will be analyzed for noble gases and the isotopes of Sr, Nd, Pb, C, and O.

Results: During FY199, we continued our analyses of the rocks and minerals collected from the deformation zones, vein fillings, and hosts along the SAF and companion fault systems. Fluid inclusion helium isotopic compositions from the various fault zone samples vary from ~0.1 - 2.5 Ra (Ra is the $^3\text{He}/^4\text{He}$ ratio in air), indicating that past fluids percolating through the SAF system contained mantle helium contributions of ~1 to ~32%, similar to that measured in present-day groundwater. This confirms the involvement of mantle fluids and shows from structural relationships observed in the field and in thin sections that these fluids are directly associated with the process of faulting.

Calcite is the dominant vein material and repeatedly occurs as an accessory mineral in deformation zones. At each sampling site, several trends in the relative depletion of ^{13}C - and ^{18}O isotopes are observed. (1) The deformation zone and vein material are the most depleted compared to their host rocks. (2) Veins that cut through deformation zones are even more isotopically depleted. (3) With increasing distance from what can be structurally defined as the core of fault zones, host rocks are less isotopically affected and the density of veins and deformation zones decreases. (4) Host-rock carbonates display progressive evolution towards greater depletion in the order limestone, marble, gneiss, granite and basalt, mirroring the increase in metamorphic grade or deep crustal origin of the host-rocks.

We infer from these trends and the isotopic compositions that (1) the fault zones have been infiltrated by fluids of deeper origin during deformation and (2) the fluids are dominated by crustal or connate water \pm CO₂. Meteoric water does not appear to represent a significant contribution and the CO₂ is inferred to have a metamorphic or mantle origin.

Clay Mineral Surface Geochemistry

Garrison Sposito (510-643-8297; Fax: 510-643-2940; gsposito@lbl.gov)

Objectives: The objectives of this project are to determine the mobility and surface speciation of Cs⁺ counterions, as well as interlayer water structure, for 12.4 Å Cs-smectite hydrates using Monte Carlo and molecular dynamics simulations.

Project Description: Smectites are clay minerals with expandable interlayers and substantial cation exchange capacities. Molecular modeling techniques can provide an understanding of the hydrated Cs-smectite interlayer necessary to predicting the permeability of clay liners to radiocesium cations at nuclear waste containment facilities.

Monte Carlo (MC) simulations were used to determine the configuration of Cs⁺ and water molecules present in stable Cs-smectites with 12.4 Å layer spacings. The program MONTE, written by Neal Skipper and Keith Refson and compiled on Cray J90s at the National Energy Research Scientific Computing Center (NERSC), was used. The smectites examined include octahedrally charged hectorite, tetrahedrally charged beidellite, and montmorillonite, which has both tetrahedral and octahedral charge sites. Molecular dynamics (MD) simulations based on MC-equilibrated Cs-smectites revealed the diffusion of Cs⁺ and water molecules over 800 ps. The code MOLDY, written by Keith Refson and compiled on the Cray T3E at NERSC, was used. Coordinate data from MD runs have been animated using RM SceneGraph in order to visualize molecular interactions. Further information may be found at <http://esd.lbl.gov/sposito/>.

Results: Monte Carlo calculations provided radial distribution function and coordination number data that revealed both the ability of Cs⁺ to organize water into a partial hydration shell, as well as the highly distorted nature of interlayer water structure as compared to bulk water.

Comparison of MD trajectories revealed the effect of clay charge site on Cs⁺ mobility. The recessed charges of hectorite held Cs⁺ in fixed locations at the midplane of the interlayer, whereas the near-surface tetrahedral charges within beidellite drew cations to fixed positions closer to the clay layers. When both charge sites were present, as in montmorillonite, the Cs⁺ became somewhat more mobile. All Cs⁺ were in inner-sphere surface complexes and moved through jump diffusion, except in Cs-montmorillonite with 2/3 water monolayer. This system featured four cations tightly bound to two tetrahedral charge sites, while two remaining Cs⁺ exhibited diffusional motion. Water molecules diffused at rates a fraction of those in bulk water.

The results confirmed the findings of experiments, which predict low mobility of Cs⁺ in smectites. Such agreement indicates the potential functions used may be reasonably accurate, and provides further evidence supporting the use of smectite clay liners within nuclear waste containment facilities in order to retard the movement of radiocesium.

Molecular-level studies of Fe-Al oxyhydroxide coating formation on quartz

G. A. Waychunas (510-495-2224; Fax: 510-486-7152; GAWaychunas@lbl.gov) with J. A. Davis, and R. Reitmeyer (both at USGS Menlo Park, CA)

Objectives: Determination of the molecular structure of initial sorbed and precipitated Fe-Al oxyhydroxides on quartz surfaces; Comparison of perfect surface reactivity with degraded perfect surfaces and with perfect surfaces exposed to natural conditions; Characterization of the effects of undersaturation on precipitate formation; Exploration of coating sorption properties to specific toxic metals and organic species.

Project Description: Fe oxyhydroxides are potent scavengers of toxic oxyanions (arsenite, selenite, chromate) over a large pH range, and can also incorporate or sorb toxic metal cations under appropriate conditions. Recent work has shown that coatings of these materials, down to nanometer thicknesses, can be ubiquitous even in the cleanest sediments, effectively creating a large surface area sorbant that dominates mineral-water interface reactivity. This project combines three efforts to understand the nature, formation and alteration of these coatings in aquifer sediments: 1) laboratory sample preparation and characterization including both perfect single crystal surfaces and high surface area silica (Aerosil). 2) emplacement of perfect single crystal surfaces into sampling wells at two aquifers where the sediments, conditions and chemistry is well described. These samples are withdrawn periodically to reveal coating formation and quartz surface degradation. 3) Characterization of coatings on natural quartz grains from these aquifers and elsewhere representing a range of formation environments. Characterization methods include synchrotron-based x-ray absorption spectroscopy in grazing incidence mode (GIXAS), transmission electron microscopy (TEM) and atomic force microscopy (AFM).

Results: Observations of initial precipitates on high surface area Aerosil and on quartz r- and m-plane surfaces shows a strong dependence on Fe^{3+} solution concentration and on dehydration. At low pH values that suppress oxyhydroxide polymerization in solution, individual inner sphere Fe^{3+} surface complexes dominate sorption only at coverages below 2% of a monolayer of surface silanol groups. With increased coverage Fe oxyhydroxyl polymers form. These have hematite-like structure for r- and m-plane quartz surfaces with strong texturing such that the hematite (0001) axis is along the surface plane normal. No definite epitaxial relationship is observed.

Drying and aging promotes polymerization (clustering and precipitation) in samples initially having only sorbed isolated complexes. This could explain how very low aqueous Fe^{3+} concentrations can lead to Fe^{3+} coating formation during drying of sediments. AFM images of clean m-plane surfaces show uniform terrace and step structure with step height of 2.6 Å, and terrace width of several thousand Å. The step edge is found to be the preferred position for precipitation development and may catalyze polymerization.

Work on the earliest samples from wells at the Cape Cod site show development of both calcite and Fe oxyhydroxide coatings, but not sufficient Fe to yield detailed structural information.

CATEGORY: Hydrogeology

Person in Charge: S. Benson

Geochemical and Isotopic Constraints on Processes in Oil Hydrogeology

B. M. Kennedy (510-486-6451; Fax: 510-486-5496; bmkennedy@lbl.gov) and T. Torgersen (University of Connecticut)

Objectives: This research project evaluates the processes which produce, dissolve and distribute noble gases and noble gas isotopes among liquid hydrocarbon, gaseous hydrocarbon and aqueous phases. This project also uses the abundances and isotopic composition of noble gases in hydrocarbon systems to evaluate hydrocarbon sources and characteristics, groundwater end-members, and migration processes, mechanisms, and time scales.

Project Description: The mechanisms, processes and time scales of fluid flow in sedimentary basins represent fundamental questions in the Earth Sciences with direct application to exploration and exploitation strategies for energy and mineral resources. This project investigates the noble gas composition of hydrocarbon samples on a basin and field scale where adequate commercial production and ancillary information are available, to provide a test of the use and applicability of noble gases to delineate end members, migration mechanism and migration paths for hydrocarbons. Samples are analyzed for the five stable noble gases (He, Ne, Ar, Kr, Xe) and their isotopes.

Results: Negotiations with various oil companies for the provision of samples in the North Sea and the Gulf of Mexico have been completed. Samples are in hand and undergoing analysis. A post doc has been added to the research team.

The solubility of noble gases in hydrocarbons and water dictate that a source area noble gas signature will be mixed with and diluted by noble gases stripped from groundwater during secondary migration. The degree of dilution is a function of the integrated water/hydrocarbon volume ratio. Plots of relative noble gas abundances ($F[Ng]$) and isotopic compositions as a function of the inverse ^{36}Ar concentration generate mixing lines reflecting the varying degrees of dilution and thus can identify the noble gas characteristics of the source area (high values of $1/^{36}Ar$) and the groundwater (the intercept at $1/^{36}Ar=0$). Noble gas data from the Alberta gas fields (Hiyagon and Kennedy, 1992) provides a proof of concept and identifies four distinct mixing lines. The spatial distribution of samples defining each dilution line is suggestive of migration flow paths, as indicated by the progression from high to low values of $1/^{36}Ar$, and are consistent with the migration flow paths of Garven (1989) and Hitchon (1984) that were identified using hydrologic arguments.

The secondary migration of Alberta hydrocarbons occurred in groundwaters with noble gas compositions consistent with air-saturated water at 10-25 °C. The source areas (distinct from source rock) for Groups B1 and B2 are characterized by very large enrichments of radiogenic 4He and ^{40}Ar , nucleogenic ^{21}Ne , and fissionogenic ^{136}Xe that is unlikely to have been derived solely from the source rock. These large excesses suggest that Tertiary orogeny preceding secondary migration degassed large volumes of older crust into the defined source areas. The noble gas characteristics of the source areas for Groups A1 and A2 indicate an enrichment in 3He . $1/^{36}Ar$ -defined flow paths trace this 3He enrichment to the only volcanic formation in Alberta, the regionally restricted Cretaceous Crow's Nest Formation. The sequence of restricted Cretaceous volcanism 'staining' the Group A source area with mantle 3He , degassing of large source area crustal volumes by Tertiary orogeny, followed by

hydrocarbon maturation and migration is defined by the mixing line analysis. Noble gas mixing line analysis thus provides a fundamental constraint on models of hydrocarbon migration and emplacement.

Reactive Chemical Transport in Structured Porous Media: X-ray Microprobe and Micro-XANES Studies

T.K. Tokunaga (510-486-7176; Fax: 510-486-7797; tktokunaga@lbl.gov)

Objectives: In subsurface reactive transport, large differences in chemical composition can be sustained in boundary regions such as sediment-water interfaces, interior regions of soil aggregates, and surfaces of fractured rocks. Studies of reactive transport in such boundary zones require information on chemical speciation with appropriate spatial and temporal resolution.

Project Description: Predicting transport of trace elements between various environmental compartments is currently often unsuccessful, partly due to lack of relevant information at compartment boundaries. Batch studies can yield insights into kinetics and equilibrium in well-mixed systems, but much of the subsurface is very poorly mixed. Without in-situ, spatially- and temporally-resolved chemical information, transport between compartments can only be described with system-specific, nonmechanistic, mass transfer models. In this project, the synchrotron x-ray microprobe and micro-XANES techniques are used to obtain such measurements in a variety of critical microenvironments. Past efforts in this project focused on selenium transport and reduction in two types of microenvironments, that found at surface water-sediment boundaries, and that found within soil aggregates. In FY 1998, the project emphasis shifted to consider reactive transport of Cr included flow-through experiments in columns of aggregated soils, including spatially resolved, real-time tracking of initial contamination processes within soil aggregates, and later characterization of Cr redistribution upon long-term drying. The complexity of reactive transport in such systems with macropore flow and intraaggregate diffusion-redox motivated simpler FY 1999 studies focused only on the latter processes.

Results: The FY 1999 studies focused on Cr(VI) diffusion and reduction to Cr(III) within soil aggregates. Experiments were designed to quantify characteristic Cr(VI) diffusion distances, reduction rates, and their dependence on intraaggregate redox conditions. Experiments were conducted on synthetic soil aggregates formed from a homogenized alkaline (pH 8.5) clay soil. The alkalinity of this soil minimized the extent of Cr(VI) sorption on mineral surfaces. A range of initial redox conditions was established within aggregates by infusing solutions containing different concentrations of organic carbon (0 to 800 ppm, as tryptic soy broth). Redox potentials were measured through arrays of microelectrodes embedded within aggregates. Cr(VI) was diffused into the aggregate microcosms at boundary concentrations ranging from 260 to 5200 ppm. Upon exposure to Cr(VI), redox potential profiles were disturbed only within the near-surface (0 to 4 mm depth interval) of the aggregates. Micro-XANES mapping was done at GSECARS beamline 13ID-C, Advanced Photon Source. Preliminary tests showed that artifacts from x-ray beam induced Cr(VI) reduction to Cr(III) could be problematic. This effect was minimized to < 5% through defocusing and short (< 30 s) exposures. Micro-XANES mapping of Cr in aggregates showed (1) deeper Cr diffusion in systems with lower organic carbon, (2) reduction of Cr(VI) to Cr(III) during transport, and (3) very sharp termination of Cr fronts in more reducing aggregates. The latter phenomenon results from rapidly increasing reduction rates over very short distances (< 10 mm). The steep concentration gradients for Cr(VI) and Cr(III) measured directly within aggregates via micro-XANES spectroscopy permit quantification of Cr reduction during diffusion.

Unsaturated Fast Flow in Fractured Rock: Testing Film Flow and Aperture Influences

T.K. Tokunaga (510-486-7176; Fax: 510-486-7797; tktokunaga@lbl.gov)

Objectives: The nature of unsaturated fast-flow in fractured rocks needs to be understood in order to obtain reasonable constraints on vadose zone transport. Water films along unsaturated fractures have recently been shown to be capable of supporting fast flow and transport, and revealed limitations of existing aperture-based models. In this project, theoretical considerations and experiments are combined to improve our understanding of unsaturated flow in fractured rocks.

Project Description: Recently, the concept of film flow was introduced as a possible process by which preferential flow could occur along truly unsaturated fractured rock. Our work concerns water films on fracture surfaces under near-zero (negative) matric potentials, and examines the possibility of fast, unsaturated flow under "tension". "Films" in this context are a complex network of thick pendular regions that form within topographic depressions and thin films on topographic ridges. Thus, the thickness and connectivity of pendular film regions is expected to be important in controlling film flow on individual fracture surfaces. We showed that at matric potentials greater than that needed to saturate the rock matrix, transmissive water films can develop on fracture surfaces. The matric potential dependence of the average film thickness and film transmissivity of a Bishop Tuff fracture surface were measured using equilibrium and steady-state methods, respectively. The water "films" investigated in the previous study as well as the present one develop on rough surfaces, range in average thickness from about 1 to 50 μm , and flow in the laminar regime. In the FY 1999 work, general conditions necessary for stable film flow were identified.

Results: Flow through unsaturated fractured rock occurs via a number of processes, including film flow. Approximate ranges of conditions necessary for the presence of thick water films along unsaturated fracture surfaces were investigated through considering rock matrix and fracture aperture saturation criteria. Stable thick films exist when the matric potential is high enough to effectively saturate the immediately underlying rock matrix, yet low enough not to saturate the fracture aperture. The lower energy limit for stable thick films was estimated through correlations between air-entry matric potentials and matrix permeabilities. The upper matric potential limit was estimated from the Laplace-Young predicted inverse fracture aperture dependence of capillary filling. With these two limiting relations, the domain for stable thick films was identified in the parameter space defined by matrix permeability, fracture aperture, and matric potential. These results show that thick films are stable over a moderate range of matric potentials when the rock matrix permeability is less than about 10^{-14} m^2 and the fracture aperture is greater than about 30 μm . Such combinations of permeabilities and apertures are common in fractured rock vadose zones. Thus, thick water films can form in these environments within the matric potential ranges identified here. It is important to keep in mind that near-zero matric potentials are necessary for the possible development of fast film flow.

Colloid Transport in Unsaturated Porous Media and Rock Fractures

J. Wan (510-486-6004; Fax: 510-495-7797; jwan@lbl.gov)

Objectives: The objective of this project is to improve the mechanistic understanding on colloid transport in unsaturated porous media. Because the classic filtration theory for predicting colloid

transport cannot be directly used for transport in unsaturated media, this research is designed to develop a comprehensive understanding and model for colloid transport through vadose environments.

Project Description: Wan and Tokunaga (1997, *Environ Sci. Technol.*) identified the mechanism of “film straining”, which hinders colloid mobility under unsaturated conditions. The premise of this hypothesis is that the gas-water interface can physically constrain colloid movement through regions of thin flowing liquid films that characterize fluid transport under unsaturated conditions. The effect of film straining on colloid removal was assumed to depend on the ratio of particle size and film thickness and on pore water velocity. Their model predicts that particle transport is inhibited if colloid size is larger than film thickness, while colloids smaller than film thickness are transported, even at saturations lower than the critical value. However, the mechanistic understanding of the effect of the characteristics of films, particles, and medium surfaces on particle motion is still lacking. The relative importance of forces in either facilitating (such as fluid drag and torque) or retarding (friction and surface tension), the motion of particles in flowing liquid films has not been previously investigated. To address some of these issues, this study was undertaken to investigate the effect of particle size/film thickness ratio on the motion of a spherical particle in a flowing liquid film.

Results: The effect of particle-size-to-film-thickness-ratio on the motion of spherical particles in a stable liquid film flowing down an inclined flat surface was studied experimentally. Previously reported models that are based on force and torque balance were modified to predict motion of particles that are smaller than film thickness. At low values of the ratio, particle velocity is observed to increase nearly linearly with particle size, reflecting the increasing influence of hydrodynamic drag as larger particles expose their surface to regions of higher fluid velocity. Good agreement between model predictions and experimental results is observed for small ratios. When the ratio is in the range of ~ 0.7 to 1, particle velocities are observed to decrease rapidly with an increase in size. This may be attributed to the effect of the proximity of the free interface to the particle surface and the deformation of the free surface induced by the moving particle. When the ratio is in the approximate range of 1 to 1.75, particles ceased to move, due to the surface tension acting on the particle along the circumference of the contact radius of the three-phase interface. For particles significantly larger than film thickness (ratio greater than about 1.7), the particle velocity is observed to increase with its size, as the particle motion is aided by the increased contribution from the gravitational force. For the range of film thicknesses and particle sizes studied, there appears to be a range over which gravity force begins to dominate over surface tension force.

CONTRACTOR: Lawrence Livermore National Laboratory

University of California
Livermore, California 94550

CONTRACT: W-6405-ENG-48

CATEGORY: Geophysics and Earth Dynamics

PERSON IN CHARGE: F. J. Ryerson

Pore Scale Simulations of Rock Deformation, Fracture and Fluid Flow in Three Dimensions

S. C. Blair (925-422-6467; Fax: 925-423-1057; blair5@llnl.gov) with A. L. Ladd (Univ. of Florida), and H. F Wang (Univ. of Wisconsin)

Objectives: The objective of this research is to provide new fundamental understanding of the coupling of rock deformation and fracture behavior at the grain scale to macroscopic rock properties and to and fluid flow.

Project Description: This project is concerned with simulation of rock deformation and fracture at grain and larger scales. This project builds on an earlier OBES project in which a 2-dimensional field-theory model for rock fracture was developed and then used to determine how heterogeneity in different microscale parameters affects rock behavior in compression, and how macroscopic stress strain behavior is related to the formation of cracks. More recently, we have extended our work to include simulation of much larger rock masses and deformation in 3-dimensions. An accelerated 2-dimensional simulator has been implemented using fast multipole methods (FMM) to perform the necessary calculations in optimal time and with reduced memory usage. This approach permits much larger problems to be solved. In particular, it is now possible to study the dependence of sample strength on sample size over several orders of magnitude in scale-up. In addition, the FMM can be “tuned” to give the desired trade-off between efficiency and accuracy.

Results: We have performed preliminary simulations of Brazilian tests to investigate the influence of scale upon strength. Although many applications involve large rock masses, it is usually only practical to test small samples, and experimentally it is observed that compressive strength decreases as sample size increases. Numerical simulations can complement laboratory results by providing a means to relate field scale properties to laboratory scale measurements. Preliminary simulations of Brazilian tests show that as expected, increased sample size resulted in decreased strength. Moreover, we found that increasing the heterogeneity of grain strength and shape led to decreased sample strength. Our results also indicate that larger perturbations of grain strength and shape induce a faster drop in strength with increasing size.

We plan to use this computational tool to consider more realistic distributions of microscale heterogeneity. In particular, failure in rock with spatially correlation of grain strength and shape will be considered.

Three-dimensional Analysis of Seismic Signatures and Characterizations of Fluids and Fractures in Anisotropic Formations

P. A. Berge (925-423-4829; Fax: 925-423-1057; berge1@llnl.gov), J. G. Berryman (925-423-2905; Fax: 925-422-1002; berryman1@llnl.gov)

Objectives: Our major objective is to obtain constraints on lithology in fluid-filled anisotropic rocks by using rock physics theories for anisotropic and poroelastic media. We are collaborating with investigators on related OBES projects at the Colorado School of Mines and Stanford University, who are developing techniques for obtaining anisotropy parameters from seismic reflection data (CSM) and relating laboratory measurement information to modeling and field data (Stanford). By using our theoretical methods to model the anisotropy parameters recovered from seismic data, we can find ways to improve analysis of seismic reflection data collected in areas where the geology is complicated by anisotropy and heterogeneity.

Project Description: CSM collaborators are generalizing anisotropic velocity analysis techniques to account properly for vertical inhomogeneity and dipping structure, so that the technique will be applicable to a wide range of exploration problems. The LLNL/Stanford group is working on developing and analyzing rock physics models that describe transversely isotropic media, particularly to determine how these models may constrain lithology. Stanford is focusing more on laboratory measurements and anisotropic signatures of fractured rocks, and LLNL is focusing on fluid effects and poroelasticity in anisotropic rocks. Topics of research include determining what constraints on lithology can be found from the anisotropy and poroelasticity parameters and what information is sufficient and necessary for the constraints. The overlying questions are how to do lithologic interpretation of the anisotropic parameters obtained from field data, and the possibility of incorporating shear-wave data into the velocity analysis and lithology interpretation.

Results: (Stanford and CSM results are described elsewhere.) LLNL researchers have shown how poroelastic parameters in rocks may differ from values generally assumed in oil industry models. These results were presented at the 1998 Biot Conference on Poroelasticity and were submitted to *Geophysics*. LLNL researchers have also developed a new method for using P and S velocities to obtain information about rock saturation. This work was presented at the 1999 annual meeting of the Society of Exploration Geophysicists and a Stanford workshop, and was submitted to the *Journal of the Acoustical Society of America* and to *Geophysics*. Results for relating fluid distribution in partially saturated anisotropic rocks to measured seismic parameters and effects of fluids on anisotropy parameters were submitted for presentation at an OBES symposium. A paper on anisotropy parameters and lithology in layered media was published in *Geophysical Prospecting*.

Visco-, Thermo-, and Poroelasticity of Rocks and Rock/Fluid Mixtures

J. G. Berryman (925-423-2905; Fax: 925-423-6907; berryman1@llnl.gov)

Objectives: Our main objective is to understand factors affecting physical properties of rocks in order to improve our ability to predict rock behavior from knowledge of rock components. One new tool developed to accomplish this objective is the recent discovery of exact results in poroelasticity and thermoelasticity for two component composite rocks and the application of these ideas to effective medium theories for poroelastic composites. This project exploits these as well as other new results, with the expectation that new insight into the poro-, thermo-, and viscoelasticity of rocks will result. Such insight should prove important for understanding partial melt in both the upper and lower mantle,

for clarifying earthquake source mechanisms, for interpreting seismic reflection survey data for oil and gas exploration, for oil field engineering practices related to drilling and pumping, and for related issues in environmental cleanup of DOE sites. This type of information is important for interpretation of both seismic and electrical geophysical field data.

Project Description: Four major approaches are being considered in this project:

- development and application of viscoelastic property bounds to rock/fluid mixtures;
- volume averaging methods for rock/fluid mixtures;
- double-porosity/dual-permeability methods for fractured reservoirs;
- development and use of a new generalization of Eshelby's formula from elasticity theory for poroelastic and thermoelastic composite inclusions analysis problems.

These types of results are all of interest in the oil and gas industry. The same basic framework can also be employed to treat reservoir characterization problems, especially regarding the effects of changing stress on matrix and fracture permeability in double-porosity models used for reservoir pumpdown studies. In addition to single-fluid reservoir analysis, related ideas have been applied to partial saturation problems, in which both gas and oil, or gas and water may be present and distributed throughout the reservoir volume in a complicated, inhomogeneous manner. Related ideas (Gassmann's fluid-substitution formulas) can play a very significant role in interpretation of seismic AVO (amplitude *versus* offset) data used as direct hydrocarbon indicators.

Results: The most exciting new work this year is in the area of partial saturation analysis. This work builds on previously funded BES work in anisotropy, wherein it was determined that the most important variable determining Thomsen's parameters in anisotropy analysis is, surprisingly, Lamé's elasticity parameter known as lambda. For rocks containing fluids, we have shown that this is also the parameter that depends most sensitively on the pore fluid's physical properties. Thus, plots of seismic velocity (both compressional and shear are required) emphasizing changes in lambda have the power not only to determine the magnitude of the liquid saturation present, but also (and this was also a big surprise to all of us) to distinguish homogeneous from inhomogeneous (patchy) saturation. Papers on this topic have been submitted to *Journal of the Acoustical Society of America* and to *Geophysics*. Our most recent work in this area shows that seismic impedance (density times velocity) data that are typically obtained in seismic reflection surveys can also be used to accomplish the same results. This fact has significant implications for improvements to seismic AVO analysis. We also discovered this year that it was possible to use Gassmann's equations to study seismic velocity decrements due to partial melt in the lower mantle. The new approach we developed takes advantage of the fact that Gassmann's equations do not depend explicitly on the microstructure of the porous Earth, but only on the fact that the pores are connected and the pertinent time scales long. A preliminary version of this work was published in *Geophysical Research Letters*. In collaboration with researchers at the University of Wisconsin, we had previously developed methods to determine and in some cases drastically reduce the number of elastic coefficients required to describe the behavior of a double-porosity system in the presence of changing pore pressure for applications to reservoir pumpdown. This work was published in the *Journal of Geophysical Research*. Subsequent work in this area has been done on elastic wave propagation through such media, leading to equations that permit the parameters that determine wave speed and attenuation to be decoupled in a significant new way. This work is scheduled to appear in *International Journal of Rock Mechanics*, and extensions of the work continue through studies of methods to estimate coefficients in these equations that can be computed from knowledge of the constituents and their

physical properties. This last mentioned work is in collaboration with Professor Steven Pride from France and will be submitted for publication sometime during the summer of 2000.

Reactive Solute Transport and Processes of Dissolution and Deposition in Single Fractures in Rock

William. B. Durham (925-422-7046; Fax: 925-423-1057; durham1@llnl.gov), B. P. Bonner, W. L. Bourcier, and A. Tompson

Objective: The objective of this research is to measure local rates of dissolution and precipitation on the walls of individual fractures and correlate differences in reaction rates to changes local fracture aperture. Much use will be made of high-resolution physical topography measurement and numerical simulation of reactive flow.

Project Description: The experiments and simulations will be done on rock samples containing a single laboratory-made or natural fracture. Detailed imaging of the fracture aperture before and after alteration will be coordinated with measurements of fracture deformation, permeability, dispersivity, and effluent composition, all as functions of pressure, temperature, temperature gradient, time, rock composition, fluid velocity, and fluid composition. For the most part we will work with simple but relevant systems in order to maximize our understanding and impact: samples will be monomineralic rocks with low porosity and low bulk permeability (such as quartzites and marbles), under fully saturated, single-phase flow conditions. We will attempt measurements in undersaturated, dual-porosity, and more chemically complex settings as success dictates.

Results: We have completed several series of dissolution experiments on single fractures in two cores of Carrara marble, have completed detailed topographic maps of all fracture surfaces before and after each dissolution experiment, and have thoroughly analyzed the data. The results are quite surprising and could significantly affect models reactive flow models currently in use. In summary, what the results seem to indicate is that the “stability” of dissolution, *i.e.*, the tendency for a dissolution front to smooth out perturbations (stable) or to amplify perturbations (unstable) is scale-dependent. This in itself is not unexpected, but in this experiment, we seem to have located the point of transformation from stable to unstable dissolution, which in turn will allow rather precise tuning of reactive flow models set up to simulate our experimental conditions. We found that at a scale of a few mm and below, dissolution is a stable process: roughness and tortuosity in the fluid flow patterns (“channeling”) tend to become smoother under the influence of dissolution. At the sample scale of many cm, dissolution is unstable: flow becomes increasingly concentrated in a single, broad flow channel as dissolution proceeds. The results have been written up in a preliminary draft, and further experiments are ongoing.

The Role of Carbon and Temperature in Determining Electrical Conductivity of Basins, Crust, and Mantle.

A. G. Duba, LLNL (925-422-7306; Fax: 925-423-1057;) with T. J. Shankland, (LANL; 505-667-4907; Fax: 505-667-8487; shankland@lanl.gov); and E. A. Mathez (American Museum of Natural History; 212-769-5379; Fax: 212-769-5339;)

Objectives: The intent of this work is to comprehend the electrical conduction mechanisms in carbon-bearing rocks and in mantle minerals for the purpose of relating electrical conductivity (σ) measured in the field to formation conditions and existing state of crustal rocks and to temperatures in the mantle.

Project Description: Electrical conductivity depends strongly on temperature T and on the presence of other phases such carbon, fluids, or ore minerals at the lower temperatures of the crust and basins. Thus, one research approach is to measure σ of mantle minerals as functions of temperature, orientation, oxygen fugacity fO_2 , and iron content. These data supply the best models for "electrogeotherms" yet available. Another approach is to document textures of carbon in crustal rocks from basins and metamorphic zones and relate them to rock conductivity. In this case texture of carbon distribution is mapped with electron microscopy in the same samples used for conductivity measurement. The approach here is to measure electrical conductivity of the mantle's most volumetrically important mineral phases under conditions appropriate to the entire mantle and to use these observations in an a priori calculation of mantle conductivity.

Results: Recent laboratory measurements of electrical conductivity of mantle minerals are used in forward calculations for mantle conditions of temperature and pressure for the entire depth of the mantle beginning at 200 km and extending to the base at ~ 2800 km. The electrical conductivity of the Earth's mantle is influenced by many factors, which include temperature, pressure, the coexistence of multiple mineral phases, and oxygen fugacity. In order to treat these factors and to estimate the resulting uncertainties, we have used several spatial averaging schemes for mixtures of the mantle minerals and have incorporated effects of oxygen fugacity. In addition, to better calculate lower mantle conductivities we report new measurements for electrical conductivity of magnesiowüstite ($Mg_{0.89}Fe_{0.11}O$). The effective medium theory averages lie between the Hashin-Shtrikman bounds (theoretical limits on calculated maximum and minimum conductivities) in the whole mantle. A laboratory-based conductivity-depth profile was constructed using the effective medium theory average. Comparison of apparent resistivities calculated from the laboratory-based conductivity profile with those from field geophysical models shows that the two approaches agree well. The results apply to our understanding of mantle dynamics, plate tectonics, and the distribution of heat sources beneath the crust.

Water distribution in partially saturated porous materials

J. J. Roberts (925-422-7108, Fax: 925-423-1057, roberts17@llnl.gov)

Objective: To determine the distribution of water in partially saturated porous materials by measuring the complex electrical properties and to investigate the relationships between electrical transport and other transport properties in materials with well-characterized microstructures.

Project Description: The purpose of this project is to measure the frequency dependent electrical properties of porous materials and relate the results to other transport properties and to improve the interpretation of field EM measurements through better understanding of physical properties of partially

saturated porous media. Measurements include dielectric constant and electrical resistivity as functions of saturation, temperature and microstructural properties. The complex impedance is measured because impedance spectra provide information regarding the number and arrangement of conduction mechanisms, distribution of liquid phase, and microstructural properties. The fluids used to saturate the samples have a range of ionic composition, and hence, electrical conductivity. This permits the comparison of impedance spectra of samples at similar saturations to better understand the relationship between fluid distribution and the corresponding conduction mechanisms. These measurements are of particular importance because field electrical measurements in unsaturated regions (including electrical resistance tomography, electromagnetic depth sounding, and induced polarization) depend on reliable laboratory measurements for accurate interpretation. A number of geophysical problems including remediation, enhanced oil recovery, geothermal reservoir evaluation and site monitoring depend on reliable information regarding the interconnectedness and distribution of the fluid phase.

Results: Laboratory impedance measurements on natural sandstones continued, with results being compared to previous measurements on fused glass bead samples. Results were presented at the 14th. Workshop on Electromagnetic Induction in the Earth, Int. Union Geodesy Geophys., held in Sinaia, Romania, 1998. Analysis of a previous dataset on olivine-basalt partial-melts, an analog for low porosity, tight rocks led to a publication in *J. Geophys. Res.* A main result of that paper was the estimate of permeabilities based on electrical measurements with varying degrees of melt fraction (porosity) using the Katz-Thompson relationship.

Collaborations with LBL investigators continued to be fruitful, with two presentations and proceedings papers at the 14th. Workshop on Electromagnetic Induction in the Earth, Int. Union Geodesy and Geophysics. in Sinaia, Romania, and the SEG.

An experimental device was constructed that permits the measurement of electrical properties and permeability on samples at temperatures up to 300°C, confining pressures up to 500 bars, pore pressures up to 250 bars. Initial results on electrical properties during boiling in porous media drew interest from the Geothermal Energy Program, the Yucca Mountain Project, and Fossil Energy.

CATEGORY: Geochemistry

PERSON IN CHARGE: F. J. Ryerson

An Experimental Investigation of Mechanisms Controlling Glass Dissolution

S. A. Carroll (925 423-5694; Fax: 925-422-0208, carroll6@llnl.gov) and W. L. Bourcier (925-423-3745; Fax: 925-422-0208; billb@llnl.gov)

Objectives: The objective of this project is to identify the underlying molecular mechanisms responsible for dissolution of glass and to utilize this understanding in the development of quantitative models for predicting glass dissolution rates in nature.

Project Description: This project uses a combination of conventional glass dissolution experiments and NMR to characterize the solution interface to determine the mechanisms controlling glass dissolution. The dissolution behavior of simple SiO₂ glass was used to develop a mechanistic model based on three principal observations: (1) the pH dependence of dissolution rates (2) the saturation effect and (3) the

effect of absorbed alkali cations on dissolution rates. The results are relevant to a number of problems including the stability of radioactive waste glasses, weathering of volcanic glasses, and obsidian hydration age dating, among others.

Results: We have combined traditional batch and flow-through dissolution experiments, multinuclear nuclear magnetic resonance (NMR) spectroscopy, and surface complexation modeling to re-evaluate amorphous silica reactivity as a function of solution pH and reaction affinity in NaCl and CsCl solutions. All of our NMR data suggest that changes in surface speciation are driven by solution pH and to a lesser extent alkali concentrations, and not by reaction time or saturation state. The ^{29}Si cross-polarization NMR results show that silanol surface complexes decrease with increasing pH. The pH dependence of the alkali surface complexes is opposite to that of the silanol complexes ($>\text{SiOH}$). The ^{23}Na and ^{133}Cs NMR results show that the alkali cations form outersphere surface complexes and that the concentration of these complexes increases with increasing pH.

We describe the silica–water surface chemistry using the triple-layer model using a combination of spectroscopic and solution analyses to determine the deprotonation constant ($\log K_{>\text{SiO}^-} = -2.5 \pm 0.5$) the exchange constants ($\log K_{>\text{SiO}^- \text{Cs}^+} = -7.5 \pm 0.4$, $\log K_{>\text{SiO}^- \text{Na}^+} = -6.6 \pm 0.4$), and the capacitance constants ($C_1 = C_2 = 6 \text{ Fm}^{-2}$). Constants derived from solution analyses alone do not fit our experimental data. The dissolution behavior of silica glass as a function of solution pH and sodium concentrations can be described as an exponential function of the concentration of ionized surface complexes ($X_{>\text{SiO}^- \frac{1}{2} >\text{SiO}^- \text{Na}^+}$) at 22°C as $\log(\text{Rate}) (\text{mol m}^{-2} \text{ s}^{-1}) = -10.9 + 2.09 X_{>\text{SiO}^- \frac{1}{2} >\text{SiO}^- \text{Na}^+}$, and at 70°C as $\log(\text{Rate}) (\text{mol m}^{-2} \text{ s}^{-1}) = -10.4 + 2.91 X_{>\text{SiO}^- \frac{1}{2} >\text{SiO}^- \text{Na}^+}$. Changes in surface chemistry cannot explain decreases in dissolution as amorphous silica saturation is approached. We find no evidence for repolymerization of the silanol surface complexes to less reactive siloxane complexes at pH 4 and 10 at longer reaction times.

Mineral Dissolution and Precipitation Kinetics: A Combined Atomic-Scale and Macro-Scale Investigation

K. G. Knauss (925-422-1372; Fax: 925-422-0208; knauss@llnl.gov), C. M. Eggleston (307-766-6769; Fax: 307-766-6679; carrick@uwyo.edu) and S. R. Higgins (307-766-3318; Fax: 307-766-6679; shiggins@uwyo.edu)

Objectives: Our objectives are to build and test an atomic force microscope (AFM) capable of operation at up to 150°C and 10 atm pressure, to apply this AFM to direct, in-situ, and real-time observation of step dynamics during dissolution and growth of oxide and silicate minerals at elevated temperature and pressure, and to use rate and stoichiometric data from parallel macroscopic dissolution and growth experiments to interpret mineral rates using a combined microscopic Burton-Cabrera-Frank and macroscopic surface-complexation model.

Project Description: This project combines atomic-scale and macro-scale approaches to the study of mineral–fluid interaction in order to significantly improve our understanding of, and ability to predict the course of, mineral dissolution and precipitation processes. We have successfully built a high temperature–pressure flow-through AFM that allows atomic-scale kinetic experiments under geologically relevant conditions for important oxide and aluminosilicate minerals. This is a unique capability. Identical conditions are being investigated using macroscopic wet-chemical rate experiments, including conditions both near and far from equilibrium. We are measuring rates of dissolution and precipitation, determining activation energies, measuring rates of step motion across surfaces (including anisotropy), and investigating step-step interactions that affect rate. With this capability, we can address

many still-open questions concerning the exact forms for rate laws near and far from equilibrium, the microscopic interpretation of these rate laws in terms of dissolution and precipitation mechanisms operating under various conditions, and the question of what exactly the "active area of interaction" and "active sites" are on mineral surfaces.

Results: During this fiscal we continued our studies of mineral dissolution and growth under hydrothermal conditions using our unique Hydrothermal AFM (HAFM). We made detailed studies of barite growth, continued investigating anorthite dissolution and began work on magnesite dissolution. The results of our work were disseminated in papers published in *Geochim. Cosmochim. Acta* and recently accepted by *J. Phys. Chem. B*. We began construction of a second HAFM at LLNL (the prototype was built at U. Wyo.). This new system will utilize a compact plumbing board to simplify control of temperature, pressure and flow. After testing expected to be completed in early FY00, the U. Wyo. system will be upgraded. We established contact with Dr. Barry Coles (Oxford) and, based on his work, are designing an inlet jet of precise geometry, which allows a priori calculation of the flow field in the immediate vicinity of the tip. This will prove critical in observations made very near equilibrium.

Collaborative Research: Studies for Surface Exposure Dating in Geomorphology

R. C. Finkel (925-422-2044; Fax: 925-422-0208; rfinkel@llnl.gov) M. Caffee (925-423-7896; Fax: 925-422-1002; caffee1@llnl.gov)

Objectives: The objective of this research is an experimental and theoretical program to fully develop the systematics of *in-situ*-produced cosmogenic nuclides in terrestrial surface samples and their application to the dating of surface features and processes. This work includes determination of precise production rates and production depth profiles, studies of altitude and latitude effects, intercalibration with other methods, isolation of *in situ* produced nuclides from other lithologies and development of *in situ* produced ^{14}C . This research is a collaborative endeavor between LLNL (Caffee, Finkel, AMS), UC Berkeley (Dietrich, geomorphology; Nishiizumi, geochemistry) and LANL (Reedy, cosmogenic nuclide modeling; Poths, noble gas mass spectrometry).

Project Description: In the past year this project, in its LLNL manifestation, has attacked two components of the overall project objectives: *In situ* ^{14}C and spallogenic ^{36}Cl . ^{14}C has a half-life, which is significantly shorter than the other commonly measured *in situ* cosmogenic nuclides. This makes it ideal for determining recent erosion rates and for burial dating of recent formations. Blank problems and difficulties in quantitatively extracting ^{14}C from rocks have limited the applicability of this nuclide. Work is nearly completed on constructing and calibrating an extraction line for determining ^{14}C in quartz samples.

Many geologic problems, *e.g.*, studies involving basalts, require dating of formations that do not contain quartz. ^{36}Cl is an alternative nuclide to use in these cases. The use of ^{36}Cl is made more complex by the existence of two modes of production: spallation from K and Ca and thermal neutron capture from Cl. The thermal neutron capture production has a very different depth profile and much greater dependence on rock composition and moisture than does spallation. We have begun chemical studies to develop methods for determining pure spallation ^{36}Cl .

Results: In the past year we have investigated the possibility of coupling ^{36}Cl determinations to our ^{10}Be and ^{26}Al work in quartz by removing thermal-neutron capture ^{36}Cl using sequential leaching before determining the spallation component. We are in the process of carrying out sequential leaching experiments on several granitic samples. ^{36}Cl has been extracted from these leaches and measured by AMS. We are currently measuring the concentration of target elements and of chlorine in the samples so that we can assess the effectiveness of this approach. We are developing techniques for the extraction of cosmogenic ^{36}Cl from calcite. Two problems are being attacked in parallel: the chemical isolation and purification of cosmogenic ^{36}Cl and the measurement of \sim ppm levels of total Cl in the dissolved rock. Like the extraction of other cosmogenic radionuclides from minerals, the separation of meteoric ^{36}Cl from in-situ cosmogenic ^{36}Cl is critical. We are testing a procedure based on a series of water leaches followed by nitric acid dissolution that appears to resolve meteoric from in-situ ^{36}Cl . It is also essential that the Cl concentration of the dissolved rock be determined. Typical techniques, such as ion chromatograph, are not useful because of the high concentration of nitrate. Other techniques, such as ion-specific-electrode, are unreliable for ppm levels of Cl. We have successfully developed an isotope dilution technique to measure the total Cl. Terrestrial $^{37}\text{Cl}/^{35}\text{Cl}$ ratios are nearly uniform in crustal materials. The addition of a ^{37}Cl spike enables the unambiguous determination of the Cl concentration of the sample. We have developed a technique to measure all three isotopes of Cl simultaneously on the Accelerator Mass Spectrometer. This technique required additional electronics and considerable modification of the data acquisition software however all this has been accomplished and successfully tested.

Dating depositional surfaces: Applications of *in situ* Cosmic-ray Exposure Dating

R. C. Finkel (925-422-2044; Fax: 925-422-0208; rfinkel@llnl.gov), M. Caffee (925-423-7896; Fax: 925-422-1002; caffee1@llnl.gov), and F.J. Ryerson (925-422-6170; Fax: 925-422-1002)

Objectives: Cosmogenic isotope abundance patterns will be determined for a number of different types of aggradational surfaces of known age in order to assess the applicability of this method for deposits of this type. Such data are required if the climate and other information held in these surfaces is to be fully exploited.

Project Description: Landscape evolution depends strongly on climate and tectonics, and landscape history may in principle be inverted to obtain information regarding these two forcing factors. A major group of landscape features consists of those involving the emplacement and modification of depositional surfaces. Providing a temporal framework based upon cosmic-ray exposure dating for the interpretation of such features is challenging, as they may be modified subsequent to deposition, and may possess a pre-depositional exposure history. In the work described here, we propose to develop and validate sampling and analytical methods for three different depositional settings in the western US: debris flow fans, lacustrine shorelines and fluvial deposits using a combination of ^{10}Be , ^{26}Al , ^{21}Ne and *in situ* ^{14}C at LLNL's Center for Accelerator Mass Spectrometry and associated facilities. Sampling strategies will exploit the depth dependence of cosmogenic nuclide production to constrain inheritance and post-depositional disturbance. The measurements will provide a basis for future investigations requiring the dating of such surfaces, and provide additional constraints on Quaternary climate and tectonics in the western US.

Results: In conjunction with Robert Anderson at UC-Santa Cruz we have dated fluvial terrace along the Fremont River, Utah using cosmogenic ^{10}Be and ^{26}Al of quartz-rich clasts. The stochastic nature of burial

depth and hence in nuclide production in individual clasts during exhumation and fluvial transport, and during post-depositional stirring, results in great variability in clast nuclide concentrations. We have generated amalgamated samples of many individual clasts in order to average over their widely different exposure histories. Depth profiles of such amalgamated samples allow us to constrain the mean inheritance, to test for the possible importance of stirring, and to estimate the age of the surface. Working with samples from terraces of the Fremont River, we demonstrate that samples amalgamated from 30 clasts represent well the mean concentration. Depth profiles show the expected shifted exponential concentration profile that we attribute to the sum of uniform mean inheritance and depth-dependent post-depositional nuclide production. That the depth-dependent parts of the profiles are exponential argues against significant post-depositional displacement of clasts within the deposit. Our technique yields ^{10}Be age estimates of 60 +/- 9, 102 +/- 16 and 151 +/- 24 ka for the three highest terraces, corresponding to isotope stages 4, 5d and 6, respectively. The mean inheritance is similar from terrace to terrace and would correspond to an error of similar to 30-40 ka if not taken into account. The inheritance likely reflects primarily the mean exhumation rates in the headwaters, of order 30 m/Ma.

Thermodynamic and Transport Properties of Aqueous Geochemical Systems

J. A. Rard (925-422-6872; Fax: 925-423-6907; rard1@llnl.gov) and D.G. Miller (925-422-8074; Fax: 925-422-0208; dmiller@llnl.gov)

Objectives: The objectives are to (1) measure precise and accurate osmotic/activity coefficients, solubilities, densities, and mutual (Fick's law) diffusion coefficients for aqueous brine salts and their mixtures and osmotic/activity coefficients for acidic sulfate mixtures; (2) develop reliable methods to estimate such properties for multicomponent solutions from binary solution properties; and (3) calculate generalized transport coefficients.

Project Description: The general techniques of classical thermodynamics and of linear irreversible thermodynamics are used to understand and model equilibrium and transport processes in brines and other aqueous electrolyte mixtures relevant to energy programs. Properties being measured are osmotic/activity coefficients and solubilities by the isopiestic method, densities by pycnometry and vibrating densimetry, and diffusion coefficients by Rayleigh and Gouy interferometry.

One major goal is to measure highly accurate data for systems involving geochemical brines and chemical pollutants. A second goal is to develop estimation methods for accurate predictions of these properties for aqueous electrolyte mixtures of arbitrary complexity, using the accurate new data as test systems. Osmotic/activity coefficients are being analyzed using extended forms of Pitzer's equations, and transport data are being analyzed as Onsager transport coefficients.

Results: We extended our diffusion and density experiments for mixtures of NaCl and Na_2SO_4 at 25°C up to a total molarity of 3.0 mol/dm³, at molarity fractions of NaCl of 0.9 and 0.75, using Rayleigh interferometry. These measurements at very high concentrations are only being made for solutions containing high mole ratios of NaCl to Na_2SO_4 , because of solubility limitations due to precipitation of mirabilite at higher Na_2SO_4 ratios. These experiments supplement our previous measurements at 0.5 – 1.5 mol/dm³ at 25°C for the full composition fraction range, and were made using the Gosting diffusimeter with computer-controlled data collection in real time. These diffusion experiments were

performed in collaboration with Professor John G. Albright and a graduate student at Texas Christian University.

Isopiestic vapor-pressure experiments were started for aqueous $\text{Na}_2\text{SO}_4 + \text{MgSO}_4$ mixtures at high molalities at 25 °C, since published isopiestic data for this system are extremely limited. We also began isopiestic experiments for the aqueous $\text{H}_2\text{SO}_4 + \text{Al}_2(\text{SO}_4)_3$ system at 25 °C, in part to understand the dissolution of aluminum minerals in acid mine waste. We attempted to prepare the $\text{H}_2\text{SO}_4 + \text{Al}_2(\text{SO}_4)_3$ solutions directly from high-purity anhydrous $\text{Al}_2(\text{SO}_4)_3$ and aqueous H_2SO_4 , but all the resulting solutions had difficulties with formation of sparingly soluble aluminum hydroxy polymers. We were able to prepare hydrolytically stable $\text{H}_2\text{SO}_4 + \text{Al}_2(\text{SO}_4)_3$ solutions using high-purity hydrated $\text{Al}_2(\text{SO}_4)_3$ and aqueous H_2SO_4 , and these solutions are being used for our isopiestic measurements. The initial measurements are at three ionic molality fractions z of H_2SO_4 of $z \cdot 6/7$, $5/7$, and $4/7$, and will later be extended to the $\text{Al}_2(\text{SO}_4)_3$ rich composition region

During this period four journal articles were published, and two others were submitted for publication. The first of these articles reports our isopiestic results for aqueous $\text{H}_2\text{SO}_4 + \text{MgSO}_4$ mixtures at 25 °C, and gives an analysis with extended ion-interaction (Pitzer) equations based on a speciation model that includes Mg^{2+} , H^+ , HSO_4^- , and HSO_4^{2-} . The analysis was done in collaboration with Simon Clegg of the University of East Anglia. The second paper is a biography of Kenneth Pitzer that served as the introduction to the Kenneth S. Pitzer Memorial Tribute, which was published by the *Journal of Solution Chemistry*. The third published paper (co-authored with Kenneth Pitzer and his post doctoral fellows) gives a method for generalizing Pitzer's ion-interaction equation to include ionic-strength dependencies for higher-order virial terms. The fourth published paper describes analogies and similarities between the extraction of ternary diffusion data for liquid and for solid solutions, and was published in *Acta Materialia*. An extensive critical review was made of the published thermodynamic data for aqueous Na_2SO_4 , a mole-fraction based equation of state was obtained that represented the available results accurately from freezing temperatures to 150.5°C, and a manuscript was written and submitted for publication. This review is in collaboration with Simon Clegg (University of East Anglia) and Donald Palmer (Oak Ridge National Laboratory). Joseph A. Rard served as the guest editor of the Kenneth S. Pitzer Memorial Tribute, which was published by the *Journal of Solution Chemistry*.

CONTRACTOR: Los Alamos National Laboratory

University of California
Los Alamos, New Mexico 87545

Contract: W-7405-ENG-36

Person in Charge: D. R. Janecky (505-665-0253; FAX 505-665-8118; janecky@lanl.gov)

CATEGORY: Geophysics and Earth Dynamics

Fast 3D Seismic Modeling and Prestack Depth Migration Using Generalized Screen Methods

M. Fehler (505-667-1925; Fax: 505-667-8487; fehler@seismo5.lanl.gov) with R.-S. Wu (U.C. Santa Cruz), M. N. Toksoz (Massachusetts Institute of Technology)

Objectives: The intent of this work is to develop and explore seismic modeling and imaging for regions of complex geology that greatly improves on the results of conventional implementation of Kirchhoff migration.

Project Description: Modeling and migration of seismic data are among the most important ways we can learn about the structure of the Earth. The demand for processing large seismic datasets to obtain high-quality images has thus become of critical importance. The finite difference method is the most popular method for modeling wave propagation through complex structures. Finite difference can also be used for migration; however, it requires enormous computational resources and is not feasible on even the largest computers. The approach taken by this project for doing efficient and reliable modeling and migration is to develop and explore use of dual-domain (space-wavenumber) methods for seismic modeling and imaging.

Results: We have continued developing a suite of methods for doing efficient and reliable seismic wave modeling and migration. The methods use generalized screen propagators for one-way wave equations. Development of the extended local Rytov Fourier migration method has been demonstrated to provide improved imaging results over standard methods and our Rytov code has been implemented into petroleum companies' processing systems. We also adapted a new method that is based on some work in EM modeling for seismic modeling and migration, resulting in images comparable to our best previous method but using considerably less computing time. Results using the methods have also been applied to earthquake seismology to improve understanding how seismic waves scatter and attenuate in interacting with the complex structure of the Earth's lithosphere

The Role of Carbon and Temperature in Determining Electrical Conductivity of Basins, Crust, and Mantle.

T. J. Shankland, (505-667-4907; Fax: 505-667-8487; shankland@lanl.gov) with A. G. Duba (LLNL; 510-422-7306; Fax: 510-423-1057; duba1@llnl.gov), and E. A. Mathez, (American Museum of Natural History; 212-769-5379; Fax: 212-769-5339; mathez@amnh.org)

Objectives: The intent of this work is to comprehend the electrical conduction mechanisms in carbon-bearing rocks and in mantle minerals for relating the electrical conductivity measured in the field to formation conditions and existing state of crustal rocks and to temperatures in the mantle.

Project Description: Electrical conductivity depends strongly on temperature T and on the presence of other phases such carbon, fluids, or ore minerals at the lower temperatures of the crust and basins. Thus, one research approach is to measure the conductivity of mantle minerals as functions of temperature, orientation, oxygen fugacity fO_2 , and iron content. These data supply the best models for "electrogeotherms" yet available. Another approach is to document textures of carbon in crustal rocks from basins and metamorphic zones and relate them to rock conductivity. In this case, the texture of carbon distribution is mapped with electron microscopy in the same samples used for conductivity measurement. The approach here is to measure electrical conductivity of the mantle's most volumetrically important mineral phases under conditions appropriate to the entire mantle and to use these observations in an *a priori* calculation of mantle conductivity.

Results: Recent laboratory measurements of electrical conductivity of mantle minerals are used in forward calculations for mantle conditions of temperature and pressure for the entire depth of the mantle beginning at 200 km and extending to the base at ~ 2800 km. The electrical conductivity of the Earth's mantle is influenced by many factors, which include temperature, pressure, the coexistence of multiple mineral phases, and oxygen fugacity. In order to treat these factors and to estimate the resulting uncertainties, we have used several spatial averaging schemes for mixtures of the mantle minerals and have incorporated effects of oxygen fugacity. In addition, to better calculate lower mantle conductivities we report new measurements for electrical conductivity of magnesiowüstite ($Mg_{0.89}Fe_{0.11}O$). The effective medium theory averages lie between the Hashin-Shtrikman bounds (theoretical limits on calculated maximum and minimum conductivities) in the whole mantle. A laboratory-based conductivity-depth profile was constructed using the effective medium theory average. Comparison of apparent resistivities calculated from the laboratory-based conductivity profile with those from field geophysical models shows that the two approaches agree well. The results apply to our understanding of mantle dynamics, plate tectonics, and the distribution of heat sources beneath the crust.

Nonlinear Elasticity in Earth Materials

P. A. Johnson, (505-667-8936; Fax: 505-667-8487; paj@lanl.gov), J. A. TenCate, T. J. Shankland, E. Smith, and R. A. Guyer)

Objectives: Research objectives are to investigate the physical manifestations of nonlinear elasticity in rock, including those indicating reservoir/repository characteristics and those affecting seismic observations, and to characterize nonlinear properties of rocks. Of primary importance is developing and applying a holistic model describing the nonlinear response of rock over broad stress-strain-frequency ranges so that practical applications can proceed.

Project Description: Increasingly rapid progress is being made in the field of dynamic nonlinear elasticity of Earth materials. Roughly ten years ago three groups of scientists (at Los Alamos, at the Institute of Applied Physics, and the Institute of Physics of the Earth in Russia) independently initiated this research field. Early and continued OBES support has been instrumental in making it possible for this research field to flourish. Today the field of dynamic nonlinear elasticity of Earth materials has recognized importance in the domains of geomaterials, materials science, and strong ground motion, and there are an ever-increasing number of researchers working within it.

Rocks display unique elastic behavior. They are extremely nonlinear, being hysteretic, possessing discrete memory, and having slow dynamics [a long term memory of strain]. Although some of these types of nonlinearities may exist in, for example, powdered metals, it is rocks that exhibit these characteristics “in spades” (to quote a colleague). Thus, a study of nonlinearity in Earth materials affords opportunities to apply research results to other materials as well. Nonlinear behavior plays a central role in developing new methods with which to characterize rock properties, for instance, interrogating the entire elastic microstructure of rock. Nonlinear attributes of rock have important consequences on processes in the Earth such as earthquake strong ground motion, reservoir subsidence, seismic wave propagation and attenuation, stress fatigue damage, hydraulic fracturing, *etc.* Our work involves developing a comprehensive theoretical and experimental framework that (1) employs static and dynamic laboratory investigation of rocks to provide a macroscopic and microscopic description of the elastic state, and (2) provides for turning the microscopic description into a prescription for rock properties that can be used to predict change in stress state, both static and dynamic.

Results: Several important questions were answered this year, many of them related to slow dynamics. Many aspects of slow dynamics are reminiscent of static creep and much of the theoretical study this year involved examining quasistatic creep systems and learning from them. An important distinction separates slow dynamics from all other forms of creep: static creep is caused by a “dc” source whereas slow dynamics is caused by an “ac” (sinusoidal) source. Several careful experiments were performed to see if slow dynamics is a thermally activated process, *i.e.*, does slow dynamics depend on temperature? The answer is yes.

CATEGORY: Geochemistry

Uranium-Series Concordance Studies

M. T. Murrell (505-667-4299; Fax: 505-665-4955; mmurrell@lanl.gov), and S.J. Goldstein (505-665-4793)

Objectives: The goal of this project is to provide unique information on the behavior of U-series members in the environment using improved capabilities for Quaternary dating.

Project Description: Uranium-series disequilibria techniques are well-established and valuable tools for geochronology and geochemistry. Such measurements have typically been made by decay counting; however, there are considerable advantages in using mass-spectrometric techniques. We have previously used BES funding to develop such techniques. The goal of this current proposal is to apply these new mass spectrometric methods to answer basic questions in Quaternary dating and geochemistry. Emphasis will be placed on: 1) modeling magma chamber processes using U-series disequilibria in

young volcanic systems at Hawaii and Mid-Ocean Ridges and 2) evaluating ^{235}U - ^{231}Pa and ^{230}Th - ^{226}Ra -Ba disequilibria as a geochronometer for young volcanics using mineral isochrons and in carbonate systems using a multi-element concordia approach. This work will provide information on the recent evolution of magmatic systems and also has application to natural hazard risk assessment, paleoclimate studies, and the carbon cycle.

Results: *Travertines Of Central Italy: Evolution And Significance (with S. Rihs and N. Sturchio):* Degassing of CO_2 -enriched water emanating from thermal springs is accompanied by formation of travertine deposits. Thus, travertines provide a record of CO_2 degassing. In this study we are correlating the U-Th ages of Italian travertines with magmatic and geothermal activity, as well as with paleoclimatic information, and we are evaluating the significance of the ages in relation to geologic and tectonic setting. Our preliminary age determinations on a limited number of samples from Italian fossil travertine deposits shows that there may have been a significant period of travertine deposition at about 250 ka.

Age Constraints on Lavas from the Axial Valley of the Mid-Atlantic Ridge, MARK Area (with M. Sturm, E. Klein, and J. Karson): Mass spectrometric measurements of U-series disequilibria were used to determine eruption ages for four basalt glasses collected by DSV ALVIN from the Mid-Atlantic Ridge (MAR) south of the Kane Fracture Zone. To our knowledge, this is the first systematic uranium-series dating study on well-located mid-ocean ridge basalts (MORB) from a slow-spreading ridge. These lavas from the most robust volcanic edifices in the MARK area are 10-20 kyr old. The age-dates are used to begin to quantify the temporal and spatial relationship of volcanic, tectonic, and hydrothermal processes at slow-spreading oceanic ridges.

Mid Ocean Ridge Basalts at the EPR (with K. Sims, M. Perfit, D. Fornari, and R. Batiza): We have measured U-Th-Ra and U-Pa disequilibria in a suite of ~20 samples from 9-10N EPR. In young axial trough samples, our results indicate that ^{226}Ra excesses vary significantly and systematically as a function of magmatic fractionation. Based on these data, upper limits on magma storage times in crustal reservoirs for these lavas range from ~300-2,000 years. These estimates of residence time also enable us to model magma chamber characteristics such as crystallization rate and magma chamber melt volumes for this segment of the EPR.

U-Series Chronologies for Deep Sea Corals and Glacial Ice (with D. Lea and K. Nishiizumi): We have applied sensitive uranium-series measurements by mass spectrometry to provide some of the first radiometric dates for deep-sea corals and polar ice samples. U-series dates for deep-sea corals are combined with radiocarbon dating to determine ventilation ages for deep-ocean water, both presently and during the past glacial maximum (16 ka). Our results indicate that glacial deep-ocean circulation was more sluggish than present, which may have significantly contributed to decreased atmospheric pCO_2 for the past glacial period. Our U-series dating results for ice samples from Allan Hills, Antarctica, suggest a young age for this ice, in conflict with published data measured by alpha spectrometry. Our results suggest that radiometric dating of polar ice based on inherited U-series disequilibria from precipitation may be feasible.

Surface Exposure Dating in Geomorphology

R. Reedy (505-667-5446; Fax: 505-665-4414; rreedy@lanl.gov), with K. Nishiizumi (U.C. Berkeley; 510-643-9361; kuni@ssl.berkeley.edu), W. E. Dietrich (U.C. Berkeley) R. C. Finkel (LLNL), and M. W. Caffee (LLNL)

Objectives: The production of cosmogenic nuclides in terrestrial surface samples and the use of these nuclides to date and characterize young (<1 Ma) surfaces are studied.

Project Description: Geological samples start accumulating cosmogenic stable and radioactive nuclides such as 0.7-Ma ²⁶Al once they are formed very near the surface or brought to the surface from depths of many meters. These nuclides are often the only way to characterize the recent-surface record of such samples, such as dating when they were exposed on the Earth's surface or inferring erosion rates. To interpret the measurements of the concentrations of these nuclides in surface samples requires good rates for their production. This project uses measurements of cosmogenic nuclides in well-characterized samples plus numerical simulations using computer codes developed at Los Alamos to get better production systematics for many in-situ-produced cosmogenic nuclides as a function of target composition, elevation, and geomagnetic latitude.

Results: Recently measured cross sections for the production of these nuclides continue to be compiled and evaluated. Work continued with Dr. J. Sisterson on measuring needed neutron cross sections at the Los Alamos Neutron Scattering Center and other sources of energetic neutrons.

The code recently developed at Los Alamos, MCNPX, has been obtained for use in this work. This code combines the latest version of the LAHET code with the low-energy-neutron code MCNP4B into a single code. This code has the high-energy physics packaged FLUKA for use with incident GCR particles having energies above ~10 GeV. The calculations done using the FLUKA package are better for regions near the Earth's equator with very high geomagnetic cutoff energies than with other packages in high-energy transport codes at Los Alamos. Calculations made with MCNPX are being compared with those calculated with other codes.

Contacts have been maintained with groups exposing artificial samples on the Earth's surface. Contacts are being continued with others on the work being done on studying production rates with natural samples. These and other measurements will be modeled using MCNPX in testing the ability of the code to model the production of in-situ-produced cosmogenic nuclides.

Microbial Dissolution of Iron Oxides

L. Hersman (505-667-2779; Fax: 505-665-6894; hersman@lanl.gov) with P. Maurice (Kent State University) and G. Sposito (U.C., Berkeley)

Objectives: Our overall objective is to determine the mechanisms of iron release during microbially enhanced iron oxide dissolution by an aerobic microorganism. During this first year, work at Los Alamos National Laboratory has been focussed on four aspects of the proposed research:

- Using high performance liquid chromatography (HPLC), purify a siderophore (produced by a *Pseudomonas* sp.) for use in dissolution experiments at UC Berkeley,
- During dissolution, determine if reductants are being produced by the *Pseudomonas* sp.,

- Conduct a series of growth experiments on various Fe oxides, and provide those same Fe oxides for atomic force microscopy (AFM) analysis at Kent State University.

Project Description: The purpose of this research is to investigate the mechanisms used by aerobic microorganisms to obtain Fe for growth. Currently little is known about Fe oxide dissolution processes in oxic environments. Understanding these mechanisms is fundamental to a wide range of bio-geochemical processes. For example, Fe oxides sorb a variety organic and inorganic pollutants, therefore understanding the mechanisms of dissolution is important to understanding pollutant transport phenomena. Los Alamos National Laboratory is investigating the growth characteristics of a *Pseudomonas* sp. whose only source of Fe is either hematite or goethite. Additionally, we supply siderophore for siderophore-mediated investigations at UC Berkeley and provide microbially reacted, Fe oxide surfaces for AFM analysis at Kent State University.

Results: We have been investigating the production of reductants/reductases by aerobic microorganisms, in response to variations in Fe availability. We have found that in addition to producing siderophores *P. mendocina* produced both extracellular and cell associated Fe reductants in response to Fe deprivation and Fe supplied as either hematite or FeEDTA.

Because our work has demonstrated that *P. mendocina* dissolved Fe(III)(hydr)oxides in excess, and because siderophore removed Pb from these oxides, it seemed probable that this microorganism also may remove sorbed metals and radionuclides from Fe(III)(hydr)oxides. Therefore, we investigated desorption of Pu from goethite by *P. mendocina*. We found that after 4 d growth at room temperature (abs. of 0.55 at 600 nm) the microorganism removed approximately 20% of the sorbed Pu.

CATEGORY: Solar-Terrestrial Physics

Energy Transport in Space Plasma

S. P. Gary (505-667-3807; Fax: 505-665-7395; pgary@lanl.gov)

Objectives: The long-term goal of this research is to understand the flow of plasma energy in the near-Earth space environment from a small-scale point of view. The objective of this research is to use plasma theory, simulations, and data analysis to express the consequences of plasma microinstabilities as concise relationships that may be used in large-scale models of space plasmas that describe the solar-terrestrial interaction.

Project Description: Particle velocity distributions and parameters observed by Los Alamos plasma instruments on scientific spacecraft as well as computer simulations are used to carry out fundamental studies of plasma instabilities and associated transport in and near the solar wind, the Earth's bow shock, and the terrestrial magnetosphere.

Results: Our most important accomplishment in 1999 was the demonstration that electromagnetic fluctuations near the electron plasma frequency observed in the polar regions of the terrestrial magnetosphere are likely to arise from electron/electron instabilities. The particle-in-cell simulations that we used to show this result may provide the basis for a more complete understanding of electron beams and their consequences in the polar magnetosphere.

The Solar Wind-Magnetospheric Interaction

J. Birn (505-667-9232; Fax: 505-665-3332; jbirn@lanl.gov)

Objectives: The goal of this research is to further the understanding of the structure and dynamics of the Earth's magnetosphere, coupled to the fast-flowing solar wind plasma on the one hand and to the ionosphere on the other.

Project Description: The focus of this research is the investigation of the large-scale structure and evolution of the Earth's magnetosphere, using theory, numerical modeling, and correlative studies of data from multiple sites within and near the magnetosphere (including the Earth itself as well as scientific satellites).

Results: Our most significant accomplishment in 1999 was a clarification of the mechanisms that cause the collapse of the magnetic field in the Earth's magnetic tail, based on computer simulations of the dynamic evolution of the tail. Microscopic effects decouple particles from the magnetic field and enable magnetic reconnection. The reconnection process then leads to accelerated plasma flow. These flows subsequently distort the magnetic field and the ionosphere-magnetospheric current system. Contrary to earlier expectations, we found that the important role in the collapse and diversion of the magnetotail-ionosphere current system is played by plasma transport processes rather than anomalous dissipation.

Energetic Particle Acceleration and Transport

G. D. Reeves (505-665-3877; Fax: 505-665-7395; reeves@lanl.gov)

Objectives: The overall goals of this project are (1) to better understand the acceleration and transport of energetic particles during magnetic storms, substorms, relativistic electron enhancements, solar energetic particle events, and other magnetospheric processes, (2) to develop empirical models of the structure and dynamics of the Earth's radiation belts and other energetic particle regions, and (3) to develop a better understanding of the space environment as a system and to better understand the effects of the space environment on spacecraft and their operations.

Project Description: This effort concerns the analysis of energetic particle data from a variety of US programmatic and NASA scientific satellites. Those include the series of geosynchronous spacecraft that carry Los Alamos energetic particle detectors, the GPS satellites that also carry Los Alamos energetic particle detectors, NASA's POLAR satellite, and others. The energies of the particles of interest range from keV to hundreds of MeV. The lower end of this range lies somewhat above the thermal plasma energies and is therefore sensitive to local acceleration processes such as magnetospheric substorms. The higher end of the energy range is well suited to the study of energetic particles in the Earth's radiation belts and those that can penetrate the Earth's magnetic field, such as galactic cosmic rays and particles produced in solar flares. We also investigate the effects of those particles on spacecraft systems and instrumentation.

Results: Our most important accomplishment in 1999 was the development of a new technique to remotely image the energetic particle populations in the Earth's magnetosphere using Energetic Neutral Atom (ENA) Imaging. Since producing the first ENA images of the Earth's radiation belts in 1997, we have had considerable success applying the technique to problems in space physics. The most recent result concerns the similarities and differences between energetic particle injections in geomagnetic

storms and the smaller and less energetic “substorms”. In other recent work we have used simultaneous measurements of the Earth’s relativistic electron belts from up to 11 satellites to create time-dependent “data synthesis” models of the Van Allen radiation belts. We have also applied that technique to four different relativistic electron events, which provided the first evidence for several common, underlying characteristics of relativistic electron acceleration.

CONTRACTOR: Oak Ridge National Laboratory

Lockheed Martin Energy Research Corporation
Oak Ridge, Tennessee 37831

CONTRACT: DE-AC05-96OR22464

CATEGORY: Geochemistry

PERSON IN CHARGE: David. R. Cole

Thermodynamic Mixing Properties of C-O-H-N Fluids

J. G. Blencoe (423-574-7041; Fax: 423-574-4961; blencoejg@ornl.gov), J. Singh, and L.M. Anovitz

Objectives: Thermophysical data for CO₂-CH₄-N₂-H₂O-NaCl fluids at high temperatures and pressures are insufficient in quantity and quality to permit formulation of accurate equations of state (EOSs) for natural, deep-seated fluids in the Earth's crust (hydrothermal waters, natural gas, *etc.*) Such equations would have numerous applications in geochemistry, including geothermal- and hydrocarbon-reservoir hydrodynamics modeling, calculation of fluid-rock equilibria, predicting permeability changes in resource host rocks, quantifying contaminant transport, and characterizing global cycling of greenhouse gases.

Project Description: Experiments are performed with binary and multicomponent mixtures of CO₂, CH₄, N₂, H₂O, and NaCl at temperature-pressure conditions similar to those encountered in deep aquifers, sedimentary basins, geothermal fields and many ore-forming environments. Volumetric properties and liquid-vapor phase relations are determined with high precision and accuracy using a unique vibrating-tube densimeter designed for operation at 50-500°C and 5-200 MPa. The activity-composition relations of the fluids are measured using another unique facility: a hydrogen-service internally heated pressure vessel capable of operation at high hydrogen fugacities, with an overall operating range of 100-1100°C and 5-800 MPa. Laboratory experiments and thermodynamic modeling are closely integrated to optimize the efficiency and effectiveness of data acquisition and EOS development.

Results: Density and liquid-vapor equilibrium data for CO₂-H₂O fluids at 300°C are scarce and of uncertain accuracy. Therefore, a vibrating-tube densimeter was used to determine the densities and liquid-vapor phase relations of CO₂-H₂O mixtures at closely spaced intervals of pressure (*P*) and mole fraction CO₂ (*X*_{CO₂}) at 300°C, 7.44-99.93 MPa.

Liquid-vapor coexistence limited the range of composition over which measurements could be made at pressures from 8.6 to ~56.5 MPa. Nonetheless, four characteristics of the data are evident:

- (1) at 7.44 MPa, fluid density increases slowly and continuously from $X_{\text{CO}_2} = 0$ to $X_{\text{CO}_2} = 1$;
- (2) at pressures from 8.6 to 99.93 MPa, and particularly at pressures below 40 MPa, H₂O-rich fluids are much more dense than CO₂-rich fluids;
- (3) the densities of CO₂-rich fluids increase sharply from 7.44 to 99.93 MPa; and
- (4) density vs. X_{CO_2} is nearly linear at 7.44-19.94 MPa, but distinctly nonlinear (concave upward) at higher pressures.

The new density data, and equations of state for CO₂ and H₂O, yield excess molar volumes (V^{ex}) for the fluids. At 7.44 MPa, V^{ex} vs. X_{CO_2} is nearly symmetric, with a peak excess molar volume of ~20 cm³/mol at $X_{\text{CO}_2} = 0.5$. However, with an increase in pressure from 7.44 to 9.94 MPa, V^{ex} vs. X_{CO_2} becomes highly asymmetric toward H₂O, with a peak excess molar volume of ~250 cm³/mol at $X_{\text{CO}_2} = 0.2$. This value is nearly 75% of the molar volume of the mixture, reflecting extreme nonideality of the fluid. At pressures above 9.94 MPa, H₂O-rich fluids have negative excess molar volumes. Finally, the results also indicate that, from 9.94 to 99.93 MPa: (1) V^{ex} vs. X_{CO_2} for H₂O-rich mixtures becomes progressively less negative; and (2) excess molar volumes for CO₂-rich fluids are continuously positive, but decrease steadily to values < 5 cm³/mol.

The vibrating-tube densimeter was also used to acquire density and LVE data for N₂-H₂O fluids at closely spaced intervals of pressure and mole fraction N₂ at 300°C, 7.44-99.93 MPa. As in the CO₂-H₂O system at 300°C, $P > 8.6$ MPa, liquid-vapor coexistence limited the range of composition over which density measurements could be made. However, in the N₂-H₂O system, the field of liquid-vapor stability is much more extensive than it is in the CO₂-H₂O system, extending up to—and beyond—100 MPa. This limits the stability field of H₂O-rich fluids to a very narrow range near the H₂O sideline. In addition, whereas—as in the CO₂-H₂O system—H₂O-rich fluids are much more dense than gas-rich compositions, this density contrast is even greater in the N₂-H₂O system. From 9.94 MPa to 99.93 MPa, the densities of N₂-rich fluids vary from ~5% to ~50% of those determined for H₂O-rich compositions. In contrast, in the CO₂-H₂O system at 300°C, 9.94-99.93 MPa, the densities of CO₂-rich compositions rise to values near 80% of those determined for H₂O-rich mixtures. Finally, the results also indicate that, at a given pressure, the effects of composition on density are more linear for N₂-rich N₂-H₂O mixtures than for CO₂-rich CO₂-H₂O fluids.

Excess molar volumes for N₂-H₂O mixtures at 300°C, 7.44-99.93 MPa, calculated from our new density data for those fluids, and equations of state for N₂ and H₂O, are similar, both in pattern and in magnitude, to those determined for CO₂-H₂O fluids. The principal differences are that:

- (1) at a given pressure and mole fraction of gas equal to or greater than 0.2, the excess molar volume of the N₂-H₂O fluid is slightly larger than that of the corresponding CO₂-H₂O fluid; and
- (2) because, at 300°C, 9.94-99.93 MPa, liquid-vapor coexistence is more extensive in the N₂-H₂O system than in the CO₂-H₂O system, the compositional range where V^{ex} is negative is much narrower in the former system than in the latter.

Fundamental Research in the Geochemistry of Geothermal Systems

J. Horita (865-576-2750; Fax: 865-574-4961; horitaj@ornl.gov), D. R. Cole, and D. J. Wesolowski

Objectives: The objective of this project is to provide fundamental information on geochemical reactions that play pivotal roles in a wide range of geological processes, but that specifically impact reservoir dynamics, corrosion, and heat extraction in active geothermal systems. The speciation of elements in aqueous solutions, mineral solubilities, kinetic and equilibrium partitioning of stable C-O-H isotopes, and other fluid-solid interactions are primary subject areas for this research.

Project Description: At Oak Ridge National Laboratory, a long-term basic research program in experimental hydrothermal geochemistry, stable isotope geochemistry, and igneous petrology has led to the development of unique methodologies for extracting rigorous and unambiguous information on a wide range of geochemical processes. This capability permits the efficient and definitive examination of

specific problems hampering the ability to quantitatively model fluid-rock interaction processes related to the discovery and exploitation of geothermal resources. Research topics in this project are selected in close cooperation with geothermal industry representatives and are frequently augmented by parallel research on more applied aspects of the same problems funded by the U.S. Department of Energy's Geothermal and Wind Technologies Program.

Results: During the current funding period, our activities have been focused the experimental and theoretical examination of the effect of pressure and fluid composition, which both vary widely in geothermal systems, on isotope partitioning between brines, steam, and minerals at elevated temperatures and pressures.

Pressure effects on D/H isotope fractionation were determined in the system brucite $[\text{Mg}(\text{OH})_2]$ -pure water at 200-500°C and at 21-8000 bars, using the partial isotope exchange technique. The measured D/H fractionation factor between brucite and water increased systematically from -31.4 to -19.3 per mil with increasing pressure from 150 to 8000 bars at 380°C. A good linear relationship was observed between the measured fractionation factor and the density of water (0.07 to 1.04 g/cm³). Our experimental results on brucite-water at 200°C at 21 bars, 300°C and 100 bars, 400°C and at 500 bars, and at 500°C and 800 bars, together with the literature data, also show a positive relationship between the D/H fractionation factor and the density of water at each temperature. D/H pressure effect appears even larger at 200-300°C.

The effect of 1-5 molal NaCl on D/H fractionation factor between brucite and water at 200-500°C showed that dissolved NaCl slightly, but consistently increased brucite-water D/H fractionation at all the temperatures studied. Our results of the effect of dissolved NaCl on brucite-water D/H partitioning at 380°C, and at 200 and 250 bars suggest that the NaCl effects are pressure-dependent. These new results demonstrate that isotope fractionation is a function, not only of temperature, but also of pressure and fluid composition.

Molecular dynamic simulations of water at elevated temperatures were also initiated. The water model SPC-mTR is a good candidate for simulations of the isotopic properties of water at elevated temperature and pressures, because this model uses an anharmonic Morse term for the intramolecular O-H stretching, and simulates the liquid-vapor curve in excellent agreement with the experimental data. H₂O and HDO simulations were carried out on both liquid and vapor at 27 and 300°C as well as on a high-density liquid (0.99 g/cm³) at 300°C. The simulated vibrational spectra reproduce experimental observations with spectroscopic methods. The O-H bands blueshifts with increasing temperature, while the H-O-H band redshifts. Pronounced peaks in the low-frequency region (bending and stretching of hydrogen bonds, librations) disappear with increasing temperature and are replaced by a rather continuous spectrum. With increasing density at 300°C, the O-H stretching redshifts and the H-O-H band blueshifts.

The raw simulated densities of water have been used to calculate reduced partition function ratios and the liquid-vapor D/H fractionation. These first results overestimated the fractionation significantly, compared to the experimental results. However, they qualitatively predict the experimentally observed crossover in liquid-vapor D/H fractionation at 220°C. In addition, the predicted pressure/density effect in the liquid at 300°C is in qualitative agreement with the experimental results.

Ion Microprobe Studies of Fluid-Rock Interaction

L.R. Riciputi (865-574-2449; Fax: 865-576-8559; i79@ornl.gov) and D. R. Cole

Objectives: The objective of this research is to investigate how the microscale elemental and isotopic record, accessible using ion microprobe analysis, can be used to understand mass transfer processes occurring during fluid-rock interaction at low to moderate temperatures in the Earth's crust, studying both natural and experimental samples.

Project Description: In this project, the ability of ORNL's Cameca 4f ion microprobe to obtain quantitative element and light (H, B, C, O, S) isotope ratio analyses with a 5-30 micron spatial resolution are being developed and applied to studies of fluid-rock interactions in a variety of settings, in both natural and experimental systems. The ion microprobe data is typically integrated with information obtained using a variety of other techniques, petrographic studies, conventional bulk gas source and thermal ionization isotope ratio analyses, electron microprobe, and fluid inclusion analysis. Primary areas of investigation include (1) use of the microscale isotope record to study mass transport during large-scale fluid-rock events, (2) determination of both diffusion rates and equilibrium water-mineral isotope partitioning factors in the O, H, and C systems, and (3) utilizing microscale isotopic and elemental disequilibrium in natural settings to study the duration of fluid-rock events.

Results: An ion microprobe study was initiated on authigenic K-feldspar and quartz cements from the Mount Simon Sandstone in the Illinois Basin (and surrounding areas) to obtain a better understanding of the regional event that formed the widespread K-feldspar cement formed across the mid-continent at ~400Ma. Six samples have been examined from a 600km, south-north traverse through southern Illinois to mid-Wisconsin. Average K-feldspar oxygen isotope values increase over 10 per mil from the southernmost, most deeply buried sample (+13 per mil) to outcrop samples from the Wisconsin Arch (+24 per mil), with oxygen isotope values in quartz cements displaying similar trends. Fluid inclusion data from three samples suggests that temperatures were relatively constant across the basin, implying that temperature fluctuations cannot be used to explain the regional isotopic gradient. These data imply that the regional gradient in oxygen isotope values is due to isotopic enrichment in the fluid resulting from progressive diagenesis. The isotopic pattern suggests a northward flow vector, with a possible source of superheated fluids from deeply buried sediments in the Reelfoot rift.

A microscale investigation of oxygen isotope zonations in the Boehls Butte Anorthosite, Idaho was conducted to better understand fluid-rock interactions during the alteration of this anorthosite. Most previous observations suggest that alteration occurred before a high pressure and high temperature regional metamorphic event between 80 and 50Ma, but cathodoluminescence observation suggests that alteration could be post-peak metamorphic. The ion microprobe reveals the presence of large (>10 per mil) isotopic gradients in single thin sections, and gross isotopic disequilibrium between slow diffusing kyanite formed during peak metamorphic conditions and fast diffusing feldspar. These observations indicate that large-scale hydrothermal alteration took place after the peak of metamorphism, during rapid uplift between 54 and 48Ma, and the lack of alteration in the feldspars suggest that fluid-rock interaction occurred while the rocks were still very hot (>500°C).

Micro-scale oxygen isotope patterns were also documented in altered feldspars from the Rico Dome hydrothermal system, San Juan Mountains, CO. Zoning profiles display a marked change in samples from the periphery of the hydrothermal system to the core. Distal samples having zoning that goes to displays increasing values relative to the cores (up to +14 per mil relative to +9 per mil), with zoning confined to narrow (<200µm) rims, and Ca/Na ratios well-correlated with oxygen isotopes.

Intermediate samples display more extensive alteration, with rims zoned to lower oxygen isotope values (<0 per mil), and some decoupling between isotope and chemical composition. Samples from the core of the system are completely exchanged isotopically (to -8 per mil), although there are still chemical zonations present. These trends indicate that isotopic and chemical exchange are somewhat decoupled, and provide insight into the nature and duration of the meteoric hydrothermal system.

Continued examination of hydrogen depth profiles to date obsidian artifacts and delineate hydrogen transport mechanisms in glasses at low (10-150°C) temperatures shows considerable promise. Both hydration depth and maximum water content in the hydration profiles correlate very well with exposure age, although the rate appears to be non-constant. Based on analysis of a suite of obsidian artifacts from the Chalco site, Mexico, an empirical rate model has been developed. Ages obtained for obsidian artifacts using this model agree quite well (typically within 50 years) of dates determined from associated charcoal using ¹⁴C dating. A series of controlled hydration rate experiments have been initiated at 30 to 150°C to help us better quantify natural hydration rates and mechanisms.

Experimental Studies of Fundamental Stable Isotope Exchange Reactions

J. Horita (865-576-2750; Fax: 865-574-4961; horitaj@ornl.gov), D. R. Cole, and D. J. Wesolowski

Objectives: The objective of this project is to obtain reliable information on the partitioning of the stable isotopes of oxygen, carbon, and hydrogen among minerals and fluids of critical importance in defining fluid-rock interaction parameters, such as fluid sources and fluxes, temperatures, and duration of fluid-rock interaction, in a variety of settings including oil, gas, and geothermal reservoirs, sedimentary basins, and waste repositories.

Project Description: This project is currently focussed on: a) the oxygen isotope partitioning between aqueous fluids and the mineral hematite and magnetite in the 25-800°C range; and b) the exchange rates and equilibrium fractionation of hydrogen and carbon isotopes among gaseous species in the system H₂O-CO₂-CH₄-H₂. Multiple novel experimental methods are used to promote recrystallization and/or synthesis of the iron oxides minerals. Synthetic catalysts and natural minerals, including magnetite and hematite, are investigated for isotopic exchange among the C-O-H gases.

Results: In our earlier work on oxygen isotope fractionation between magnetite and water, we used either hematite to magnetite or iron metal to magnetite reactions at elevated temperatures and pressures. These two reaction pathways, although, kinetically fast, proved to be somewhat problematic for the purposes of facilitating equilibrium isotope fractionation. A new series of high temperature-high pressure experiments have been conducted using a very fine-grained magnetite starting material reacted with three of four isotopically different waters each containing 0.5 molal NaCl. Experiments at 1-2 kbars have been completed at 500, 600, 700, and 800°C for durations ranging from 232 hrs (800°C) to as long as 1798 hrs (600°C). Experiments of a similar nature are in progress at 300 and 400°C, 1kbars. SEM observations indicate that considerable grain growth occurred during these experiments with some grains coarse enough (>100 micrometers in diameter) for analysis by the ion probe. XRD results demonstrate that magnetite is the only phase present in the run products. Nearly 100% exchange was obtained at 600, 700, and 800°C; and over 90% at 500°C. We obtained the following fractionation factors: -5.56, -6.34, -6.99, and -7.81 per mil at 800, 700, 600, and 500°C, respectively.

Isotopic fractionation was investigated during microbial siderite precipitation. Iron-reducing and fermentative bacteria were cultured at 10-65°C in the presence of amorphous FeOOH and dissolved CO₂.

Fine grained (2-5 micrometers), cubic or rhombohedral siderite was precipitated together with magnetite. $^{18}\text{O}/^{16}\text{O}$ values of siderite precipitated microbially slightly increases in early stages of the incubation (<1 week), and then decreased several per mil to a nearly constant value after a month of incubation. These results suggest that oxygen isotope partitioning of microbial siderite was controlled by a biological effect in early stages, and later modified by an inorganic aging process (*i.e.*, dissolution-precipitation), gradually approaching toward equilibrium values. Our measured values of the oxygen fractionation factor are reproducible and nearly constant regardless the species, and change systematically with temperature. In addition, our values of microbial siderite fall along those of inorganically precipitated siderite and theoretical calculations in the literature.

Experimental determination of the equilibrium carbon isotope partitioning between CO_2 and CH_4 was completed between 200 and 600°C at a 50°C interval. A mixture of CO_2 and CH_4 was reacted in the presence of a Ni catalyst. At all the temperatures investigated, the gas composition changed significantly. Constant values of carbon isotope fractionation factor between CO_2 and CH_4 were reached within analytical error from the opposite directions (complete isotopic reversal). Our experimentally determined fractionation factor is slightly, but systematically (0.6-1.0 per mil) higher than those calculated on the basis of statistical mechanics in the literature. All of our experimental data were satisfactorily fitted to a simple equation. The behavior of carbon isotopes was investigated during the formation of hydrocarbons from dissolved CO_2 under hydrothermal conditions. Dissolved CO_2 were converted to CH_4 via intermediate product HCOOH in the presence of a Ni/Fe alloy at 200 and 300°C and at 500 bars. The concentrations of CO_2 , HCOOH , and CH_4 can be modeled with a first-order reaction with a decreasing reaction rate. The $^{13}\text{C}/^{12}\text{C}$ values of CO_2 increased during the reaction, while that of CH_4 formed was significantly lower than that of CO_2 , accompanied by a large kinetic isotope fractionation. The observed carbon isotope profiles can also be understood with a first-order model with two negative kinetic carbon isotope fractionations in each step. The $^{13}\text{C}/^{12}\text{C}$ values of the abiogenic CH_4 formed were as low as (-54 per mil) those typically for biogenic CH_4 in nature.

Potentiometric Studies of Geochemical Processes

D.J. Wesolowski (865-574-6903; Fax: 865-574-4961; wesolowskid@ornl.gov) and P. Bénézeth

Objectives: The objective of this project is to utilize ORNL's unique, high temperature, hydrogen-electrode, pH-measurement cells and other potentiometric approaches to study aqueous reactions and water/mineral interactions relevant to DOE's geoscience mission areas.

Project Description: The pH is considered the master variable in aqueous systems, controlling the nature of dissolved species, the rates of homogeneous and heterogeneous reactions, the solubility and absorbtivity of rock minerals, the transport and deposition of contaminants and ore components, the volatility of mineral acids and the thermal stability of organic acids. In this program we develop and use unique experimental facilities to directly measure the pH of aqueous solutions and the activities of important dissolved ions over broad ranges of temperature, salinity and pH, and use these measurements to quantify the dissociation constants of inorganic and organic acids and bases, the hydrolysis and complexation of metal ions in solution and the solubilities and surface properties of minerals.

Results: The kinetics of gibbsite ($\text{Al}(\text{OH})_3$) and boehmite (AlOOH) dissolution and precipitation are being investigated at temperatures of 50 to 200°C using a unique pH-perturbation method in ORNL's high-temperature, hydrogen-electrode, pH-measurement cells (HECC's). Solutions are permitted to equilibrate with these solids, then acid or base titrant is added and the relaxation of the system back to

the equilibrium state is observed by continuous pH monitoring and periodic sampling to determine the total dissolved aluminum content of the solutions. In this way, the detailed rates and mechanisms of mineral dissolution and growth at near-equilibrium conditions can be precisely determined, a region difficult to study by conventional approaches, even at room temperature.

Detailed studies employing the HECC have also been completed on the proton-induced surface charge of magnetite (Fe_3O_4) in 0.03 to 0.3 molal sodium trifluoromethanesulfonate (NaTr, a “non-complexing” 1:1 electrolyte) from 50 to 290°C. ORNL pioneered this approach with studies of rutile (TiO_2) surface charge, in collaboration with Dr. Michael L. Machesky of the Illinois State Water Survey, and the magnetite studies constitute only the second mineral phase for which the proton-induced surface charge has been determined as a function of pH and salinity at temperatures above 95°C. Studies have also been initiated in collaboration with Dr. Machesky and Dr. Moira K. Ridley of Texas Tech University on the effect of sulfate and oxalate on the surface charge of rutile at 25-75°C. It has been found that SO_4^{2-} interacts with the positively charged rutile surface (at pH's below the point of zero charge) much more weakly than the divalent oxalate anion, possibly due to the formation of bidentate or multidentate complexes with charged surface sites.

The HECC was also used to complete a major study (in collaboration with Dr. Scott A. Wood of the University of Idaho) of the solubility of $\text{Nd}(\text{OH})_3$ in dilute NaCl solutions from 30 to 290°C. The pH was monitored continuously and samples were periodically withdrawn for total neodymium analyses. Thermodynamic reversibility was demonstrated by subsequent additions of acid and base titrant under near-equilibrium conditions. These studies permitted extraction of the stability constants for Nd^{3+} and $\text{Nd}(\text{OH})_3^\circ$ over a wide range of temperatures, and the intermediate species $\text{Nd}(\text{OH})^{2+}$ and $\text{Nd}(\text{OH})_2^+$ at the highest temperatures. The complete hydrolysis of Nd^{3+} (an excellent analog for trivalent actinides) to the neutral tri-hydroxide occurs over a very narrow pH range, and no evidence for an anionic species, such as $\text{Nd}(\text{OH})_4^-$, was observed, even at quite high pH's. These represent the first such studies of the solubility and speciation of a rare earth element at temperatures above 100°C.

A new potentiometric concentration cell employing $\text{Hg}/\text{Hg}_2\text{SO}_4$ electrodes was developed for highly precise and accurate measurement of the difference in SO_4^{2-} concentration between a reference solution of known sulfate concentration and a test solution in which the complexation of metal ions by sulfate is investigated. With this apparatus the stability constants of $\text{Al}(\text{SO}_4)^+$ and $\text{Al}(\text{SO}_4)_2^-$ complexes were determined in 0.3, 0.5 and 1.0 molal NaCl solutions at 10, 25 and 50°C. These results were fit using a Pitzer-type activity coefficient model and the resulting infinite-dilution constants were found to be higher than any previously published work at low temperature. These new results agree quantitatively at 50°C with the aluminum sulfate complexation studies conducted earlier in this program at the same temperature from gibbsite solubility measurements and at 50-125°C from homogeneous titrations in the HECC. The new results place important constraints on weathering rates and aluminum toxicity associated with acid rain and acid mine drainage (where high sulfate concentrations and very low pH's are encountered) in sensitive environments.

HECC cell studies were also completed on the complexation of cadmium, a highly toxic metal encountered in mixed wastes, with acetate, the most abundant organic acid anion found in groundwaters and landfill leachates. The stabilities of $\text{Cd}(\text{Ac})^+$ and $\text{Cd}(\text{Ac})_2^\circ$ were determined in 0.1, 0.3 and 1.0 molal NaTr solutions from 50 to 250°C.

Mechanisms and Rates of Isotope Exchange in Mineral-Fluid Systems

D. R. Cole (865-574-5473; Fax: 865-574-4961;coledr@ornl.gov), L. R. Riciputi and J. Horita

Objectives: The major objective of this research is to measure the rates of isotopic exchange between mineral and fluids controlled by one of two general mechanisms: surface reactions leading to recrystallization and volume diffusion.

Project Description: Equilibrium isotope fractionation factors and rates of isotopic exchange (via diffusion or mineral transformation mechanisms) form the cornerstones for interpretation of stable isotope data from natural systems. Microscale studies (high precision of small sample sizes or *in situ* spot analysis) of mineral-fluid interaction in natural systems indicate that: (a) isotopic heterogeneity and disequilibrium may be more widespread than previously realized, (b) isotopic disequilibrium can occur at high as well as low temperatures, (c) different minerals exhibit varying susceptibilities to retrograde fractionation and re-equilibration, and (d) the mechanisms of isotopic exchange are varied depending on the prevailing geochemical conditions (*e.g.*, temperature, pressure, fluid chemistry, fluid/solid ratio, *etc.*). Because of the recent advances in analytical techniques, the need for accurate, reliable fractionation factors and rate constants has never been greater. Realizing this need, we have focused our BES research on the experimental determination of rates and equilibrium fractionations for a variety of geologically relevant mineral-fluid (gas) systems for which data are either lacking, limited or, in some cases, controversial.

Results: We determined the diffusivity of C and O in calcite reacted with dry CO₂ to establish the lower limit on the rate of diffusion. Experiments in cold-seal hydrothermal vessels were performed at 100 MPa over a range in temperature from 600 to 800°C. The starting materials were single crystals of Mexican calcite that were pre-annealed to remove any non-equilibrium defects before the experiment. The single crystals were placed in platinum capsules with CO₂ consisting of 99% ¹³C and 90% ¹⁸O. After heating for periods ranging from 7 to 147 d, C and O diffusion profiles were measured with the ion microprobe. The diffusivity of C is $D_{\text{Carb}} = 7.77 \times 10^{-9} \exp(-166 \pm 16 \text{ kJ/mol/RT}) \text{ cm}^2/\text{s}$ and of O is $D_{\text{Oxy}} = 7.5 \times 10^{-3} \exp(-242 \pm 39 \text{ kcal/mol/RT}) \text{ cm}^2/\text{s}$. The activation energies are lower than those for C and O diffusion at 1 atm, and the pre-exponential factor for C is several orders of magnitude lower than that measured at low pressure. The combination of low activation energies for both C and O and the very low pre-exponential factor for C is consistent with diffusion by a simple vacancy mechanism in the intrinsic region. Carbon appears to diffuse as a carbonate anion group, and oxygen appears to diffuse primarily as a single anion. Closure temperatures were calculated for isotopic exchange by diffusion.

In conjunction with single-crystal hydrogen isotope exchange studies, we have initiated hydrogen diffusion studies in epidote, amphiboles, brucite, and chlorite. A variety of museum-quality crystals of epidote, brucite, chlorite, pargasite, and tremolite have been mineralogically characterized (*e.g.*, SEM; electron microprobe), cut, and carefully polished prior to hydrothermal experimentation. For example, single crystals of epidote were reacted with varying amounts (50 – 100 mg) of 99% D₂O at temperatures between 200 and 600°C and a pressure of 2 kbar. Only those crystals that exhibited minimal roughness ($\pm 0.1 \mu\text{m}$) and an absence of surface mineral growth were selected for SIMS analysis. The ion microprobe was used to determine D/H profiles parallel to the \underline{b} crystallographic orientation (faster direction). The diffusion coefficients for epidote between 200-600°C are slower than those estimated from either a plate or cylinder model using more ambiguous bulk powder-water exchange data. It is clear that we are just beginning to understand the reactivity of hydrous phases, the rates of H-isotope diffusion in natural hydrous phases obtained from the ion probe, and how to quantify the factors that govern hydrogen transport in hydrous phases.

CONTRACTOR: Pacific Northwest Laboratory

Batelle, PNNL
Richland, WA

CONTRACT: DE-AC06-76RLO 1830

CATEGORY: Geochemistry

PERSON IN CHARGE: A. Felmy (509-376-4079; Fax: 509-376-3650; ar.felmy@pnl.gov)

Local Reactions on Carbonate Surfaces: Structure, Reactivity, and Solution

D.R. Baer (509-375-2375; Fax: 509-375-5965; dr_baer@pnl.gov), and J.E. Amonette (509-372-6125; Fax: 509-376-6328; je_amonette@pnl.gov)

Objectives: The purpose of this program is to develop a fundamental, microscopic understanding of the structure and chemistry of carbonate surfaces, including the interactions between adsorbates and mineral surfaces.

Project Description: This project involves an interdisciplinary theoretical and experimental effort designed to gain a fundamental, molecular-level understanding of carbonate mineral surface structure and chemistry. Carbonate minerals are particularly important in the global carbon dioxide cycle and in subsurface contaminant migration processes. The availability of large, single crystals allows fundamental measurements to be made on well-defined surfaces. By linking experimental studies of geochemical reactions on single-crystal surfaces with first-principles quantum-mechanical model calculations to describe the surface and interfacial structure and chemistry, a systematic study of the factors controlling the surface chemistry of carbonate minerals can be made. In particular, the effects of substitutional impurities and other point chemical defects on the structure and geochemical reactivity of carbonate mineral surfaces and interfaces can be isolated and quantified. Moreover, this improved microscopic understanding will eventually provide insights into the behavior of these materials in natural systems.

The approach to meeting program goals involves three interdependent efforts: 1) developing *ab initio* models for interpreting experimental observations regarding the structure and chemistry of the calcite cleavage surfaces; 2) studying the structure and chemistry of the cleavage surface in vacuum; and 3) comparing surfaces in vacuum with those in model geochemical environments. Many of the experimental measurements involve the use of Atomic Force Microscopy. Collaboration with Prof. Larry Sorensen at the University of Washington facilitates the comparison of the real space AFM with inverse space x-ray scattering.

Results: In FY1999, experimental work centered on observing growth of an Mn-containing phase on the calcite cleavage surface in solution and measuring the impact of Ca on pit growth and fill-in.

The growth of a Mn-induced phase on the calcite surface had been observed in our previous investigation of Mn-solution effects on calcite dissolution. This phase has a striking visual character due to the rapid growth in one direction and growth to a maximum size in height and width (as shown in Figure 1). Among the interesting properties of these Mn precipitates are the wide range of length, the constant 3-nm height, and the small width variation of approximately 200 nm. We find that the

precipitate growth rate initially increases with Mn concentration, subsequently slows as the general rate of calcite dissolution decreases, and then increases again at higher Mn concentrations. However, at the highest Mn levels, the high degree of orientation of the crystals decreases. Other measurements show that initially the crystals grow in both width and length until the width reaches approximately 230 nm at which time the width ceases to change, and the rate of overall length growth decreases slightly. The height of the crystals is roughly that expected for a critical thickness within which there is no defect formation. We assume that the width growth is limited by a strain effect. We have been unsuccessful at fully characterizing the small phase; as a result, we do not have important information about lattice mismatch, which is needed to further explain these observations.

A Masters of Science in Chemical Engineering thesis “Solution Effects on Calcite Dissolution” was completed that extended our previous carbonate work in two areas. First a mixed kinetic rate expression that relates step retreat velocities to the surface reaction and to the hydrodynamic conditions of the AFM flow cell was developed. This expression facilitates an understanding of the experimental data from the AFM for conditions in which both flow and solution composition effects play important roles. Second, the effect of calcium solution concentrations on dissolution was measured. Earlier measurements had shown that when HCO_3^- ions were added to the solution they influenced primarily one type of site along one type of step. Ca^{++} on the other hand, influenced both step types and did not enhance pit rounding. Another interesting result of this work was the observation that when solution concentrations reach saturation, the corner of the closed steps serves as a nucleation site and pits begin to fill in. Having one specific corner serve as the primary site allows the rate of that specific active site to be determined during pit fill-in or calcite growth.

Several models for interpreting experimental observations were developed. A “blocking” version of the terrace-ledge-kink (TLK) model was used to explain the effects of Mn and Sr on the rates of step retreat or pit growth. If Mn or Sr ions sorbed on a step block dissolution when present then there may be a fundamental change in behavior when the rate of arrival of a blocking ion becomes nearly identical to the rate of double kink formation along a step. This model appears to explain experimental observations quite nicely. The addition of back reactions to our Kinetic Monte Carlo (KMC) model for dissolution was used to understand the sorption processes that occur during general dissolution. A 2-D cellular automata KMC model simulates the effects of dissolution, re-adsorption, diffusion, and fluid flow on calcite surface crystallographic step evolution and rate of motion. It reproduces the AFM wet cell data in both the reaction-controlled regime (fast flow) and the diffusion-controlled (slower flow) regions. As part of the MS thesis, a more engineering “solution flow” model helped to further our understanding of the flow rate on solution and surface behaviors was developed.

Geometric and Electronic Structure of Oxide Surfaces

A. C. Hess (509-375-2052; Fax: 509-375-2426;anthony.hess@pnl.gov)

Objectives: Our program of study involves the development and use of first principles solid state quantum mechanical methods to gain a fundamental understanding of the geometric and electronic structure and chemical properties of oxide, transition metal oxide and aluminosilicate surfaces.

Project Description: Activities focus on detailed investigations of the adsorption, desorption and diffusion of molecular and atomic species and the dissociative chemisorption of molecular entities at the internal and external surfaces of such materials.

Results: A brief overview of the basic theory associated with periodic Gaussian basis density functional theory will be given with particular emphasis on describing our recently completed formulation and implementation of analytical first derivatives of the total crystal energy with respect to nuclear coordinates (atomic forces). The addition of this new capability to the existing solid-state program GAPSS has greatly increased our ability to investigate the geometric structure of complex surface-adsorbate complexes. The overall behavior of the new force method, including absolute and relative accuracy, will be illustrated by presenting detailed results from selected systems. To provide a self-contained example of how first-principles methods can be used to understand the mechanisms by which adsorbates influence surface geometric and electronic properties (and *vice-versa*) and to illustrate some of the primary sources of error in such calculations we will discuss the details of Group Ia metals co-adsorbed with CO on a MgO (001) surface over a range of coverages. The metal to non-metal transitions found at selected metal atom surface coverages and the influence of the metal electronic and magnetic structure on the adsorption properties of CO will be presented in detail. Finally, the sensitivity of both the geometry and energetics of the total co-adsorption system and its principle components to the choice of gradient and non-gradient corrected density functionals will be described. The purpose of this latter activity is to demonstrate how sensitive selected properties of weakly bound (or physisorbed) systems can be to this common change in formalism.

Structure and Reactivity of Iron Oxide and Oxyhydroxide Surfaces and Interfaces

J.R. Rustad (509-376-3979; Fax: 509-376-3650; james.rustad@pnl.go), A.R. Felmy (509-376-4079; Fax: 509-376-3650), D. A. Dixon (509-372-4999; Fax: 509-375-663); David.Dixon@pnl.gov), M. Dupuis (509-376-4921; Fax: 509-376-0420)

Objectives: The objectives of this program are to (1) develop molecular models of hydroxylated ferric and ferrous oxide and oxyhydroxide surfaces (2) use these models to better understand the relationship between structure and reactivity for this class of minerals, and (3) use this knowledge to improve thermodynamic calculations using surface complexation models.

Project Description: Ferric oxides have high specific surface areas, high affinities for oxyanions and heavy metals, and actively respond to changes in redox conditions in natural environments. These minerals are therefore important in a variety of low-temperature geochemical processes, particularly those in which adsorption and dissolution couple with fluctuations in redox potential. For many solutes, measurements of sorption density *versus* aqueous concentration suggest the presence of a heterogeneous array of surface sites having a range of affinities for the probing solute. Crystallographic differences in coordination and geometrical arrangements of surface oxide sites are a fundamental aspect of this heterogeneity. In this project, the effects of crystal chemistry on adsorption are evaluated using computational molecular modeling techniques. These results are then used to produce a more robust thermodynamic description

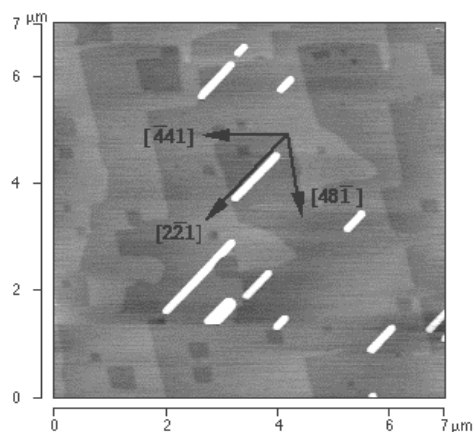


Figure. AFM image of calcite cleavage surface in solution showing an Mn-rich rod-like phase.

of adsorption at the mineral-water interface.

Results: Plane Wave Pseudopotential Calculations on Fe and Al Oxyhydroxides: The equation of state of diasporite (α -AlOOH) was investigated theoretically using the plane-wave pseudopotential method. Both norm-conserving and ultrasoft pseudopotentials were used in conjunction with both the local density and generalized gradient approximations to generate pressure-volume relations for diasporite to 25 Gpa. All the resulting structures converged to Pbnm, which is the experimentally determined space group for diasporite. The local density approximation with both the ultrasoft and norm-conserving pseudopotentials gives bulk moduli about 10 percent too large. The ultrasoft pseudopotentials, when used with either the local density or generalized gradient approximations, tend to give unit cell volumes which are too small. The combination of the generalized gradient approximation and the norm-conserving pseudopotential gives excellent results for lattice parameters at pressures up to 25 Gpa, and bond lengths and bond angles measured from x-ray diffraction at ambient pressure, agreement in all cases being better than 1 percent. These calculations suggested a re-interpretation of the main compression mechanism identified in diasporite and goethite.

Plane-wave pseudopotential methods were used to investigate the structures and total energies of AlOOH and FeOOH in the five canonical oxyhydroxide structures: diasporite (goethite), boehmite (lepidocrocite), akaganeite, guyanaite, and grimaldiite. The local density approximation was used in conjunction with ultrasoft pseudopotentials in full optimizations of both AlOOH and FeOOH in each of these structures. Structures are in reasonably good agreement with experiment, with lattice parameters and bond lengths within 3 percent of the experimental ones. Neither AlOOH nor FeOOH have been identified in the grimaldiite or guyanaite structures, however we find that total energies for AlOOH and FeOOH in these structures are comparable to or lower than the total energies of the commonly observed polymorphs (with the exception of FeOOH in the grimaldiite structure, which is anomalously high energy). For diasporite and boehmite we also provide calculations using the generalized gradient approximation and norm-conserving pseudopotentials to assess the extent to which the results depend on the particular level of theory used. We find that while diasporite has a lower energy in the local density approximation, boehmite has a lower energy in the generalized gradient approximation, in contradiction to experimental observations. Thus, while one may reasonably conclude that the differences in total energies of the various (Al, Fe)oxyhydroxide polymorphs are small, current electronic structure methods do not appear to be capable of accurately resolving these small differences. These findings provide further confirmation that the structures of oxyhydroxide polymorphs and surface precipitates are more likely to be a function of kinetics than of intrinsic lattice stability.

The excellent agreement with experiment on the diasporite equation of state justified use of the plane-wave pseudopotential method on the hydroxylated corundum (012) surface. A study similar to our earlier work on hematite (012) (see last year's FWP) was carried out on corundum (012). This work was carried out to provide an additional check on the molecular dynamics studies on hematite (012) (corundum is at least in some respects a good model for hematite, but is more computationally tractable for ab initio calculations). The goal of this work was to estimate the extent of dissociation of water on corundum (012), and compare the result with that calculated for hematite (012). Density functional calculations confirmed our predictions based on empirical potentials, that at least 50 percent of the water on the (012) surface. Water adsorption energies were lower for the DFT calculations than for the empirical potentials, but hydroxylation energies were still negative for the DFT calculations (*i.e.* the water adsorption energy is greater than the cleavage energy), as is the case for the calculations using empirical potentials.

Classical Simulation of the Hydroxylation and PZC of the Magnetite (001) “A” and “B” Terminations: A classical polarizable potential model is used in a molecular dynamics model of the magnetite (001) surface. The model, previously applied to the tetrahedral, or “A” termination of magnetite (001) is here applied to the octahedral or “B” termination, as well as to the hydroxylation of both the “A” and “B” termination. Surface relaxations for the “B” terminated surface are small, and consistent with the observed $(\sqrt{2} \times \sqrt{2})R45$ cell observed in LEED experiments. Additionally, it is shown that the relaxation of a tetrahedral defect on the “B” terminated surface does not give rise to the same relaxation mechanism as that calculated for the tetrahedral sites on the “A” surface. The lack of a “ccurr” forming at the defect site is consistent with recent STM studies. Calculations on charge-ordered magnetite slabs indicate that, within the context of the ionic model used here, the surface energy of the “A” termination of magnetite is lower than that of the “B” termination over a wide range of oxygen fugacities. Hydroxylation has a negligible effect on the relative energies of the “A” and “B” surfaces, however, the large gain in energy associated with tetrahedral ion relaxation on the “A” surface could explain the lack of two high temperature peaks expected for successive removal of adsorbing waters from the same tetrahedral site (C. H. F. Peden *et al.*, unpublished).

Proton affinity and acidity calculations were carried out for the “A” terminated surface to check whether the predicted pH of zero charge was less than that of hematite, as generally predicted experimentally. Our prediction, based on our previous methods, using a linear free energy relationship between the surface acidity and the deprotonation energy, gave erroneous results, with the PZC occurring around 9.6, less acidic than either the hematite or goethite PZC. We hypothesize that solvent effects account for this discrepancy by enhancing the acidity of the tetrahedral Fe^{3+} at the surface.

Na-OH-H-SiO₄ –PO₄-SO₄ Crystal Structures: We have made considerable progress testing our *ab-initio*-based potential functions on a variety of oxyanion hydrate crystal structures. To do this, we introduced sodium ion into the set of potential functions. This was deemed necessary because of the large amount of experimental data available for the hydrated Na salts with the oxyanions of interest to us. We tested the results on sodium hydroxide hydrate crystal structures: $\text{NaOH}(1,3,5,4,7) \cdot \text{H}_2\text{O}$ lattice constants and Na-O bond lengths were within 5 percent of experiment in all cases. The hydrated hydrogen silicate and dihydrogen silicate sodium salts $\text{Na}_2\text{H}_2\text{SiO}_4 \cdot (4,5,7,8)\text{H}_2\text{O}$ and $\text{Na}_3\text{HSiO}_4 \cdot (1,2,3)\text{H}_2\text{O}$ were gave lattice constants within our 5 percent target error, and gave stable protonation states in agreement with experimental ones. This is not a trivial result and the proton affinity of the hydrogen silicate anion is more than enough to hydrolyze water in the gas phase. The fact that we did not observe these hydrolysis reactions in solution provides some validation that the solvent stabilization of the hydrogen silicate anion is in the right range. Similar calculations are in progress on the sulfate and phosphate structures.

Parametrization of the Chromate Model: Using quantum mechanical calculations, we have also parameterized a model for chromate which is valid over all relevant protonation states over the range of oxidation states from (VI) to (IV). The deprotonation energies and bond lengths are very good, except for the proton affinity of H_3CrO_4^- , we are working on improving this latter value, its effect is that the intermediate species $\text{H}_4\text{Cr(IV)O}_4$ is in fact much more acidic than orthosilicic acid, and will readily hydrolyze. We have used the model to examine coordination changes from tetrahedral to octahedral as the chromium becomes reduced in aqueous solution. We find no coordination change for the Cr(IV) species, which is of significance because it has been speculated for some time that this coordination change is the rate limiting step in the reduction of chromate. We are investigating Fe(III)-Cr(IV) complexes to investigate whether complexation has any effect on the coordination of Cr(IV) in aqueous solution

Electron Transfer at the Fe(III) Oxide-Microbe Interface

J. M. Zachara (509-376-3254; Fax: 509-376-3650; john.zachara.pnl.gov), J. K. Fredrickson (509-376-7063; Fax: 509-376-1321; jim.fredrickson@pnl.gov), Y. Gorby (509-373-6177; Fax: 509-376-1321; yuri.gorby@pnl.gov), and T. Beveridge (519-824-4120; Fax: 519-837-1802; tjb@micro.uoguelph.ca)

Objectives: The project objectives are to 1) develop an improved understanding of the interfacial mechanisms of electron transfer between dissimilatory Fe(III)-reducing bacteria and Fe(III) oxides; and 2) define the mineral structural, thermodynamic, and kinetic factors that control the rate and extent of bacterial Fe(III) oxide reduction as a basis for predicting microbiologically driven reduction rates and transformations in subsurface environments.

Project Description: Bacterial iron (III) reduction is a key process in sediments and subsurface environments that controls the aqueous and solid phase speciation of Fe and other polyvalent metals, radionuclides, and contaminants (*e.g.*, Co, U, Cr, Tc, *etc.*). In spite of its widespread importance, the mechanisms of bacterial electron transduction to Fe(III) oxides and the factors that control it remain unknown. Research in this project is investigating microscopic aspects of bacterial iron (III) oxide reduction using spatially-resolved synchrotron based spectroscopies, high resolution electron and scanning probe microscopies, and transmission and conversion electron Mössbauer spectroscopies. Laboratory experiments using a well studied bacterium (*Shewanella putrefaciens*) and abiotic reductants (ascorbate, cysteine, AQDS); and synthetic, epitaxial iron oxide films and crystallites of known face exposure and variable defect densities (hematite, magnetite) are used to investigate fundamental hypotheses related to electron transfer at the oxide-organism interface. Focal points of the research include: 1.) the influence of Fe(III) oxide surface structure and energy on microbiologic reduction and the nature/spatial distribution of geochemical products formed; and 2.) the architecture of the bacteria-mineral association including the spatial location of the cytochromes and exopolysaccharide (EPS) relative to the oxide surface and areas of reduction.

Results: FY 99 research has investigated thermodynamic controls on bacterial Fe(III) oxide reduction using magnetite and hematite as model systems. Both of these Fe(III) oxides are extremely stable and are bacterially reducible only under certain conditions for reasons that are not well understood. Magnetite (Fe_3O_4), a mixed valence oxide [Fe(II)/Fe(III)], is considered a stable mineral phase under anoxic conditions and not susceptible to bacterial reduction. Accordingly it has been used as a heavy-mineral geochemical marker of provenance (*e.g.*, sediment origin). We have shown, however, that magnetite can be reduced by subsurface bacteria under typical subsurface geochemical conditions. Importantly, it has been observed that the identity, thermodynamics, and precipitation mechanism of the biomineralization products controls the rate and extent of bacterial magnetite reduction. The accompanying figure is an SEM image of fine-grained magnetite that has been contacted with *S. putrefaciens* in bicarbonate buffer with

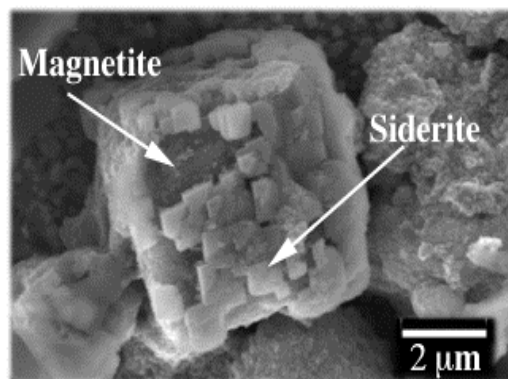


Figure. Bacterial reduction of goethite (FeOOH) to magnetite (Fe_3O_4) and siderite (FeCO_3)

lactate as an electron donor. Bioreduction only occurred in association with siderite precipitation. Siderite formation provided a thermodynamic lever that was exploited by the organism to gain internal energy in the magnetite. Siderite formation occurred topotactically to the magnetite, leading to a unique morphologic association of magnetite-cored siderite. This mineral association has been observed in anoxic geologic environments and sediments, and its mode of formation has previously been enigmatic. Our results define a plausible diagenetic mechanism.

Researchers have long puzzled over the factors that control the availability of crystalline Fe(III) oxides such as goethite, hematite, and lepidocrocite to microorganisms. Are oxide free energies, surface areas, or surface structures more important? We have shown using a series of hematites of differing morphologies and surface area, that crystallite face exposure, and accordingly surface energy and structure, are key determinants of the bioreducibility of a Fe(III) oxide. The basal plane (001), which often predominates hematite crystallites in terms of total surface area, appears recalcitrant to microbial attack. Discussions with other BES collaborators (*e.g.*, Rustad and Felmy) suggest that this recalcitrance results from the surface coordination structure of (001) which is dominated by hydroxyls with high coordination number (*e.g.*, >1). Research planned for FY00 will examine crystallite face issues in more detail, using epitaxially grown hematite and tabular hematite crystallites with different aspect/surface area ratios of (001) to bounding faces.

CONTRACTOR: Sandia National Laboratories

Lockheed Martin
Albuquerque, New Mexico 87185

CONTRACT: DE-AC04-94AL85000

CATEGORY: Geophysics and Earth Dynamics

PERSON IN CHARGE: H. R. Westrich

Effects of fluid flow on inelastic deformation and failure in dilating and compacting rock

W. A. Olsson (505-844-7344; Fax: 505-844-7345; waolss@sandia.gov) and D. J. Holcomb

Objectives: One of the proposed strategies for mitigation of carbon dioxide emissions is to sequester CO₂ in depleted oil or gas reservoirs. For the implementation of this strategy, it is critically important to understand how producing the original contents of the reservoir has changed the stress and deformation states and the properties of the rocks making up the reservoir trap. For example, certain deformation structures, such as shear and compaction bands, often compartmentalize a hydrocarbon reservoir before or during production. Thus, inelastic deformation during earlier production or reinflation with CO₂ may produce structures that interfere with fluid migration and make the reservoir unattractive as a potential CO₂ repository.

Project Description: We are applying coordinated experimental, theoretical, and numerical techniques to the problem through an existing university-national laboratory collaboration. J. W. Rudnicki at Northwestern University, is addressing the theoretical and numerical aspects; and W. A. Olsson and D. J. Holcomb at Sandia National Laboratories are designing and carrying out the experimental part of the program. Deformation experiments are being performed on porous sandstone characteristic of oil and tgas reservoirs. The Three main objectives of this work are: (1) to illuminate the phenomenology of dilatant/compactive rock containing pore fluid in the drained and the undrained response, and test predictions of current theory, (2) to collect the appropriate constitutive data constrained and suggested by developing theoretical models, and (3) to construct well-posed experiments that can be used as validation tests against a numerical implementation of the theory to be developed as part of this research. Additional aspects of compaction of porous rock will also be included; porous rock is known to have a cap on the yield surface and this will be addressed in the considerations. The theoretical analytical model will be implemented into a numerical model for comparison to the validation experiment.

Results: Triaxial compression experiments on Castlegate sandstone (porosity = 28%) under certain conditions lead to compaction banding. To better understand the dynamics of the compaction process in these experiments we instrumented cylinders of Castlegate with 12 acoustic transducers and then subjected the specimens to triaxial loading at 45 to 80 Mpa confining pressure. Acoustic emissions (AE) were monitored continuously throughout the experiments, and then locations of the events were determined. During triaxial loading, near peak stress, one or two narrow tabular zone(s) of AE events, perpendicular to the maximum compression direction, appear near one or both ends of the cylinder. These zone(s) move toward the center of the specimen with increasing applied axial strain, and can be forced to coalesce by continuing to increase the shortening. Microscopic observations show that the

rock behind the AE zones are highly compacted, thus we interpret these moving zones of AE events to be the boundaries or fronts between compacted and uncompacted material. Therefore, compaction of the specimens occurs nonuniformly by the initiation and slow propagation of compaction fronts into the uncompacted material. This appears to be a previously unrecognized mode of deformation of porous rock.

Permeability measurements are being made axially across the specimens during experimentation. The permeability drops dramatically upon formation of the band(s), and then continues to decrease steadily with propagation of the band(s). Total change in permeability is about 2 orders of magnitude.

Inversion of Full Waveform Seismic Data for Shallow Subsurface Properties

D. F. Aldridge (505-284-2823; Fax: 505-844-0240; dfaldri@sandia.gov), G. J. Elbring, and D. E. Womble)

Objective: This research plans to demonstrate the applicability of full waveform seismic inversion methodologies to shallow subsurface environmental characterization or remediation targets.

Project Description: Inversion of full waveform seismic data is a large-scale, nonlinear, geophysical inverse problem. A successful attack on this problem requires robust computational tools for i) calculating realistic simulated seismic data from a prescribed Earth model, and ii) inverting these data to recover the Earth model properties. The general inversion procedure entails iteratively refining a candidate Earth model until an acceptable match is obtained between predicted (*i.e.*, computed) and observed seismic data. Typically, a least squares measure of data misfit is adopted. Imposition of model regularization constraints during each iteration restricts the non-uniqueness associated with the problem, and allows noisy data to be examined. This formal inversion approach for recovering Earth model properties may be especially relevant to shallow subsurface targets where the seismic arrivals (reflections, refractions, diffractions, surface waves, *etc.*) are not easily separated *via* conventional data processing techniques.

Results: A seismic wave propagation algorithm appropriate for three-dimensional (3D) isotropic elastic media has been developed. The algorithm is based on the velocity-stress equations of linear elastodynamics, a system of nine, coupled, first-order partial differential equations. Solution yields the three components of the particle velocity vector, and the six independent components of the stress tensor. An explicit, time-domain, finite-difference (FD) numerical scheme is used to solve this system. Centered spatial and temporal FD operators possess 4th-order and 2nd-order accuracy in the discretization intervals, respectively. The nine dependent variables are stored on uniform, but staggered, spatial and temporal grids.

The computational algorithm is a direct numerical implementation of the governing partial differential equations of linear isotropic elasticity. No theoretical approximation, such as far-field distances, high frequencies, weak scattering, or one-way wave propagation, is adopted. Hence, the algorithm generates all seismic arrival types (P-waves, S-waves, reflections, refractions, multiples, mode-conversions, diffractions, head waves, surface waves, *etc.*) with fidelity, provided the spatial and temporal gridding intervals are chosen appropriately.

Special attention is devoted to representing the large variety of energy sources and receivers common in the seismic exploration arena. Most such sources may be idealized as one or more stationary point

forces, dipoles, couples, torques, explosions/implosions, surface tractions, *etc.* Multiple point sources may be activated simultaneously, with independently specified orientations, magnitudes, and waveforms. Hence, spatially extended source arrays may be modeled. Seismic energy receivers are considered to be particle velocity sensors (geophones), acoustic pressure transducers (hydrophones), or particle rotation sensors. The directional transducers may be oriented in any direction. Hence, multicomponent recording is easily simulated. Finally, general (*i.e.*, fully 3D) recording geometries are permitted; sources and receivers may be distributed at arbitrary locations on and/or within the 3D Earth model.

In order to simulate seismic conditions at the Earth's surface, an explicit representation of a plane, vanishing-stress surface boundary is included in the algorithm. Point traction sources, with arbitrary orientations, may be imposed on this surface. Nonplane surface topography will be incorporated into the algorithm in the future. However, preliminary testing indicates that a nonplane stress-free surface can be mimicked by assigning the material properties of air to grid nodes above the surface. Algorithm stability is maintained by making the earth/air interface gradational.

Significant computational resources are required to execute this 3D elastic wave propagation algorithm. In order to treat realistic-sized Earth models (*e.g.*, tens of millions of spatial gridpoints) and trace durations (*e.g.*, tens of thousands of timesteps) with reasonable execution times, parallel versions of the algorithm have been developed and sited on appropriate computational platforms. Parallel codes use Message Passing Interface (MPI) and Parallel Virtual Machine (PVM) coding protocols to maintain algorithm portability.

Synthetic seismograms replicating borehole experiments conducted at Bayou Choctaw Salt Dome in Louisiana have been computed, and are a reasonable match to the field-recorded data, although with reduced spectral bandwidth. A primary goal of these field experiments is to record reflected energy from the nearby, nearly vertical, salt dome flank. Computational modeling of these data assist in understanding the various geological and geophysical factors that influence the strength, character, and even existence, of salt flank reflections.

The 3D elastic wave propagation algorithm described above forms the "driver" for an iterative full waveform inversion scheme. We are presently investigating two specific inversion approaches: i) the gradient method, and ii) the subspace method. Each has merits, and we intend to develop a hybrid approach incorporating the advantages of each. For example, the gradient method does not involve solving a large system of linear, algebraic equations to obtain the model update. However, it is difficult to incorporate *a priori* geological/geophysical constraints into the inversion methodology. In contrast, the subspace method allows the straightforward introduction of constraints, but requires the solution of a linear system of equations.

Micromechanical Processes in Porous Geomaterials

J. T. Fredrich (505-844-2096; Fax: 505-844-7354; fredrich@sandia.gov) and T. Wong (State University of New York at Stony Brook)

Objectives: This project focuses on the systematic investigation of the microscale characteristics of natural Earth materials, and how these micro-scale characteristics control the macroscopic deformation and transport behavior. The research uses an integrated approach consisting of experimental rock mechanics testing, quantitative 2D and 3D microscopy and statistical microgeometric characterization, and theoretical and numerical analyses. The objective is to enhance fundamental understanding of

failure and transport processes in geologic materials, and thereby strengthen the theoretical basis for the application of laboratory results to various technological operations of importance.

Project Description: Knowledge of the microscale characteristics and behavior of rocks is important for several energy-related applications, including global climate change and carbon management; oil field geoscience; geotechnical engineering efforts such as design and assessment of geologic nuclear waste repositories; and environmental remediation efforts at contaminated DOE and/or DoD installations. We use an integrated approach consisting of experimental rock mechanics testing, quantitative microscopy, and theoretical and numerical analyses. The experimental investigation provides a detailed understanding of the microstructure of geologic materials and how the microscale characteristics affect macroscale behavior including brittle failure and fluid transport. Detailed and quantitative microstructural studies complement laboratory rock mechanics experiments. The results are used to formulate and evaluate theoretical and numerical models of rock deformation and fluid flow.

Results: (1) Pore-scale lattice Boltzmann numerical simulations require flow definition at the model ingress and exit; however, this condition is not definable a priori for flows in complex porous media. Instead, this requirement is typically handled by “wrapping” flow around the model boundaries. But, because of the geometric mismatch at the model boundaries for complex porous media, this requires mirroring the model domain (in 3 dimensions). Because of the computational cost associated with this approach, alternative formulations were developed to define the flow conditions at the boundaries implicitly, rather than explicitly. (2) The sensitivity of the flow simulations to image segmentation is being assessed quantitatively. The 3D image data are gathered at 8-bit resolution and typically 10-15% of voxels contain a mixture of solid and void phase. We are comparing two global and one local segmentation scheme. (3) Work was initiated to develop a numerical framework to allow the raw unsegmented image data to be mapped directly onto the LB flow simulation. (4) A collaboration was initiated with Prof. Kohlstedt at the Univ. of Minnesota. We are performing 3d flow simulations to calculate the permeability of partially molten mantle rocks using binarized image data from serial sectioning. This is a unique application as the permeability of the system of interest can only be assessed through numerical simulation. (4) Optical and scanning electron microscopy studies are being performed to elucidate the micromechanics of compaction in an analogue reservoir sandstone. The microscopy, that includes quantitative stereological measurements, suggests that compaction of this weakly cemented sandstone under a triaxial load path was accommodated in two distinct stages. The first stage of compaction was associated with breakage of the minimal cement bonding the framework grains and subsequent rotation of the intact framework grains to yield a more compact grain packing. This stage reduced the macroporosity by an estimated 27%. The second stage of compaction was associated with intense grain comminution and subsequent rotation of the grain fragments and resulted in substantial additional reduction in porosity and bulk volume.

Resolution and Accuracy of 3-D Electromagnetic Imaging

G. A. Newman (505-844-8158; Fax: 505-844-7354; ganewma@sandia.gov) and D. L. Alumbaugh

Objectives: The objective of this research two fold. The first objective is to develop and analyze techniques for quantifying the resolution of, and appraising the accuracy of images produced by 2D and 3D electromagnetic inversion schemes, and to apply these techniques to field data. The second objective is to develop and the implement 3D magnetotelluric (MT) modeling and inversion schemes to

demonstrate expected resolution improvements compared to standard, and much faster, 2D data analysis over 3D targets.

Project Description: Non-linear electromagnetic inversion for 2D and 3D subsurface imaging of electromagnetic properties has rapidly evolved over the last decade due to its potential benefit in the areas of contaminant waste site characterization, oil and mineral exploration and delineation, and ground water resource evaluation. However, before we can proceed on inverting field data and interpreting the resulting images with any level of confidence, methods of appraisal and error analysis must be developed. The purpose of this project is to examine established methods for this purpose such as calculating the model covariance and model resolution matrices through direct matrix inversion using Bakus-Gilbert theory, and examine procedures that estimate these resolution parameters without direct matrix inversion; the latter is required when iterative techniques such as Conjugate Gradients are employed within the inversion scheme.

An outstanding problem in the interpretation of 3D magnetotelluric (MT) data sets have been the lack of robust and computationally efficient 3D inversion schemes. Whilst 3D forward modeling can be applied to these types of data sets, it is often too cumbersome to use for trial and error fitting of observed data. To overcome the computational barriers of 3D inversion, we have implemented a preconditioned non-linear conjugate gradient solution on massively parallel computing platforms. Thus, large 3D MT data sets can now be analyzed and it is now possible to study the resolving power of 3D inversion compared to standard 2D data analysis.

Results: Linearized methods have been developed for appraising resolution and parameter accuracy in images generated with two- and three-dimensional (2D and 3D) non-linear electromagnetic inversion schemes. When direct matrix inversion is employed, the model resolution and a posteriori model covariance matrices can readily be calculated. Traditionally the main diagonal of the model resolution matrix has been employed to estimate the resolution properties of the inversion process. However, because this parameter alone cannot distinguish how the resolution varies in the different directions, we chose analyzing individual columns the model resolution matrix, which allows the spatial variation of the resolution in the horizontal and vertical to be estimated. Plotting the diagonal of the model covariance matrix provides an estimate of how errors in the inversion process such as data noise and incorrect *a priori* assumptions map into parameter error, and thus provides valuable information about the uniqueness of the resulting image.

Methods were also derived for linearized image appraisal when the iterative conjugate gradient technique is applied to solve the inverse problem rather than direct inversion. This technique must be employed for the 3D problem as direct inversion is computationally too demanding. An iterative statistical method was demonstrated to yield accurate estimates of the model covariance matrix as long as enough iterations are employed. Although determining the entire model resolution matrix in a similar manner is computationally prohibitive, individual columns of this matrix can be determined. Thus, the spatial variation in image resolution can be determined by calculating the columns of this matrix for key points in the image domain, and interpolating between. These linearized image analysis techniques were conducted on 2D and 3D synthetic cross well EM data sets, as well as a field data set collected at the Lost Hills Oil Field in Central California.

Because the above methods are linearized about a final model, there is uncertainty of how realistic an estimate they provide given that we are solving a nonlinear inverse problem. To investigate this aspect of image appraisal, a nonlinear technique for determining estimates of parameter uncertainty was developed for 2D cross-well EM inversion, and the results of this appraisal method compared to those

provided by the linearized technique. Here, parameter variance estimates are determined using the same Monte Carlo technique as employed above, except the entire nonlinear inversion rather than just the last iteration is rerun N times. Two oil field examples from California indicate that the linearized approach produces the same general pattern in the uncertainty estimates as the nonlinear estimation process. However, the linearized estimates are smaller in magnitude and show less spatial variation compared to the full nonlinear estimates, and the deviation between the two techniques increases as the contrast between the maximum and minimum parameter values increases within the inversion domain.

Three-dimensional (3D) magnetotelluric (MT) forward and inverse solutions have been implemented and applied in a resolution study for sub-salt imaging of an important target in marine magnetotellurics for oil prospecting. In the forward problem, finite difference methods are used to efficiently compute predicted data and cost functional gradients. A fast preconditioner is introduced at low induction numbers to reduce the time required to solve the forward problem. We demonstrate a reduction of up to two orders of magnitude in the number of Krylov subspace iterations and an order of magnitude reduction in time needed to solve a series of test problems. For the inverse problem, we employ a nonlinear conjugate gradient solution developed on massively parallel computing platforms. Solution stabilization is achieved with Tikhonov regularization. To further improve the image resolution of sub-salt structures, we have also incorporated two additional constraints within the inversion process. The first constraint allows for the preservation of known structural boundaries within the inverted depth sections. This type of constraint is justified for the sub-salt imaging problem because the top of salt is constrained by seismic data. The other constraint employed places variable lower bounds on the electrical conductivity above and below the top of salt. Cross sections of the inversion results over the center of the salt structures indicate that the 3D analysis provides somewhat more accurate images compared to faster 2D analysis, but is computationally much more demanding. On the flanks of the structures, however, 3D analysis is necessary as 2D inversion shows significant image artifacts arising from the 3D nature of the data. We conclude, however, that 3D inversion may not be cost effective for the sub-salt imaging problem. Very fine data sampling along multiple profiles employed in the 3D analysis yielded only a marginal improvement in image resolution compared to 2D analysis along carefully selected data profiles. The study also indicates that in order to provide resolution that is required to accurately define the base of the salt, additional constraints beyond that employed here, need to be incorporated into the 3D inversion process.

CATEGORY: Geochemistry

PERSON IN CHARGE: H. R. Westrich

Atomistic Simulations of Clay Minerals and Their Interaction with Hazardous Wastes: Molecular Orbital and Empirical Methods

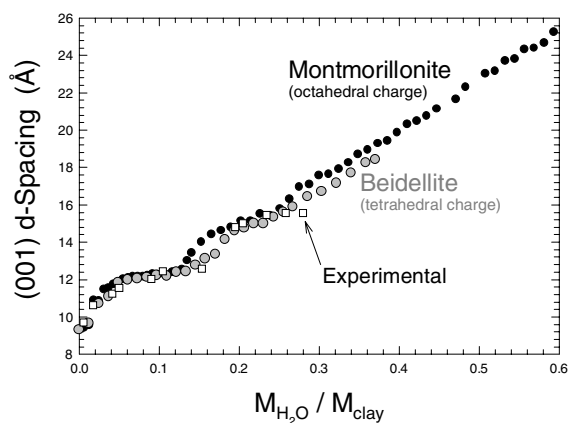
R. T. Cygan (505-844-7216; Fax: 505-844-7216; rtcyan@sandia.gov) and Jian-Jie Liang

Objectives: Examine the interaction of selected metal ions, anions, and organic contaminants on the external and interlayer surfaces of clay minerals using molecular orbital and empirical simulation methods. The computer simulations will improve our understanding of the fundamental mechanisms of

adsorption processes and may help to predict and optimize environmental approaches for the mitigation of hazardous waste.

Project Description: Modeling of clay and clay-fluid systems combine energy minimization and molecular dynamics methods using both molecular cluster and periodic system representations of the bulk clay minerals, their external and interlayer surfaces, and the interacting fluids. One set of modeling techniques uses an empirically derived forcefield to describe the energy of all atomic interactions. Bulk structures, relaxed surface structures, and intercalation processes are evaluated and compared to experimental and spectroscopic findings for validation. More sophisticated calculations incorporate state-of-the-art molecular orbital methods that complement the empirical models. *Ab initio* approaches based on density functional theory (DFT) are used to examine the electronic structure of various clay minerals. Massively parallel computers provide the capability to obtain fully optimized periodic structures for large unit cell structures typical for clay minerals. Electron density distributions, deformation maps, HOMO/LUMO extents, and electrostatic potentials are used to evaluate the crystallographic control and mechanisms for contaminant sorption. This project is being performed in collaboration with Cynthia J. Hartzell (Northern Arizona University), Andrey G. Kalinichev (University of Illinois), and Kate Wright (Royal Institution of Great Britain).

Results: We have developed a molecular mechanics forcefield based on the structures of simple hydroxide phases and quantum-based partial charges for modeling natural hydrous phases. The forcefield incorporates octahedral substitution involving Mg and Fe (for Al) and tetrahedral substitution of Al (for Si), thereby allowing the evaluation of different charge distributions within the clay sheets. The forcefield is flexible and allows all atoms and cell parameters to be unconstrained. Theoretical models of the bulk structures of kaolinite, pyrophyllite, and smectite clays are in excellent agreement with published refinements. The simulation of swelling phenomena involving water molecules, metal ions, and organic complexes provide crystallographic basal d-spacings that are in very good agreement with experiment (see Figure). We have used molecular dynamics methods to simulate the intercalation of metal organophosphate complexes in smectite and the intercalation of hydrazine in kaolinite. Fully optimized structures based on electronic structure calculations using density functional methods at the nonlocal level were also performed. The quantum methods provide theoretical structures that are in excellent agreement with known refinements, and help to evaluate electron densities, electrostatic potential maps, bond lengths, bond angles, and bond critical points.



CATEGORY: Hydrology

PERSON IN CHARGE: H. R. Westrich

Multi-component Convection in Porous Media and Fractures

R. J. Glass (505-844-5606; Fax: 505-844-6023; rjglass@sandia.gov), H. W. Stockman, and S. W. Tyler (Desert Research Institute) and C. A. Cooper (Desert Research Institute)

Objectives: This research seeks to understand the physical and chemical processes controlling multi-component convection in porous and fractured media and to develop quantitative relationships between system parameters (solute concentrations, permeability and system geometry), system stability, flow field structure, and convective transport.

Project Description: We apply high resolution, full field light transmission techniques to study the onset and development of convection in simulated porous media (Hele-Shaw cells) and fractures. The light transmission technique allows quantitative measurement of the solute concentration fields in time thus allowing direct measurements of the mass flux of components. Experiments are first designed to test theoretical stability relations as a function of the solute concentrations, solute diffusivities and the medium's permeability.

Structural evolution and convective transport as a function of dimensionless control parameters is then determined across the full range of parameter space. We also consider the application of lattice gas automata techniques to numerically model the onset and development of convection.

Results: The dimensionless buoyancy ratio (R_p), given by the ratio of fluid density contributions by the two components, is one of three dimensionless parameters required to define system behavior. We designed experiments where we systematically increased the buoyant driving force while keeping R_p constant. Experiments covered the entire range of concentrations up to the solubility limits for the salt-sucrose (denoted by subscripts 1 and 2 respectfully) system while maintaining a constant R_p of 1.08. This approach allowed us to investigate system response over a three order of magnitude increase in the buoyant driving forces ($\Phi = \beta_1 C_1 + \beta_2 C_2$) where β is the volumetric expansion coefficient and C is the concentration.

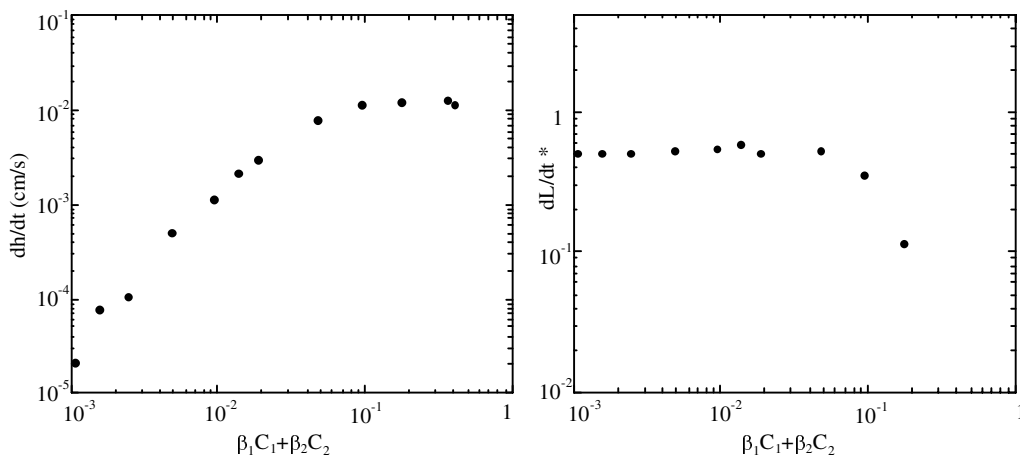


Figure. Vertical growth rate of fingers as a function of Φ

The vertical length scale, (h), defined by the tips of the growing fingers, was found to increase linearly in time for all 14 experiments regardless of the magnitude in Φ ; however, the vertical growth rate of h shows strong dependence on Φ (bottom left figure). For values of Φ on the order of 10^{-2} , the relationship takes the form, $w = 0.2\Phi$. As Φ increases to 10^{-1} , the scaling relationship becomes $w = 0.003\Phi$ and w shows only slight dependence on Φ . A further increase in Φ , results in a decrease in the vertical growth rate. The horizontal growth rate shows $t^{0.54}$ dependence for $10^{-3} < \Phi < 0.05$, therefore, regardless of the initial frequency of the fingers, the growth rate remains unchanged. However, as Φ approaches its maximum, the relationship takes the form $t^{0.11}$, which suggests that the finger frequency at instability is maintained throughout evolution (bottom right figure).

It has been common in the double-diffusive literature to report results as a function of R_p suggesting that this independent parameter governs system behavior. Based on these results, it is clear that system response is quite variable even though R_p is invariant.

The functional dependency of both vertical and horizontal growth rates of the instabilities emphasizes the importance of careful, systematic characterization of this phenomenon in order to understand the influence of critical controlling parameters.

Laboratory Investigation of Permeability Upscaling

V. C. Tidwell (505-844-6025; Fax: 505-844-6023; vctidwe@sandia.gov) and John L. Wilson (New Mexico Institute of Mining and Technology)

Objectives: The goal of this research is to better understand the process of permeability upscaling. Physical and numerical experimentation forms the basis for testing conceptual and theoretical models of permeability upscaling as well as exploring alternative measures and models of this process.

Project Description: Investigation of permeability upscaling is predicated on the results of physical experimentation. These experiments are unique in that: 1) permeability data are collected over a range of different sample supports (sample volumes), each subject to consistent measurement conditions; 2) data are collected on densely sampled grids providing detailed resolution in the spatial distribution of permeability; and 3) experiments are repeated on a variety of geologic materials each differing in their structural/textural attributes. A specially designed gas minipermeameter provides a rapid, precise, and non-destructive means of collecting permeability data. By varying the size of the minipermeameter tip seal, measurements spanning five orders of magnitude on a per-volume basis are made subject to consistent boundary conditions and flow geometry. Thousands of measurements on multiple faces of meter-scale blocks of rock are collected with each of five different tip seals (0.31 - 5.08 cm ID) plus a single large tip seal (15.24 cm ID) designed to integrate over the entire sampling domain. To quantify permeability upscaling, key summary statistics are calculated from the acquired data sets and analyzed with reference to their corresponding sample support. Results are interpreted in light of the physical characteristics of the porous medium and measurement characteristics of the sampling instrument. Detailed numerical modeling is also employed to further explore and quantify the empirical upscaling behavior and to extend the studies to a broader suite of materials.

Results: Inversion of the permeability from air minipermeameter measurements is based on a numerically determined geometric factor. For a variety of reasons, we sought a more exact solution

using both analytical and numerical methods. The two independent solutions agree to five significant digits and provide much improved precision over the previously published results.

We have also developed an adjoint state method for theoretically determining the spatial filter function of the air minipermeameter. We implemented this procedure with a finite element model and were able to plot the three-dimensional filter function for the tip seal design used in our current work. The function shows great sensitivity to the permeability just below the inner tip seal radius and a lower but still significant sensitivity to the permeability just below the outer tip seal radius. The filter function also appears to be proportional to the velocity squared, a previously unreported observation for any instrument. We plan to use the derived function to better interpret the empirical filter functions we recently published [Tidwell *et al.*, 1999].

Finally, we derived finite element numerical solutions for a layered permeability system consisting of a surface layer of one permeability overlying a substratum of a second permeability. This solution will assist us with determining the importance of surface disturbances from sawing and other rock preparation effects on minipermeameter measurements.

Two-Phase Immiscible Fluid Flow in Fractured Rock: The Physics of Two-Phase Flow Processes in Single Fractures

R. J. Glass (505-848-0556; Fax: 505-848-0558; rjglass@nwer.sandia.gov), H. Rajaram (University of Colorado, Boulder) and M. J. Nicholl (Oklahoma State University)

Objectives: The objective is to develop a quantitative understanding of critical fundamental processes controlling two-phase flow and transport in fractures, based on detailed physical experiments and high-resolution numerical simulations. This understanding may subsequently be abstracted for use in conceptual models applied to large-scale problems in petroleum extraction, isolation of hazardous or radioactive waste, remediation of contaminated subsurface media and CO₂ sequestration.

Project Description: Under two-phase immiscible flow conditions, the phase geometry associated with each phase controls the fluid flow and solute transport characteristics. The phase geometry is in-turn determined by a combination of the aperture variability, the capillary and viscous effects inherent in the two-phase flow processes themselves and external forces such as gravity. If one of the fluids can slightly dissolve in the other, then transport of the dissolved fluid also influences phase geometry.

In this collaborative project between Sandia National Laboratories, Oklahoma State University and University of Colorado at Boulder, systematic physical experimentation is coupled with concurrent numerical simulation to explore the factors controlling phase-structure, flow, transport, and inter-phase mass transfer in rough-walled fractures. A high-resolution light-transmission technique has been developed to facilitate acquisition of accurate experimental measurements of aperture, phase geometry and solute concentrations in transparent analog fractures. Use of this technique will lead to data of unprecedented accuracy for evaluating current understanding of invasion, flow and transport processes, and motivate refinement of theoretical concepts.

Results: A Modified Invasion Percolation (MIP) algorithm has been developed and comprehensively tested, to simulate phase invasion processes influenced by capillary and gravity forces. An essential feature of the MIP algorithm in the context of application to rough-walled fractures is the incorporation of an in-plane curvature term. The inclusion of this term is critical to obtaining phase structures that correspond closely with experimentally measured phase structures. The in-plane curvature term is not

incorporated in previously proposed approaches such as standard percolation (SP) or traditional invasion percolation (IP, incorporating only an out-of-plane curvature across the aperture).

To allow a meaningful experimental evaluation of current conceptual models of flow, transport, and inter-phase mass transfer, aperture measurement errors were minimized and quantified. Each component of the light transmission system was evaluated with respect to its contribution to measurement error and the individual errors were combined to yield estimates of the total error at any location within the flow field. This effort indicated that minimizing aperture measurement errors requires a trade-off between precision errors resulting largely from signal noise and accuracy errors resulting from the nonlinearity of light absorbance by the dye used for measurements. The optimal measurement process is fracture and system specific and thus must be carefully evaluated for each new fracture or measurement system.

A careful re-evaluation of saturated and unsaturated flow experiments in rough-walled fractures is in progress, to identify the sources of discrepancy between experimental results and numerical simulations employing the Reynolds equation. It is expected that these efforts will lead to unambiguous and comprehensive evaluations of the Reynolds equation. Several issues related to the numerical implementation of the Reynolds equation and the adequacy of data resolution are also being investigated.

A series of experiments on solute transport in partially saturated fractures was carried out. These experimental results highlight the importance of solute diffusion into and out of low velocity regions adjacent to the entrapped non-flowing phase. Because of these low velocity regions, the front edge of a solute plume appears to be more influenced by flow channeling and the tail portion appears to be stretched out. These experimental results will be compared against numerical simulations of solute transport in order to better understand the importance of the low velocity regions.

Continuum and Particle Level Modeling of Concentrated Suspension Flows

L. Mondy (505- 844-1755; Fax: 505-844-8251; lamondy@sandia.gov), A. Graham (Texas Tech University), M. Ingber (University of New Mexico)

Objectives: The purpose of this program is to combine experiments, computations, and theory to make fundamental advances in our ability to predict transport phenomena in concentrated, multiphase, disperse systems, particularly when flowing through geologic media.

Project Description: The proposed research will elucidate the underlying physical principles that govern concentrated multiphase systems in areas essential to continued progress in geosciences. In order to be of use in real world applications, significant enhancements to currently available continuum-level suspension flow models will be required. We will use both experimentation and high performance computing to obtain microstructural information that is necessary to the development and refinement of the continuum models. For example, we expect to use this microstructural information to gain insight into the physics of particle bridge formation and collapse and particle sedimentation, which are particularly important in sand control issues found in petroleum production. Further, we expect that continuum-level modeling could eventually be directly implemented in codes currently used to predict hydraulic fracturing operations in the petroleum industry. The understanding gained about the physics of multiphase flows will, however, have much broader application in geosciences.

Results: The continuum models originally developed by Phillips *et al.* (1992) and Nott and Brady (1994) has been extended to account for normal stress contributions. This allows accurate predictions of

suspended particle migration in curvilinear flows. The Phillips-type model currently also allows for non-neutrally buoyant particles and non-Newtonian suspending liquids. Results from the new models, which have been implemented into a general-purpose finite element computer code, show good agreement with experimental measurements based on nuclear magnetic resonance (NMR) imaging. In addition, massively parallel computing has allowed particle level simulations, based on the boundary element method (BEM), with up to a thousand particles. These simulations are currently being used to determine the magnitude of the normal stresses developing from particle interactions, as well as to develop more accurate hindered settling functions for particles interacting with other types of particles or in a porous medium. These simulations lead to detailed information on individual particle and fluid motion that is unobtainable through experiments. In addition, a multipole-accelerated boundary element method (BEM) has been developed to simulate many thousands of individual interacting particles. Two-dimensional dynamic simulations show qualitative agreement with (three-dimensional) laboratory experiments, and three-dimensional simulations are now possible for “snapshots” of interacting particles.

PART II: OFF-SITE

GRANTEE: American Museum Of Natural History

Department of Mineral Sciences
New York, New York 10024

GRANT: DE-FG02-92ER14265

Influence of carbon on the electrical properties of crustal rocks

E.A. Mathez (212-769-5379; Fax: 212-769-5339; mathez@amnh.org)

Objectives: Understand the adsorption of carbon on silicate surfaces in the presence of carbonaceous gases; determine the nature and origin of carbon in deep crustal rocks; and seek applications to a section of the San Andreas Fault system currently the object of seismic research.

Project Description: The adsorption study will be conducted by fracturing rocks and single crystals of synthetic forsterite, natural olivine, quartz, and amphibole under identical conditions in the presence of CO-CO₂ gas mixtures, using experimental and analytical techniques developed in our previous studies. The composition and distribution of carbon in a suite of deep crustal rocks will be determined using time-of-flight secondary ion mass spectroscopy (ToF-SIMS) and electron probe techniques. To learn if carbon deposition plays a role in active fault systems, we shall also determine the nature and distribution of carbon in rocks and outcrops at Parkfield, CA. This is a joint project with A.G. Duba (LLNL) and T. J. Shankland (LANL).

Results: The nature and distribution of carbonaceous matter in microcracks and grain boundaries in amphibolite samples from 4.6 and 9.1 km depth in the KTB borehole have been investigated using electron probe and ToF-SIMS. In the sample from 9.1 km depth, the carbon is dominantly to completely elemental. In contrast, the carbonaceous matter in the samples from 4.6 km depth comprises a mixture of elemental carbon and hydrocarbons. The latter are believed to include simple alkanes and lesser amounts of alcohols, ethers, ketones or aldehydes. Small quantities of haloalkane or thiol compounds may also be present. The microcracks containing carbonaceous matter are also occupied by a retrograde micro-assemblage consisting of ferri-oxy-hydroxide, calcite, and possibly clay minerals, suggesting that the carbonaceous matter and retrograde minerals formed together. These features formed at crustal levels above the brittle-ductile transition (*ca.* 10 km) after the time of peak metamorphism.

Carbon compounds form extensive, quasi-continuous coats on microcrack and grain boundary walls and likely influence *in situ* rock electrical conductivity. Retrograde metamorphism, in which graphite in the mid- and deep crust is transformed to a mixture of graphite and hydrocarbons in the shallow crust during uplift, may increase rock resistivity. This chemical destruction of the interconnectivity of electrical pathways may contribute to the diminished conductivity of the shallow crust in relation to the deep crust.

GRANTEE: Arizona State University

Departments of Geology and Chemistry/Biochemistry
Box 871404
Tempe, Arizona 85287-1404

GRANT: DE-FG03-95ER14533

Reaction Mechanisms of Clay Minerals and Organic Diagenesis: An HRTEM/AEM Study

P. R. Buseck (602-965-3945; Fax: 602-965-8102; pbuseck@asu.edu)

Objectives: The objectives of this study were to gain an improved understanding of the microstructures and reaction mechanisms for diagenetic reactions in selected layered silicate minerals and organic materials found in surficial environments. The project was subsequently expanded to include studies of iron oxyhydroxides both because of their role in surficial environments, specifically soils, and their potential importance as scavengers of heavy metals, including toxic waste products.

Project Description: We studied clay and detrital minerals as well as organic matter in sequences of Upper Cretaceous and Lower Tertiary clastic rocks from the southern Rocky Mountains using a range of analytical and structural techniques. We were especially interested in: (1) the berthierine-to-chamosite reaction, (2) smectite illitization, (3) organic diagenesis, (4) XRD *versus* TEM size distributions of clay minerals, and (5) ferrihydrite, a poorly crystalline iron oxide of the types found in surficial environments.

A study of ferrihydrite and related iron oxyhydroxides was added in an attempt to understand their definition, structure, and character as an aid to determining their potential as heavy-metal scavengers and natural repositories for such metals.

Results: Ferrihydrite (also known as "amorphous iron oxide," "hydrous ferric oxide," and "colloidal ferric oxide") is a common, poorly crystalline iron oxide that forms in surface environments. Numerous studies of synthetic ferrihydrite have addressed its ability to adsorb or coprecipitate with organic compounds and ions of elements that include Ba, Na, P, V, Cd, Cr, Sr, Li, Tl, Sn, Zn, Cu, Ni, Ag, Co, Se, As, Hg, Sr, Pb, U, and Np. Ferrihydrite is an effective adsorbent of CoII EDTA²⁻ and NiII EDTA²⁻ complexes, which are used as chelating agents for radionuclides in waste disposal, and it is used in industrial waste-water treatment. We successfully used electron microscopy and electron nanodiffraction to provide significant new insights into the structure of this ubiquitous and yet somewhat mysterious material.

Natural ferrihydrite samples, because of their poor crystalline structure, unusually fine-grained character (< 6 nm), and variability in minor and trace element contents, are extremely difficult to study. They also display considerable variability in both structural and chemical properties. X-ray diffraction patterns show two to six broad peaks, corresponding to lattice-plane spacings of ~0.15 to 0.26 nm. Ferrihydrite with two peaks is known as "2-line" ferrihydrite (2LFh), and that with six peaks is commonly called 6-line ferrihydrite (6LFh). Numerous models have been proposed but have been difficult to test. We applied a new method to this problem - single-crystal nanodiffraction. Such patterns from synthetic 2LFh were divided into three groups corresponding to a highly disordered structure consisting of close-packed anionic, a structure with close similarities to highly ordered distorted ferrihydrite, and a maghemite-like material. Nanodiffraction patterns with characteristics intermediate between the highly disordered structure and each crystalline structure suggest continuous variation in the degree of ordering.

Our proposal that the observed characteristics are dominated by those of the highly disordered structure leads to interpretations that differ in important respects from those of previous researchers. Although we find that there is no single 2LFh crystal structure, the high degree of disorder suggests that an understanding of the average structure may suffice to explain the observed chemical and phase-transition behavior of synthetic 2LFh. The average structure can be inferred from methods such as XRD, SAED, and synchrotron data, which measure bulk properties; however, details require methods such as transmission electron microscopy that can provide higher spatial resolutions.

GRANTEE: Arizona State University

Center for Solid State Science
Box 871704
Tempe AZ 85287-1704

Grant: DE-FG03-94ER14414

Chemical Dynamics of Hydrocarbon Reservoirs Investigated by Secondary Ion Mass Spectrometry

R. L. Hervig (602-965-3107; Fax: 602-965-9004; richard.hervig@asu.edu) and L. Williams (602-965-5081; Fax: 602-965-8102; lynda.williams@asu.edu)

Objectives: Microanalyses of oxygen and boron isotopes in authigenic silicates are being obtained to determine their variation in hydrocarbon-producing sedimentary basins. These analyses can be used to constrain mass transport processes occurring during diagenesis and hydrocarbon migration.

Project Description: Current research examines the isotopic heterogeneity of authigenic silicates (quartz, feldspar, clay minerals) in the Gulf Coast Sedimentary Basin in order to interpret the chemical environment of precipitation during burial diagenesis. *In situ* analyses of O-isotopes help determine the timing of reservoir cementation and the volumes and chemistry of the paleofluids responsible. Concurrent changes in B-isotopes were investigated as an aid to interpretation of the sources of fluids. Organic matter is a potential source of B in clastic sedimentary basins undergoing burial and thermal maturation. Understanding sources of B is required to interpret mass transport processes and develop better models to explain fluid flow and hydrocarbon migration.

Results: In 1999 the experiments to determine B-isotope fractionation as a function of temperature were completed. With this information, an isotope fractionation curve was deduced. The validity of the fractionation curve was tested using samples from the U.S. Gulf of Mexico Sedimentary Basin, Alberta Basin, and a Cretaceous black-shale intruded by a dike. Following are the major conclusions of these investigations.

A linear fit to the isotopic fractionation of B determined by the experimental reaction of smectite to illite, together with data from higher and lower temperature experiments, produced the following relationship:

$$\Delta(T)_{(\text{mineral-water})} = -10.12 * (1000/T \text{ (K)}) + 2.44$$

It appears that this relationship is based on the coordination change of B from trigonal in solution to tetrahedral sites in the silicates. This curve applies specifically to silicates that incorporate B in tetrahedral coordination, such as clay minerals.

The B-content and isotopic composition of oil field brines in the U.S. Gulf Coast reservoirs showed changes both laterally across the reservoir and vertically among stacked reservoirs. There appeared to be a ¹¹B enrichment of waters with distance of migration, that could result from the 10B preference for clay minerals. However, this trend might also reflect a separation of gaseous or light hydrocarbons with a higher δ¹¹B.

Kerogen extracted from source rock in the Gulf Coast contains >100 ppm B, similar to the quantities observed in the pore-filling clay minerals of the reservoir, and in many oil field brines. The isotopic

composition is light (0 to -10%), therefore organic matter is a potential source of ^{10}B during thermal maturation. This research deduced that B is released by processes of late hydrocarbon maturation, possibly during dry gas generation. Although kerogen makes up only a small percentage of any sedimentary basin, its significance as a source of boron in deep sedimentary basins cannot be ignored when considering its reactivity compared to clay minerals.

The kinetics of the illitization reaction was demonstrated by a time-series of samples analyzed during the reaction progress. The results showed that metastable equilibrium is attained with respect to B-isotopes during R1 ordering of the I/S, but that equilibrium conditions require long range ordering (R3), indicative of neoformation of authigenic illite. In general, there was a 5-fold increase in the B-content of the illite during recrystallization. This indicates that illite is a sink for B, not a source of B during burial diagenesis.

The neoformation of illite at depths similar to those of hydrocarbon generation makes boron a sensitive monitor of pore fluid changes related to organic maturation. If the B-isotopic composition of reservoir fluids can be linked to a specific source rock, then authigenic illite might record the presence of fluids related to hydrocarbons.

Authigenic illite is a reservoir for ^{10}B , even at high temperatures ($\sim 500^\circ\text{C}$). This was demonstrated by the very high B-content (500 ppm) of a bentonite sample taken near a dike in the presence of metasomatic fluids. Other samples in the bentonite showed a 20% decline in $\delta^{11}\text{B}$ of the I/S during long-range ordering. Applying a Rayleigh distillation model to this bentonite (using the isotopic fractionation from (1) above) successfully predicts the range of boron isotopic compositions observed.

Application of the isotopic fractionation curve to a steam-injected reservoir in the Alberta Basin demonstrated that the $\delta^{11}\text{B}$ of the hydrothermal fluids could be predicted by the isotopic composition of the pumice in the reservoir as a function of temperature. The pumice contained the highest concentrations of B and was the most reactive constituent of the reservoir.

The successful application of the new B-isotope fractionation curve to prediction of the pumice-water fractionation demonstrates that the curve is not limited to clay minerals, but can be applied to other silicate minerals undergoing recrystallization, as long as there is a coordination change for B from trigonal (aqueous) to tetrahedral (mineral). This makes B-isotopes a useful geothermometer in hydrothermally stimulated oil-reservoirs and potentially other high temperature environments such as geothermal wells.

GRANTEE: Boston University

Physics Department
590 Commonwealth Avenue
Boston, MA 02215

GRANT: DE-FG02-95ER14498

**Nonlinear Systems Approach to Understanding the Origin of Geodetic Crustal Strains
(Collaborative Research)**

W. Klein (617- 353-2188) and J. B. Rundle (303-492-5642; Fax: 303-492-5070)

Objectives: To develop a physical understanding of the origins of geodetic crustal strains in nonlinear geomechanical systems, to examine the space-time patterns and correlations that occur in these systems, and to use these patterns to forecast the future activity that may produce disasters affecting a wide variety of critical energy facilities.

Project Description: A variety of nonlinear dynamical processes operate within the complex Earth system. Signatures of these processes include the appearance of scaling (fractal distributions), global and local self-organization, intermittancy, chaos, and the emergence of coherent space-time correlations, patterns, and structures. The geodynamical effects observed in earthquake systems, particularly crustal straining, dynamical segmentation, and intermittent seismicity, are being modeled in massively parallel simulations in an effort to clarify the origins of these phenomena. Simulations and theoretical investigations are particularly aimed at quantifying the limits of predictability for catastrophes (disasters) that occur within the Earth system. We are currently developing both the simulation methods for earthquake models, and the statistical mechanical analysis techniques needed to understand and interpret the results. From these simulations, we will then predict geodetic and other deformation associated with impending earthquakes to be tested against Global Positioning System, Synthetic Aperture Radar, seismicity, and other field data.

Results: We have made important progress in several fundamental problem areas. These include: 1) Stochastic evolution of stress fields on faults. Using numerical simulations, we have made a fundamental advance in understanding how failure and frictional processes influence the size of earthquakes. Stable precursory slip in a variety of current friction laws, such as the slip-dependent and rate-and-state laws, acts to smooth the stress distribution. Smoothing processes are thus associated with stable (aseismic) slip, whereas roughening processes are associated with unstable slip (earthquakes). 2) Space-time patterns in crustal deformation and seismicity with implications for forecasting. We analyzed the eigenpatterns and space-time structure of earthquake seismicity in southern California and found that systematic variations in seismicity can be seen prior to large earthquakes. These precursory patterns may prove useful in anticipating the occurrence of large earthquakes. 3) Earthquake physics and observational tests. We have found that earthquake physics can be understood as rotations of state vectors in mean-field, phase dynamical systems. These results strongly suggest that the largest events are accompanied by precursors that can be observed in crustal deformation and seismicity data. Analysis indicates that the largest repeating events are associated with long-lived space-time structures in the stress field.

GRANTEE: California Institute Of Technology

Division of Geological and Planetary Sciences
Pasadena, California 91125

GRANT: DE-FG03-85ER13445

Infrared Spectroscopy and Hydrogen Isotope Geochemistry of Hydrated Silicate Glasses

S. Epstein (818-356-6100; epstein@gps.caltech.edu) and E. Stolper (818-356-6504; Fax: 818-568-0935; ems@expet.gps.caltech.edu)

Objectives: The focus of the proposed project is the combined application of experimental petrology and geochemistry with stable isotope geochemistry to problems in petrology and geochemistry, with particular emphasis on the behavior of the volatile components, H₂O and CO₂, in geological systems ranging from high to low temperatures.

Project Description: This project integrates (1) laboratory studies directed toward the development of analytical techniques and a solid understanding of the physical chemistry of geological systems through carefully controlled experiments, and (2) syntheses and field studies in which these techniques and chemical principles are applied to specific petrological and geochemical problems. A key feature of this project is the combination of methodologies from stable isotope geochemistry with those from other fields (*e.g.*, experimental petrology, mineralogy, and atmospheric science). Results of this work will continue to be applied to developing quantitative constraints on geological processes involving H₂O and CO₂. Our results also contribute to a deeper understanding of the chemical and physical properties of volatile-bearing systems and have applications to both Earth and materials science.

Results: (1) Experiments and analyses were undertaken to determine O-isotope fractionation between CO₂, minerals, and silicate melts. Such experiments are essential for using O-isotopes quantitatively to constrain the origin and evolution of magmas. An experimental technique for determining O-isotope fractionations between CO₂ and silicate melts using laser fluorination techniques has been developed. Most experiments thus far have been on a sodic melilite composition that is an analog for basaltic melt. The results have been reversed at 1250°C and give a precise value for vapor-melt fractionation consistent with but more precise than the range expected for CO₂-basalt based on extrapolations of previous experimental data and empirical calculations. (2) 1-liter samples of air have been collected at 1-2 day intervals for almost 1.5 years on the Caltech campus. Comparison of CO₂ concentrations and isotopic compositions were compared with a set of data collected in 1972-73 in a similar location. Excellent correlations between concentration and $\delta^{13}\text{C}$ confirm that Pasadena has had an increase in CO₂ concentration of ~50 ppm and that the heaviest end member has become lighter by ~0.5‰ over the past 26 years. Both of these observations reflect the effects of fossil fuel combustion. CO₂ concentrations are significantly higher overall than oceanic sites and isotopically lighter. Unlike seasonal variations in CO₂ concentrations observed at sites dominated by oceanic influences at the same latitude, the data for the Caltech campus shows no seasonal variation because the pollution effects overwhelm them. Several candidates for the “pollutant” end member have been examined, and the trend for the air samples corresponds well with automobile exhaust. The CO₂ concentrations and isotopic compositions on the Caltech campus correlate well with NO₂ data from sites ranging from Hawthorne (*i.e.*, near the ocean) to Pomona (*i.e.*, well inland of Pasadena), demonstrating that the observed trends are not local phenomena.

GRANTEE: California Institute Of Technology

Division of Geological and Planetary Sciences
Pasadena, CA 91125

GRANT: DE-FG03-88ER13851

Isotope Tracer Studies of Diffusion in Silicates and of Geological Transport Process in Aqueous Systems Using Actinide Elements

G. J. Wasserburg (626-395-6139; Fax: 626-796-9823; isotopes@gps.caltech.edu)

Objectives: The research program was directed to three principal objectives: 1) The determination of the concentration and isotopic composition of Os in rivers, estuaries and the oceans; 2) The nature of U transport on colloids and particles in natural waters.

Project Description: We are carrying out studies of the transport of actinide and platinum group elements in rivers, bogs, estuarine environments and the oceans. This involves development of advanced laboratory analytical procedures and improved field filtering techniques. The distribution of U and Th on colloids and in solution was studied. These techniques have been applied to both oxic and anoxic environments and establish clear relationships for element transport in natural conditions. The analytical techniques involve high sensitivity mass spectrometry (TIMS and NTIMS), ICPMS and very low blank-level chemical procedures

Results: 1) The role of colloids in the transport of ^{238}U and ^{234}U in rivers and the removal and exchange that result from mixing with saline waters in estuaries has been studied. It was found that colloids dominate the riverine transport of U and that a substantial fraction of the U is removed by the aggregation and sinking of Fe-organic rich colloids in the initial mixing in the estuarine environment.

2) A detailed study of the transport of ^{238}U , ^{234}U , ^{232}Th , ^{234}Th , ^{230}Th , ^{226}Ra and ^{210}Pb were carried out in a well-defined, pristine watershed that feeds into an estuary. The area also includes mires. It is shown that Th is dominantly transported on Fe-rich particles in the rivers with contributions from both authigenic riverine particles and detrital grains. Only a small fraction of the Th dissolved. The Th not on particles is predominantly associated with organic colloids upon discharge into the estuary. The residence time is determined to be ~50 days due to particle scavenging.

3) For the first time, the Os isotopic composition and concentration was determined in the Ganges, Brahmaputra and Indus rivers. This study was undertaken to establish the extent to which the Himalayan uplift could be responsible for the increase in $^{187}\text{Os}/^{188}\text{Os}$ over the last 17 My. It was shown that these rivers cannot be the cause of the changes in the seawater Os isotopic composition. The overall trend for both Sr and Os that had been previously attributed to this source is not justified. The overall oceanic trend could be explained by a regularly increasing input of global continental weathering, but the Himalayas themselves do not appear to be the dominant source. (Sharma *et al.*, 1999 *Geochim. Cosmochim. Acta* 63, pp4005-12).

4) The first determination of the Os isotopic composition and concentration in hydrothermal fluids was successfully carried out. Most high temperature hydrothermal fluids are buffered at about the seawater concentration level but are predominantly of isotopic composition reflecting the mantle. A simple theoretical model was developed that appears to explain the data and the interaction with both seawater and with the rocks. It was shown that the hydrothermal fluids originally had very high concentrations of

Os (and presumably other platinum group elements), which are deposited below the seawater interface. The results show that these fluids, now almost stripped of Os are injected into seawater. These cannot significantly affect the seawater balance. However, there are low temperature fluids with greatly elevated Os concentrations that could provide large amounts of mantle Os into the oceans.

GRANTEE: University Of California, Berkeley

Department of Geology and Geophysics
Berkeley, California 94720

GRANT: DE-FG03-85ER13419

Advective-Diffusive/Dispersive Transport of Chemically Reacting Species in Hydrothermal Systems

H. C. Helgeson (510-642-1251; Fax: 510-643-9980; brogie@Socrates.Berkeley.edu)

Objectives: The overall research objective of this project is to quantify the reaction process responsible for the generation of petroleum in sedimentary basins using thermodynamic calculations and compositional information to characterize metastable equilibrium states (Shock, 1988; Helgeson *et al.*, 1993; Seewald, 1994) and the causes and consequences of irreversible reactions in hydrocarbon source rocks and reservoirs.

Project Description: The formation and evolution of petroleum in sedimentary basins is generally attributed to the thermal catagenesis of kerogen; *i.e.* kinetically controlled irreversible generation of high molecular weight liquid hydrocarbons in bitumen from kerogen and their progressive conversion to the lighter species that predominate in petroleum as a result of increasing temperature and time with increasing depth of burial. This widely accepted time/temperature paradigm is based largely on extrapolation of the results of laboratory pyrolysis experiments to the natural process of petroleum generation by correlating the products of the experiments with observed changes in kerogen composition with depth in sedimentary basins. However, high-temperature pyrolysis experiments are by design irreversible, and the extent to which the results of these experiments represent, or can even be reliably extrapolated to account for petroleum generation in nature has never been adequately documented.

Although the phenomenological association of petroleum generation and maturation with increasing temperature and time during burial is self-evident, the causal implications of this association are highly questionable. In fact, it has been shown that in closed systems, source rocks with hydrogen-rich organic matter may retain their petroleum generating potential at temperatures far greater than those normally associated with the formation of crude oils. It can be demonstrated that degradation of organic matter with increasing depth is an oxidation/reduction process that requires the presence of H₂O.

Theoretical considerations and thermodynamic calculations have led to the hypothesis that hydrolytic disproportionation of hydrocarbons plays a crucial role in the diagenetic deoxygenation of immature kerogen, as well as the generation and maturation of crude oil in hydrocarbon source rocks. Recent field and laboratory evidence supporting this hypothesis indicates that hydrolytic disproportionation of organic matter is not only a dominant process in petroleum source rocks and reservoir systems, but that it plays a widespread and important role in ore deposition and high-temperature metasomatism of sedimentary, granitic, and mantle-derived rocks.

Results: Research carried out in the current budget period has been primarily concerned with 1) thermodynamic description of model Type II kerogens in successive states of deoxygenation with increasing burial of hydrocarbon source rocks and 2) carrying out Gibbs free energy minimization calculations for various bulk compositions in the system C-H-O to determine the extent to which metastable equilibrium states can be achieved among the model kerogens, H₂O, and hydrocarbon species

in crude oil with increasing depth and temperature. The calculations carried out so far indicate that diagenetic deoxygenation of kerogen in source rocks in the upper part of the burial sequence is an irreversible open system process which is driven by reaction of H_2O with the oxygenated kerogen to produce CO_2 and a less oxygenated, more hydrogenated kerogen. The calculations also indicate that the Gibbs free energy minimum toward which the irreversible process proceeds corresponds to a metastable equilibrium state among the deoxygenated kerogen species, the aqueous phase, and liquid hydrocarbons, which signals the onset of oil generation. In accord with analytical data reported in the literature, further burial and metamorphism of the deoxygenated kerogen leads to increasing production of crude oil with increasing concentrations of lighter hydrocarbon species in the liquid and a progressively more oxidized (aromatized) kerogen, all of which remain in metastable equilibrium with each other.

GRANTEE: University Of California, Berkeley

Space Sciences Laboratory
Berkeley, California 94720-7450

GRANT: DE-FG03-96ER14676

Collaborative Research: Studies for Surface Exposure Dating in Geomorphology

K. Nishiizumi (510-643-9361; Fax: 510-643-7629; kuni@ssl.berkeley.edu), W. E. Dietrich (510-642-2633, bill@geomorph.berkeley.edu), M. W. Caffee (Lawrence Livermore National Laboratory), R. C. Finkel (Lawrence Livermore National Laboratory), and R. C. Reedy (Los Alamos National Laboratory)

Objectives: An experimental and theoretical program to fully develop the systematics of *in situ* produced cosmogenic nuclides in terrestrial surface samples and their application to the dating of surface features and processes.

Project Description: Surface exposure dating utilizing cosmogenic nuclides is now acknowledged as a successful means with which to date many terrestrial surfaces. It is also recognized that there are many new applications for these techniques. Although the method rests on a firm physical and geochemical foundation, there are examples of conflicting results. This project includes determination of precise production rates and production depth profiles, studies of altitude and latitude effects, intercalibration with other methods, isolation of *in situ* produced nuclides from other lithologies. The effort will focus on chemical isolation of cosmogenic nuclides of geologic and artificially exposed samples, on implementation of surface exposure dating methods using new radionuclides such as *in situ* ^{14}C and pure spallation ^{36}Cl , measurements of proton and neutron cross sections and development of theoretical production rate calculation.

Results: After testing a wide range of chemical reagents, a procedure was developed by which the concentration of meteoric ^{10}Be in olivine could be reduced by a factor of 1000. In order to verify that meteoric ^{10}Be can be totally removed, we have applied the developed procedures to a young volcanic lava sample from Kilauea, Hawaii, erupted in 1840. The expected *in situ* produced ^{10}Be and ^{26}Al for this sample is 650 atoms/g olivine and 2000 atoms/g olivine, respectively. Surprisingly we obtained a ^{10}Be concentration of 1.6×10^5 atoms/g olivine. There are two possibilities for the high ^{10}Be : 1) meteoric ^{10}Be has diffused into the olivine crystal and has not been removed by our leaching procedures; 2) contaminant ^{10}Be , *i.e.*, ^{10}Be not produced *in-situ* by cosmic rays, has been incorporated into the olivine crystal during crystallization. Conceivably this contaminant could have been scavenged from local rock during the emplacement of the basalt. If the latter is the case, it may imply alteration of the upwelling melts during Hawaii volcanic activity. To further investigate this observation, ^{10}Be from various sources encompassing a wider range geologic settings will be investigated. Similar tests on procedures for removal of meteoric ^{10}Be from calcite will also be conducted.

GRANTEE: University Of California, Berkeley

Environmental Engineering and Health
Sciences Laboratory
Berkeley, California 94720-1766

GRANT: DE-FG03-96ER14667

Microbial Dissolution of Iron Oxides

G. Sposito (510-643-8297; Fax: 510-643-2940; sposito@ce.Berkeley.edu), L. E. Hersman (Los Alamos National Laboratory), and P. A. Maurice (Kent State University)

Objectives: The overall objective of this research is to determine the rates and mechanisms whereby bacteria dissolve Fe(III)(hydr)oxides in aerobic soil environments, where Fe is insoluble. Information about the rates and mechanisms of Fe(III)(hydr)oxide dissolution is fundamental for a wide range of hydrobiogeochemical soil, surface-water, and aquifer processes, yet little is known about dissolution by aerobic bacteria. Fe(III)(hydr)oxides sorb radionuclides and organic contaminants; thus, their dissolution may cause remobilization of these pollutants.

Project Description: Research at Berkeley has focused on the dissolution of goethite by the siderophore, desferrioxamine B (DFO-B) in competition with a common biologically produced ligand, oxalate. Continuous flow stirred-tank reactors were used in the dissolution experiments. The reactors were immersed in a constant temperature water bath at 25°C, the entire assembly being wrapped in aluminum foil to exclude light. The concentration of the goethite suspension was 10.0 g/l. The flow rate of the reactor was controlled using a variable-speed peristaltic pump and determined by collecting effluent over a fixed period. Division of the volume of the effluent by the time taken gives the flow rate. The composition of the influent solution was 0.01 M NaClO₄, 5 mM MOPS buffer, and fixed ligand concentrations at pH 5.

Results: The rate of dissolution of goethite as a function of DFO-B concentration roughly paralleled the adsorption isotherms of DFO-B on goethite, indicating that the dissolution rate is a function of adsorbed ligand concentration and that dissolution is via ligand-promoted mechanism. The goethite dissolution rate as a function of oxalic acid concentration was negligible below 100 μM, but increased linearly above 100 μM. The goethite dissolution rate as a function of DFO-B concentration, with an oxalic acid concentration fixed at 40 μM, was at least twice that of simply adding the goethite dissolution rates in the presence of each ligand alone at the concentrations used. The goethite dissolution rate as a function of oxalic acid concentration, with a DFO-B concentration fixed at 40 μM, was also much higher than the sum of dissolution rates in the presence of each ligand alone. At low oxalic acid concentrations, the dissolution rate increased linearly as the oxalic acid concentration increased.

In systems where both DFO-B and oxalic acid were present, the dissolution rate of goethite was significantly enhanced, suggesting a synergistic effect of the two ligands. Before putting forward hypotheses on this phenomenon, we shall collect data on adsorption of DFO-B and oxalic acid. This will determine whether adsorption of the two ligands is competitive or promotive. Thus, we shall be able to test the applicability of rate additivity in our systems.

GRANTEE: University Of California, Davis

Department of Land, Air and Water Resources,
Department of Geology
and the Department of Chemistry
Davis, California 95616

GRANT: DE-FG03-96ER14629

The Kinetics of Dissociation of Aluminum-Oxygen Bonds in Aqueous Complexes

W. H. Casey (530-752-3211; Fax: 530-752-1552; whcasey@ucdavis.edu) and B. L. Phillips

Objectives: We determine rates for key elementary reactions in dissolved aluminum complexes that help establish a general reactivity scale for processes in more-complicated settings.

Project Description: At a molecular scale, most reactions of geochemical importance involve a bonded atom or molecule that is replaced with another. The rates of bond cleavage depend very sensitively on the other ligands that are also in the inner-coordination sphere of the metal. We probe these effects at the most fundamental level by coupling NMR spectroscopy and aqueous experiments.

Results: In the first year of the grant we constructed an NMR probe suitable for ^{17}O -NMR experiments at pressures of up to 5 kbar. High pressures are needed because the mechanisms of reactions are determined through the activation volumes, which derive from the pressure dependence of the reaction rate. The first system we examined is the pressure dependence of solvent exchange in the $\text{AlF}^{2+}(\text{aq})$ and $\text{AlF}_2^+(\text{aq})$ complexes. This work is conducted in collaboration with Prof. Thomas Swaddle at the University of Calgary and we modeled the exchange process via *ab initio* molecular orbital calculations with Prof. Jack Tossell, of the University of Maryland [Phillips *et al.*, 1999]. In our studies we found that a single fluoride in the inner-coordination sphere of Al^{3+} enhances the rates of dissociation of Al-O bonds to water molecules by a factor of 10^2 . Addition of a second fluoride, to form the $\text{AlF}_2^+(\text{aq})$ complex, enhance the rates by a second factor of 10^2 . The preliminary activation volume of 6-7 cm^3/mole is consistent with a dissociative-interchange mechanism for reaction.

These measurements elucidate fluoride-promoted dissolution of bayerite ($\beta\text{-Al}(\text{OH})_3(\text{s})$) and ^{19}F -NMR studies of adsorbate complexes on the surface (Nordin *et al.*, 1999). Bayerite has a particularly simple surface chemistry that is similar to the basal planes of most dioctahedral clays. From the ^{19}F -MAS-NMR of wet samples we can make fluoride assignments to different structural sites at the dissolving surface. Substitution of a fluoride for a terminal hydroxyl functional group can be detected in the NMR spectra as a peak at -143 ppm [Figure, top]. This substitution is analogous to substitution of a fluoride for a single hydration water in aqueous complexes. Correspondingly, fluoride adsorption at terminal sites causes a large increase in the rate of dissolution, just as it causes rates of Al-O bond dissociation to increase in aluminum fluoride complexes. Substitution of fluoride for a bridging hydroxyl site, however, has an enormous effect on the reaction rate and can be detected in the NMR spectra as a peak at -131 ppm.

Phillips, B. L., Tossell, J. A., and Casey, W. H. (1998) Experimental and theoretical treatment of elementary ligand exchange reactions in aluminum complexes. *Environ. Sci. Technol.* **32**, 2865-2870.

Nordin, J. P., Sullivan, D. J., Phillips, B. L., and Casey, W. H. (1999) Mechanisms for fluoride-promoted dissolution of bayerite [β -Al(OH) $_3$ (s)] and boehmite [γ -AlOOH(s)]- 19 F-NMR spectroscopy and aqueous surface chemistry. *Geochim. Cosmochim. Acta* **63**, 3513-3524.

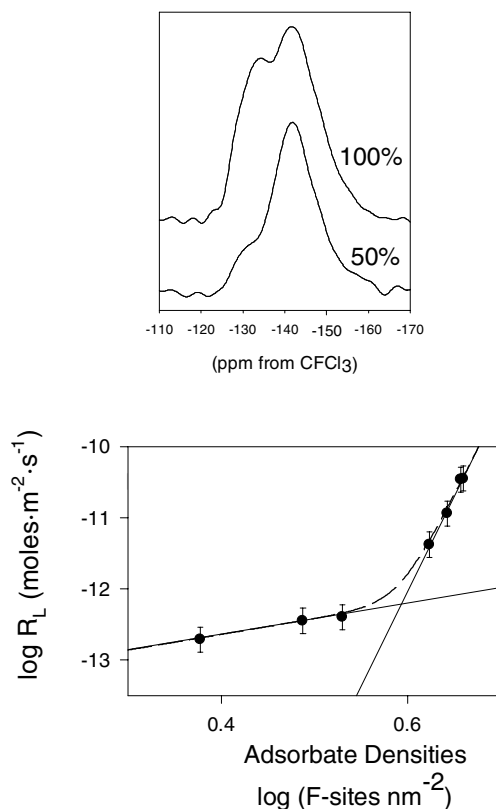


Figure: **(Top)** 19 F-MAS-NMR spectra of fluoride adsorbates on bayerite (β -Al(OH) $_3$ (s)) as a percentage of full adsorbate density at pH=5. Conspicuous peaks are present in the spectra that vary with adsorbate concentration. The peak at -143 ppm is assigned to 19 F at terminal sites and the peak at -131 ppm is assigned to 19 F replacing hydroxyls bridging two aluminums at the surface. **(Bottom)** Dissolution rate of bayerite as a function of adsorbed fluoride concentrations (Nordin *et al.*, 1999) at pH=5. Note that the dissolution rates vary nonlinearly with F-adsorbate concentration even on a logarithmic scale. The lines correspond to contributions to rate from terminal and bridging fluorides, based up the NMR spectra.

GRANTEE: University Of California, Davis

Thermochemistry Facility
Department of Chemical Engineering and Materials Sciences
One Shields Ave.
Davis, California 95616-8779

GRANT: DE-FG03-97ER14749

Thermodynamics of Minerals Stable Near the Earth's Surface

A. Navrotsky (530-752-9289; Fax: 530-752-9307; anavrotsky@ucdavis.edu)

Objectives: The goals of the project are to increase both the database and the fundamental understanding of the thermodynamics of volatile-bearing mineral phases (amphiboles, micas, clays, zeolites, carbonates) important to surficial, sedimentary, and shallow crustal processes.

Project Description: Using high temperature solution calorimetry, this research determines the enthalpies of formation of hydrous silicates and carbonates. Systematics in energetics of ionic substitutions are sought in order to predict the thermodynamics of complex multicomponent minerals. Mixing properties of mica, amphibole, clay, zeolite, and carbonate solid solutions are also studied.

Results: *Clays:* Work on kaolinite has been extended to synthetic samples with better control of composition, crystallinity, and impurity content. The conclusions found earlier, namely that all the samples are very similar in enthalpy despite differences in disorder, is confirmed and extended. Kaolinite is the thermodynamically stable kaolin polymorph.

Hydration energetics: Using data for manganese oxide minerals and for zeolites, a model is being developed in which the cation hydration (described by the number of water molecules per extra-framework cation) is the major factor influencing enthalpies of formation relative to anhydrous stable phases. This concept unifies, explains, and predicts enthalpies of formation of a large number of hydrated frameworks. Negative (exothermic) enthalpies of formation of hydrated open frameworks from anhydrous dense ones plus liquid water correlate linearly with negative entropies of formation. This implies that the "structuring" of water around alkali and alkaline earth cations is the major driving force for the stability of low temperature open framework minerals such as zeolites.

New Projects: Exploratory work on hydrotalcites and sulfate minerals has been initiated. The behavior of sulfate in the two calorimetric solvents, $2\text{PbO}\cdot\text{B}_2\text{O}_3$ and $3\text{Na}_2\text{O}\cdot\text{MoO}_3$ is being characterized. Preliminary results suggest that the sulfate remains dissolved up to a concentration of about 1 wt. %, forming a reproducible and satisfactory calorimetric final state.

GRANTEE: University Of California, Davis

Department of Chemistry and the
Department of Land, Air and Water Resources
Davis, CA 95616

GRANT: DE-FG03-92ER14307

Electrochemical Measurements of Thermodynamics Properties of Minerals and the Processes of Reconstruction at Mineral Surfaces

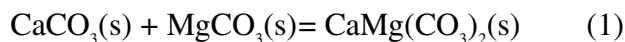
P. A. Rock (530-754-8918; Fax: 530-754-9057; rock@lsdo.ucdavis.edu) and W. H. Casey (530-752-3211; Fax: 530-752-1552; whcasey@ucdavis.edu)

Objectives: We are: (1) measuring thermodynamic properties for carbonate solid-solution minerals that are important in soils and aquifers; (2) devising new theoretical approaches to the calculation of the energetics of calcite-structure metal carbonates in pure and binary phases; (3) and, using AFM to explore the processes of reconstruction at mineral surfaces.

Project Description and Results: We have extended our new theoretical method for calculating lattice energies of calcite-structure metal carbonates (G. Mandell and P.A. Rock, *J. Phys. Chem. Solids* 59, 95-702 and 703-712, 1998) to metal carbonate solid solutions. Theoretical excess energies for solid solutions (Ca,M)CO₃(ss) [where M=Cd, Mn or Fe] have been calculated (G. Mandell, *et. al.*, *J. Phys. Chem. Solids* 60, 651-661 (1999)). A comparison between our theoretical results and experimental results is encouraging, especially for the Ca_xCd_{1-x}CO₃(ss) and Ca_xMn_{1-x}CO₃(ss) systems.

Recently, we have discovered how to extend the theory to carbonates with the aragonite structure. This advance enables us to explore the energetics of the calcite <-> aragonite phase transition, as well as metal carbonate solid solution with the aragonite structure; for example, as Ca_xSr_{1-x}CO₃(ss) for which we have independently obtained experimental excess Gibbs energy data.

We have used our electrochemical cell technique (Rock, *et. al.*, *Geochim. Cosmochim. Acta* 58, 4281-4291, 1994) to determine ΔG_f° for dolomite. Our value of ΔG_f° of $-2147.82 \pm 2.20 \text{ kJ} \cdot \text{mol}^{-1}$ for dolomite, together with new ΔG_f° data for MgCO₃(s) (determined in our lab) and literature data for CaCO₃(s) yield for the equation:



$$\Delta G_f^\circ = -11.56 \pm 2.20 \text{ kJ}$$

whereas the calorimetric data of Capobianco and Navrotsky (1987) yield a value of $\Delta H_f^\circ = -11.48 \pm 0.50 \text{ kJ}$ for reaction (1). Because, as Navrotsky has pointed out, $\Delta S_{rxn}^\circ(11) = 0$, the agreement of the independent electrochemical and thermochemical method is remarkable.

We have also used our lattice energy theory to calculate $\Delta G_{rxn}^\circ(1)$; the result obtained was -12.64 kJ which is in excellent agreement with the experimental data.

Dissolution Kinetics of Calcite:

Atomic force microscopy (AFM) was used to study the rates of migration of the (1014) plane of a single-crystal of calcite dissolving in 0.1 M NaCl aqueous solutions at room temperature. The solution pH and P_{CO_2} was controlled in the ranges $4.4 < \text{pH} < 12.2$ and $0 < P_{CO_2} < 10^{-3.5}$ atm (ambient), respectively. Measured step velocities were compared with the mineral dissolution rates determined from the calcium fluxes. The step velocity is defined as the average of the velocities of the obtuse and acute steps. Rates of step motion increased gradually from $1.4(\pm 0.2)$ at pH 5.3 to $2.4(\pm 0.3)$ nm s^{-1} at pH 8.2, whereas the rates inverted and decreased to the minimum value of $0.69(\pm 0.18)$ nm s^{-1} at pH 10.8. For $\text{pH} > 10.8$, only the velocity of the obtuse steps increased as pH increased, whereas that of acute steps gradually decreased (see Figure).

The dissolution rate of the mineral can be calculated from the measured step velocities and average slope, which is proportional to the concentration of exposed monomolecular steps on the surface. The average slope of the dissolving mineral, measured at pH 5.6 and 9.7, was $0.026 (\pm 0.015)$. Using this slope, we calculate bulk dissolution rates for $5.3 < \text{pH} < 12.2$ of $4.9(\pm 3.0) \times 10^{-11}$ to $1.8(\pm 1.0) \times 10^{-10}$ $\text{mol cm}^{-2} \text{s}^{-1}$. The obtained dissolution rate can be expressed by the following empirical equation:

$$R_{\text{dss}} = 10^{-4.66(\pm 0.13)} [\text{H}^+] + 10^{-3.87(\pm 0.06)} [\text{HCO}_3^-] + 10^{-7.99(\pm 0.08)} [\text{OH}^-]$$

We propose that calcite dissolution in these solutions is controlled by elementary reactions that are similar to those that control the dissolution of other amphoteric solids, such as oxides. The mechanisms include the proton-enhanced hydration and detachment of calcium-carbonate ion pairs. The detachments are enhanced by the presence of absorbed nucleophiles, such as hydroxyl and bicarbonate ions, and by protons absorbed by key oxygens. A molecular model is proposed that illustrates these processes (Shiraki, *et al.*, *Aquatic Geochemistry* **6**, 87-108, 2000).

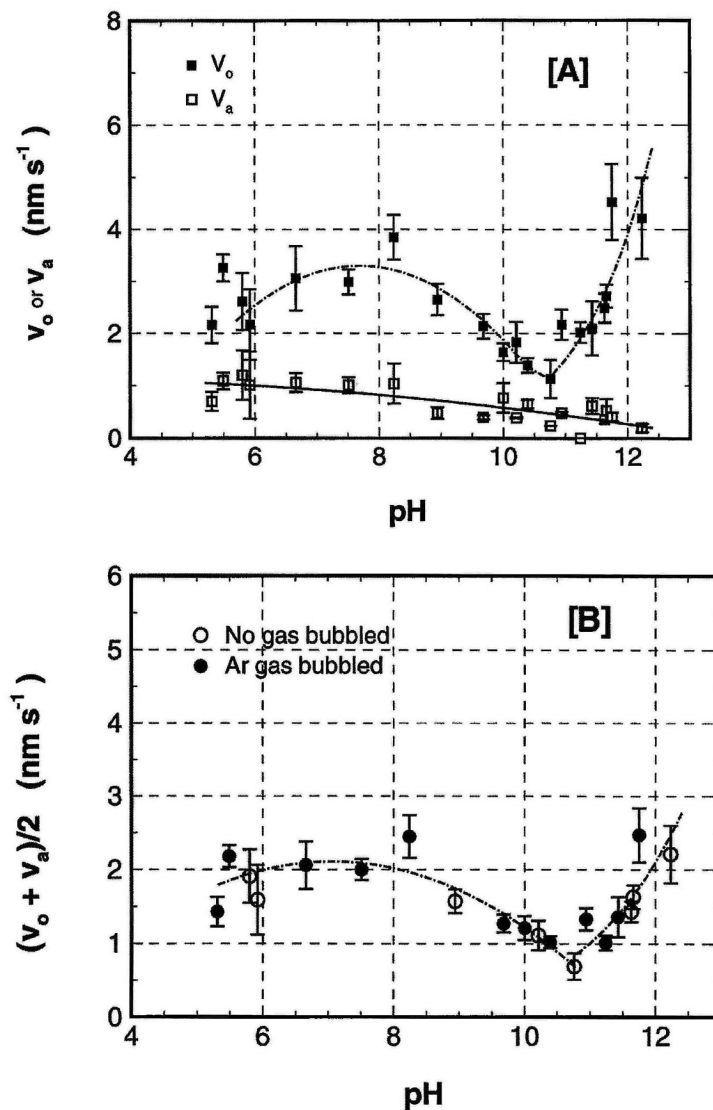


Figure 1. [A] The velocity of the obtuse and acute steps, v_o and v_a vs. pH. [B] The average velocity, $(v_o + v_a)/2$, vs. pH (● No gas was bubbled, ○ argon gas was bubbled).

GRANTEE: University Of California, Los Angeles

Department of Earth and Space Sciences
Los Angeles, CA 90095-1567

GRANT: DE-FG-03-89ER14049

Application of $^{40}\text{Ar}/^{39}\text{Ar}$ thermochronometry and ion microprobe stable isotope geochemistry to the evolution of petroleum reservoirs and hydrothermal systems

T.M. Harrison (310-825-7970; Fax: 310-825-4396; tmh@argon.ess.ucla.edu)

Objectives: Understanding the rates and mechanisms involved in the formation of exploitable geological energy sources, including fossil fuel, geothermal, and fissionable materials, requires knowledge of the age of origin and subsequent thermal history of the system over geological time. The objective of this research is to assess the utility of micro-scale isotopic techniques in deriving both fluid evolution and thermal history results for crustal environments that bear upon energy exploration and reservoir assessment.

Project Description: We are using coupled application of the ion microprobe and $^{40}\text{Ar}/^{39}\text{Ar}$ thermochronometry to: (1) assess the thermal and diagenetic histories of sedimentary basins (southern San Joaquin basin, central California); (2) study the intrusion history and thermal evolution of a young geothermal system (Geysers steam field, northern California) to resolve fundamental questions regarding its origin; and (3) develop tools to investigate the stability of uraninite in the presence of fluid and radiation effects to better understand the nature of unconformity-type uranium deposits (Athabasca Basin). Some of these efforts require significant developmental work to make meaningful progress. In particular we have found it necessary to develop a robust ion microprobe calibration for isotope ratio analysis of oxygen and carbon isotopes of complex carbonate compositions in order to investigate rock-fluid interactions. Similar developments have been required to study the U-Pb and oxygen isotopic systematics of uraninites and associated phases.

Results: 1) *Thermal and diagenetic histories of sedimentary basins.* Carbonate cements are an important feature of hydrocarbon reservoirs throughout the world because they control fluid flow thereby influencing hydrocarbon accumulation. While we have made substantial progress in developing *in situ* stable isotopic analyses of carbonate phases from which to infer fluid evolution trajectories, our methods have thus far been restricted to end member carbonates because significant matrix effects on secondary ionization yields require empirical calibrations. This effect is a significant limitation as carbonates exhibit an extensive solid solution in basin environments. To achieve our goal of obtaining better than $\pm 1\%$ precision from a $\sim 10\ \mu\text{m}$ spot in non-endmember carbonates in less than 5 minutes, we have begun synthesis of complex carbonates covering a broad range of compositions across the Ca-Fe-Mg ternary. Both hydrothermal and piston-cylinder approaches to synthesis have been investigated and over a dozen candidate materials produced. The chemical homogeneity of these materials are then assessed and appropriate samples isotopically characterized using both combustion and fluorination methods prior to gas-source mass spectrometry. Once a comprehensive set of ion microprobe standards for O and C isotopic analysis have been developed, we will systematically assess matrix effects by comparing the conventionally obtained results with ion microprobe analyses. To date we have been successful at synthesizing about two dozen different compositions along the calcite-siderite join, siderite

with 20 wt% MgO, and ferromagnesite. Homogeneous, naturally occurring carbonates have been obtained for endmember compositions and along the dolomite-ankerite join.

2) *Thermal energy potential of active magmatic-hydrothermal systems.* We have been able to establish granitoid emplacement and the subsequent thermal evolution in the Geysers geothermal field with sufficient precision ($\pm 25^\circ\text{C}$, ± 50 ka) to constrain quantitative thermal models. Ion microprobe analyses of 74 zircon crystals from four granite samples from the plutonic complex that underlies the Geysers geothermal field yield concordant ages ranging from 1.13 ± 0.04 Ma to 1.25 ± 0.04 (1σ) Ma. The U-Pb ages coincide closely with $^{40}\text{Ar}/^{39}\text{Ar}$ age spectrum ages from coexisting K-feldspars and with the eruption ages of overlying volcanic rocks. The data indicate that the granite had cooled below 350°C by ~ 0.9 - 1.0 Ma. Interpretation of the feldspar $^{40}\text{Ar}/^{39}\text{Ar}$ age data using multi-diffusion domain theory indicates that post-emplacement rapid cooling was succeeded either by slower cooling from 350 - 300°C between 1.0 and 0.4 Ma or transitory reheating to 300 - 350°C at about 0.4 - 0.6 Ma. Subsequent rapid cooling to below 260°C between 0.4 - 0.2 Ma is in agreement with previous proposals that vapor-dominated conditions were initiated within the hydrothermal system at this time. Heat flow calculations constrained with K-feldspar thermal histories and the present elevated regional heat flow anomaly demonstrate that appreciable heat input from sources external to the known Geysers plutonic complex is required to maintain the geothermal system. This requirement is satisfied by either a large, underlying, convecting magma chamber (now solidified) emplaced at 1.2 Ma or episodic intrusion of smaller bodies from 1.2 - 0.6 Ma.

3) *U-Pb and O-isotopic studies of stratiform uraninites.* Understanding the genesis of unconformity-type uranium deposits is important because they contain the highest-grade source of nuclear fuel and also serve as natural laboratories in which to study the potential migration of radionuclides from geologic repositories. Their evolution remains poorly understood, in part because of the extreme textural heterogeneity and fine-scaled inter-growths of the mixed uranium-bearing phases. To overcome this limitation, we have developed a rapid and accurate technique to perform *in situ* U-Pb and O isotopic measurements on the same spot of uranium oxide minerals. The advantages of this approach are: mineral separation and chemical digestion are obviated; homogenous uranium oxide standards are not required; and precise and accurate U-Pb ages on *ca.* $10\ \mu\text{m}$ spots can be obtained in a matter of hours. We have applied this method to study the distribution of U-Pb ages in complexly intergrown uranium minerals from the unconformity-type Cigar Lake uranium deposit, Athabasca basin, Saskatchewan. *In situ* U-Pb results from early uraninite and paragenetically late coffinite ($\text{USiO}_4 \cdot n\text{H}_2\text{O}$) define well-correlated arrays on concordia with upper intercepts of 1461 ± 47 Ma, 1176 ± 9 Ma, and 876 ± 14 Ma ($\pm 1\sigma$). These ages, interpreted as the minimum ages of mineralization, are consistent with the age of associated clay alteration. The high spatial resolution and precision of the ion microprobe have allowed us to measure $\delta^{18}\text{O}$ values in unaltered portions of uraninites developed at the 10 's of μm -scale. The narrow range of $\delta^{18}\text{O}$ values (-34 to $-20\ \text{‰}$) are among the lowest reported for unconformity-type deposits confirming that conventional fluorination analyses of material sampled at the mm-scale are insufficient to avoid contamination from isotopically heavier coffinite and calciouranoite.

GRANTEE: University Of California, Santa Barbara

Department of Geological Sciences
Santa Barbara, California 93106

GRANT: DE-FG03-96ER14620

The Hydrodynamics of Geochemical Mass Transport and Clastic Diagenesis: San Joaquin Basin, California

*J. R. Boles (UC-Santa Barbara; 805-893-3719; Fax: 805 893-2314; boles@magic.geol.ucsb.edu)
and G. T. Garven (Johns Hopkins University; 410-516-8689; Fax: 410 516-7933; garven@jhu.edu)*

Objectives: Deep groundwater migration plays an important role in many geologic processes, including diagenesis in sedimentary basins that directly affects other processes such as overpressuring, oil migration and sediment-hosted ore mineralization during burial because of the control on permeability and porosity. The principal objective is to quantify the hydrogeologic regimes for clastic diagenesis, using the San Joaquin basin of California to establish geologic constraints for numerical modeling at the basin and formation scale.

Project Description: Few hydrogeologic models have been developed or applied to field data sets, rigorously couple geochemical processes, or test conceptual models for diagenesis beyond abstract formation-scale numerical simulations or core-scale laboratory studies. The approach used here is to develop coupled hydrodynamic-geochemical models with computer simulations constrained by geochemical and hydrologic observations for the San Joaquin basin of California. This project has involved the compilation and general mapping of geologic, pore pressure, salinity, and temperature data for the main aquifers in the basin to build a clearer picture of flow patterns as they exist today at the regional scale. The principal task for us has been to quantify the paleohydrology and thermal history of the San Joaquin basin with a new finite-element code for simulating fluid migration and pressure changes during sedimentation, uplift, and erosion. After the hydrogeologic history has been explored in a hydrodynamic sense, we will conduct reactive-flow simulations to assess mechanisms for diagenesis and chemical mass transport in the clastic wedge. Different diagenetic fluid-flow hypotheses such as compaction dewatering, episodic pulses, meteoric invasion, and cross-formational flow are tested with the coupled hydrogeologic models through a sensitivity analysis.

Results: Our previous fluid flow modeling results formed the regional-scale framework for sets of new numerical experiments aimed at simulating reactive flow fields within the Stevens Sandstone, a Miocene-age reservoir in the San Joaquin basin for which extensive amounts of geochemical and petrophysical data exist. We developed simulations to predict the coupled processes of fluid flow, heat transport, and reactive chemical transport to investigate effects of mass transfer on the diagenesis of a permeable bed during compaction-driven flow. The models included a new kinetic rate expression for plagioclase dissolution that appears to drive precipitation of calcite and kaolinite and albitization reactions in the Stevens Sandstone. Calcium transport in the basin seems to be most important during burial and compaction, with transport distances of up to 10 km during the 5 million years of burial simulated. Sensitivity studies were used to illustrate the range of diagenetic fabrics that might be generated depending on the range of model parameters such carbon dioxide partial pressures, permeability heterogeneity, and formation dispersion coefficients. More focused flow along fracture or faults seems to be required to explain the volumes of cements observed in the basin.

GRANTEE: University Of California, Santa Barbara

Department of Geological Sciences
Santa Barbara, California 93106

GRANT: DE-FG03-91ER14211

Magma Rheology, Mixing of Rheological Fluids, Molecular Dynamics Simulation, and Lithospheric Dynamics

F. J. Spera (805-893-4880; Fax: 805-893-8649; spera@magma.geol.ucsb.edu)

Objectives:

- Laboratory measurements of magma rheological properties on magma
- Determination of the structure and properties of multicomponent silicate melts and glasses at elevated temperature and pressure.
- Numerical modeling of porous media thermohaline convection
- Geochemical material balance modeling of assimilation and fractional crystallization subject to energy constraints.

Project Description: This collaborative project with D. A. Yuen at the University of Minnesota will improve our understanding of the thermal, chemical, dynamical and mechanical state of the continental crust and subcrustal lithosphere with particular focus on the interactions between the various subsystems. The work-plan includes: (1) new rheological laboratory measurements on melts and magmatic suspensions (2) Determination of the thermodynamical and transport properties of molten silicates by MD simulations (3) Mixing processes of rheological fluids in convection and visualization of complex processes (4) Coupling between mantle convection with temperature-dependent and non-Newtonian rheology and mantle diapirs on the thermal regime and subsidence curves of rift-related basins (5) The dynamical influences of lithospheric phase transitions on the thermal-mechanical evolution of sedimentary basins (6) The development of stress fields and criteria for faulting in the crust and finally (7) Modeling of heat and mass transport driven by thermal and compositional heterogeneities in porous media (8) Open system geochemical modeling of magmatic systems.

Results: Results cited below are for the UCSB part of this project. Additional results are given in the summary of activities by the University of Minnesota team lead by D. A. Yuen. Molecular Dynamics (MD) simulations have been carried out on 5 liquids in the system $\text{NaAlO}_2\text{-SiO}_2$ at temperatures ranging from 4000 -6000 K and pressures from 0 to 55 GPa. We have studied changes in melt structure as a function of pressure to better comprehend the known pressure-dependent properties of network and partially networked silicate melts. One result is that the activation volume for diffusion of Oxygen in melts across the join $\text{NaAlO}_2\text{-SiO}_2$ varies smoothly with composition such that $V_a = -10\text{cm}^3/\text{mol}$ for silica and $+4\text{cm}^3/\text{mol}$ for soda aluminate (NaAlO_2) at low pressures. We also extend the heuristic Adams-Gibbs configurational entropy model and explain both the variation of the activation volume for viscous flow and the anomalous viscosity behavior as a function of composition for all melts along the join $\text{NaAlO}_2\text{-SiO}_2$. Details of this work may be found in *American Mineralogist*, 84, 1999, pp.345-356. Other MD simulation research includes a study of the microscopic dynamics of the glass transition in equilibrium liquid, metastable (supercooled) liquid and glassy $\text{CaAl}_2\text{Si}_2\text{O}_8$. This work has been submitted

to *American Mineralogist*. Structural relaxation at the macroscopic level may be explained microscopically by a stochastic trapping diffusion model with a defined waiting time distribution for activated hopping that diverges as the glass transition is approached. This model can be applied to quantitatively model diffusion in geological materials at elevated temperatures and pressures.

In experimental rheological work, measurements of the viscosity of bubble-bearing rhyolite emulsions have been completed. We show that for Capillary numbers in the range 1-100 the relative viscosity is a monotonically decreasing function of porosity (volume bubble-fraction) and that at 50 vol. % bubbles, the shear viscosity is smaller, by a factor of ten, relative to the single-phase (zero porosity) melt at the same pressure and temperature. In a separate publication (*Earth Planet. Sci. Lett.*, 175, 2000, pp.327-331) we discussed a paper in the literature (*Earth Planet. Sci. Lett.*, 166, 1999, pp71-84) and show how the authors came to incorrect conclusions based on an inadequate appreciation of errors inherent in high viscosity experimental rheometry.

The final piece of research completed this year involves development of a petrological model for describing the geochemical evolution of open magmatic systems subject to simultaneous assimilation, recharge and fractional crystallization. This work consists of about 120 manuscript pages of text and figures and has been accepted for publication in the *Journal of Petrology*. This study presents an algorithm for modeling the trace element evolution of a magmatic system treated as an open system subject to exchange of mass and energy with its surroundings. We show how certain seemingly inscrutable geochemical systems such as Long Valley Caldera system in eastern California can be readily interpreted based on this new model.

GRANTEE: University Of California, Santa Cruz

Institute of Tectonics
Santa Cruz, CA 95064

GRANT: DE-FG03-98ER14845

Fast 3-D Modeling and Prestack Depth Migration Using Generalized Screen Methods

R.-S. Wu (831-459-5135; Fax: 831459-2423; wrs@es.ucsc.edu)

Objectives: Develop high accuracy and high efficiency numerical methods for seismic modeling/imaging in three-dimensional complex structures. The methods are based on the generalized screen propagator theory that uses the MFSB (Multiple Forward-scattering Single Backscattering) approximation.

Project Description: The project is a collaborative effort of three institutions, LANL, MIT, and UCSC. The research at UCSC is implemented at the Modeling and Imaging Laboratory, Institute of Tectonics. The approach is based on the fast one-way wave propagation methods with dual-domain (space and wavenumber domains) implementation. The method bridges the gap between high-frequency asymptotic methods and full-wave equation methods, and can generate excellent modeling/imaging results with high efficiency.

Results: The windowed screen propagator (Jin and Wu, 1999), hybrid pseudo-screen method (Jin and Peng, 1999, Jin, Wu and Peng, 1999), wide-angle screen propagator based on the Pade approximation (Mignet and Xie, 1999) and Generalized local Born Fourier method (Huang, Fehler and Wu) are all been tested and improved. Both synthetic SEG/EAGE salt data, Marmousi data and real data from complex regions in the Gulf of Mexico are tested with these methods. The results showed superior image quality.

The 3D post-stack and pre-stack migrations for the SEG/EAGE salt model are conducted with the pseudo-screen method and wide-angle Pade screen propagator (Wu, Jin, Xie and Mosher, 2000; Xie, Mosher and Wu, 2000). For both 2D and 3D migrations, the above mentioned methods give much better image results than the Kirchhoff method and conventional split-step Fourier method.

The common-offset migration based on the pseudo-screen method are introduced and tested for the 2D Marmousi model (Jin and Wu, 1999). Compared with the common-source migration, which uses more than 300 sources, the common-offset migration uses only 48 offsets and gives the same image quality.

An absorbing boundary is introduced in the boundary element method (Fu, *et al.* 1999) and the resulted method has been used to remove the rugged-topography scattering effects in surface seismic data. The studies under this project also include the improvement of the wide-angle elastic wave modeling (Wu and Wu, 1999; Xie and Wu, 1999), and parallelization of the prestack migration code (Guan and Wu, 1999).

Fu, L.Y., R.S. Wu and H. Guan, 1999, Removing rugged-topography scattering effects in surface seismic data, Expanded abstracts, SEG 69th Annual Meeting, 453-456.

Guan, H. and R.S. Wu, 1999, Parallel prestack migration with the generalized screen propagator method, Expanded abstracts, SEG 69th Annual Meeting, 1520-1523.

Huang, L.J., M. Fehler and R.S. Wu, 1999, Generalized local Born Fourier migration for complex structures, Geophysics, in press.

- Jin, S. and C. Peng, 1999, Experimenting with the hybrid pseudo-screen migration, Expanded abstracts, SEG 69th Annual Meeting, 1449-1452.
- Jin, S., and R.S. Wu, 1999, Depth migration with a windowed screen propagator: Journal of Seismic Exploration, 8(1), 27-38.
- Jin, S., Wu, R.S., and Peng, C., 1999, Seismic depth migration with screen propagators: Computational Geosciences, 3, 321-335.
- Jin, S., and Wu, R.S., 1999, Common-offset pseudo-screen depth migration: Expanded abstracts, SEG 69th Annual Meeting, 1516-1519.
- Mignet, F.C. and X.B. Xie, 1999, Wide angle screen method applied to pre-stack migration of a 2D synthetic salt-like model, Expanded abstracts, SEG 69th Annual Meeting, 1536-1539.
- Wu, X.Y. and R.S. Wu, 1999, Wide-angle thin-slab propagator with phase matching for elastic wave modeling, Expanded abstracts, SEG 69th Annual Meeting, 1867-1870.
- Wu, R.S., Jin, S., Xie, X.B and Mosher, C.C., 2000, 2D and 3D generalized screen migrations, submitted to: EAGE Annual Meeting.
- Xie, X.B. and Wu, R.S., 1999, Improving the wide angle accuracy of the screen propagator for elastic wave propagation, Expanded abstracts, SEG 69th Annual Meeting, 1863-1866.
- Xie, X.B, Mosher, C.C. and Wu, R.S., 2000, The application of wide angle screen propagator to 2D and 3D depth migrations, submitted to: SEG 70th Annual Meeting.
- .

GRANTEE: The University Of Chicago

Department of the Geophysical Sciences
Chicago, IL 60637

GRANT: DE-FG02-97ER14773

Kinetic isotope fractionation

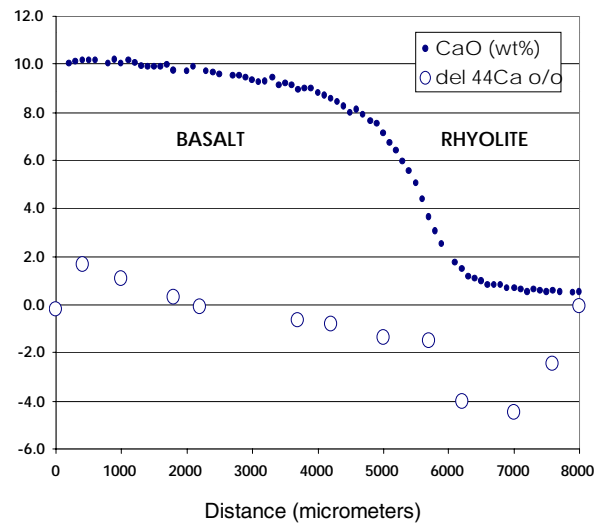
F. M. Richter (773-702-8118; Fax: 773-702-9505; richter@ geosci.uchicago.edu)

Objectives: The main theme of our present research is to better understand fluid-mineral chemical exchange mechanisms and associated transport mechanisms. The specific focus is on kinetic isotope fractionations associated with transport by diffusion.

Project Description: Our project has evolved from measuring the mass dependence of isotope mobility (self diffusion coefficients) in doped, isochemical, and isothermal diffusion couples to studies of kinetic isotope fractionation by chemical diffusion between natural fluids. The systems being investigated include molten rhyolite-basalt, supercritical water with dissolved silica, and water at near room temperature conditions with dissolved Ca salts. The Ca experiments are preliminary to studies involving dissolution and transport of CaCO_3 . In the case of dissolved Ca^{2+} we need to resolve the effect, if any, of codiffusers on the kinetic isotope fractionation in aqueous solutions. Electrical neutrality requires that Ca^{2+} have co-diffusing anions, for which we can explore a range of masses by using Cl^- , Br^- , and I^- .

Results: We have completed a series of basalt-rhyolite diffusion couples using natural starting materials run in a piston cylinder apparatus for various lengths of time at $T=1400^\circ\text{C}$ and $P=10$ kbars. The starting materials were mid ocean ridge basalt and a natural low Ca rhyolite. We have measured the Ca and Li isotopic fractionation associated with the diffusion of Ca and Li, between basalt and rhyolite. The results are in excellent agreement with our earlier predictions (see Fig. 8, *Geochem. Cosmochem. Acta*, v63, pp2853-2861, 1999): $\sim 6\%$ change in $\delta^{44}\text{Ca}$ (see below) and $\sim 30\%$ in $\delta^7\text{Li}$. Thus, we have clear evidence that diffusion in silicate liquids can produce kinetic isotope fractionations that are more than an order of magnitude larger than present analytical precision (*e.g.*, $\pm 0.2\%$ for $\delta^{44}\text{Ca}$).

The Li diffusion experiments gave a most unexpected result that may turn out to be very useful in terms of constraining the residence times of magmas in the crust. We found that the diffusion coefficient for Li in both basalt and rhyolite is almost two orders of magnitude larger than that of the next fastest diffuser, Na. This was not expected and clearly at odds with the commonly made suggestion that Li diffuses more or less like Na. The very rapid diffusion of Li has great potential for translating observed Li variations in erupted magmas into constraints on the fractionation, geometry and residence time of the magma in the crustal reservoir. We should be



able to answer questions as to how long could a particular batch of magma have been in the crust (or last fractionated) without diffusion having erased all variations in Li content?

We have also been carrying out kinetic isotope fractionation experiments in aqueous fluids. These involve diffusion along a capillary connecting two reservoirs. The supercritical water experiments involve dissolved silica and are done in a special two-chamber piston cylinder assembly developed by Bruce Watson for measuring solubility and the diffusion coefficient of dissolved silica. In our application, we also measure the Si isotopic composition of the material deposited in the lower temperature chamber. The same general approach is used at room temperature and one bar for studies of diffusion and isotope fractionation of dissolved Ca

GRANTEE: The University Of Chicago

Center for Advanced Radiation Sources
5640 S. Ellis Avenue
Chicago, IL 60637

Grant: DE-FG02-94ER14466

GeoSoilEnviroCARS: A National Resource for Earth, Planetary, Soil and Environmental Science Research at the Advanced Photon Source

S. R. Sutton (630-252-0426; Fax: 630-252-0436; sutton@cars.uchicago.edu) and M. L. Rivers (630-252-0422; Fax: 630-252-0436; rivers@cars.uchicago.edu)

Objectives: GeoSoilEnviroCARS is a national consortium of Earth scientists whose goal is to design, construct and operate, as a national user facility, two synchrotron radiation beamlines (one sector) at the Advanced Photon Source, Argonne National Laboratory.

Project Description: The GeoSoilEnviroCARS sector will include instrumentation for: (1) absorption spectroscopy and anomalous scattering; (2) fluorescence microprobe analysis and microtomography; (3) powder and microcrystal diffraction; (4) high-pressure research with diamond anvil cells; and (5) high-pressure research with the large-volume press. The availability of these facilities, dedicated to Earth science research, will allow extension of current research at synchrotron facilities to much lower concentration levels, low Z elements, low dimensionality materials (surfaces and interfaces), small volume samples, and transient phenomena. Focus research areas include migration and remediation of toxic metals and radioisotopes in contaminated sediments, redox chemistry of transition metals at the root-soil interface and its role in agriculturally-relevant plant diseases, the chemical nature of hydrothermal fluids and evolution of hydrothermal systems, chemical reactions on mineral surfaces, petrogenesis of strategic elements, phase transitions in mantle minerals, and the properties of the Earth's core.

Results: Techniques which have been commissioned in the three operating experimental stations are: 13-ID-C: Microspectroscopy; XRF microprobe; single crystal diffraction, surface scattering; surface spectroscopy; microtomography. 13-ID-D: Energy dispersive and monochromatic diffraction experiments in the DAC with laser heating. 13-BM-D: 250-ton multi-anvil press (energy dispersive diffraction, viscosity), microtomography, microcrystal diffraction, XRF microprobe.

GeoSoilEnviroCARS is currently making beam time available (<http://gsecars.uchicago.edu>) to the general Earth science community for the following techniques: XRF microprobe/microspectroscopy, microtomography, energy-dispersive diffraction in the diamond anvil cell and multi-anvil press. During FY99, eighty beamtime proposals have been received and one hundred and forty users have conducted experiments.

Scientific highlights include: *The Water - Corundum (0001) Interface Structure Measured by Crystal Truncation Rod Diffraction*: Collaborators - P. Eng, M. Newville, S. Sutton (University of Chicago), T. Trainor, G. E. Brown, Jr., J. Fitts, D. Grolimund (Stanford University), G. Waychunas (LBNL). Crystal truncation rod studies showed that a stable double water layer exists on the surface of hydroxylated (0001) alumina. This result differs significantly from those of Guenard *et al.* (1997) for the "clean" α -Al₂O₃ (0001) surface, indicating the importance of performing ambient measurements. Moreover, the

results clearly indicate that the common assumption that metal oxide surfaces in contact with bulk water are simple terminations of the bulk structure is incorrect.

Plutonium Sorption onto Yucca Mountain Tuff: Collaborators - P. Bertsch, M. Duff, D. Hunter (Savannah Research Ecology Laboratory, Univ. of Georgia); P. Eng, M. Newville, S. Sutton (University of Chicago): In a study of Pu sorption on tuff, Pu was highly associated with Mn-rich phases (*e.g.*, rancieite), and all but absent in the zeolitic and iron oxide grains that dominate the rock. This result is contrary to expectations of high association with Fe-rich minerals based on single component experiments and demonstrates the need for sorption studies on complex natural materials. The XANES spectra are most consistent with Pu being Pu⁵⁺ though further measurements will be required to fully explore the possibility of contributions from Pu⁴⁺ and Pu⁶⁺. First-shell microEXAFS of Pu shows six oxygen atoms coordinating Pu at 2.25Å, which is consistent with Pu⁴⁺ and Pu⁵⁺ compounds.

GRANTEE: The University Of Chicago

Center for Advanced Radiation Sources
5640 S. Ellis Avenue
Chicago, IL 60637

Grant: DE-FG02-92ER14244

Synchrotron X-ray Microprobe and Microspectroscopy: Technical Development for Advanced Photon Source Research and Low Temperature Geochemistry Applications

S. R. Sutton (630-252-0426; Fax: 630-252-0436; sutton@cars.uchicago.edu)

Objectives: The objectives are to develop and apply a synchrotron-based x-ray microprobe that can be used to determine the composition, structure, oxidation state, and bonding characteristics of Earth materials with trace element sensitivity and micrometer spatial resolution.

Project Description: The project focuses on development and application of the x-ray fluorescence microprobe on beamline X26A at the National Synchrotron Light Source (NSLS), Brookhaven National Laboratory. Geochemical problems that are under investigation include the nature of hydrothermal fluid inclusions, toxic metal and radioisotope speciation in contaminated sediments, determinations of the chemical histories of contaminated sites through microanalytical studies of indigenous organisms, and redox chemistry of metals at the root-soil interface.

Results: Examples of research projects include the following: *Hydraulic properties of water films on fracture surfaces* (with T. Tokunaga, LBNL): Research has focused on film flow and developing new methods for measuring relations between average film thickness, matric potential, and film hydraulic diffusivity. The initial results showed approximate power law matric potential dependence of the average film thickness, and monotonically increasing film hydraulic diffusivity with increased film thickness (and with increased matric potential). Fast film flow (average velocities greater than 10^{-7} m s⁻¹ under unit gradient conditions) was observed for average film thicknesses greater than 2 μ m and matric potentials greater than -2 kPa. The results of this research provide important constraints on chemical transport in sediments.

Redistribution of manganese in soils by microbial activity (with D. Schulze, Purdue University): The redox chemistry of soil manganese plays an important role in Mn uptake by plants, the mobility of trace elements absorbed on or occluded within Mn-oxide minerals, and the etiology of some soil-borne plant fungal diseases. MicroXANES studies at X26A have allowed in-situ analyses on Mn redox chemistry in both soils and live plants. This work has allowed detection and quantification of Mn²⁺, Mn³⁺, and Mn⁴⁺ in mixed systems and showed that Mn can be redistributed in soils by microbial activity.

Redox histories of igneous and metamorphic systems (with J. Delaney, Rutgers University; D. Dyar, U. Mass-Amherst): The relative oxidation state of iron in rock forming minerals is an important indicator of exchange reactions, kinetics, and biogenic activity in near-surface systems. Experiments at X26A have shown that synchrotron microXANES allows microscale determinations of Fe³⁺ and Fe²⁺ on spot sizes < 10 x 15 μ m. This permits examination of redox zoning in minerals, allows realistic characterization of these cations for thermodynamic modeling, permits study of oxidation kinetics at microscale, and potentially, coupled with ion probe H measurements, will allow distinction of dehydrogenation vs. oxidation processes in environmental samples

GRANTEE: The City College Of The City University Of New York

Benjamin Levich Institute & Department of Physics
New York, New York 10031

GRANT: DE-FG02-93-ER14327

Particulate Dynamics in Filtration and Granular Flow

J. Koplik (212-650-8162; Fax: 212-650-6835; koplik@sci.ccny.cuny.edu)

Objectives: We propose to seek a better understanding of the dynamics of collective particulate motion in deep-bed filtration processes, in flows in geological fracture systems, and in gravity-driven granular flows.

Project Description: Three general topics will be considered. First, the results of our previous studies of the motion of particles suspended in a fluid flowing in a porous medium will be used in network-model simulations of deep-bed filtration processes. Secondly, we will study transport processes (fluid flow, passive tracer dynamics, and suspended particle dynamics) in geological fractures, where the rock surface is a self-affine fractal. Here we will use scaling arguments and lattice Boltzmann numerical simulations, and collaborate with an experimental group at Orsay. Third, we will consider several topics in granular flows, specifically segregation and mixing processes, simple models of the effects of surrounding fluid in granular flows, and the structure of the wake of an obstacle placed in a gravity-driven flow.

Results: This year's progress on the topics listed above is as follows. (1) We conducted simulations of filtration in a network model of a porous medium, and found behavior qualitatively consistent with experiment, but the calculations are very time-consuming, and the results are extremely sensitive to the details of pore size distribution. The general features of filtration can be understood based on simpler cellular automaton models. A paper has been submitted for publication. (2) We started by developing estimates for the permeability of a self-affine fracture, and have begun lattice Boltzmann simulations to verify them. (3) The effects of temperature gradients on the mixing of granular systems were investigated by event-driven simulations. The temperature gradient can either enhance or discourage mixing of particles of different mass or different size, depending on the arrangement. A simple model of fluidization, in which the fluid flow intervening between the particles is modeled using Darcy's law, was shown to give qualitatively reasonable results.

GRANTEE: University Of Colorado

Cooperative Institute for Research in Environmental Sciences
Colorado Center for Chaos & Complexity
Department of Physics
Campus Box 216, Boulder, CO 80309

GRANT: DE-FG03-95ER14499

Nonlinear Systems Approach to Understanding the Origin of Geodetic Crustal Strains (Collaborative Research)

*J. B. Rundle (303-492-5642; Fax: 303-492-5070; rundle@cires.colorado.edu) and W. Klein
(Department of Physics, Boston University)*

Objectives: To develop a physical understanding of the origins of geodetic crustal strains in nonlinear geomechanical systems, to examine the space-time patterns and correlations that occur in these systems, and to use these patterns to forecast the future activity that may produce disasters affecting a wide variety of critical energy facilities.

Project Description: A variety of nonlinear dynamical processes operate within the complex Earth system. Signatures of these processes include the appearance of scaling (fractal distributions), global and local self-organization, intermittency, chaos, and the emergence of coherent space-time correlations, patterns, and structures. The geodynamical effects observed in earthquake systems, particularly crustal straining, dynamical segmentation, and intermittent seismicity, are being modeled in massively parallel simulations in an effort to clarify the origins of these phenomena. Simulations and theoretical investigations are particularly aimed at quantifying the limits of predictability for catastrophes (disasters) that occur within the Earth system. We are currently developing both the simulation methods for earthquake models, and the statistical mechanical analysis techniques needed to understand and interpret the results. From these simulations, we will then predict geodetic and other deformation associated with impending earthquakes to be tested against Global Positioning System, Synthetic Aperture Radar, seismicity, and other field data.

Results: We have made important progress in several fundamental problem areas. These include: 1) Stochastic evolution of stress fields on faults. Using numerical simulations, we have made a fundamental advance in understanding how failure and frictional processes influence the size of earthquakes. Stable precursory slip in a variety of current friction laws, such as the slip-dependent and rate-and-state laws, acts to smooth the stress distribution. Smoothing processes are thus associated with stable (aseismic) slip, whereas roughening processes are associated with unstable slip (earthquakes). 2) Space-time patterns in crustal deformation and seismicity with implications for forecasting. We analyzed the eigenpatterns and space-time structure of earthquake seismicity in southern California and found that systematic variations in seismicity can be seen prior to large earthquakes. These precursory patterns may prove useful in anticipating the occurrence of large earthquakes. 3) Earthquake physics and observational tests. We have found that earthquake physics can be understood as rotations of state vectors in mean-field, phase dynamical systems. These results strongly suggest that the largest events are accompanied by precursors that can be observed in crustal deformation and seismicity data. Analysis indicates that the largest repeating events are associated with long-lived space-time structures in the stress field.

GRANTEE: University Of Colorado

Department of Geological Sciences
Boulder, CO 80309-0399

GRANT: DE-FG03-95ER14518

Evolution of Rock Fracture Permeability During Shearing

S. Ge (303-492-8323; Fax: 303-492-2606; ges@spot.colorado.edu)

Objectives: To investigate the evolution of fracture apertures from the initial crack to a state with a certain amount of slip displacement under shearing.

Project Description: Significant progress has been made in understanding how fracture permeability relates to geometric factors of fracture surfaces and stress conditions. However, the history of the Earth reveals a dynamic environment in which small fractures dislocate after their initial separation and large faults slip over observable distances. Yet, limited effort has been made to study the evolution of fracture permeability under varying stress and deformation conditions. Understanding how apertures change dynamically during shearing would help interpret how fracture permeability varied in the past and thereby enhance our ability to infer paleo-systems of fluid flow and mineral or energy transport. This project aims at studying the evolution of fracture permeability in a shear deformation environment.

Results: Using four artificial fractures, a constant head fracture permeameter, and an LGA numerical model, we examined how fluid moves through an assortment of rough geometries. All flow experiments and numerical simulations were under laminar and fully saturated flow conditions. In each case, we achieved a good agreement between the flow rates observed in the experiments and the flow rates simulated using the lattice gas automata (LGA) model. Using variations of the mated sinusoidal and the sheared sinusoidal geometries, we found that the parallel plate model overpredicted the flow rate in all cases. The overprediction became more extensive as the tortuosity of the fluid path increased.

From the improved theoretical understanding, experimental data, and numerical simulation results, we recognized the role of true aperture and tortuosity and proposed a new model for fracture permeability. The new model uses an averaged normal aperture divided by the averaged tortuosity, and is called Averaged Normal Aperture (ANA) model. Comparing the observed data to the proposed ANA model, we found that the cubic law can be applied to these sinusoidal geometries by redefining the aperture and pressure gradient. Instead of using the vertical separation, the fracture aperture must be measured normal to the flow path and averaged according to a harmonic averaging scheme. In addition, the pressure gradient must include the extension in the path length when dealing with tortuous pathways. When the average normal aperture and the tortuosity are included in the cubic law, *i.e.*, when the aperture parameter in the cubic law is replaced by the proposed averaged normal aperture, we achieved a good match with the observed data in all cases

To examine the extent to which the minimum aperture in the fracture is a controlling factor in fluid flow, we made some additional measurements through less tortuous fractures that had obvious constrictions in the fluid path. One of these fracture geometries was composed of a combination of the sinusoidal and flat surfaces, and another used flat surfaces in a wedge configuration. After comparing experimental and LGA results, we found that using the minimum aperture in the cubic law could not adequately predict the flow rate. The best estimation of the effective aperture through both geometries was still the proposed average normal aperture model.

On the numerical study front, we made progress in advancing from the LGA model to a more sophisticated lattice Boltzmann (LB) model that is capable of yielding good approximation solutions to the Navier-Stokes equations. The LB method provides an efficient tool in studying flow in rock fractures, especially under non-linear or non-Darcian flow conditions. We adopted and modified a Sandia LB model that simulates not only fluid flow but also solute transport in rock fractures. We have tested the LB model, and initial simulation results indicate that the fluid and solute transport mechanism is strongly affected by fracture geometry. Shear deformation could lead to turbulent flow conditions and cause more solute dispersion.

GRANTEE: University Of Colorado

Department of Geological Sciences
Boulder, Colorado 80309-0399

GRANT: DE-FG03-99ER14979

Nucleation and Growth Kinetics of Clays and Carbonates on Mineral Substrates

K. L. Nagy (303-492-6187; Fax 303-492-2606; kathryn.nagy@colorado.edu)

Objectives: To investigate the kinetics of nucleation and growth of clays and carbonates on mineral substrates. Data are needed to model reactive fluid flow in porous media as applied to the natural processes of soil formation and sediment diagenesis, and to engineered processes such as subsurface CO₂ sequestration.

Project Description: Secondary mineral nucleation and growth is a major process that controls global cycling of elements during weathering at the Earth's surface, irreversible sequestering of dissolved contaminant metals in the environment, and changes in porosity, permeability, and fluid flow pathways in sedimentary basins. Typically, secondary minerals do not form homogeneously from solution, but nucleate and grow on substrate minerals. Although numerical simulations of fluid flow can now handle complex representations of reactions between minerals and fluids in natural porous media they still cannot simulate the real world because of the lack of kinetic data, especially kinetic data describing nucleation and growth.

Kinetics experiments will be conducted to nucleate and grow clays and carbonate minerals onto mica, quartz, and feldspar surfaces as a function of pH, saturation state, ionic strength, and temperature. Substrate mineral characteristics that control nucleation such as distribution and type of surface charge and molecular-scale structure will be evaluated. Rates will be determined from solution compositional changes and from atomic force microscopy images of precipitate volume. Synchrotron X-ray reflectivity and Extended X-ray Absorption Fine Structure spectroscopy measurements will be applied to determine nucleation mechanisms, in collaboration with Neil Sturchio of Argonne National Laboratory and Alain Manceau of the University of Grenoble, respectively. Quantitative expressions for nucleation and growth kinetics of clays and carbonates will be constructed from all data.

Results: This project was started on Sept. 1, 1999, and is in part a continuation of an earlier project to Nagy and R. T. Cygan at Sandia National Laboratories. Here are summarized results from the earlier experimental research. Nagy, Cygan, Hanchar, and Sturchio (1999, *Geochim. Cosmochim Acta*) measured gibbsite growth rates at 80°C, pH 3 on powdered kaolinite and single crystal muscovite substrates in stirred-flow reactors. They quantified growth rates on muscovite by measuring precipitate volume from three-dimensional microtopographic data collected in atomic force microscopy images. These data also showed that the gibbsite precipitated as thin films and elongated crystallites in crystallographic alignment with the structure of the muscovite basal surface. Gibbsite growth rates on gibbsite, kaolinite, and muscovite were expressed as one rate law with a dependence on solution saturation state and with adjustment of the percentage reactive surface areas of each substrate to be 100% for gibbsite and muscovite, and ~10% for kaolinite. The kaolinite surface was considered reactive only along edges under the experimental conditions. Manceau, Schlegel, Nagy, and Charlet (1999, *J. Colloid Interface Sci.*) demonstrated that Co-trioctahedral clays could be nucleated on quartz grain surfaces at room temperature in six days using a combination of Extended X-ray Absorption Fine

Structure (EXAFS) spectroscopy, solution chemistry experiments, and thermodynamic calculations of clay mineral stabilities. Hanchar, Nagy, Fenter, Finch, Beno, and Sturchio (2000, in press, *Amer. Mineral.*) used rotating anode X-ray powder diffraction (XRD) to quantify the amount of gibbsite grown on the kaolinite substrate experiments reported in Nagy *et al.* (1999). Hanchar *et al.* (2000) showed that these measurements can be obtained relatively quickly and quantitative determination can be made easily to 0.1 wt. % gibbsite using standard mixtures of powdered gibbsite and kaolinite. Results indicated that some of the gibbsite grown on the kaolinite was X-ray amorphous and that the discrepancy between the quantity of gibbsite determined by XRD and the quantity determined from solution compositional analyses exhibited a slight dependence on the aqueous Al concentration.

GRANTEE: University Of Colorado

Department of Civil, Environmental and Architectural Engineering
Boulder CO 80309-0428

Grant: DE-FG0396ER14590

Two-Phase Immiscible Fluid Flow in Fractured Rock: The Physics of Two-Phase Flow Processes in Single Fractures

H. Rajaram (303-492-6604; Fax: 303-492-7317, hari@colorado.edu), R. J. Glass (Sandia National Laboratories), and M. J. Nicholl (Oklahoma State University)

Objectives: The objective is to develop a quantitative understanding of critical fundamental processes controlling two-phase flow and transport in fractures, based on detailed physical experiments and high-resolution numerical simulations. This understanding may subsequently be abstracted for use in conceptual models applied to large-scale problems in petroleum extraction, isolation of hazardous or radioactive waste, remediation of contaminated subsurface media and CO₂ sequestration.

Project Description: Under two-phase immiscible flow conditions, the phase geometry associated with each phase controls the fluid flow and solute transport characteristics. The phase geometry is in-turn determined by a combination of the aperture variability, the capillary and viscous effects inherent in the two-phase flow processes themselves and external forces such as gravity. If one of the fluids can slightly dissolve in the other, then transport of the dissolved fluid also influences phase geometry.

In this collaborative project between Sandia National Laboratories, Oklahoma State University and University of Colorado at Boulder, systematic physical experimentation is coupled with concurrent numerical simulation to explore the factors controlling phase structure, flow, transport and inter-phase mass transfer in rough-walled fractures. A high-resolution light-transmission technique has been developed to facilitate acquisition of accurate experimental measurements of aperture, phase geometry and solute concentrations in transparent analog fractures. Use of this technique will lead to data of unprecedented accuracy for evaluating current understanding of invasion, flow and transport processes, and motivate refinement of theoretical concepts.

Results: A comprehensive evaluation of the Reynolds equation for saturated flow in rough-walled fractures was accomplished by combining high-resolution experiments with careful numerical simulations. Highly accurate aperture measurements in three transparent analog fractures (a Hele-Shaw cell, a fracture assembled using one rough and another flat glass plate and a fracture constructed with two rough plates) were an essential element in this evaluation. While numerical simulations based on the Reynolds equation closely reproduced the experimentally determined effective transmissivity of the Hele-Shaw cell, the discrepancies were in the range of 22-47% in the other two fractures. A careful evaluation of numerical and experimental errors suggested that these could only account for about 2% of the discrepancy. We therefore concluded that the Reynolds equation is inadequate for predicting effective transmissivities in the experimental rough-walled fractures.

A comprehensive study of solute dispersion in rough-walled fractures was carried out, combining high-resolution experimental measurements of fracture aperture and solute concentrations, with a three-dimensional computational model. The flow field in the computational model was determined by solving the Reynolds equation. The experimental results indicated a nonlinear dependence between the effective dispersion coefficient and the Peclet number (Pe). This feature was interpreted using a

theoretical model in which the total dispersion coefficient is expressed as a sum of the molecular diffusion, macrodispersion (induced by aperture variability, linear in Pe) and Taylor dispersion (induced by the velocity profile across the fracture, quadratic in Pe) coefficients. The Taylor dispersion term was shown to be most important at large values of Pe , corresponding to a quadratic dependence. While the theoretical model and numerical simulations qualitatively reproduced the nature of Pe -dependence of the dispersion coefficient, the magnitude of the dispersion coefficient was underestimated by about 35% at the highest Pe (750) value in the experiments. We concluded that the discrepancy between the theoretical and experimental results is largely attributable to the limitations associated with the Reynolds equation.

The factors controlling relative permeability in a partially saturated fracture were investigated based on experiments involving a wide range of entrapped phase structures. A numerical simulator was developed for modeling flow around the entrapped non-wetting phase. Results indicated close agreement between experimental and modeled relative permeabilities, suggesting that the inaccuracies associated with the Reynolds equation "cancel out", because they appear in both the saturated and absolute permeabilities. A conceptual model based on effective medium theory was proposed to explain the variation of the relative permeability with phase structure. The conceptual model involves four factors - the phase saturation, the in-plane tortuosity induced by the entrapped phase, the change in mean aperture within the flowing phase and a parameter representing change in aperture distribution within the flowing phase. The in-plane tortuosity induced by the entrapped phase was identified as the most dominant controlling factor, followed by the phase saturation.

GRANTEE: University Of Colorado

CIRES / Dept. of Geological Sciences
Boulder, Colorado 80309

Grant: DE-FG03-94ER14419

Seismic Absorption and Modulus Measurements in Single Cracks and Porous Rocks: Physical and Chemical Effects of Fluids

H. Spetzler (303-492-6715; Fax: 303-492-1149; spetzler@colorado.edu)

Objectives: We are studying the effects of small amounts of organic substances (*e.g.*, alcohols, ketones) on the mechanical properties of partially saturated porous rocks. The eventual goal is the development of a tool for monitoring changes in organic contaminant levels near waste sites.

Project Description: Small amounts of adsorbed organic substances on a surface significantly change the physical behavior (*e.g.*, wettability) of that surface. In porous rocks, this changed wettability can inhibit fluid flow, and thus change the bulk mechanical properties of the rock. An apparatus has been developed that measures Young's modulus and attenuation ($1/Q$) of both real rocks and artificial samples. The complexity of the dependence of the physical properties of a real rock (Lyons Sandstone) on contamination conditions and frequency of deformation has inspired measurements of the properties of a single crack. These properties have been successfully modeled using an energy-minimization scheme with independently supplied physical parameters. Findings from single-crack experiments and modeling are now being applied to artificial rocks made of sintered glass beads, and to natural sandstone samples. An intermediate-scale ($\sim 1 \text{ m}^3$ sample) experiment is planned.

Results: Attenuation measurements of a single crack contaminated with 2-propanol and partially saturated with distilled water show a large increase in attenuation at frequencies of 10-100 Hz. This effect is attributed to viscous dissipation caused by local fluid flow. Another attenuation increase at frequencies of 0.001-1 Hz is attributed to inhibited fluid flow due to changed surface wettability (contact angle hysteresis). This has been modeled by assuming that the shape of the meniscus and the position of the wetting front are in a minimum energy state. This state depends only on the surface energies of each of the present phases. Independent measurements of surface energy in both static and dynamic experiments have been made. Results from these measurements are used to supply model parameters to single-crack attenuation calculations. In addition to the strong frequency dependence mentioned earlier, modeled single-crack attenuation is very sensitive to crack aspect ratio and deformation amplitude.

Attenuation measurements have also been made of artificial and natural rock samples. The artificial rocks were sintered from 250 μm glass beads, and were chosen because of their simple (nearly hexagonal close packing) pore geometry. Modeling results from single cracks correctly predicted very low contaminant-induced attenuation due to the small aspect ratio of pore spaces in these samples. Real rocks, despite having more complicated pore geometry, have much thinner crack spaces. Modeling predicts that contaminant-induced attenuation is an important contributor to overall attenuation in Lyons Sandstone at frequencies of 0.001-1 Hz. Measurements of this type are currently under way, in preparation for finite-element modeling of attenuation in a meter-scale rock sample.

GRANTEE: Colorado School Of Mines

Center for Wave Phenomena
Green Center, Golden, CO 80401-1887.

GRANT: DE-FG03-98ER14908

Three-Dimensional Analysis of Seismic Signatures and Characterization of Fluids and Fractures in Anisotropic Formations.

I. Tsvankin (303-273-3060; Fax: 303-273-3478; ilya@dix.mines.edu), V. Grechka, and K. L. Lerner.

Objectives: The main goal of the project is to develop efficient velocity analysis and parameter estimation methods for azimuthally anisotropic reservoirs using the 3-D (azimuthal) variation in seismic signatures. The anisotropic parameters can then be related to the reservoir properties which control the flow of hydrocarbons.

Project Description: The CSM group is working on the inversion of azimuthally dependent reflection traveltimes and prestack amplitudes for the effective parameters of azimuthally anisotropic media. Combination of P-waves and converted PS-waves helps to estimate a representative set of the anisotropic parameters for models containing subvertical fracture systems or tilted transversely isotropic layers. The project includes theoretical studies, development of inversion and processing algorithms and their application to 3-D seismic field data. The inverted anisotropic model makes it possible to evaluate the physical parameters of fracture networks and the lithologic properties of source and reservoir rocks; the rock-physics part of the project is addressed by the groups from LLNL and Stanford University. The project results should provide a foundation for high-resolution characterization of heterogeneous anisotropic reservoirs using wide-azimuth multicomponent seismic surveys.

Results: *3-D moveout inversion in azimuthally anisotropic media with lateral velocity variation:* A velocity-analysis method capable of separating the influence of azimuthal anisotropy and lateral velocity variation on normal-moveout (NMO) velocity was developed and successfully applied to 3-D data acquired over a fractured reservoir in the Powder River Basin, Wyoming.

Analytic description of nonhyperbolic (long-spread) moveout in azimuthally anisotropic media: A concise nonhyperbolic moveout equation for stratified azimuthally anisotropic media provides analytic insight into the behavior of long-spread moveout and can be efficiently used in anisotropic traveltime modeling and inversion.

NMO-velocity surfaces and Dix-type formulae in heterogeneous anisotropic media: NMO-velocity surfaces, built by plotting NMO velocities in 3-D space at a fixed common-midpoint (CMP) location, help to devise Dix-type averaging and differentiation algorithms for parameter estimation in heterogeneous anisotropic media.

Inversion of azimuthally dependent NMO velocity in transversely isotropic media with a tilted axis of symmetry: Inversion of the 3-D NMO equation yields all parameters of tilted TI media responsible for kinematic signatures of P-waves.

Estimation of fracture parameters of transversely isotropic media with a horizontal symmetry axis (HTI) from reflection seismic data: Analysis of the dependence of the anisotropic parameters of HTI media on the physical properties of the fracture network was used to devise fracture-characterization procedures based on the reflection signatures of P- and PS-waves.

3-D moveout velocity analysis and parameter estimation for fractured reservoirs with orthorhombic symmetry: The equation of the NMO ellipse was used to invert multi-azimuth P-wave reflection traveltimes for the parameters of vertically inhomogeneous orthorhombic media.

GRANTEE: Columbia University

Lamont-Doherty Earth Observatory
Palisades, New York 10964-8000

GRANT: DE-FG02-95ER14572

Rock Varnish Record of Holocene Climate Variations in the Great Basin of Western US

T. Liu (845-365-8441; Fax 845-365-8155; tanzhuo@ldeo.columbia.edu) and W. S. Broecker (845-365-8413; Fax 845-365-8169; broecker@ldeo.columbia.edu)

Objectives: The objective of this research is to document Holocene climate variations recorded in rock varnish from the Great Basin of western US.

Project Description: Rock varnish is a very slowly accreting (<1 to 40 $\mu\text{m}/\text{ky}$) patina on subaerially exposed rock surfaces in arid to semi-arid deserts. Due to its sedimentary origin, rock varnish displays layered stratigraphy. Our previous work funded by the DOE indicates that the chemical composition of varnish stratigraphy changes markedly with climate. During dry periods it is manganese-poor and during wet periods manganese-rich. Such climate-related stratigraphy in varnish can be correlated across a given geographic region, suggesting that the climate signals recorded in varnish are of regional extent. In the Great Basin of western US, manganese-poor varnish layers formed during interglacials when the Great Basin was unusually dry, and manganese-rich layers were deposited during periods of glaciation when the Great Basin was wetter than at present. Therefore, rock varnish can be used as a recording media to study the climate, in particular moisture history of the world's deserts.

Varnish samples will be collected from a number of independently and radiometrically dated geomorphic features of latest Pleistocene and Holocene age in the entire Great Basin. These samples will then be thin-sectioned to uncover the distinct lamination patterns in rock varnish that recorded Holocene climate variations. Microchemical analyses with electron probe will be used to quantitatively characterize the varnish lamination patterns. The ages of the sampled geomorphic features will be utilized to provide radiometric time constraints for calibration of the Holocene lamination sequence. In addition, relative thickness of rock varnish will be used to interpolate ages for the internal layers within the varnish stratigraphy.

Results: Based on examinations of hundreds of varnish samples from the radiometrically dated geomorphic features in the Great Basin of western US, we have established the Holocene lamination sequence. This sequence consists of at least twelve evenly spaced weak dark layers, interfingering with thirteen orange layers. The six dark layers in the upper portion of the sequence are likely to be deposited during the Neoglaciation and Little Ice Age when the Great Basin was relatively wetter than at present. The five dark layers in the lower portion of the sequence probably formed in response to the early Holocene wet phases. There is also one dark layer at the middle point of the sequence, possibly recorded one wet phase around the middle Holocene. All of the orange layers in the sequence are diagnostic of the dry phases during the Holocene. This rock varnish record of Holocene climate variations is generally consistent with other regional climate records in the Great Basin. Most importantly, the first-order periodicity of the twelve dark layers appears to match the millenium-scale climate cycles that have already been documented in a number of Holocene climate records worldwide.

GRANTEE: University Of Connecticut

Department of Marine Sciences
1084 Shennecossett Road
Groton, CT 06340-6097

GRANT: DE-FG02-95ER14528

Geochemical and Isotopic Constraints on Processes in Oil Hydrogeology

T. Torgersen (University of Connecticut; 860-405-9094; Thomas.Torgersen@Uconn.edu; Fax: 860-405-9153) with B.M. Kennedy (Lawrence Berkeley National Laboratory; 510-486-6451; kennedy@ux5.lbl.gov; Fax: 510-486-5496)

Objectives: This research project (with LBNL) will evaluate the processes that produce, dissolve and distribute noble gases and noble gas isotopes among the liquid hydrocarbon, gaseous hydrocarbon and aqueous phases. This project will use measures of the noble gases and noble gas isotopes from several hydrocarbon fields to evaluate source characteristics, groundwater endmembers, migration processes and mechanisms

Project Description: The mechanisms, processes, and time scales of fluid flow in sedimentary basins represent a fundamental question in the Earth Sciences with direct application to exploration and exploitation strategies for energy and mineral resources. This project investigate hydrocarbon samples from regions where adequate commercial production and ancillary information are available to provide a test of the use and applicability of noble gases to delineate end members, migration mechanism and migration paths for hydrocarbons. Samples will be analyzed for five noble gases and multiple isotopes.

Results: The solubility of noble gases in hydrocarbons and water dictate that a source area noble gas signature will be mixed and diluted with noble gases stripped from groundwater during secondary migration. The degree of dilution is a function of the water/hydrocarbon volume ratio. Plots of relative noble gas abundances ($F[{}^i\text{Ng}]$) and isotopic compositions as a function of the inverse ${}^{36}\text{Ar}$ concentration generate mixing lines reflecting the varying degrees of dilution and thus can identify the noble gas characteristics of the source area (high values of $1/{}^{36}\text{Ar}$) and the groundwater (the intercept at $1/{}^{36}\text{Ar}=0$). Noble gas data from the Alberta gas fields (Hiyagon and Kennedy, 1992) provides a proof of concept and identifies four distinct mixing lines. The spatial distribution of samples defining each dilution line is suggestive of migration flow paths, as indicated by the progression from high to low values of $1/{}^{36}\text{Ar}$, and are consistent with the migration flow paths of Garven (1989) and Hitchon (1984) that were identified using hydrologic arguments.

The secondary migration of Alberta hydrocarbons occurred in groundwaters with noble gas compositions consistent with air-saturated water at 10-25 °C. The source areas (distinct from source rock) for Groups B1 and B2 are characterized by very large enrichments of radiogenic ${}^4\text{He}$ and ${}^{40}\text{Ar}$, nucleogenic ${}^{21}\text{Ne}$, and fissionogenic ${}^{136}\text{Xe}$ that is unlikely to have been derived solely from the source rock. These large excesses suggest that Tertiary orogeny preceding secondary migration degassed large volumes of older crust into the defined source areas. The noble gas characteristics of the source areas for Groups A1 and A2 indicate an enrichment in ${}^3\text{He}$. $1/{}^{36}\text{Ar}$ -defined flow paths trace this ${}^3\text{He}$ enrichment to the only volcanic formation in Alberta, the regionally restricted Cretaceous Crow's Nest Formation. The sequence of restricted Cretaceous volcanism 'staining' the Group A source area with mantle ${}^3\text{He}$, degassing of large source area crustal volumes by Tertiary orogeny, followed by

hydrocarbon maturation and migration is defined by the mixing line analysis. Noble gas mixing line analysis thus provides a fundamental constraint on models of hydrocarbon migration and emplacement.

GRANTEE: University Of Delaware

Department of Chemistry and Biochemistry
Newark, DE 19716

Grant: DE-FG02-89ER14080.A003

Development of an Experimental Database and Theories for Prediction of Thermodynamic Properties of Aqueous Electrolytes and Nonelectrolytes of Geochemical Significance at Supercritical Temperatures and Pressures

R. H. Wood (302-831-2941; Fax: 302-831-6335; rwood@udel.edu) and E. L. Shock (314-726-4258; Fax: 314-935-7361; shock@zonvark.wustl.edu)

Objectives: The objectives of this research are to combine new experimental measurements on heat capacities, volumes, and association constants of key compounds with theoretical equations of state and with first-principles quantum mechanical predictions to generate predictions of thermodynamic data, which in turn allow quantitative models of geochemical processes at high temperatures and pressures.

Project Description and Results: This project is part of ongoing collaboration between Prof. Everett Shock of Washington University and Prof. Robert Wood of the University of Delaware, which involves:

- 1) experimental measurements on key compounds;
- 2) making substantial improvements in theoretical equations of state for aqueous nonelectrolytes and electrolytes based largely on these experimental measurements;
- 3) pursuing novel applications of these equations of state to the study of high temperature/pressure geochemical processes involving aqueous fluids; and
- 4) developing and using *ab initio* quantum calculations with Molecular Dynamics simulations to predict chemical potentials of aqueous solutes where experimental measurements are impossible or not available.

The experimental work is conducted at the University of Delaware. Geochemical applications of the data are done at Washington University. Efforts to improve the equations of state and develop predictive methods are shared between the two labs, because this task in particular requires close collaboration between the two Principle Investigators.

We have been developing equations of state that allow the predictions at high temperatures and pressures of the properties of almost all solutes in water given either no or limited experimental data at room temperatures. Using fluctuation solution theory as a basis, we have developed an equation to predict aqueous electrolytes and non-electrolytes and this has now been published, Sedlbauer, *et al. Chem Geology* 2000, 163, 43-63. A follow up paper in which we use the above equation of state together with a functional group approach and fit the thermodynamic data for as many organic functional groups as possible has been published, Yezdimer, *et al., Chem Geology*, 2000, 164, 259-280. This greatly expands the predictions of thermodynamic properties.

The above equation has limitations. It has not as accurate as wished at low water densities and high temperatures. We have developed another equation which is better at low water densities and high temperatures but which is only appropriate for non-electrolytes and which requires estimates of gas phase virial coefficients. However, we appear to have good accuracy up to even 1000°C and believe that

this is a very worthwhile advance. Our first paper on this equation applies it to properties above the critical point of water and this paper has been published, Plyasunov *et al.*, *Geochim, Cosmochim. Acta*, 2000, 64, 495-512. An extension of this equation to temperatures below the critical point of water has been submitted. (Plyasunov *et al.*, *Geochim, Cosmochim, Acta*).

We have been developing a molecular dynamic plus quantum chemistry method of predicting (within about 5 kJ) the chemical potential of any solute in water at essentially any temperature and pressure. We have been doing further tests on water at high temperatures and find that the method works even better at high temperatures (about 800°C) where experimental measurements are available for water (Sakane *et al.*, *J. Chem. Phys.* accepted). We have predicted water at up to 2000°C and densities up to 1.8 gms/cm³ and the results are being written up. We are just starting our calculations on predicting the properties of aqueous silica. This new method of predicting properties shows great promise of making predictions where experimental measurements and extrapolation of empirical theories are not accurate.

We have experienced delays in getting our conductance apparatus operational. We have developed equations for the conductance of mixtures and tested them on Na₂SO₄ (aq). The association constant we obtain agrees with previous literature data (Sharygin *et al.*, *J. Phys. Chem.*, submitted).

GRANTEE: University Of Florida

Chemical Engineering Department
Gainesville, Florida 32611-6005

GRANT: DE-FG02-98ER14853

Pore Scale Simulations of Rock Deformation, Fracture, and Fluid Flow in Three Dimensions

A. J.C. Ladd (352-392-6509; Fax: 352-392-9513; ladd@che.ufl.edu)

Objectives: The overall research objective of this project is to develop micro-mechanical models for the dissolution of porous rocks by a chemically reacting fluid. The aim of the work is an improved understanding of how the coupling between chemical reactions, hydrostatic pressure, and fluid flow produces morphological changes in the sample.

Project Description: Numerical simulation techniques are being developed to model the flow of a chemically reacting fluid through a porous matrix. These simulations will combine a very fast fluid flow code with a stochastic simulation of the transport of chemical reactants and products. The code iterates between fluid-flow simulations and cycles of chemical transport and reaction, to predict the changes in morphology arising from the coupling between chemical reactions at the solid-fluid surfaces and the flow of fluid through the pore spaces. The motivation for this work is to explain the observations of Dr. William Durham (Lawrence Livermore National Laboratory), who found that chemical erosion tends to reduce the small-scale spatial heterogeneity in narrow fractures, while enhancing it on larger scales.

Results: A new boundary condition for the lattice-Boltzmann model has been developed, which allows a no-slip condition to be specified at scales less than the resolution of the grid (R. Verberg and A.J.C. Ladd, *Lattice-Boltzmann model with sub-grid scale boundary conditions*, Phys. Rev. Lett. 84:2148-2151, 2000). This makes a significant advance in the application of the lattice-Boltzmann method, since it allows for the subtle changes in the shape of the rock matrix as the surfaces erode.

By introducing a continuous variable, specified at each node and representing the fluid volume fraction associated with that node, 2nd-order accuracy is obtained for boundary surfaces at arbitrary positions and orientations with respect to the grid. The method does not require that surface normals be specified, and thus can be used in irregular geometries such as porous media. The new rules conserve mass and momentum, maintain stick boundary conditions, and reduce to the link (or midway) bounce-back rule at aligned planar interfaces. The figure below shows the improved convergence of the flow field in a narrow fracture obtained with the new boundary rules. A quantitative flow pattern is obtained with 250 μm resolution (lower-left image), despite the fact that the mean fracture height is only about 1.3 lattice spacings. Bounce-back boundary conditions (A.J.C. Ladd, *J. Fluid Mech.*, **271**, 285-309 311-325, 1994) require about twice the resolution (125 μm) for the same accuracy.

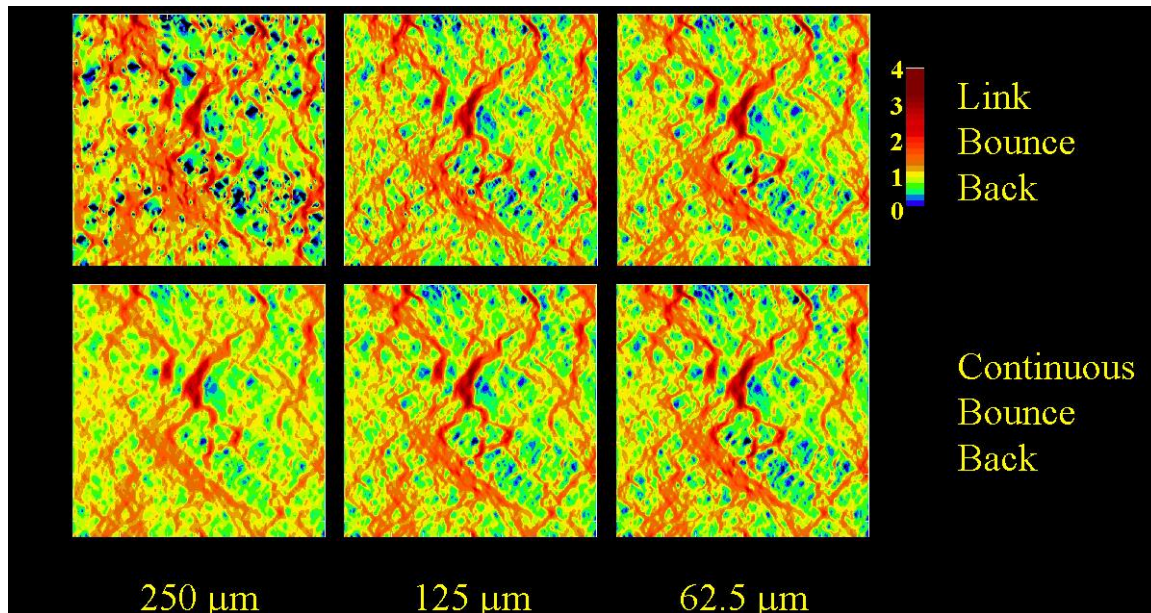


Figure: Visualization of fluid flow in a narrow fracture. The contours of a rough fracture, 4mm high, 32mm wide and 32 mm deep have been measured using a mechanical profilometer with a spatial resolution of 0.25mm. Fluid flow in the fracture, driven by a constant pressure gradient, has been simulated using the lattice-Boltzmann method. The figure shows a contour plot of the volumetric flow in the fracture, using spatial resolutions of 250, 125 and 62.5 microns to discretize the height profile. Contours indicate the local volumetric flow relative to the mean flow velocity. Results are shown for two different boundary conditions at the solid fluid interfaces: the link bounce-back rule [1] and the recently proposed continuous bounce-back rules.

GRANTEE: Georgia Institute Of Technology

School of Earth and Atmospheric Sciences
Atlanta, Georgia 30332-0340

GRANT: DE-FOG5-95ER14517

Biom mineralization: Organic-Directed Controls on Carbonate Growth Structures and Kinetics Determined by *In Situ* Atomic Force Microscopy

P. M. Dove (540-231-2444; Fax: 540-231-3386; dove@vt.edu)

Objectives: To determine the kinetics and mechanisms by which selected amino acids interact with calcite surfaces during crystal growth to govern the polymorph and surface structure that forms. The long-term goal is to develop a mechanistic understanding of the physical basis for biom mineralization and the larger role of organic compounds in governing carbonate precipitation and growth in natural and engineered Earth systems.

Project Description: Primary biom minerals form through biologically mediated activities of marine and freshwater organisms. They result from organic-directed crystal nucleation and growth processes acting in concert to yield chemically and morphologically complex structures. When combined with a macromolecular matrix of proteins, polysaccharides, and lipids, these structures fulfill specific physiological functions such as providing stiffness and strength to mineralized skeletal tissues. An understanding of organic-mineral surface interactions also has application to 1) avoidance strategies for cementation/scaling in oil/gas fields; 2) role of organics in the long-term behavior of carbonates in waste repositories; 3) new biomaterial technologies for synthesis of lightweight mineral-based composites.

Previous studies have found that the matrix macromolecules involved in regulating biological crystal growth have an acidic character and often contain aspartic or glutamic acid-rich domains. *In vitro* studies suggest that these macromolecules possess inhibitory properties that stabilize unusual crystallographic faces by site-specific binding. The mechanistic explanation for this inhibitory effect has focused upon the orientation and interactions of side-chain carboxylates with calcite surfaces and their ability to create extended calcium-interacting domains.

This project combines *in situ* Atomic Force Microscopy (AFM) investigations with kinetic measurements and surface chemical modeling to determine the rates and mechanisms by which amino acids modify the crystallization and dissolution of calcium carbonate minerals.

Results: 1) Reversed Calcite Carbonate Morphologies Induced by Microscopic Kinetics: Insights into Biom mineralization (*Geochimica Cosmochimica Acta*, 1999, v.63, p. 2507). This investigation of calcite growth quantifies baseline relationships between solution supersaturation and the rates of step advancement. Using *in situ* Fluid Cell Atomic Force Microscopy, we show that the movement of monomolecular steps comprising growth hillocks on $\{10\bar{1}4\}$ faces during growth of this anisotropic material is specific to crystallographic direction. By quantifying the sensitivity of step growth kinetics to supersaturation, we produce spiral hillocks with unique geometries. These forms are caused by a complex dependence of step migration rates, v_{S+} and v_{S-} , upon small differences in solution chemistry along the conventional 'fast' and 'slow' crystallographic directions. As solute activity, a , decreases, v_{S+} and v_{S-} converge and the growth hillock expresses a pseudo-isotropic form. At lower supersaturations where a approaches its equilibrium value, a_e , an inversion in the rates of step advancement produces

hillocks with unusual reversed geometries. Comparisons of the kinetic data with classical theoretical models suggest that the observed behavior may be due to minute impurities that impact the kinetics of growth through blocking and incorporation mechanisms. These findings demonstrate the control of crystallographic structure on the local-scale kinetics of growth to stabilize the formation of unusual hillock morphologies that may occur at the near equilibrium conditions found in many natural environments.

2) *Kinetics of Calcite Growth: Surface Processes and Relationships to Macroscopic Rate Laws*: This study links classical crystal growth theory with observations of microscopic surface processes to quantify the dependence of calcite growth on supersaturation and show relationships to the same dependencies of approximated by affinity-based expressions.

3) *Selective Binding of Amino Acids to the Atomic Steps of Calcite*: The Emergence of Chiral Structures: Results of this study show that the conventional paradigm for understanding geometrical and chemical aspects of biomineralization should be reevaluated. Using complementary experimental and theoretical methods, we use chiral forms of aspartate to show that new facets are stabilized by site-selective changes in the energy landscape of the surface.

GRANTEE: University Of Hawaii

Department of Geology and Geophysics
1680 East-West Road
Honolulu, HI 96822 USA

GRANT: DE-FG03-95ER14525 A004

Growth of Faults, Scaling of Fault Structure, and Hydrologic Implications

S. Martel (808-956-7797; Fax: 808-956-5512; martel@soest.Hawaii.edu), with K. Hestir (Utah State University; 801-797-2826; Fax: 801-797-1822; hestir@sunfs.math.usu.edu) J. P. Evans (Utah State University; 801-797-2826; Fax: 801-797-1588; jpevans@cc.usu.edu), and J.C.S. Long (University of Nevada at Reno; 702- 784-6987; Fax: 702-784-1766; jcslong@mines.unr.edu)

Objectives: The main research objectives are: (a) to determine how faults grow in three dimensions in brittle crystalline rocks (granites and basalts), and (b) to further develop physically based stochastic models for predicting geometric and hydrologic properties of such faults.

Project Description: We are investigating how faults of different scale grow in granite and basalt in three-dimensions. We are systematically examining the geometries, structure, and mechanics of faults with trace lengths of a few meters to several kilometers, and using this knowledge to develop physically based stochastic models for predicting the geometry of faults over a wide range of scale and for analyzing their hydraulic behavior. The main effort this year has been to assess how fault tip deformation scales by documenting and comparing the style and extent of deformation near the ends of strike-slip faults and normal faults that range in length from several meters to several kilometers. Information on the structure near the ends of large faults will provide insight into how linkages develop along large faults, how these linkages change with scale, and how faults grow.

Results: Fracturing in granites at the ends of strike-slip fault zones a few kilometers long is distributed over a broad region and connects a network of small faults. In contrast, fracturing along small faults several meters long occurs near the immediate ends of the faults and does not necessarily link faults together. A three-dimensional region of well-connected fractures around the perimeter of a large fault zone allows fluids to be conducted more readily around its perimeter than the perimeter of a small fault. Along scarps of unpaired normal faults in basalt, gaping vertical fissures open on the uplifted footwall but not on the down-dropped, hanging wall. These fissures have apertures as large as several meters for scarps twenty meters tall. Additionally, steeply inclined cavities develop beneath the scarps as flexed basalt layers delaminate above a normal fault that has not breached the surface. These cavities can have apertures of several meters on scarps only a couple of meters tall. Blocks collapsed from fissure walls and cavity roofs prop open the fissures and cavities. These features must strongly influence the hydrologic properties of the normal faults; these findings should be relevant to several DOE sites in the western United States.

GRANTEE: Indiana University

Laboratory for Computational Geodynamics
Department of Chemistry
Bloomington, Indiana 47405

Grant: DE-FG02-91ER14175

Basin Nonlinear Dynamics and Self-Organization

P. J. Ortoleva (812-855-2717; Fax 812-855-8300; ortoleva@indiana.edu)

Objective: The goal of this project is the development of new models and rate laws to describe mechanical processes as these play a central role in the creation and dynamics of fracture zones and faults.

Project Description: Fracture zones and faults play a key role in many nonlinear basin phenomena including episodic fluid flows, self-organized compartments and chaotic fault mechanical and fluid flow processes. We are developing a new multi-phase flow law that more realistically captures the changing geometry of the phases within the pore space and the coupling of this changing geometry and the overall flow-through.

Results: Our conjecture is that many of the features of a sedimentary basin from the grain scale to tens or hundreds of kilometers have self-organized over geological time through coupled reaction, transport and mechanical (RTM) processes. Once again, we found the sedimentary basin has a great richness of self-organization phenomena on a wide range of spatial scales. Our findings are summarized in the following paragraph extracted from the indicated papers. We start from the grain scale where it was shown how needle and other diagenetic outgrowth phenomena or pitting could emerge as a morphological instability for coated grains. We then present our findings on faults.

Development of Pits and Needles on Coated Grains: Observed needles and other outgrowths or pits on coated grains are explained via a reaction kinetic model of grain growth/dissolution and shape change. The coupling between grain coating thinning or fracturing occurring due to nonplanar growth is shown to underlie an instability to needle-like outgrowth (or the converse; pitting) in undersaturated conditions. Examples for clay-coated quartz are presented. A quantitative model of couple quartz growth and coating dynamics is shown to imply many of the observed features. Deposition of a coating during growth of the underlying quartz grain is shown to have an important influence on the morphology of the grain. These morphological instability phenomena are an interesting example of geochemical self-organization.

Failure, memory and cyclic fault movement: A model based on incremental stress rheology and rock texture dynamics is introduced that emphasizes the interplay of rock competency, porosity and other texture variables with stress and strain. The deformation mechanisms taken into consideration are poroelasticity and viscosity. The rheologic equations are strongly coupled to the evolution equations of rock texture and pore fluid flow. The model is used to gain an understanding of several oscillatory modes of fault movement. The roles of rock competency, fluid pressure, and continuous deformation in these oscillations is illustrated for various conditions. The approach is shown to be a natural starting point for a theory of the three dimensional, multi-process dynamics of fault nucleation, growth, morphology, reactivation and continuous vs. seismic behavior.

A model for understanding rock competency/failure and grain-size distribution evolution in faults: Fault movement is shown to have complex temporal dynamics when rock competency/failure dynamics is coupled with gouge, diagenesis and fluid flow. In this study, our previous models for rock competency/failure and gouge-diagenesis are combined to quantitatively investigate the temporal evolution of the grain size distribution, rock competency, porosity, stress and fluid pressure. Our conclusions are based on a model coupling incremental stress, rock competency, a Markov theory of gouge and diagenesis, and fluid flow.

Sedimentary Basin Deformation: An Incremental Stress Approach: A key component of sedimentary basin evolution is the spatial distribution and temporal variation of stress and deformation. The many deformation processes (poroelasticity, fracturing, irreversible nonlinear viscosity, and pressure solution) are inextricably bound in a tightly coupled network, which, in turn, is coupled to a myriad of basin diagenetic, thermal and hydrologic processes. In our approach, the various deformation processes are integrated through an incremental stress approach. Together with mass, momentum and energy conservation, this approach yields a complete, fully coupled basin model that captures basin and fault phenomena that are beyond the scope of simpler or decoupled models. We have developed a numerical simulator using a moving, adapting, accreting finite element discretization grid. Sedimentation/erosion history and the deformation at the basin lateral and bottom boundaries (*i.e.*, overall tectonics) are imposed. The finite element grid is allowed to deform and to grow and adapt with the addition of sediment to capture smaller sedimentary features. As a result, our fully coupled, comprehensive model allows one to solve a number of key problems in basin and fault dynamics. These include compaction, fractured reservoir and compartment genesis and dynamics.

Salt tectonics as a self-organizing process: A reaction, transport and mechanics model: Salt tectonics is placed within the theory of nonlinear dynamical systems. Features such as waves, diapirs, and tears are viewed as natural consequences of the symmetry breaking instabilities and related self-organized dynamics of the deforming salt body coupled to the reaction, transport, and mechanics (RTM) of the surrounding sediments. The fundamental nonlinearities are in the surrounding-rock and salt rheology. Our findings are based on a 3-D coupled RTM model simulated using finite element techniques. The centerpiece of the rheology of both rocks and salt is a nonlinear incremental stress formulation that integrates poroelasticity, continuous irreversible mechanical deformation (with yield behavior), pressure solution and fracturing. In contrast to previously presented studies, in our approach, the descriptive variables of all solid and fluid phases (stress, velocity, concentrations, *etc.*) and porous medium (texture, *i.e.*, volume fractions, composition, *etc.*) are solved from RTM equations accounting for interactions and interdependencies between them.

A Forward Model of Three-Dimensional Fracture Orientation and Characteristics: A new forward modeling approach to simulate the extension/closure and orientation statistics of evolving fracture networks is presented. The model is fully dynamical and couples fracturing to other processes. Thus, fracturing affects hydrology and, in turn, its development is affected by fluid pressure. In this way, highly pressured fluids can enhance their own migration while low-pressured ones may become trapped. Fracturing affects the stress tensor through rock volumetric changes and stress affects fracture dynamics. The statistical aspect of fracture network dynamics is described by assuming a probability distribution characterizing variations in rock strength within a nominally uniform lithology. The dependence of fracture density and length on the rate of fluid pressure or stress variation is thereby captured. By imbedding the model in a 3-D basin finite element simulator, we illustrate the dynamical nature of the location and character of fracture zones in a sedimentary basin.

GRANTEE: The Johns Hopkins University

Department of Earth and Planetary Sciences
Baltimore, Maryland 21218

Grant: DE-FG02-96ER14619

The Hydrodynamics of Geochemical Mass Transport and Clastic Diagenesis: San Joaquin Basin, California

G. Garven (410-516-8689; Fax: 410-516-7933; garven@jhu.edu) and J. R. Boles (UC-Santa Barbara; 805-893-3719; Fax: 805-893-2314; boles@magic.geol.ucsb.edu)

Objectives: Deep groundwater migration plays an important role in many geologic processes, including diagenesis in sedimentary basins that directly affects other processes such as overpressuring, oil migration and sediment-hosted ore mineralization during burial because of the control on permeability and porosity. The principal objective is to quantify the hydrogeologic regimes for clastic diagenesis, using the San Joaquin basin of California to establish geologic constraints for numerical modeling at the basin and formation scale.

Project Description: Few hydrogeologic models have been developed or applied to field data sets, rigorously couple geochemical processes, or test conceptual models for diagenesis beyond abstract formation-scale numerical simulations or core-scale laboratory studies. The approach used here is to develop coupled hydrodynamic-geochemical models with computer simulations constrained by geochemical and hydrologic observations for the San Joaquin basin of California. This project has involved the compilation and general mapping of geologic, pore pressure, salinity, and temperature data for the main aquifers in the basin to build a clearer picture of flow patterns as they exist today at the regional scale. The principal task for us has been to quantify the paleohydrology and thermal history of the San Joaquin basin with a new finite-element code for simulating fluid migration and pressure changes during sedimentation, uplift, and erosion. After the hydrogeologic history has been explored in a hydrodynamic sense, we will conduct reactive-flow simulations to assess mechanisms for diagenesis and chemical mass transport in the clastic wedge. Different diagenetic fluid-flow hypotheses such as compaction dewatering, episodic pulses, meteoric invasion, and cross-formational flow are tested with the coupled hydrogeologic models through a sensitivity analysis.

Results: Our previous fluid flow modeling results formed the regional-scale framework for sets of new numerical experiments aimed at simulating reactive flow fields within the Stevens Sandstone, a Miocene-age reservoir in the San Joaquin basin for which extensive amounts of geochemical and petrophysical data exist. We developed simulations to predict the coupled processes of fluid flow, heat transport, and reactive chemical transport to investigate effects of mass transfer on the diagenesis of a permeable bed during compaction-driven flow. The models included a new kinetic rate expression for plagioclase dissolution that appears to drive precipitation of calcite and kaolinite and albitization reactions in the Stevens Sandstone. Calcium transport in the basin seems to be most important during burial and compaction, with transport distances of up to 10 km during the 5 million years of burial simulated. Sensitivity studies were used to illustrate the range of diagenetic fabrics that might be generated depending on the range of model parameters such carbon dioxide partial pressures, permeability heterogeneity, and formation dispersion coefficients. More focused flow along fracture or faults seems to be required to explain the volumes of cements observed in the basin.

GRANTEE: The Johns Hopkins University

Dept. of Earth and Planetary Sciences
Baltimore, MD 21218.

Grant: DE-FG02-96ER-14616

Predictive Single-site Protonation and Cation Adsorption Modeling

D. A. Sverjensky (410-516-8568; Fax: 410-516-7933; sver@jhu.edu)

Objectives: The overall goal of this research is to develop a predictive model of adsorption processes at the mineral-water interface that can be applied to a fundamental understanding of the role of adsorption in geochemical processes such as weathering, diagenesis, the chemical evolution of shallow and deep groundwaters and ore-forming fluids, and the fate of contaminants in groundwaters.

Project Description: The research is aimed at generating a comprehensive, internally consistent, quantitative description of proton and cation adsorption on oxides and silicates using an extended triple layer model. The model will be developed to integrate the available experimental information on proton and cation adsorption based on internally consistent assumptions. By so doing, it will considerably facilitate the comparison of experimental data from different investigators. In addition, the model will permit predictions of surface speciation to supplement the lack of experimental adsorption data for many systems of geochemical interest. In addition, it will provide a basis for extending applications of the concept of surface complexation to oxide and silicate dissolution kinetics. The proposed extended triple layer model will include: (1) Internally consistent assumptions and methods of estimating site densities and capacitances; (2) Explicit recognition of ion solvation; (3) Explicit recognition of proton attraction-repulsion; (4) Inclusion of the extended Debye-Huckel model for aqueous ionic activity coefficients; and (5) Inclusion of a geochemical thermodynamic data file for aqueous species and minerals.

Results: To improve the ability to predict surface protonation and surface-charge development at the oxide-electrolyte-water interface, additional studies of the capacitances have been carried out. By taking account of the adsorption of a layer of water molecules, as well as a parallel layer of electrolyte ions, the model structure of the oxide-water interface is specified in more detail. As a result, on some minerals (*e.g.*, rutile, anatase and magnetite), the adsorbed alkali ions are dehydrated, forming inner-sphere complexes, whereas on other minerals (*e.g.*, goethite, hematite, quartz and amorphous silica), the adsorbed alkali ions are hydrated, forming outer-sphere complexes. This enables a better prediction of the inner layer capacitance, which improves predictive capabilities with regard to surface charge as a function of electrolyte type and concentration.

Work to determine the ionic strength dependence of the adsorption of divalent transition and heavy metals has been completed (Criscenti and Sverjensky, 1999, *Am. J. Sci.*, v299, pp828-99). A corresponding effort has also been carried out on the issue of metal adsorption as a function of metal concentration. The results of this study indicate the utility of the single-site approach over wide ranges of metal concentration.

Finally, an analysis of the adsorption of alkaline earth metals on oxides is underway. Preliminary results indicate that minerals with a wide range of surface characteristics seem to adsorb alkaline earths with similar speciation mechanisms.

GRANTEE: The Johns Hopkins University

Department of Earth and Planetary Sciences
Baltimore, MD 21218

GRANT: DE-FG02-95ER14074

Reaction and Transport of Toxic Metals in Rock-Forming Silicates at 25°C

*D. R. Veblen (dveblen@jhu.edu; 410-516-8487) and D. C. Elbert (Elbert@jhu.edu; 410-516-5049)
with E. S. Ilton (esi2@Lehigh.edu; 610-758-5834)*

Objectives: This project is an investigation of reactions between silicate minerals and toxic metal-bearing aqueous fluids. We are specifically exploring the mechanisms of oxydation-reduction reactions at the mineral-fluid interface and transport of reactive components along the grain-boundary interface in rocks.

Project Description: This project has three main components: 1) experimental investigation of Cr and U reduction and sorption by micas; 2) high-resolution transmission electron microscopy (HRTEM) characterization of grain boundaries; and 3) experimental investigation of transport and sorption of heavy metals along grain boundaries. The first component includes development of X-ray photoelectron spectroscopy (XPS) methodologies to probe sorption behavior. The second component includes molecular-dynamical modeling of grain-boundary structures to provide insight into their transport properties. This second component also includes development of near-atomic-resolution analysis and imaging methodologies of electron-energy-loss spectroscopy (EELS), high-angle-annular-dark-field imaging (HAADF) and energy-filtered-transmission-electron-microscopy (EFTEM) in mineralogical systems. The third component combines the geochemical and mineralogical studies to elucidate transport properties and mechanisms important in Earth materials.

Results: Geochemical work has focused on the sorption and reduction of aqueous U(VI) on biotite (Ilton *et al.*, 1999a). Experiments have been done at 25°C and pH = 4.5, with solutions containing 0.5 mM U(VI) and 0.8 mM Na⁺ or K⁺. Oxidation is avoided in these experiments by working in an argon atmosphere.

XPS analysis of biotite basal planes and edges utilized U4f-spectra to identify the presence of U(IV) on reacted samples. The analyses show that U(VI) in solution has been reduced to U(IV) on the mica surface. The degree of reduction is sensitive to mica orientation and chemistry, and the associated alkali. Greater reduction of U was found on edge sites than on basal planes. More ferrous biotite was found to reduce more U(VI). Potassium ions limit reduction of U(VI) relative to sodium ions.

The mineralogical component of the project has centered on HRTEM imaging and modeling of a range of silicate-silicate and silicate-oxide grain boundaries. The work continues to show that boundaries between minerals are tight and semi-coherent. These boundaries contain defects that create through-going channels (nanopores) that form a rapid network for chemical transport (Veblen and Elbert, 1999).

We have migrated our work to the new CM-300 FEG microscope at Johns Hopkins and begun the energy-filtered imaging component. This work shows that energy-filtered imaging (EFI) offers distinct advantages in spatial resolution over energy-filtered, scanning transmission electron microscopy and can produce chemical maps with two-to three-orders of magnitude finer spatial resolution than X-ray spectroscopic methods (Elbert, Veblen, Schubel, 1999). We have collected the first energy-filtered

images of clinopyroxene-orthopyroxene interfaces and nearly atomistic images of basal planes of biotite. In the biotite images, we are able to image the atoms in isolated A-sites stacked up in the sample. We have also imaged mica samples with sorbed uranium. Our goal is the imaging of individual uranium atoms on biotite surfaces. Such imaging will allow direct identification of preferred sorption sites. Although we have, to date, failed to accomplish individual atom imaging, we are investigating several different sample preparation techniques to further that part of the project.

- Elbert D.C. and Veblen D.R. (1999) Mineralogical applications of energy filtered imaging (EFI) in a conventional transmission electron microscope (TEM). *Geol. Soc. of Amer. Abstracts with Programs* 28.
- Ilton E.S., Moses C.O. and Veblen D.R. (in press) Using X-ray photoelectron spectroscopy to discriminate among different sorption sites of micas: with implications for heterogeneous reduction of chromate at the mica-fluid interface. *Geochimica Cosmochimica Acta*.
- Ilton E.S., Moses C.O. and Veblen D.R. (1999a) X-ray photoelectron spectroscopic evidence for coupled sorption and reduction of aqueous U(VI) by ferrous micas. *Geol. Soc. of Amer. Abstracts with Programs* 28. A-67
- Ilton E.S., Moses C.O. and Veblen D.R. (1999b) XPS analysis of cation sorption by phyllosilicates: a methodology for interpreting small binding energy differences for sorbed chromium. *EUG* 10 , 664
- Ilton E.S. (1999) Interpreting small binding energy differences for cations sorbed to micas: With Implications for heterogeneous electron transfer reactions. *Geosciences Research Symposium VI: Interfacial Processes*. U.S. Department of Energy OBES, February 1-2, Richland WA.
- Moore K.T., Howe J.M., Elbert D.C., (1999a) Analysis of diffraction contrast as a function of energy loss in energy-filtered transmission electron microscope imaging, *Ultramicroscopy*, v. 80, 203-219.
- Moore K.T., Howe J.M., Veblen D.R., Murray T.M., Stach E.A., (1999b) Analysis of electron intensity as a function of aperture size in energy-filtered transmission electron microscope imaging, *Ultramicroscopy*, v. 80, 221-236.
- Veblen D.R. and Elbert D.C. (1999) Structures of planar defects and grain boundaries in minerals, XVIII Congress IUCr.

GRANTEE: Kent State University

Department of Geology
Kent, OH 44242-001

GRANT: DE-FG02-96ER14668

Microbial Dissolution of Iron Oxides

P. A. Maurice (currently at: Dept. of Civil Engineering & Geological Sciences, University of Notre Dame, Notre Dame, IN 46556; 219-631-9163; Fax: 219-631-9236; pmaurice@nd.edu) in collaboration with L. Hersman (LANL) and G. Sposito (U.C., Berkeley)

Objectives: The overall goal of this research is to determine the mechanisms whereby an aerobic *Pseudomonas sp.* bacterium acquires Fe from Fe(III)(hydr) oxides. Specific objectives are to characterize the types of attachment features used by the microorganism, and to determine how dissolution varies with mineral surface properties.

Project Description: The overall objective of this research is to determine the mechanisms of Fe release during microbially enhanced Fe (III) (hydr)oxide dissolution by an aerobic bacterium. Understanding the mechanisms whereby microorganisms acquire Fe in aerobic environments is fundamental to a wide range of bio-geo-chemical phenomena. For example, given that hydrous Fe(III) oxides adsorb an array of organic and inorganic components, understanding microbial dissolution is key to modeling pollutant transport phenomena. This research utilizes atomic force microscopy (AFM) and scanning electron microscopy (SEM) to characterize the types of attachment features used by the microorganisms to attach to mineral surfaces, and the structures of dissolution features that form upon reaction. An additional goal is to determine how dissolution varies as a function of hydrous Fe(III) oxide surface structure, micromorphology, and surface area. These research objectives represent important first steps towards understanding microbially mediated dissolution mechanisms.

Results: Although microorganisms have been shown to play important roles in the weathering of Fe(III)-(hydr)oxide minerals, little is known regarding microbial-mineral interactions in aerobic environments. Our research focused on determining the rates and mechanisms by which obligate aerobic *Pseudomonas* bacteria obtain Fe from geologic materials. In research conducted in collaboration of Dr. L. Hersman (LANL), we have grown colonies of *Pseudomonas* species in suspensions of Fe(III)-(hydr)oxides in which the mineral materials are the only sources of Fe. The bacteria could only grow to population sizes great than those of controls by acquiring Fe from the solid phase. Enhanced microbial growth in the presence of the Fe(III)-(hydr)oxides provided evidence that the bacteria enhanced dissolution in order to acquire Fe. Atomic-force microscopy (AFM), scanning electron microscopy (SEM), and epifluorescence microscopy showed that the bacteria colonize mineralogic aggregates, forming networks of fiber-like attachment features intertwined through amorphous-looking 'ooze'. In addition, close associations were observed between bacterial flagella and growth-medium salts (as determined by SEM/EDS) that precipitate on drying, which suggests that the flagella are hydrophilic. Our SEM, AFM, and epifluorescence images concur with, and further enhance, our understanding of the importance of microbial adhesion to mineral surfaces.

GRANTEE: Lehigh University

Department of Earth and Environmental Sciences
Bethlehem, PA 18015

GRANT: DE-FG02-95ER14507

Reaction and Transport of Toxic Metals in Rock-Forming Silicates at 25°C

E. S. Ilton (esi2@Lehigh.edu; 610-758-5834), with D. R. Veblen (dveblen@jhu.edu; 410-516-8487) and D. C. Elbert (Elbert@jhu.edu; 410-516-5049)

Objectives: This project is an investigation of reactions between silicate minerals and toxic metal-bearing aqueous fluids. We are specifically exploring the mechanisms of oxydation-reduction reactions at the mineral-fluid interface and transport of reactive components along the grain-boundary interface in rocks.

Project Description: This project has three main components: 1) experimental investigation of Cr and U reduction and sorption by micas; 2) high-resolution transmission electron microscopy (HRTEM) characterization of grain boundaries; and 3) experimental investigation of transport and sorption of heavy metals along grain boundaries. The first component includes development of X-ray photoelectron spectroscopy (XPS) methodologies to probe sorption behavior. The second component includes molecular-dynamical modeling of grain-boundary structures to provide insight into their transport properties. This second component also includes development of near-atomic-resolution analysis and imaging methodologies of electron-energy-loss spectroscopy (EELS), high-angle-annular-dark-field imaging (HAADF) and energy-filtered-transmission-electron-microscopy (EFTEM) in mineralogical systems. The third component combines the geochemical and mineralogical studies to elucidate transport properties and mechanisms important in Earth materials.

Results: Geochemical work has focused on the sorption and reduction of aqueous U(VI) on biotite (Ilton *et al.*, 1999a). Experiments have been done at 25°C and pH = 4.5, with solutions containing 0.5 mM U(VI) and 0.8 mM Na⁺ or K⁺. Oxidation is avoided in these experiments by working in an argon atmosphere.

XPS analysis of biotite basal planes and edges utilized U4f-spectra to identify the presence of U(IV) on reacted samples. The analyses show that U(VI) in solution has been reduced to U(IV) on the mica surface. The degree of reduction is sensitive to mica orientation and chemistry, and the associated alkali. Greater reduction of U was found on edge sites than on basal planes. More ferrous biotite was found to reduce more U(VI). Potassium ions limit reduction of U(VI) relative to sodium ions.

The mineralogical component of the project has centered on HRTEM imaging and modeling of a range of silicate-silicate and silicate-oxide grain boundaries. The work continues to show that boundaries between minerals are tight and semi-coherent. These boundaries contain defects that create through-going channels (nanopores) that form a rapid network for chemical transport (Veblen and Elbert, 1999).

We have migrated our work to the new CM-300 FEG microscope at Johns Hopkins and begun the energy-filtered imaging component. This work shows that energy-filtered imaging (EFI) offers distinct advantages in spatial resolution over energy-filtered, scanning transmission electron microscopy and can produce chemical maps with two-to three-orders of magnitude finer spatial resolution than X-ray spectroscopic methods (Elbert, Veblen, Schubel, 1999). We have collected the first energy-filtered

images of clinopyroxene-orthopyroxene interfaces and nearly atomistic images of basal planes of biotite. In the biotite images, we are able to image the atoms in isolated A-sites stacked up in the sample. We have also imaged mica samples with sorbed uranium. Our goal is the imaging of individual uranium atoms on biotite surfaces. Such imaging will allow direct identification of preferred sorption sites. Although we have, to date, failed to accomplish individual atom imaging, we are investigating several different sample preparation techniques to further that part of the project.

- Elbert D.C. and Veblen D.R. (1999) Mineralogical applications of energy filtered imaging (EFI) in a conventional transmission electron microscope (TEM). *Geol. Soc. of Amer. Abstracts with Programs* 28.
- Ilton E.S., Moses C.O. and Veblen D.R. (in press) Using X-ray photoelectron spectroscopy to discriminate among different sorption sites of micas: with implications for heterogeneous reduction of chromate at the mica-fluid interface. *Geochimica Cosmochimica Acta*.
- Ilton E.S., Moses C.O. and Veblen D.R. (1999a) X-ray photoelectron spectroscopic evidence for coupled sorption and reduction of aqueous U(VI) by ferrous micas. *Geol. Soc. of Amer. Abstracts with Programs* 28. A-67
- Ilton E.S., Moses C.O. and Veblen D.R. (1999b) XPS analysis of cation sorption by phyllosilicates: a methodology for interpreting small binding energy differences for sorbed chromium. *EUG* 10 , 664
- Ilton E.S. (1999) Interpreting small binding energy differences for cations sorbed to micas: With Implications for heterogeneous electron transfer reactions. *Geosciences Research Symposium VI: Interfacial Processes*. U.S. Department of Energy OBES, February 1-2, Richland WA.
- Moore K.T., Howe J.M., Elbert D.C., (1999a) Analysis of diffraction contrast as a function of energy loss in energy-filtered transmission electron microscope imaging, *Ultramicroscopy*, v. 80, 203-219.
- Moore K.T., Howe J.M., Veblen D.R., Murray T.M., Stach E.A., (1999b) Analysis of electron intensity as a function of aperture size in energy-filtered transmission electron microscope imaging, *Ultramicroscopy*, v. 80, 221-236.
- Veblen D.R. and Elbert D.C. (1999) Structures of planar defects and grain boundaries in minerals, XVIII Congress IUCr.

GRANTEE: University Of Maryland

Department of Chemistry and Biochemistry
College Park, Maryland 20742

GRANT: DE-FG02-94ER14467

Theoretical Studies on Metal Species in Solution and on Mineral Surfaces

J. A. Tossell (301-405-1868; Fax: 301-314-9121; tossell@chem.umd.edu)

Objectives: This study utilizes the techniques of computational quantum chemistry to study the structures, energetics and properties of various metal species in solution, in mineral glasses, or absorbed on mineral surfaces. Our focus in the past year has been on complexes of Cu^+ with thioarsenites in sulfidic solutions (studied experimentally by Clark and Helz, Univ. of Maryland), on inorganic and organometallic complexes of Hg, on Na-aluminate and Na-silicate ion pairs, on Be and Al hydrolysates and complexes with oxalate and methylmalonate and on the calculation of ^{23}Na and ^{17}O NMR shieldings in silicates and aluminosilicates.

Project Description: To understand the mechanisms of dissolution of minerals and formation of ore deposits one must understand the structures and properties of metallic species in aqueous solution. In the first three years of this project we calculated the structures, energetics and spectral properties of a number of different Au, As and Sb sulfide, chloride and hydroxide species. Calculating the properties of such species in the gas-phase is relatively easy - the difficult problem is to describe with accuracy their interaction with the solvent water. More recently, we have studied Hg compounds, both purely inorganic species such as Hg chlorides and sulfides and organometallic methyl-Hg species. Aluminosilicate species are also a continuing interest, from a geochemical point of view addressing the effects of water upon melt properties as well as the modeling of aluminosilicate surfaces, and from a materials science point of view, as an opportunity for suggesting possible new materials with interesting properties. We have also studied the interaction of Cu^+ in aqueous solution with a number of different ligands, both simple ones like Cl^- and complex ones like $\text{AsS}(\text{SH})(\text{NH}_2)^-$, to help understand the great stability determined by Clark and Helz for the $\text{CuAsS}(\text{SH})(\text{OH})$ complex. To better understand the relationship of NMR spectral properties and local structures we have begun to systematically study ^{23}Na and ^{17}O NMR shieldings for a range of silicates and aluminosilicates.

Results: To obtain an atomistic understanding of the structure and stability of the copper thioarsenite complex, CuH_2AsO_2 , characterized experimentally by Clark and Helz (UMCP) in their study of the solubility in sulfidic solution of covellite, CuS , digenite, $\text{Cu}_{1.8}\text{S}$, and arsenosulvanite, Cu_3AsS_4 , we have carried out quantum mechanical calculations on several isomers of the Cu-thioarsenite complex, a number of related complexes and the corresponding uncomplexed ligands. Using an *ab initio* molecular orbital approach which includes electron correlation (2nd order Moller-Plesset perturbation theory using a polarized double zeta valence orbital basis and effective core potentials) we calculate the lowest energy isomer to be $\text{CuS}(\text{SH})\text{As}(\text{OH})$ (with bonds from Cu to S, SH and As), which has a calculated enthalpy of formation (from $\text{Cu}^+(\text{aq})$ and $\text{AsS}(\text{SH})(\text{OH})^-(\text{aq})$) of about -110 kJ/mol. If entropic effects are ignored, this gives a log K value of about 19.1 for the formation constant, (fortuitously) close to the value of 19.8 determined by Clark and Helz. More significantly, our method reproduces the experimental trend in log K values for the formation of the simpler complexes CuCl_2^- , $\text{Cu}(\text{SH})_2^-$ and $\text{Cu}(\text{CN})_2^-$, and allows us to understand why the $\text{CuS}(\text{SH})\text{As}(\text{OH})$ complex is so stable. We find that the complexes of Cu^+ with $\text{AsS}(\text{SH})_2^-$, $\text{AsS}(\text{SH})(\text{NH}_2)^-$ and $\text{AsS}(\text{SH})(\text{CH}_3)^-$ are also very stable, while the

complexes with related As(V), P(III) and P(V) S-containing ligands are considerably less. The determining chemical characteristic of the strongly complexing ligands is the presence of two coordinating S atoms (one -S and one -SH) and an electron-rich As center. Electron withdrawing substituents such as F on the As greatly reduce the stability of the complex, breaking the Cu-As bond. Preliminary studies indicate similar strong complexation with thioarsenites for other “soft” cations, such as Ag^+ , Au^+ and Hg^{2+} .

We have developed a procedure for calculating the ^{23}Na NMR shielding in aluminosilicates, using either a calculation on a large cluster containing the Na and its 1st and 2nd coordination sphere atoms, or an additivity approach using calculations only on individual Na-O bonds. The additivity approach is much cheaper and more intuitive and reproduces trends in isotropic shieldings quite well, particularly for low coordination number sites. The larger cluster calculations are necessary to describe larger coordination number sites and to evaluate electric field gradients and shielding anisotropies

We have also undertaken a systematic study of the acidities in aqueous solution of $\text{Si}(\text{OH})_4$ and its oligomers (including a silica surface model, $\text{Si}_7\text{O}_{12}\text{H}_{10}$) and related molecules, like H_3PO_4 . Our goal is to calculate gas-phase deprotonation energies at the quantum mechanical state-of-the-art, accurate to better than 2 kcal/mol, and to evaluate hydration enthalpies at as high a level of accuracy as possible. This will allow us to determine the physics and chemistry behind the differing pKa's of $\text{Si}(\text{OH})_4$ and the silica surface.

The properties of the $\text{Na}^+ - \text{Si}(\text{OH})_3\text{O}^-$ ion pair, are also being studied, using procedures similar to those employed for $\text{Na}^+ - \text{Al}(\text{OH})_4^-$. For this species, we can concentrate upon available ^{23}Na and ^{29}Si NMR shielding data to identify the ion-pair species. We have established that in this species both the Na and the Si are deshielded compared to the isolated ions, in agreement with experiment

The interaction of water with aluminosilicate glasses is another topic of great interest to both theoreticians and experimentalists and we continue to address this topic using molecular cluster calculations. Our calculations have revealed the important role of additional water molecules, hydrating the species formed by initial water attack on Si-O-Al bonds, in much the same way that the dissociation of water on the MgO surface is made possible by hydration of the Mg-OH species formed. The species formed in the Si-O-Al system is basically a H_3O_2^- ion, (OH^- strongly H-bonded to H_2O), which has been characterized in hydroxo sodalite systems

In collaboration with Drs. Cody, Mysen and Saghi-Szabo at the Geophysical Laboratory we are also calculating NMR shieldings for phosphate species formed in Na_2O , Al_2O_3 , SiO_2 , P_2O_5 glasses. In addition to Na_3PO_4 and $\text{Na}_4\text{P}_2\text{O}_7$ species, we have characterized a number of species with varying numbers of second-neighbour Al's. In collaboration with Dr. Cohen of the Geophysical Laboratory, we are calculating Al and O electric field gradients in the Al_2SiO_5 minerals silimanite, andalusite and kyanite, using both density functional band theory and molecular cluster approaches.

In collaboration with Dr. Sahai, a NSF Postdoctoral Fellow at UMCP, we are using MO calculations to understand the role of silicon-organic ligand interactions in biomineralization. One project involves determining the stabilities and NMR shifts of various silica-amino acid and silica-polyalcohol complexes, which are present in biogenic silica. The second project is to determine the mechanism of apatite nucleation at silica bioceramic surfaces, which are used as prosthetic implants in bones and teeth.

GRANTEE: Massachusetts Institute Of Technology

Department of Earth, Atmospheric, and Planetary Sciences
Cambridge, MA 02139-4307

Grant: DE-FG02-97ER14760

Evolution of Pore Structure and Permeability of Rocks under Hydrothermal Conditions

B. Evans (617-253-2856; Fax: 617-258-0620; brievans@mit.edu) and Y. Bernabé (Université Louie Pasteur, Strasbourg, France)

Objectives: The goal of the project is to understand the mechanisms and kinetics of evolution of pore structure and transport properties in porous rocks and granular aggregates under hydrothermal conditions and under hydrostatic and triaxial loading.

Project Summary: Pore structures and transport properties of rocks, including fluid permeability and electrical conductivity, can be altered in the Earth by a wide variety of diagenetic, metamorphic, and tectonic processes. To provide fundamental information on the way that pore structure changes, measurements of transport properties are conducted on samples while subject to elevated temperature and pressure. The samples and conditions of measurement are designed, if possible, to isolate a single mechanism, *e.g.*, roughening by diagenetic reaction or compaction by plastic flow. Extensive optical and scanning microscope observations of the pore structure are done to quantify changes in surface roughness, porosity, and pore dimensions. Computations using network techniques and cellular automata help to model the mechanisms of porosity evolution. A better understanding of these processes is important for improving resource recovery, predicting rates of metamorphism, understanding fault mechanics and fault stability, and estimating rates of deformation by pressure solution.

Results: When the porosity of synthetic sandstone made of feldspar glass beads is filled with water and heated to 190-250°C in the presence of water at 20 MPa pore pressure and 75 MPa confining pressure for periods of two to seven days fibrous to webby overgrowths of natrosilite, quartz, and perhaps gmelinite are formed in the pore space. The overgrowths are very similar to those found in diagenetically altered sandstones in nature. The long-term chemical alteration of porous silicate glass was examined first. Chemical alteration affects pore volume and connectivity as well as pore wall roughness. The experiments indicate very steep decrease of permeability at essentially constant porosity for early alteration times. During the late stages of alteration, the permeability decline slowed down significantly while a sharp decrease of porosity occurred. The results are very similar to the laboratory data compiled by others in natural sandstones and shales, but quite different from other natural sandstone where cementation is prevalent, *e.g.*, Fontainebleau, or from granular aggregates being compacted by plastic flow. Initial observations using laser scanning confocal microscopy and scanning electron microscopy show that roughing forms narrow throats that constrict flow, a condition very similar to clay-laden sandstones recovered from natural settings. The results are consistent with the idea that the roughening results in decreases in the proportion of porosity that is effective during fluid transport.

GRANTEE: University Of Michigan

Department of Geological Sciences
Ann Arbor, MI 48109-1063

Grant: DE-FG02-96ER14615

Combined Noble Gas and Stable Isotope Constraints on Nitrogen Gas Sources within Sedimentary Basins

C. J. Ballentine (Now at ETH Zurich, ballentine@erdw.ethz.ch), A. N. Halliday, and B. Sherwood-Lollar (University of Toronto)

Objectives: To combine the information provided by both noble gas and stable isotope systematics in order to constrain the origin of nitrogen gas sources, transport behavior and mass balance within sedimentary basin systems.

Project Summary: Nitrogen is one of the major non-hydrocarbon gases found in natural gas reservoirs. Many regions in which the gas fields have a high-nitrogen content also show a relationship between the concentration of nitrogen and crustal-radiogenic helium. The crustal He will be associated with crustal ^{40}Ar and ^{21}Ne . Noble gases derived from other sources such as the air dissolved in groundwater and magmatic sources can be quantified from the noble gas isotopic composition. Combined with the distinct elemental abundance patterns it is possible to resolve the extent of crustal, mantle and atmosphere-derived noble gas involvement in these systems.

The Kansas/Texas Hugoton/Panhandle giant gas field has perhaps the best-documented He/N_2 relationship of any system. This program focuses on samples from these and neighboring fields which preserve different but distinct regional He/N_2 ratios. The noble gas and stable isotope composition are compared to enable us to identify any regional nitrogen gas isotopic end members; quantify the extent of their contribution to the sedimentary fluid regime; constrain the conditions for deep nitrogen release and transport; and by comparison with samples which show rare gas abundance fractionation, identify the mechanism of fractionation (*i.e.*, mass-dependent transport fractionation, solubility/phase fractionation) and assess its impact on the stable isotope systematics.

Results: We have completed analysis on samples from producing wells giving full geographic coverage of the entire Hugoton-Panhandle system. We show that the crustal derived He is directly proportional to the groundwater derived Ne and that the Nitrogen has two sources, one that is associated with the groundwater and crustal He, and another that is not associated with the noble gases. Using the noble gases we have identified the nitrogen isotopic composition of these end-member components and are currently assessing the origin of both nitrogen components based on this information. A simple conceptual model linking the regional groundwater system to He-associated nitrogen occurrence in natural gases is being developed. In addition to the He/N_2 study we have expanded our understanding of the way in which magmatic noble gases are input into shallow fluid systems (Ballentine, *Earth and Planet. Sci. Lett.* 1997).

GRANTEE: University Of Minnesota, Twin Cities

Dept. of Geology and Geophysics and Minnesota
Supercomputer Institute
Minneapolis, MN, 55415-1227

GRANT: DE-FG03-91ER14212

Magma Rheology, Mixing of Rheological Fluids, Molecular Dynamics Simulation , and Lithospheric Dynamics

D.A. Yuen (612-624-1868; Fax: 612-624-8861; davey@krissy.mni.umn.edu) in collaboration with F. J. Spera, (University of CA, Santa Cruz)

Objectives: Mixing efficiency in complex rheology, molecular dynamics of complex fluids and micro-scale Rayleigh-Taylor instabilities, effects of complex rheology in lithospheric dynamics.

Project Description: This project will improve our understanding of the thermal, chemical, dynamical and mechanical state of the continental crust and subcrustal lithosphere with particular focus on the interactions between the various subsystems. The work plan includes: (1) rheological laboratory measurements on melts and magmatic suspensions; (2) Determination of the thermodynamical and transport properties of molten silicates by MD simulations; (3) Mixing processes of rheological fluids in convection and visualization of complex processes; (4) Coupling between mantle convection with temperature-dependent and non-Newtonian rheology and mantle diapirs on the thermal regime and subsidence curves of rift-related basins; (5) The dynamical influences of lithospheric phase transitions on the thermal-mechanical evolution of sedimentary basins; (6) The development of stress fields and criteria for faulting in the crust; (7) Modeling of heat and mass transport driven by thermal and compositional heterogeneities in porous media; and (8) Open system geochemical modeling of magmatic systems.

Results: The results described below are for the U of Minnesota part of this project. Additional results are given in the summary of activities can be found in the summary of activities by the University of California team led by F.J. Spera. We have studied with 2-D molecular dynamics the mixing phenomenon in the microscale, between 500 and 10 000 Å. We have employed up to 3 million particles interacting with a two-body potential and up to one million time-steps were integrated. We have focused on the temporal evolution of the mixing layer between two superimposed particle systems in a gravitational field directed from the heavier to the lighter particle ensemble. We have compared the micro properties with those observed in the macroworld. We found that the bubble-and spikes stage of mixing process is similar in both the micro (molecular scale) and macro worlds. The mixing layer growth constant A , which can be obtained from molecular dynamics, is approximately the same as that obtained for 2-D simulations in the macroscale. The occurrence of Rayleigh-Taylor instability in the microscale, and its similarity to the same process in the macroscale, can also expand the concept of turbulence to microscaled flows on the nanoscale. This work has been published in *Physica D*, 137, 157-171, 2000.

We have studied the mixing properties and differences between Newtonian and non-Newtonian convection. Both the line and field methods were employed. The line-method is based on monitoring of passive particles linked into lines, while the field method relies on the advection of a passive scalar field by solving a partial differential equation with a hyperbolic character. Both visual and quantitative estimates revealed that the efficiency of the Newtonian mixing is greater than that for non-Newtonian

(power-law) rheology. A chemical heterogeneity placed in the non-Newtonian convection forms preferentially horizontal structures, which may persist for at least 1 Ga in the upper-mantle. In addition, the non-Newtonian medium reveals a lesser amount of stretching of the lines than the Newtonian material. The rate of the Newtonian stretching fits well with an exponential time-dependence, while the non-Newtonian rheology shows the stretching rate close to a power-law dependence with time. Due to the non-linear character of the power-law rheology, the non-Newtonian fluid offers a natural scale-dependent resistance to deformation, which prevents efficient mixing at the intermediate length scales. This paper has several movies and can be found in *Electronic Geosciences*, 4:1, 1999.

We have studied the effects of low-temperature plasticity on the formation of shear zones. A thermal-mechanical model has been developed for describing the shear deformation of Maxwell viscoelastic material with a rheology close to dry olivine. In addition to diffusion and dislocation creep, we have included deformation by low-temperature plasticity, called the Peierls mechanism, which is significant at low temperatures and has a strong exponential dependence on the shear stress. When a sufficient magnitude of heat is produced by the rapid conversion of the elastically stored energy into viscous dissipation, thermal instability takes place and the deformation localizes in a narrow zone. For dry olivine and realistic values of the strain-rate, the effect of low-temperature plasticity is influential for temperatures between around 800 and 1000 K. This finding suggests that low-temperature plasticity may be crucial in regulating thermal-mechanical stability in the shallow portion of subducting slabs. This work has appeared in *Earth Planet Sci. Lett.*, 168, 159-172, 1999.

We have studied the effects of non-Newtonian rheology in producing ultra-fast plumes, which can spread out rapidly in horizontal direction upon impacting the lithosphere. These plumes can move at upward velocities in excess of meters / year and are considerably faster than the Newtonian plumes. These results show a direct separation of timescales between the rapidly rising non-Newtonian plumes and the ambient mantle circulation. This work has come out in *Tectonophysics*, Vol. 311, 31-43, 1999.

We have also studied mantled inclusions, commonly encountered in mylonites, which can record the deformation history. We have carried out two-dimensional numerical studies of time-dependent deformation behavior of inclusion and its dependence on rheology under simple shear. The inclusion is taken to be deformable and having its own intrinsic rheological properties. The results of numerical modeling shows that a key factor of structural appearance is the effective viscosity contrast between the inclusion and the matrix material. A high viscosity contrast from non-Newtonian rheology inhibits the stretching of the inclusion, preserving its round shape. This result is similar to our results in mixing. Wings or tails can only be developed in mineralogic systems with a high effective viscosity contrasts. This work has been published in *Earth Planet. Sci. Lett.*, 165, 25-35, 1999.

More information can be found at Prof. Yuen's web site at <http://banzai.msi.umn.edu>

GRANTEE: National Academy of Sciences, Board on Earth Sciences and Resources

The National Academies
2101 Constitution Ave., N.W.
Washington, DC 20418

GRANT: DE-FG02-97ER14810

Board on Earth Sciences and Resources and Its Activities

C. M. Schiffries (through December 1998) and A. R. de Souza (202-334-2744; Fax: 202-334-1377; adesouza@nas.edu)

Objectives: The purpose of the Board on Earth Sciences and its committees is to provide a focal point for National Research Council activities related to Earth science policy.

Project Description: The Board addresses the following strategic Earth science issues: identifying the frontiers of basic and applied research in the Earth sciences; strengthening multidisciplinary programs and integrated approaches to research; assessing mineral and energy resources; investigating human interactions with the Earth; understanding environmental change; improving access to and use of scientific and geospatial data and information; evaluating breakthrough technologies for mitigating environmental problems; and enhancing Earth science education.

Results: During FY 99, the Board on Earth Sciences and Resources produced 10 reports. In addition to producing reports, the board and its standing committees convened meetings to exchange information among scientists, engineers, and policy makers from government, university, and industry. Also, the board cosponsored with the U.S. Geological Survey a symposium on Natural Resources and Hazards: Challenges for the 21st Century.

GRANTEE: University Of Nevada, Reno

Department of Geological Sciences
Reno, NV 89512

GRANT: DE-FG03-98ER14885

Growth of Faults, Scaling of Fault Structure, and Hydrogeologic Implications

J. C. S. Long (University of Nevada, Reno; 702- 784-6987; Fax: 702-784-1766; CSLONG@mines.unr.edu) and D. Benson (Desert Research Institute; 775-673-7496; Fax: 775-673-7363; dbenson@dri.edu), in collaboration with S. Martel (808-956-7797; Fax: 808-956-3148; martel@soest.hawaii.edu), K. Hestir (Utah State University; 801-797-2826; Fax: 801-797-1822; hestir@sunfs.math.usu.edu) J. P. Evans (Utah State University; 801-797-2826; Fax: 801-797-1588; jpevans@cc.usu.edu)

Objectives: Our main objective is to find applicable equations of flow and transport in faulted and fractured zones based on their three-dimensional structure.

Project Description: We are developing an appropriate set of mathematical tools that can be used to evaluate the results of field tests in fractured and faulted rock. Previous hydraulic equations were based on a finite-sized representative elementary volume and small contrasts in media properties. Newer models that use fractional-order derivatives are based on very heterogeneous and scaleless media. We are examining the relationship between these equations and the measureable properties of fully and partially water saturated media, particularly the distribution of very high and very low velocity regions. The probability densities and connectivity of these regions directly affects the order of the governing differential equation. In particular, solute transport in a highly variable velocity field has a dispersion term of order $0 < \alpha \leq 2$. This models heavy-tailed and super-Fickian transport, both of which are characteristic of tracer tests in fractured media.

We are collaborating with a team from University of Hawaii and University of Utah that is performing detailed analysis of the three-dimensional permeability structure of faults in crystalline rocks, and developing field-based mechanical models for the nucleation and growth of faults in three dimensions. We aim to take this information and build forward models of large-scale transport in these networks. This research integrates fieldwork with deterministic and stochastic modeling to gain insight into how three-dimensional hydraulic conductivity structure of a fault develops through time. This work will lead to an increased understanding of fault zones from geologic, geomechanical, and hydrologic points of view, and to the development of a methodology for building physically realistic stochastic models for fault-zone hydrology.

Results: Previous derivation of fractional-order transport equations relied on a Lagrangian statistical mechanical viewpoint. An Eulerian setting was used to recast a fractional ADE (Schumer, *et al.*, preprint), with the added bonus of a surprising result: all plumes should be maximally skewed. This eliminates the skewness parameter from the equation and explained why the MADE site plumes are maximally skewed. More importantly, it explains how a fractional derivative works, and how the concept of a representative elementary volume (REV) is not valid in a fractional setting. In short, the fractional derivative describes the proportion of flux out of a box to the number of boxes that the solute traverses in a certain amount of time. This proportion drops like a power law of the number of boxes. An integer-order derivative (leading to the classical ADE) requires that all flux travels only one box,

which defines the REV. Aquifers with power-law velocity (*via* K or aperture statistics) and/or connected fracture lengths obviates the notion of an REV and suggests that the fractional approach is preferred for physical, rather than parsimonious reasons.

A fractional-in-space equation is most easily justified in highly heterogeneous media (Benson *et al.*, in press, *Transport in Porous Media*), such as fractured and faulted rock. But since the equation is a limit equation (Benson, *et al.*, *Water Resour. Res.*, 36(6), 1413, 2000), the fractional behavior should be observed in all inhomogeneous material (see Schumer *et al.*, preprint). Several tests that should be relatively homogeneous show fractional dispersion: a lab-scale sandbox model and the Cape Cod aquifer. The order of spatial differentiation for the sandbox is about 1.55 and the Cape Cod bromide plume follows an equation of order 1.65 to 1.8 (Benson, *et al.*, *Water Resour. Res.*, 36(6), 1403, 2000).

Previous fractional-order 3-D equations predict the same scaling in all directions. The plume grows with $t^{1/\alpha}$, resulting in a measured variance that grows like $t^{2/\alpha}$, with $0 < \alpha \leq 2$. Most plumes do not have this kind of scaling; they tend to scale more rapidly in the longitudinal direction than the laterally. The order of differentiation (α) should be different in any direction. When the scaling is allowed to be variable in any direction, the resulting equation can be represented by a combined second and fractional-order equation that allows a mixture of classical and fractional dispersion. The order of fractional dispersion may be considered a vector with directional scaling rates. This behavior is supported by experiments in granular media. For example, the Cape Cod experiment showed longitudinal spreading on the order of $\alpha = 1.65$, with Fickian ($\alpha = 2$) lateral spreading. The MADE plume showed much stronger spreading, with an obvious difference between the longitudinal ($\alpha = 1.1$) and lateral ($\alpha = 1.5$). Both plumes showed little vertical spreading, so a 2-D treatment is adequate.

A drawback of the fractional ADE is that solutions to forced-gradient tests are hard to come by. The mathematical process of subordination is a reasonable approximation and provides a model with very realistic physics and various subsets already found in the literature (Baeumer, *et al.*, preprint). Subordination starts with the assumption that the classical ADE is valid at some small scale. A particle at this scale is undergoing Brownian motion, $B(t)$. If the particle's mean velocity never changed, then the ADE would describe its probable position. If the velocity changes along a trajectory, it is as if the time spent in the Brownian motion were variable: sometimes time goes fast (which is equivalent to traveling and dispersing fast) and sometimes time goes by slowly. This leads to a random "operational time," $T(t)$. A particle's random motion is then a subordinated Brownian motion with random time $B(T(t))$. If we know something about the mean velocity density in an aquifer, we have information about $T(t)$. Similarly, if we know about the local, small-scale dispersion, we know about the Brownian motion $B(t)$. Solutions to any boundary value problem are then easily had through a simple integral transform involving the solution to the classical ADE (the subordinand) and a density (the subordinator) that is directly related to the velocity density measured at points in the aquifer. In the special case that the subordinator is a heavy-tailed, alpha-stable density, then the governing equation has a fractional-order divergence operator. These solutions in 1-D share most of the desirable properties of prior fractional approaches, with the addition of an observed mean velocity of a plume that increases with time. This is similar to the accumulating evidence that measured hydraulic conductivity (K) is larger with larger test scales: more of the high K material is integrated. The subordination approach has already appeared in various simplified forms. For example, if one assumes that a large number of particles have different (random) velocities, but the velocity stays constant for each particle while it travels, then the subordination is the "streamtube" or "transfer function" approach (Jury, 1982; Cvetkovic and Dagan, 1994). Conversely, if particles diffuse with no advection, then subordination recovers all alpha-stable diffusions. These two end-members demonstrate the robustness of the subordination approach.

GRANTEE: New England Research Inc.

331 Olcott Drive
White River Junction, VT 05001

GRANT: DE-FG02-98ER14906

The Role of Fracture Intersections in the Flow and Transport Properties of Rock

S. R. Brown (802-296-2401; Fax: 802-296-8333; sbrown@ner.com), H. W. Stockman (Sandia National Laboratories), and A. Caprihan (New Mexico Resonance)

Objectives: Fluid flow in fractured rock is an important phenomenon to understand in connection with energy production and containment or disposal of toxic wastes. Both discrete fracture and effective continuum approaches to the modeling of flow and transport in fracture networks need to be based on a sound understanding of flow in single fractures, how flow is transferred across intersections, and how multiple fractures form a network. We suggest that due to surface roughness and the consequent channeling in single fractures, volume flow and solute mixing behavior at fracture intersections will be considerably different from that expected based on simple assumptions and experiments with smooth-walled fractures. The objective of this project, therefore, is to gain a more complete understanding of flow channeling by physically modeling and analyzing several configurations of flow and transport through fracture intersections.

Project Description: We are addressing several problems concerning flow and transport through fracture intersections using a combination of numerical modeling, quantitative measurements, and visual observation of processes in real rough-walled fractures. Our observations include: channeling in single fractures, channeling within and through single fracture intersections, and channeling through fracture networks. These studies consider bulk flow, transport of solutes, and transport of multiple immiscible phases. These observations will ultimately be used to develop quantitative models describing the channeling and mixing behavior in 3-D intersections of rough-walled fractures.

This work makes use of our abilities to (1) quantify surface roughness through profilometry, (2) construct high quality replicas of actual fractured rock in transparent plastics, (3) simulate surface roughness with the computer, (4) construct bench-scale fracture systems, (5) observe actual flow and transport with quantitative visualization techniques, and (6) conduct detailed numerical simulations of flow and transport in heterogeneous media. For this work, we use a combination of quantitative measurements, visual and magnetic resonance imaging (MRI) observations of flow through real rough-walled fractures, and numerical modeling via lattice Boltzmann (BGK) methods.

Results: Field specimens of natural intersecting rock joints have been collected. Several samples were chosen for detailed study. Silicon rubber molds were used to construct epoxy replicas of selected specimens. Additionally, a calibration sample consisting of an ideal Hele-Shaw parallel plate intersection was made. To this point in the project, we have only been studying the properties of the ideal intersection by injecting clear and dyed fluids into the fracture pore space. We are able to observe the effect of the intersection on the dye flow by injecting fresh and dyed water into two separate legs of the intersection and observing the fluid traversing the outlet legs. The fluid pressure is pulsed alternately in each inlet to create a "stripe" of dye in the normally pure-water outlet leg, which moves along with the bulk fluid as a tracer. By observing the behavior of these dye stripes and the stream lines recorded in them we have seen the regularizing effect on the bulk flow of the intersection, dispersion of the dye

parallel to the flow, gravity driven stratification of dye, and the transition from laminar flow to turbulence (see Figure).

To enable us to eventually tie our results to field applications we have built a portable hand-held air permeameter to be used for measurement of effective fracture flow apertures at field sites. The operator builds pressure in a chamber with a hand pump, and then discharges the compressed air into a fracture through a rubber nozzle. Calibrations show that this device can be used to accurately derive fracture apertures in the range 25 to 2000 microns. This device will be used in the field to determine the variability of apertures in fracture networks, specifically around fracture intersections.

Measurement and analysis techniques are currently being developed for discerning flow and mixing of multiple liquid phases through intersections using pulsed magnetic resonance imaging (MRI). Numerical modeling efforts have been focused on elucidating problems in laboratory experiment design and analysis. It has been previously noted that laboratory experiments performed in finite-sized rectangular ducts give significantly different dispersion results than expected for fractures of infinite extent. We have shown through lattice Boltzmann (BGK) numerical simulations that surface roughness and flow channeling in real fractures tend to diminish the errors due to finite duct size, lending support for the performance of meaningful laboratory experiments on rough fractures.

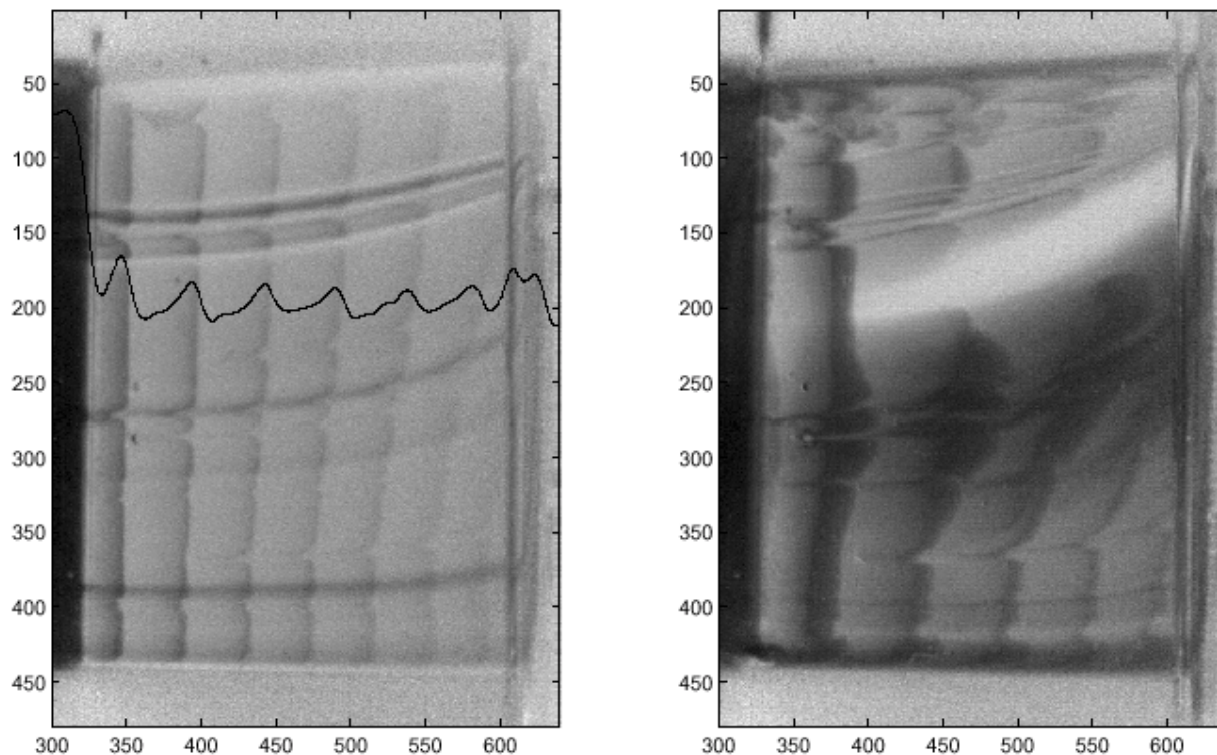


Figure: *Left:* Laminar flow of dye stripes emanating from an ideal Hele-Shaw fracture intersection. Only one outlet leg of the intersection is shown, with the vertical intersection itself located approximately at horizontal pixel number 320. Flow is from left to right from the intersection to a single outlet on the upper right hand side of the fracture. Traces of the streamlines are developed by perturbations in dye concentration due to tiny air bubbles and gravity stratification of dye. The uppermost dark streamline leads to the outlet port. At vertical pixel number 200 the variability of the dye concentration along the flow is indicated by the irregular curve superimposed on the image. *Right:* Turbulent flow in the same fracture brought on by a dramatically increased flow rate. Note the dye stripes are considerably more dispersed and irregular than for laminar flow.

GRANTEE: University Of New Mexico

Mechanical Engineering Department
Albuquerque, NM 87131

Grant: DE-FG03-97ER14778

Continuum and Particle Level Modeling of Concentrated Suspension Flows

M. Ingber (505-277-6289; ingber@me.unm.edu), with A. Graham (806-742-3553; Fax: 806-742-3552; Alan.Graham@coe.ttu.edu) and L. Mondy (Sandia National Laboratory, 505-844-1755; Fax: 505-844-825;)

Objectives: The purpose of this program is to combine experiments, computations, and theory to make fundamental advances in our ability to predict transport phenomena in concentrated, multiphase, disperse systems, particularly when flowing through geologic media.

Project Description: The proposed research will elucidate the underlying physical principles that govern concentrated multiphase systems in areas essential to continued progress in geosciences. In order to be of use in real world applications, significant enhancements to currently available continuum-level suspension flow models will be required. We will use both experimentation and high performance computing to obtain microstructural information that is necessary to the development and refinement of the continuum models. For example, we expect to use this microstructural information to gain insight into the physics of particle bridge formation and collapse and particle sedimentation, which are particularly important in sand control issues found in petroleum production. Further, we expect that continuum-level modeling could eventually be directly implemented in codes currently used to predict hydraulic fracturing operations in the petroleum industry. The understanding gained about the physics of multiphase flows will, however, have much broader application in geosciences.

Results: The continuum models originally developed by Phillips *et al.* (1992) and Nott and Brady (1994) has been extended to account for normal stress contributions. This allows accurate predictions of suspended particle migration in curvilinear flows. The Phillips-type model currently also allows for non-neutrally buoyant particles and non-Newtonian suspending liquids. Results from the new models, which have been implemented into a general-purpose finite element computer code, show good agreement with experimental measurements based on nuclear magnetic resonance (NMR) imaging. Also, massively parallel computing has allowed particle level simulations, based on the boundary element method (BEM), with up to a thousand particles. These simulations are currently being used to determine the magnitude of the normal stresses developing from particle interactions, as well as to develop more accurate hindered settling functions for particles interacting with other types of particles or in a porous medium. These simulations lead to detailed information on individual particle and fluid motion that is unobtainable through experiments. In addition, a multipole-accelerated boundary element method (BEM) has been developed to simulate many thousands of individual interacting particles. Two-dimensional dynamic simulations show qualitative agreement with (three-dimensional) laboratory experiments, and three-dimensional simulations are now possible for “snapshots” of interacting particles.

GRANTEE: New Mexico Institute Of Mining And Technology

Department of Earth & Environmental Science
Socorro, New Mexico 87801

Grant Number: DE-FG03-96ER14589

Investigation of Permeability Upscaling

J. L. Wilson (Department of Earth & Environmental Science, New Mexico Institute of Mining and Technology, 505-835-5308; Fax: 505-83506436; jwilson@nmt.edu) and V. C. Tidwell (Sandia National Laboratories; 505-844-6025; Fax: 505-844-6023; vctidwe@sandia.gov)

Objectives: The goal of this research is to better understand the process of permeability upscaling. Physical and numerical experimentation forms the basis for testing conceptual and theoretical models of permeability upscaling as well as exploring alternative measures and models of this process.

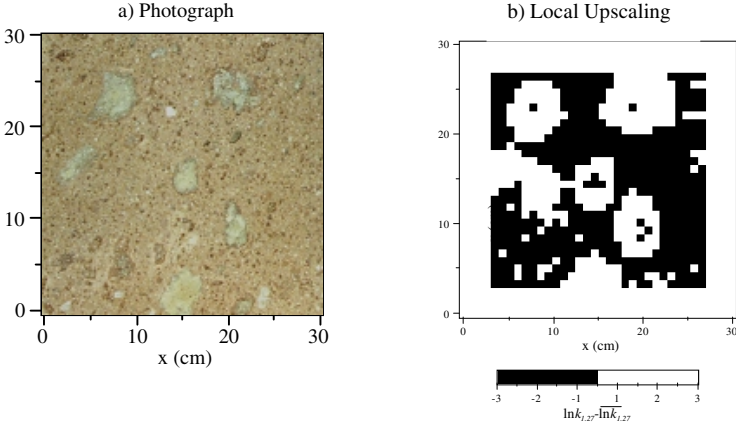
Project Description: Investigation of permeability upscaling is predicated on the results of physical experimentation. These experiments are unique in that: 1) permeability data are collected over a range of different sample supports (sample volumes), each subject to consistent measurement conditions; 2) data are collected on densely sampled grids providing detailed resolution in the spatial distribution of permeability; and 3) experiments are repeated on a variety of geologic materials each differing in their structural/textural attributes. A specially designed gas minipermeameter provides a rapid, precise, and non-destructive means of collecting permeability data. By varying the size of the minipermeameter tip seal, measurements spanning five orders of magnitude on a per-volume basis are made subject to consistent boundary conditions and flow geometry. Thousands of measurements on multiple faces of meter-scale blocks of rock are collected with each of five different tip seals (0.31 - 5.08 cm ID) plus a single large tip seal (15.24 cm ID) designed to integrate over the entire sampling domain. To quantify permeability upscaling, key summary statistics are calculated from the acquired data sets and analyzed with reference to their corresponding sample support. Results are interpreted in light of the physical characteristics of the porous medium and measurement characteristics of the sampling instrument. Detailed numerical modeling is also employed to further explore and quantify the empirical upscaling behavior and to extend the studies to a broader suite of materials.

Results: Intuitively we recognize that permeability is in some way related to the textural and structural attributes visible in the host rock; however, establishing such a relationship is problematic. The ability to discern such relationships is of significant value to site characterization programs, as this type of information would aid in predicting permeability at unsampled locations. We explore the potential for such relationships in our data by comparing measured permeabilities from two of our sandstone samples and one tuff sample with digital image data taken from the corresponding block faces. We found direct correlation between the permeability and any textural measure drawn from the digital image data to be very difficult to establish. Alternatively, correlation in the spatial patterns was easily affirmed, beginning with visual comparison of the digital image and permeability data. This relationship was also demonstrated quantitatively *via* semivariogram analysis and on the basis of the size, shape, orientation, and location of features distinguished by spatial contrast in image gray-level/permeability.

New insights into permeability upscaling were realized with the analysis of data collected from a block of volcanic tuff. A bimodal permeability distribution, which corresponds to the distinct textural contrast between the porous pumice fragments and the tight rock matrix, characterizes this sample. Upon

developing a novel conditional expected value model, local (*i.e.*, limited neighborhood about each sampling point) analysis of the permeability upscaling was conducted. Results of the local analysis reveal strong variability in permeability upscaling from point to point throughout the sampling domain. Specifically, the permeability upscaling exhibited by zones rich in pumice is very different from zones dominated by matrix, unless the averaging volume is significantly larger than the spatial correlation scale.

Figure: a) photograph of the sampled tuff block, and b) two-dimensional map showing the difference in permeability upscaling between zones rich in pumice (positive values) *versus* those dominated by matrix (negative values).



GRANTEE: State University Of New York At Stony Brook

Department of Geosciences
Stony Brook, New York 11794-2100

GRANT: DE-FG02-94ER14449

High Precision Radiometric Dating of Sedimentary Materials

G.N. Hanson (631-632-8210; Fax 631 632 8240; gilbert.hanson@sunysb.edu) and W.J. Meyers

Objectives: To develop field, petrographic and geochemical criteria to allow high precision U-Pb dating of sedimentary minerals within rapidly deposited sequences of carbonate and clastic rocks.

Project Description: The original goal was to obtain radiometric ages for sedimentary material with uncertainties of three million years or less to date the times of sedimentation. We have since shown that it is possible to obtain uncertainties of 1 Ma or less.

We started with the dating of soil calcite and have since considered the potential of U-Pb dating of sedimentary apatite and lake, swamp and spring calcite. The most obvious applications for precise ages for times of sedimentation are:

- 1) providing more precise duration's for unconformity bound genetic packages in sequence stratigraphy;
- 2) more precisely calibrating the geologic time scale;
- 3) correlation between marine and terrestrial stratigraphic sections; and
- 4) correlation between fossil-rich and fossil-poor stratigraphic sections.

Results: *Mississippian Paleosols from Kentucky:* Based on our previous success with dating brown calcite from caliches developed on marine carbonates, brown caliche crusts were selected from the Mississippian (Lower Carboniferous) section of Kentucky. Fission track maps of thin sections reveal that in these rocks uranium is concentrated in chert. The chert preferentially replaces paleo-caliche. This replacement is interpreted to have occurred near the time of formation of the caliche. Results from other studies suggest there is a strong attraction of uranium for opal. The conversion of opal to chert can take millions of years but if this is the case, the U-Pb data should show scatter. One chert sample has an outer part that is chalky and porous and an inner dense vitreous zone. While the outer porous zone is discordant and shows evidence of open system behavior, the vitreous chert has U-Pb systematics that suggest that it behaved as a closed system and gives an age of about 350 Ma.

The Medial Miocene Barstow Fm., Rainbow Basin, Mojave Block, So. California: U-Pb ages of a lacustrine tufa show great potential for improving time resolution in terrestrial sections. The range in $^{238}\text{U}/^{206}\text{Pb}$ of 4000 provides enough spread in the Pb isotopic ratios to precisely define the ^{238}U - ^{206}Pb isochron. The concordant U-Pb age of a tufa deposit that occurs at the top of the Owl Conglomerate Member in the undated section at Owl Canyon is 14.7 ± 0.4 Ma. The tufa is composed of alternating bands of fibrous and micritic calcite, with higher and lower uranium concentrations respectively. The fibrous calcite exhibits a gradual increase in the concentration of uranium in the outward growth direction of the calcite with a homogenous dull luminescence under cathodoluminescence. These observations are consistent with cyclic mixing of varying proportions of U poor and Ca-rich water from springs and U-rich and Ca-poor evaporative lake water during the precipitation of the tufa. Mono Lake tufa deposition is a modern analogue.

GRANTEE: State University Of New York At Stony Brook

Department of Applied Mathematics and Statistics
Stony Brook, New York 11794-3600

GRANT: DE-FG02ER14261

Medial Axis Analysis of Porous Media

W. B. Lindquist (631-631-8361; Fax: 631-632-8490; lindquis@ams.sunysb.edu)

Objectives: The goal of this work is to develop and utilize a package of software tools to extract quantitative information on the geometry of the void and grain microstructure of rock starting from high resolution, three dimensional (*e.g.*, X-Ray microtomographic) images.

Project Description: High resolution (1 to 5 micron), three-dimensional images of rock samples are segmented to provide specific grain/pore identification for each voxel in the image. Appropriate transforms are then applied to the segmented, digitized images to produce medial axis (co-dimension two) representations of the void (or grain) structure. Geometric properties of the rock are either measured directly from the medial axis, or the axis is utilized as a search path to locate regions where measurements are to be made.

Results: An analysis [1] of the microstructure of a suite of Fontainebleau sandstones ranging from 7.5 to 22% porosity has been completed. This represents the most extensive analysis on geometric properties of rock at the pore scale. The data samples were imaged at 5.7-micron resolution by X-ray computed microtomography; each sample studied has a volume of 46.7 cubic mm. An example of the geometric analysis is presented in the accompanying figure for a 22% porosity core sample. The results indicate: exponential distributions for the nodal pore coordination number (Fig. (c)) and channel throat areas (Fig. (e)); log-normal distribution of nodal pore volumes (Fig. (f)); Weibull-type distribution of channel lengths with a strong exponential range (Fig. (d)). These distributional forms hold over the entire porosity range of 7.5 to 22% enabling measurement of porosity dependence of the distribution parameters.

The absence of 3D-based distribution information for real rock has been a problematic issue in the goal to bulk property values to pore scale structure. In collaboration with researchers at Australian National University, we have commenced an investigation of the influence of these distributions on network model-based studies of residual saturation in two-phase flow. The investigations [2] show strong evidence of the importance of pore-pore correlation influences (Fig. (g)).

[1]. W.B. Lindquist, A. Venkatarangan, J. Dunsmuir and T.-f. Wong, Pore and throat size distribution measured from synchrotron X-ray tomographic images of Fontainebleau sandstones. Submitted to *J. Geophys. Research*.

[2]. R.M. Sok, M.A. Knackstedt, A.P. Sheppard, W.V. Pinczewski, W.B. Lindquist, A. Venkatarangan, and L. Paterson, Direct and stochastic generation of network models from tomographic images: Effect of topology on two phase flow properties. Submitted to *Transport in Porous Media*.

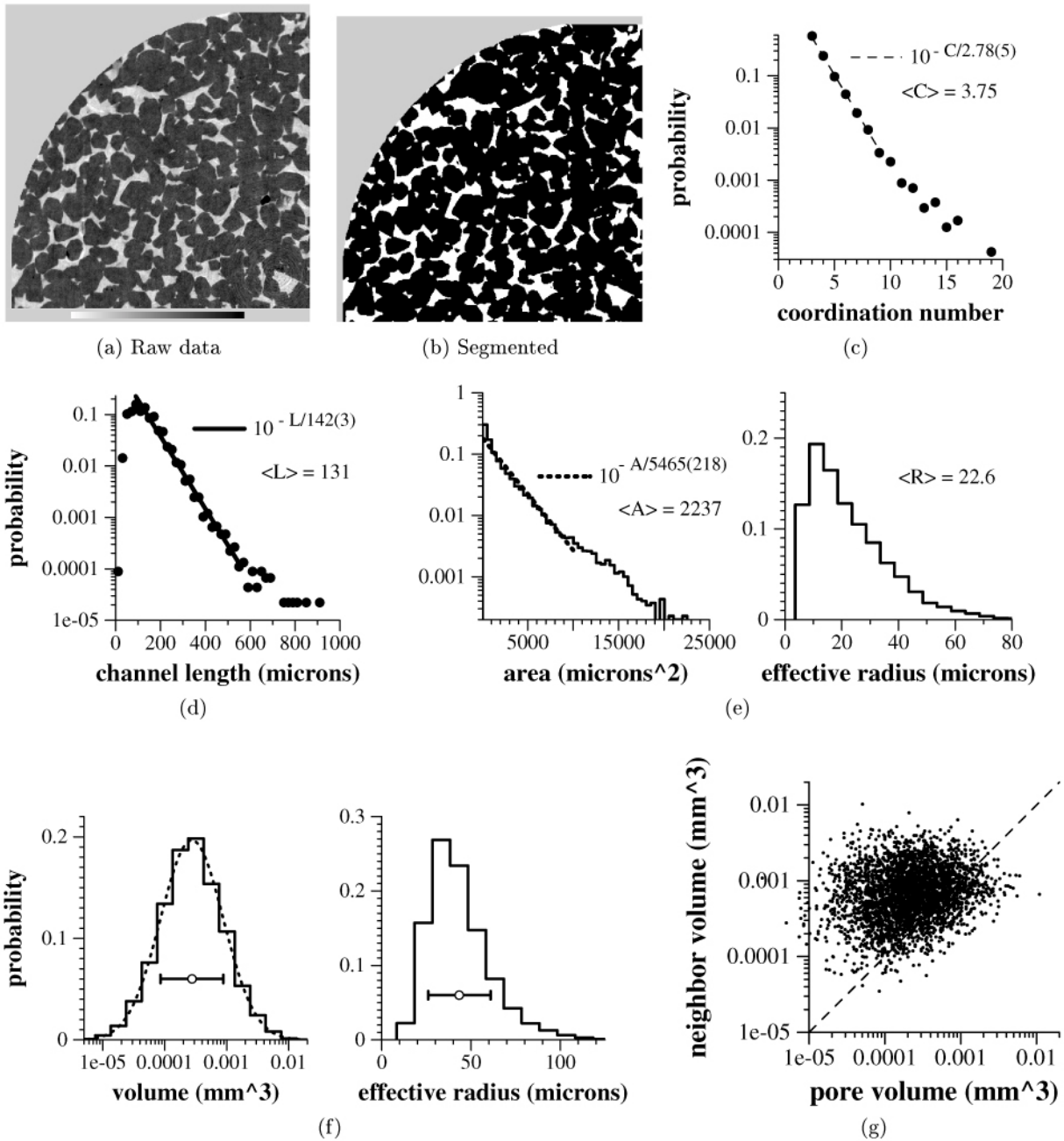


Figure. (a) A quarter slice from a 22% porosity core image. (b) The segmented quarter slice. (c) Nodal pore coordination number distribution. (d) Channel length distribution. (e) Distribution of: left - throat surface area; right -effective throat radius. (f) Distribution of: left - nodal pores volume; right - effective nodal pore radius. (g) Nearest neighbor pore-pore volume correlations.

GRANTEE: State University Of New York At Stony Brook

Department of Geosciences
Stony Brook, NY

GRANT: DEFG029ER14633

Surface Chemistry of Pyrite: An Interdisciplinary Approach

M. A.A. Schoonen (Department of Geosciences, State University of New York, Stony Brook, NY; 516-632-8007; mschoonen@notes.cc.sunysb.edu), and D. R. Strongin (215-204-7119; Fax: 215-204-1532; dstrongin@nimbus.ocis.temple.edu)

Objectives: The primary goal of this research program is to understand the microscopic aspects of pyrite oxidation. Determining the charge development on pyrite surfaces and evaluating the interaction of the pyrite surface with an array of simple inorganic and organic molecules are the immediate goals. Through a combination of macroscopic observations and observations at the atomic/molecular level new insights are gained that will lead to a better understanding how pyrite reacts in a range of chemical environments.

Project Description: The charge development, interaction with inorganic and organic constituents, and the reactivity of pyrite are being investigated. Emphasis is placed on integrating macroscopic information from low-temperature techniques such as electrophoresis and microscopic information from modern surface science techniques that are used in the ultra high vacuum (UHV) environment. Using model, atomically clean “as-grown” surfaces of pyrite, electron spectroscopies in UHV are used to understand the atomic composition and the nature of the functional groups on pyrite after exposure to the aqueous solutions. The integration of the UHV and low-temperature studies will provide a complete picture of the type of surface functional groups at the pyrite surface, their acid-base behavior, and interaction with selected aqueous constituents.

Results: In the third year of funding our studies have further characterized the oxidation chemistry of pyrite with surface science and aqueous techniques. Furthermore, significant emphasis has been placed on understanding the chemistry of phosphate on pyrite.

Surface Science Studies of pyrite structure and oxidation: Photoelectron Spectroscopy was used to investigate the surface structure and reactivity of {100} planes of pyrite that have been prepared by two commonly employed means. Specifically, synchrotron-based photoelectron spectroscopy was used to investigate the structure of two {100} pyrite surfaces. One was prepared by exposing a {100} pyrite growth surface to HCl, and one was produced by mechanical fracture. Results show that acid-washed growth surface (*i.e.*, exposed to HCl) showed a higher concentration of elemental sulfur and/or polysulfide impurities. Perhaps, surprisingly, the surfaces showed similar initial oxidation reactivity under well-controlled H₂O/O₂ gaseous environments. This result implied that the fraction of both surfaces that underwent the initial oxidation reaction were similar in structure. The oxidation activity of these surfaces were, however, were experimentally determined to be significantly less than the initial oxidation activity of an acid-washed {111} growth surface. Photoelectron and ion scattering spectroscopy suggest that a reason for this structure sensitivity may be due to differences in the concentration of Fe in the outermost layer of the different crystallographic planes of pyrite.

Studies of the pyrite-phosphate interaction: Electrophoresis and surface science experiments have been carried out to understand the interaction between phosphate and pyrite. Electrophoresis experiments

show that under anoxic conditions only a relatively small fraction (no more than 10 %) of dissolved phosphate irreversibly sorbs onto the pyrite surface. Surface science studies suggest that this irreversibly bound pyrite adsorbs to non-stoichiometric sites on pyrite. Results to date indicate that phosphate is preferentially bound to sulfur-deficient (possibly Fe^{3+}) defect sites. Research carried out in prior funding cycles suggests that these sites play a critical role in the oxidation of pyrite by dissolved O_2 . Aqueous-based oxidation experiments and experiments carried out in a combined ultra-high vacuum/high pressure apparatus suggest that this relatively small amount of adsorbed phosphate results in a significant oxidation suppression of pyrite. This result emphasizes how minority sites (non-stoichiometric sites) control the oxidation reactivity of pyrite.

GRANTEE: State University Of New York At Stony Brook

Department of Geosciences
Stony Brook, New York 11794-2100

GRANT: DE-FG02-94ER14455

Micromechanics of Failure in Brittle Geomaterials

T.-F. Wong (631-632-8212; Fax: 631-632-8240; Teng-fong.Wong@sunysb.edu) and J. T. Fredrich (Sandia National Laboratories)

Objectives: This project focuses on the systematic investigation of the micro-scale characteristics of natural Earth materials, and how these micro-scale characteristics control the macroscopic deformation and transport behavior. The research uses an integrated approach consisting of experimental rock mechanics testing, quantitative 2D and 3D microscopy and statistical microgeometric characterization, and theoretical and numerical analyses. The objective is to enhance fundamental understanding of failure and transport processes in geologic materials, and thereby strengthen the theoretical basis for the application of laboratory results to various technological operations of importance.

Project Description: Knowledge of the micro-scale characteristics and behavior of rocks is important for several energy-related applications, including global climate change and carbon management; oil field geoscience; geotechnical engineering efforts such as design and assessment of geologic nuclear waste repositories; and environmental remediation efforts at contaminated DOE and/or DoD installations. We use an integrated approach consisting of experimental rock mechanics testing, quantitative microscopy, and theoretical and numerical analyses. The experimental investigation provides a detailed understanding of the microstructure of geologic materials and how the micro-scale characteristics affect macro-scale behavior including brittle failure and fluid transport. Detailed and quantitative microstructural studies complement laboratory rock mechanics experiments. The results are used to formulate and evaluate theoretical and numerical models of rock deformation and fluid flow.

Results: (1) *Investigation of water-weakening effect on the strength of porous sandstones.* Our comprehensive data on the weakening effect of water on brittle strength and ductile compaction of several porous sandstones has allowed us to formulate a micromechanical model to consistently interpret the dilatant and compactive failure behaviors due to presence of water and initial damage in a fracture mechanics framework.

(2) *Triaxial compression experiments on 2 limestones (of initial porosities of ~3% and 14%) and detailed characterization of the failure envelopes in both the brittle and cataclastic flow regimes.* Preliminary data show that inelastic and failure behaviors in the Indiana limestone are qualitatively similar to those in porous clastic rocks. Experiments have been completed and microstructural observations are still in progress. We have also completed a study on the relatively compact Solnhofen limestone. For the first time, a fairly complete set of data on porosity change and the brittle-ductile transition in the Solnhofen limestone have been acquired. The failure modes are associated with complex interplay of dilatancy, pore collapse and crystal plasticity processes, and several micromechanical models have successfully been employed to interpret the phenomena.

(3) *Quantitative characterization of the pore geometry of 4 Fontainebleau sandstone samples using synchrotron x-ray tomography.* The data elucidate the 3-dimensional geometry and connectivity of the pore space in a suite of Fontainebleau sandstone with porosities ranging from 7.5% to 22%. Algorithms

were developed to quantify the distributions of coordination number, channel length, throat size and pore volume. This unique set of computed synchrotron X-ray tomographic data provide important constraints on geometric attributes of importance in the realistic modeling of permeability and fluid transport.

(4) Damage evolution during the formation of a compaction band. Preliminary data show that localization mode in the form of compaction bands orthogonal to the maximum compressive stress is widely observed in porous sandstones in the transition from brittle faulting to cataclastic flow. We are systematically investigating the inelastic and compactive behaviors that promote such localization features.

GRANTEE: Northwestern University

Department of Civil Engineering
Evanston, IL 60208-3109

GRANT: DE-FG02-93ER14344

Factors Affecting Shear Strain Localization in Rocks

J.W.Rudnicki (847-491-3411; Fax: 847-491-4011; jwrudn@northwestern.edu)

Objectives: To obtain an improved understanding of the occurrence, development and evolution of shear localization zones (faults) in rocks and their relation to the macroscopic constitutive description, especially that governing multi-axial response, and microscale mechanisms of deformation.

Project Description: Because of the significance of fractures to energy production, waste disposal, and mineral technologies, prediction of their causative stresses, location, orientation, thickness and spacing becomes paramount. This project examines the applicability of a theory of localization that describes faulting as an instability of the constitutive description of homogeneous deformation. The predictions of localization depend strongly on the constitutive description; consequently, a correlative objective is to improve constitutive model, particularly those aspects governing abrupt changes in the pattern of deformation. Investigations of constitutive behavior include both phenomenological models, derived from laboratory tests, and micromechanical models, based on the growth and interaction of microcracks and resulting increase in overall compliance of the solid. Constitutive relations are calibrated by comparison with axisymmetric compression tests and then used to predict the response in more complex experiments, *e.g.*, compression-torsion, and plane strain. Comparison of numerical studies with experiments addresses the effects of more realistic geometries and boundary conditions.

Results: A new microcrack damage model has been developed to describe the inelastic behavior of brittle rock under compressive stresses. An explicit expression for the macroscopic effective constitutive tensor (compliance or stiffness) makes it possible, in principle, to determine the critical damage intensity at which the localization condition is satisfied. Application of the model to a French granite and Tennessee marble yields good agreement with stress-strain curves, including the occurrence of dilatancy and the increase in compliance upon unloading.

Reexamination of theoretical results for shear localization reveals that solutions for compaction bands are possible in a range of parameters typical of brittle rock. Compaction bands are narrow planar zones of localized compressive deformation perpendicular to the maximum compressive stress, which have been observed in high porosity rocks in the laboratory and the field. Solutions for compaction bands, as an alternative to homogeneous deformation, are possible when the inelastic volume deformation is compactive and is associated with stress states on a yield surface "cap." Because the density of the material within the bands is increased, and, presumably, the permeability is decreased, the occurrence of these structures may be a significant factor affecting the withdrawal and injection of fluids from porous reservoirs.

GRANTEE: Oklahoma State University

School of Geology
Stillwater, OK 74078

Grant: DE-FG03-99ER14944

Two-Phase Immiscible Fluid Flow in Fractured Rock: The Physics of Two-Phase Flow Processes in Single Fractures

M. J. Nicholl (405-744-6041; Fax: 405-744-7841; nicholl@okstate.edu), H. Rajaram (University of Colorado), and R. J. Glass (Sandia National Laboratories)

Objectives: The objective is to develop a quantitative understanding of critical fundamental processes controlling two-phase flow and transport in fractures, based on detailed physical experiments and high-resolution numerical simulations. This understanding may subsequently be abstracted for use in conceptual models applied to large-scale problems in petroleum extraction, isolation of hazardous or radioactive waste, remediation of contaminated subsurface media and CO₂ sequestration.

Project Description: Under two-phase immiscible flow conditions, the phase geometry associated with each phase controls the fluid flow and solute transport characteristics. The phase geometry is in-turn determined by a combination of the aperture variability, the capillary and viscous effects inherent in the two-phase flow processes themselves and external forces such as gravity. If one of the fluids can slightly dissolve in the other, then transport of the dissolved fluid also influences phase geometry.

In this collaborative project between Sandia National Laboratories, Oklahoma State University and University of Colorado at Boulder, systematic physical experimentation is coupled with concurrent numerical simulation to explore the factors controlling phase structure, flow, transport and inter-phase mass transfer in rough-walled fractures. A high-resolution light-transmission technique has been developed to facilitate acquisition of accurate experimental measurements of aperture, phase geometry and solute concentrations in transparent analog fractures. Use of this technique will lead to data of unprecedented accuracy for evaluating current understanding of invasion, flow and transport processes, and motivate refinement of theoretical concepts.

Results: A comprehensive evaluation of the Reynolds equation for saturated flow in rough-walled fractures was accomplished by combining high-resolution experiments with careful numerical simulations. Highly accurate aperture measurements in three transparent analog fractures (a Hele-Shaw cell, a fracture assembled using one rough and another flat glass plate and a fracture constructed with two rough plates) were an essential element in this evaluation. While numerical simulations based on the Reynolds equation closely reproduced the experimentally determined effective transmissivity of the Hele-Shaw cell, the discrepancies were in the range of 22-47% in the other two fractures. A careful evaluation of numerical and experimental errors suggested that these could only account for about 2% of the discrepancy. We therefore concluded that the Reynolds equation is inadequate for predicting effective transmissivities in the experimental rough-walled fractures.

A comprehensive study of solute dispersion in rough-walled fractures was carried out, combining high-resolution experimental measurements of fracture aperture and solute concentrations, with a three-dimensional computational model. The flow field in the computational model was determined by solving the Reynolds equation.

The experimental results indicated a nonlinear dependence between the effective dispersion coefficient and the Peclet number (Pe). This feature was interpreted using a theoretical model in which the total dispersion coefficient is expressed as a sum of the molecular diffusion, macrodispersion (induced by aperture variability, linear in Pe) and Taylor dispersion (induced by the velocity profile across the fracture, quadratic in Pe) coefficients. The Taylor dispersion term was shown to be most important at large values of Pe, corresponding to a quadratic dependence. While the theoretical model and numerical simulations qualitatively reproduced the nature of Pe-dependence of the dispersion coefficient, the magnitude of the dispersion coefficient was underestimated by about 35% at the highest Pe (750) value in the experiments. We concluded that the discrepancy between the theoretical and experimental results is largely attributable to the limitations associated with the Reynolds equation.

The factors controlling relative permeability in a partially saturated fracture were investigated based on experiments involving a wide range of entrapped phase structures. A numerical simulator was developed for modeling flow around the entrapped non-wetting phase. Results indicated close agreement between experimental and modeled relative permeabilities, suggesting that the inaccuracies associated with the Reynolds equation "cancel out", because they appear in both the saturated and absolute permeabilities. A conceptual model based on effective medium theory was proposed to explain the variation of the relative permeability with phase structure. The conceptual model involves four factors - the phase saturation, the in-plane tortuosity induced by the entrapped phase, the change in mean aperture within the flowing phase and a parameter representing change in aperture distribution within the flowing phase. The in-plane tortuosity induced by the entrapped phase was identified as the most dominant controlling factor, followed by the phase saturation.

GRANTEE: University Of Oklahoma

School of Geology and Geophysics
Norman, Oklahoma 73019

GRANT: DE-FG03-96ER14643

Development and Application of a Paleomagnetic/Geochemical Method for Constraining the Timing of Fluid Migration and Other Diagenetic Events

R.D. Elmore (405-325-3253; Fax: 405-325-3140; delmore@ou.edu) and M.H. Engel

Objectives: The goal of this project is to develop paleomagnetic methods for dating diagenetic events in sedimentary rocks. Specific objectives include testing the hypotheses that fluid flow (*e.g.*, basal fluids, hydrocarbons), clay diagenesis and organic matter maturation are viable mechanisms for the occurrence of pervasive chemical remanent magnetizations (CRMs) that are commonly observed in sedimentary systems.

Project Description: Investigations of diagenetic processes such as fluid migration and the maturation of organic matter commonly lack temporal control. The ability to constrain the time of oil migration, for instance, would be of significant benefit for exploration. The paleomagnetic dating method is based on a genetic connection between diagenetic processes and the precipitation of authigenic magnetite. Isolation of the magnetization carried by the magnetite and comparison of the corresponding pole position to the apparent polar wander path allows the timing of diagenetic events to be determined. The research involves paleomagnetic field and laboratory tests to constrain appropriate chemical and physical conditions for magnetite authigenesis.

Results: Field and laboratory studies were conducted to constrain factors responsible for chemical remanent magnetizations (CRMs) in sedimentary rocks, in particular fluid migration and mineral diagenetic transformations. For example, hematite authigenesis in dolomites was investigated along the Highland Boundary Fault (HBF) in the Lower Paleozoic Highland Border Group of central Scotland. The HBF is exposed for 230 km from Arran to Stonehaven. Paleomagnetic results suggest that there was a fluid flow event that caused dolomitization and hematite authigenesis along the HBF in the late Carboniferous/early Permian. The fact that the fluid-related magnetizations occur at all sampling localities (up to 150 km apart) along the fault suggests that the fluid migration that triggered this event was pervasive. Although meteoric fluids may have been involved, the presence of relatively high temperature fluid inclusions in the altered rocks as well as evidence for the formation of high-temperature clays suggests that the fluids were more likely hydrothermal in origin. These fluids caused precipitation of hematite and acquisition of the associated CRM. In addition, the hot fluids probably reset a preexisting magnetization of the serpentinite present in an oceanic or back-arc assemblage that occurs immediately south of the fault plane. These fluids may have been derived from the intrusion of late Carboniferous dikes in central Scotland or from a hypothesized regional scale flow event that caused extensive remagnetization in Scotland. The dolomite along the HBF may be related to dolomite in the Dalradian schist, which occurs as linear vein-fillings that contain brecciated country rock. These veins occur from Kintyre to Loch Lomondside. Paleomagnetic analysis indicates that hematite authigenesis occurred in the Permo-Triassic, probably due to oxidative weathering. Petrographic evidence, however, indicates that the dolomitization predated the hematite authigenesis. Geochemical evidence suggests that the dolomitizing fluids were basinal brines. The dolomite veins probably formed during late Carboniferous extension and may be related to the dolomite that occurs along

the HBF. Thus, there was at least one widespread dolomitizing and hematite-precipitating fluid alteration event in central Scotland during the late Carboniferous.

Mineral transformations associated with burial diagenesis may also result in magnetite authigenesis and associated CRMs. Our recent paleomagnetic results from Jurassic age sediments on Skye, Scotland, are consistent with the hypothesis that authigenic magnetite and an associated CRM can form during the conversion of smectite to illite. Sediment in north Skye, where smectite is abundant and the clays are unaltered, contains a weak and unstable magnetization. The same age sediment in south Skye, where the clays have been altered to illite by moderate heating (150-200°C), contains a multi-component CRM residing in magnetite and/or pyrrhotite. The CRM was acquired during the early Tertiary, which is consistent with the timing of igneous intrusions and associated hydrothermal activity that caused this alteration.

Simulation experiments were performed in which samples of smectite-rich sediments and samples of powdered pyrite dispersed in plaster of paris (to minimize the skin effect) were heated. In both cases, magnetite was observed to form at 350°C and was not observed in the blanks. Thus, this alternative pathway for magnetite authigenesis via prolonged heating of sediments at moderate burial temperatures merits further investigation as a viable alternative for the occurrence of pervasive CRMs in sedimentary basins.

GRANTEE: The Pennsylvania State University

Department of Geosciences
Univ Park, PA 16802

Grant: DE-FG02-95ER14547.A000

Dissolution of Feldspar in the Field and Laboratory

*S. L. Brantley, Dept. of Geosciences (814-863-1739; Fax: 814-865-3191; Brantley@geosc.psu.edu)
and C. Pantano, Dept. of Material Sciences and Engineering*

Objectives: In this project, three questions are being investigated concerning the dissolution of feldspar under ambient conditions: 1) What are the structures of altered layers on crystalline and glassy feldspars dissolved in the laboratory? 2) What techniques can be used to investigate near-equilibrium dissolution of feldspar? 3) How are the weathering rates of feldspar affected by internal porosity and surface coatings?

Project description: One of the most debated questions today in low-temperature geochemical kinetics centers upon the rate and mechanism of dissolution of feldspar, the most common mineral in the crust. In this project, the mechanisms of feldspar dissolution are investigated by emphasizing experiments with feldspar glass and crystal while comparing surface and solution chemistry. Surface sensitive analytical techniques (x-ray photoelectron spectroscopy, secondary ion mass spectrometry, Auger electron spectroscopy, atomic force microscopy) are used on samples reacted not only in the laboratory, but also in natural field settings. Specifically, laboratory work focuses on the structure of altered surface layers on feldspars, the rate of dissolution of feldspar crystal and glass in near-equilibrium and dilute solutions, and the presence of porosity and surface coatings on feldspars. In a complementary field project, the use of Sr concentrations and isotopic ratios are used to calculate feldspar dissolution rates.

Results: Atomic force microscopy was used to investigate surfaces of feldspar powders. For oligoclase and anorthite, mesopores were imaged infrequently. These powders sometimes show hysteresis in gas adsorption experiments, also suggesting porosity. Naturally weathered soil samples of plagioclase and potassium feldspar from California also show hysteresis in gas adsorption, consistent with growth of mesopores during weathering. Using AFM to image powders is difficult, however, so this tool was also used to image feldspar plates. Total roughness of dissolved surfaces of albite crystal and glass was quantified by AFM through analysis of roughness and spatial distribution (fractal dimension, D). Crystalline samples dissolved at pH 2 became spatially less complex (D decreased) while glass samples showed no change in D. The decrease in D indicates that high-aspect ratio features on the crystal were dissolved, leaving etched defects of lower aspect ratio. These latter defects presumably consisted of both crystallographic defects and polishing scratches. In contrast, D of glass remained unchanged with dissolution, perhaps because of the lack of line and plane defects. Using AFM to measure dissolution rates may be possible if roughness and D can be correlated to rate. However, some phases (*e.g.* bytownite) form leached surface layers which flake off and which are hard to image with AFM. To better understand this leached layer and controls upon its formation, a suite of plagioclase glasses has been synthesized for dissolution and surface chemistry analysis.

GRANTEE: Purdue University

Department of Earth and Atmospheric Sciences
West Lafayette, IN 47907-1397

Grant: DE-FG02-98ER14886

Mechanical Models of Fault-Related Folding

A.M. Johnson (765-494-0250; Fax 765-496-1210; gotesson@purdue.edu)

Objectives: The underlying goal of the proposed research is to provide a unified, mechanical infrastructure for studies of fault-related folding and to apply that infrastructure to studies of a wide range of field examples. The mechanical theory will be presented via programs that have graphical user's interfaces (GUI) so that structural geologists may model a wide variety of folds. The proposed research will provide practical methods of predicting forms of folds and other structural traps accessory to each type of fault-related fold.

Project Description: The research project can be divided into four parts. The first part is to investigate the geometric characteristics that identify fault-related folds of different types. In addition to exploring existing literature and seismic profiles, field mapping of fault-related folds in central Utah and along the southwest side of the Big Horn Basin in Wyoming will be combined with borehole data and seismic profiles of the structures. This combination of data will relate the folding observed in the field to the underlying faulting. The second part of the research is to derive mechanical analogs of idealized field examples of fault-related folds as well as various geometric models of fault-related folding. The combination of boundary conditions, rheological properties, and mechanisms that produce fault-related folds will be determined. The third component of the research is to explore what kinds of secondary structures occur together with primary structures, such as ramp anticlines and synclines, décollement folds, fault-arrest folds and fault-propagation folds, that would suggest new targets for petroleum exploration. The last component of the research is to develop methods that will allow practitioners to generate their own examples of ideal fold forms, by specifying the conditions the practitioner suspects to be important in the tectonic environment.

Results: Four theoretical analyses were completed. The first is an analysis of ramp folding in a thrust system in which up to four detachment surfaces are active simultaneously or independently. The second analysis explains mechanically how a kink-band propagates. A key to this analysis is the relationship of the amount of shift across the band to the amount of shear stress required to make the shift increase and the energy released as the kink band extends an incremental distance into the layered medium. The third analysis is on the mechanics of formation of deformation bands. This analysis of propagation of deformation bands in porous sandstones largely explains why the offset is accommodated across a deformation band rather than across a fault with a distinct slip surface. The fourth theoretical analysis resulted in a Graphical User's Interface (GUI) to model simple to complex ramp folding.

In addition to the theoretical investigations, data was collected from fault-related folds. The strains and displacement fields were measured from street surveys to study the growth of a fault-related fold along the Sylmar fault segment that was active during the 1971 San Fernando earthquake. Small faults were mapped in a section of the monocline on the eastern side of the San Rafael Swell, Utah to analyze the stress state at the time of folding.

GRANTEE: Purdue University

Department of Physics
West Lafayette, IN 47907-1396

Grant: DE-F602-93-ER14391

Effects of Micro- and Macro-Scale Interfaces on Seismic Wave Propagation in Rock and Soil

L. J. Pyrak-Nolte (765-494-3027; Fax: 765-494-0706; ljpn@physics.purdue.edu)

Objectives: The objective of this proposal is to determine the effects of multi-scale heterogeneity on seismic wave propagation through soils and rocks. Specifically, we will address (1) heterogeneity within a fracture; (2) heterogeneity from multiple fractures and fracture networks; and (3) discontinuities in unconsolidated and poorly consolidated media.

Project Description: Soils and rocks are open, multiphase, biogeochemical systems that play an important role in the production of oil and gas, the maintenance of environmental quality, and the geotechnical stability of a site. They consist of solid, liquid, and gaseous phases that produce heterogeneity on multiple length scales that may vary temporally because of participation in the hydrogeologic and tectonic cycles. Because the physical heterogeneities can change in time, active monitoring techniques need to be developed for quantifying the changes in soils and rocks. Some sources of heterogeneity in soils and rocks arise from the physical structure of these media, such as pore and grain distributions, grain contacts, cracks, fractures, stratification, and laminae, as well as heterogeneity from the distribution of fluids within the structural components of these media. Meeting the proposed research objectives depends on the determination of the effect of micro-scale phenomena on macro-scale measurements by a combination of laboratory experiments and numerical analyses

Results: Acoustic mapping and wavefront imaging data were collected for samples containing a single fracture and multiple parallel fractures to predict fracture specific stiffness. For a fracture with a uniform distribution of specific stiffness, the same value of fracture specific stiffness should fit the data at all frequencies. Normal fracture specific stiffnesses that were extracted from the acoustic mapping data for all of the samples found to be frequency dependent and an increase in fracture specific stiffness was predicted for increasing frequency. From the analysis of the acoustic mapping data and wavefront imaging data, it is noted that the prediction of fracture specific stiffness for single fractures and multiple parallel fractures is complicated by kinematic mechanisms (as opposed to dynamical effects), which can produce an "apparent" frequency-dependent fracture specific stiffness. For a single fracture, an inhomogeneous distribution of asperities within the fracture can result in a variation in fracture stiffness amongst different subregions of a fracture plane, which can produce an "apparent" frequency-dependent fracture stiffness. For multiple parallel fractures, an "apparent" frequency-dependent fracture specific stiffness will be predicted if the fractures are assumed to have the same fracture stiffness but in reality have fracture specific stiffnesses that differ for each fracture within the set. The measured acoustic wavefront indicated that stiffness of the fractures was not uniform. For a single fracture, the apparent frequency-dependent stiffness has the potential to provide information on the fracture void geometry. However, for a set of multiple parallel fractures, it is not clear that there is a unique solution for predicting the stiffness of each individual fracture. If a method can be devised to distinguish the difference between the different geometrical and dynamical mechanisms that produce frequency-dependent fracture specific stiffness, interpretation of seismic data from fractured rock masses can be improved.

GRANTEE: Rensselaer Polytechnic Institute

Department of Earth and Environmental Sciences
Troy, New York 12180-3590

GRANT: FG02-94ER14432

Transport Phenomena in Fluid-Bearing Rocks

E. B. Watson (518-276-8838; Fax: 518 276 6680; watsoe@rpi.edu)

Objectives: The goal of this project is to provide insight into the phenomena leading to geochemical transport in the Earth's crust and upper mantle in the presence of C-O-H fluids. There are two principal thrusts: 1) characterization of grain-scale permeabilities of fluid-bearing rocks whose microstructures result from protracted mineral-fluid interaction at conditions where the minerals are soluble and grain coarsening is effective; and 2) development and implementation of techniques for measuring diffusion coefficients of aqueous solutes (and mineral solubilities) at deep-crustal conditions.

Project Description: This is a multifaceted program of experimental research on the behavior and properties of aqueous fluids and the rocks that contain them at depths exceeding ~20 kilometers in the Earth. The objectives described in the preceding paragraph are pursued using solid-media, high pressure-temperature techniques developed during the initial grant period (1994-1997). The two main thrusts of the proposed work — solute diffusion and rock permeability — are viewed as complementary aspects of the problem of fluid-assisted mass transport that are important for different reasons: diffusion determines the efficacy of mass transport through a stationary fluid, and permeability controls the velocity of fluid flow in response to a given pressure gradient (mineral solubility is important in both cases because of its contribution to the total flux of dissolved material).

A conventional piston-cylinder apparatus is used to achieve the P-T conditions of interest (0.5-2.0 GPa; 500-1000°C). In the permeability studies, metal-jacketed synthetic rocks are prepared by high P-T treatment leading to near-equilibrium microstructures in the presence of aqueous fluid. After quenching and depressurization, the samples are mounted for permeability characterization at room conditions using conventional gas-flow techniques. For the diffusion and solubility measurements, specially designed diffusion cells are heated and pressurized at mid- to deep-crustal conditions. These cells are machined from solid silver and consist of two chambers (~0.05-0.1 cm³) connected by a platinum capillary through which diffusion occurs at the experimental conditions. Diffusive transport—driven by a small difference in temperature between the two chambers—is quantified after each experiment by measuring the time-integrated mass of material transported.

Results: During the past year, efforts related to permeability focused on understanding two phenomena: 1) development of fluid-filled channels in synthetic rocks subjected to a modest temperature gradient; and 2) localization of fluid in fine-grained portions of rocks under equilibrium conditions. The "channelization" phenomenon, first produced inadvertently in the course of "routine" porous-rock synthesis, occurs when a modest temperature gradient (1-10°/mm) is imposed along the sample axis. The channels are oriented parallel to this gradient, with size depending on sample mineralogy: they may span a few grain edges (~100-200 microns) or traverse a significant fraction of the sample (*i.e.*, millimeters). A combination of finite-element modeling and graphical analysis was used to show that: a) the straightening and elongation of normal pores to form channels is a natural consequence of grain-scale diffusive fluxes and dissolution/precipitation processes; and b) it is not the temperature gradient

per se but a solute concentration gradient that drives channel development. In fact, a temperature gradient is not required to produce channels—they can arise in any situation in which the fluid composition varies spatially in a nonlinear fashion (*e.g.*, due to local buffering by mineral reactions). Significantly enhanced permeability can be expected in the direction parallel to the channels.

About a dozen high P-T experiments were completed which clearly demonstrated that fluid-bearing rocks consisting of discrete fine- and coarse-regions show significant enrichment of fluid (or melt) in the fine-grained portions. This fluid localization results from the tendency of the system to equalize pore wall curvature and dihedral angle over the volume of rock through which the fluid is interconnected. Localization of fluid within fine-grained regions can impart a permeability that is higher (due to higher porosity) than that of adjacent coarse-grained areas.

Advances were also made during the past year in the characterization of diffusion in fluids at elevated P-T conditions. In our 2-chambered diffusion cell, the reaction calcite + quartz = wollastonite + CO₂ was used to extract interdiffusion coefficients for CO₂ and H₂O at 1 GPa and 550°-650°C; the values fall in the range 2×10^{-8} - 1×10^{-7} m²/s. These diffusivities are similar to values for aqueous SiO₂ diffusion determined earlier in this study; significantly, they approach to within an order of magnitude the diffusivity of heat in rocks.

GRANTEE: Rice University

Chemical Engineering Department
Houston, TX 77251-1892

GRANT: DE-FG03-95ER14552

Transition Metal Catalysis in the Generation of Petroleum and Natural Gas

F. D. Mango (281-497-0384; Fax: 713-285-5478; ceng@pop.rice.edu or fmango@compuserve.com)

Objectives: This project started on the hypothesis that the light hydrocarbons in petroleum are formed catalytically from the transition metals in carbonaceous sedimentary rocks. The conventional view that oil and gas are the products of thermal cracking was viewed inadequate given the stability of hydrocarbons and the fact that laboratory attempts to duplicate the process had been unsuccessful. The transition metals are ubiquitous in organic sediments and could, in theory, become catalytically active during diagenesis, promoting the formation of lighter hydrocarbons and natural gas. This project's objective was to test this idea and to explore generally the catalytic properties of transition metals under realistic geologic conditions.

Project Description: Various natural sources of transition metals including the asphaltene fraction of petroleum, source rocks, and minerals (takovite and chlorite) are being analyzed for catalytic activity. Pure transition metal complexes (metal porphyrins, acetylacetonates, oxides and sulfides) are also under study. Reactions are being conducted in gas manifold systems under steady-state and batch reactor conditions and products analyzed by high-resolution gas chromatography.

Results: Crude oil is believed to be unstable in the Earth, thermally cracking to natural gas at temperatures > 150°C. Although the process (crude oil → gas) is well documented geologically, it has never received convincing support in the laboratory. Petroleum hydrocarbons are surprisingly stable and their cracking products do not resemble natural gas.

We have found crude oil to catalytically decompose to gas under mild laboratory conditions over the transition metals in carbonaceous sediments (Mango *et al.*, *Nature*, **368**, 535, 1994; Mango, *Org. Geochem.* **24**, 977, 1996; Mango & Hightower, *Geochim. Cosmochim. Acta.* **61**, 5347, 1997). Like natural gas in deep basins, it becomes progressively enriched in methane: initially 80% (wet gas) to a final composition of 100% methane (dry gas). Catalytic gas exhibits the carbon isotopic signature of natural gas (Mango & Elrod, *Geochim. Cosmochim. Acta.* in press) and is thus indistinguishable from natural gas.

The light hydrocarbons (LHs) are probably intermediates in the catalytic decomposition of oil to gas:



Two lines of evidence support this. First, it was duplicated experimentally under moderate conditions. Second, natural LHs exhibit the characteristics of catalytic products, in particular a proportionality between isomers:

$$(xy_i)/(x_iy) = \alpha$$

(where x and x_i are isomers; y and y_i are isomers that are structurally similar to x and x_i; and α is a constant). It holds for all oils over LH concentrations ranging from .001 to 10 % (total oil) with a

coefficient of correlation $r^2 = 0.99$ (see Figure below). Isomer ratios change systematically with concentrations, some approaching thermodynamic equilibrium, others not.

The correlations reported here are the strongest yet disclosed for the LHs. Isomers are related in triads (*e.g.*, n-hexane \leftrightarrow 2-methylpentane \leftrightarrow 3-methylpentane), consistent with cyclopropane precursors. The LHs obtained experimentally are indistinguishable from natural LHs in $(xy)_i/(x,y)$. These relationships are not explained by physical fractionations, equilibrium control, or non-catalytic modes of origin. A catalytic origin, on the other hand, has precedence, economy and experimental support.

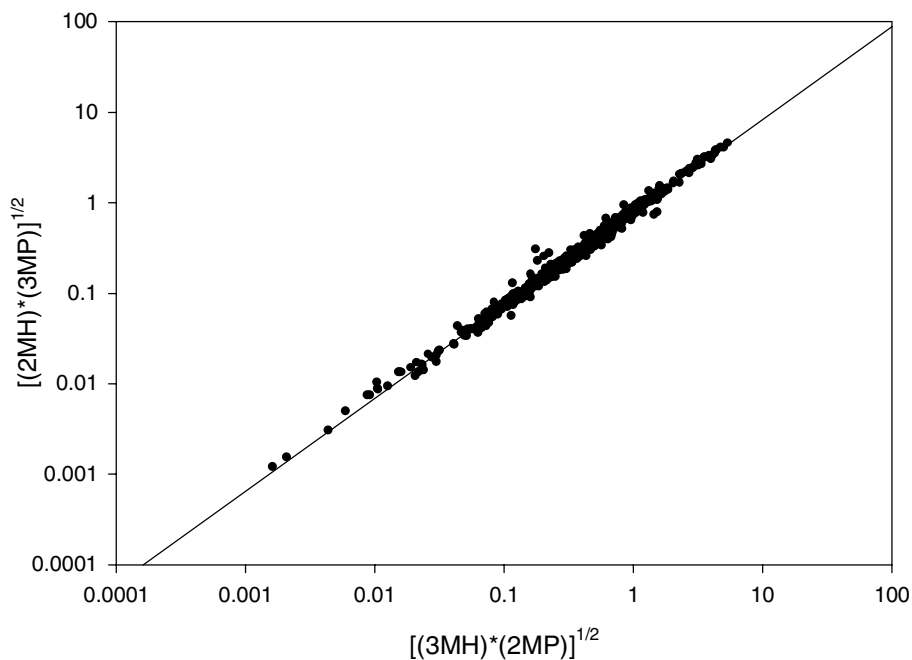


Figure. 900 crude oils. Concentrations in % wt total oil: 2-MP = 2-methylpentane, 3-MP = 3-methylpentane, 2-MH = 2-methylhexane, 3-MH = 3-methylhexane.

GRANTEE: Scripps Institution Of Oceanography

IGPP - University of California at San Diego
9500 Gilman Drive - Dept. 0225
La Jolla, California 92093-0225

GRANT: DE-FG03-97ER14757

Joint Inversion of Acoustic and Induction Log Data for Enhanced Resistivity Structure

C. de Groot-Hedlin (858-534-2313; Fax: 858-534-5332; cdh@eos.ucsd.edu) and S. Constable

Objectives: To combine several types of borehole logging data in order to enhance the resolution of geological structures. A connection between acoustic and electrical properties of the rock formations is sought which will allow for a joint inversion of different data types.

Project Description: We are developing inversion methods that combine several types of logging data to determine high-resolution images of the subsurface, for models in which the physical parameters vary both as a function of depth and distance from the borehole. The determination of a detailed model fitting the data is a large, nonlinear inverse problem, which can be solved most efficiently with approximate inverse methods. We will test several approximate inverse methods to explore the efficiency *versus* accuracy trade-off for each method.

We will also develop methods of combining sonic and electrical logging data to provide significantly improved resolution compared to that obtained from a single logging method. Effective medium methods will be developed to relate acoustic properties to electrical properties of the subsurface.

Results: We have made continuing progress on our algorithm to invert borehole induction data, described in the results for FY98. Jacobean sensitivities are computed using a skin-depth correction to the Doll's approximation.

Results on inversions of both real and synthetic induction logging data indicates that the algorithm provides smooth models that fit the data, and reconstruct the broad features of the original model. Radial boundaries are more poorly resolved than horizontal boundaries by traditional, focussed induction logs. Greater radial resolution may be afforded by the use of array induction tools, by jointly inverting several types of well logging data, or by incorporating a priori information on the conductivity model.

GRANTEE: Stanford University

Department of Geological and Environmental Sciences
Stanford, California 94305-2115

GRANT: DE-FG03-93ER14347-A007

Metal Ion Sorption at Oxide Surfaces and Oxide-Water Interfaces: Spectroscopic Studies and Modeling

G. E. Brown, Jr. (650-723-9168; Fax: 650-725-2199; gordon@pangea.stanford.edu) and G. A. Parks

Objectives: This project concerns chemical interactions between metal ions in aqueous solution and oxide surfaces representative of those found in the Earth's crust. These “sorption” reactions partition the metal between fluid and solid phases and must be understood at a molecular level to develop both quantitative understanding of the geochemistry of mineral surfaces and the macroscopic models required to predict the fate of contaminants in Earth surface environments. Our objectives are (1) to characterize sorption reactions by determining composition, molecular-scale structure, and bonding of the surface complexes produced using direct sorption measurements, synchrotron-based x-ray absorption fine structure (XAFS) spectroscopy and x-ray standing wave fluorescence spectroscopy, x-ray photoelectron spectroscopy (XPS), and UV/Vis/IR spectroscopy; (2) to investigate how these properties are affected by the solid surface, the composition of the aqueous solution, the presence of simple organic ligands containing functional groups common in more complex humic and fulvic substances, the presence of microbial biofilms, and time; and (3) to develop molecular-level and macroscopic models of sorption processes. In FY 99 we made good progress in each of these areas and continued our grazing-incidence XAFS and X-ray standing wave (XSW) studies of the interaction of heavy metals with mineral surfaces and with biofilm-coated alumina and goethite surfaces. In addition, we have used the results of our model system studies to help determine the speciation of heavy metals and metalloids in contaminated natural systems.

Project Description and Results: (1) *Long-period XSW Study of Pb(II) and Se(VI) at the mineral-solution interface:* The long-period XSW technique has recently been shown to be capable of studying diffuse metal ion distributions at charged metal-solution interfaces. We have applied the technique to investigate the partitioning of aqueous Pb(II) and Se(VI) at the oxide-solution interface as a function of solution conditions for several oxide surfaces including α -Al₂O₃(0001), α -Al₂O₃(1-102), and amorphous silica surfaces.

At low Pb(II) concentrations we observe a relatively sharp XSW fluorescence profile that broadens toward the low angle side with increasing Pb(II) concentration. This sequence suggests that the ratio of surface-bound to solution Pb(II) is decreasing with increasing Pb(II) concentration, likely due to saturation of available adsorption sites. The inclusion of selenate in the system allows us to study the distribution of an anionic solution species simultaneously with the cationic species (dominantly SeO₄²⁻ and Pb²⁺ under the solution conditions considered). We observe that increasing the selenate concentration leads to a broadening of the Pb(II) fluorescence yield signal. Our initial interpretation is that the broadening of the Pb(II) signal results from an increase of diffuse layer Pb(II) due the accumulation of negative charge at the interface associated with selenate adsorption.

(2) *Pb(II) sorption on biofilms on high-surface-area-minerals*: The modes of Pb sorption onto high surface area metal oxides such as α -Al₂O₃ and α -FeOOH, in the presence and absence of complexing ligands, have previously been characterized by our group. Using this base of information, we are now studying the mode of Pb(II) sorption on these same minerals in association with biofilms. In particular, we have used EXAFS spectroscopy to (a) determine the fraction of metal bound to the biofilm vs. the mineral surface component, (b) determine whether or not the fraction of metal associated with the mineral surface forms the same type of complexes as found in the biofilm-free studies, and (c) determine whether or not the mineral substrate has any effect on the mode of Pb(II) binding to the biofilms. We have prepared several high surface area metal oxides coated with *Burkholderia cepacia* and have reacted them with Pb(II) at various concentration levels. Pb(II) was found to bind most strongly to the goethite surface even in the presence of the biofilm, whereas, it partitions more evenly between the alumina surface and the biofilm in the Pb(II)/alumina/*B. cepacia* system.

(3) *Grazing-Incidence XAFS and XSW Studies of Pb(II) and Se(IV) Interacting with Biofilm-Coated Single Crystal Surfaces*: Coupled XSW and GI-XAFS measurements of heavy metals sorbed to biofilms formed on single-crystal surfaces can be used to obtain complementary information on the location and speciation of sorbed species. We have measured the partitioning of Pb(II) and Se(VI) between the mineral surface and a monolayer (~1 μ M) of biofilm comprised of *B. cepacia* embedded in a hydrated exopolysaccharide matrix. These measurements can be used to compare quantitatively the partitioning of the metal or metalloid between the biofilm and the mineral surfaces, which vary in their surface structure and reactivity. For Pb(II), we find that the mineral surface sites preferentially bind Pb(II) relative to the biofilm at the lowest metal concentrations tested but are eventually out-competed by the biofilms at higher metal concentrations as the most reactive sites on the crystal surface are saturated. When we add Pb(II) and Se(VI) simultaneously, with a tenfold excess of Se(VI) relative to Pb(II), we find that Pb(II) is preferentially bound to the biofilm (as expected at pH 4.5) and the Pb(II) profiles are not affected by Se(VI). However, Se(VI) uptake is enhanced by the presence of Pb(II), especially at low Se(VI) concentrations.

(4) *EXAFS Determination of the Chemical Speciation and Sorption Processes of Pb, Hg, Cr, Sr, As, and Se in Natural and Model Systems*: We have used XAFS spectroscopy to study the molecular-scale speciation of selected heavy metals and metalloids in contaminated mine wastes, natural sediments and soils from various localities. For example, in Pb-contaminated mine wastes from Leadville, CO, we found that surface-bound Pb(II) is the dominant form of Pb in a carbonate-buffered tailings pile, whereas Pb is present in relatively insoluble sulfates, carbonates, and phosphates in more acidic tailings piles. Our DOE-funded XAFS work on Pb sorption on mineral surfaces in model systems proved to be invaluable in obtaining these results on complex environmental samples. In FY 1999 we conducted additional model system studies including the effects of sulfate and carbonate ligands on Pb(II) sorption on goethite and As(III,V) sorption on manganese oxides, and Se(IV) sorption on manganese oxides.

GRANTEE: Stanford University

Geophysics Department
Stanford, California 94305-2215

GRANT: DE-FG03-99ER14933-A001

Seismic Signatures of Fluids in Anisotropic Rocks

G. M. Mavko (650-723-9438; Fax: 650-723-1188; gary@pangea.stanford.edu) and Francis Muir

Objectives: Conduct theoretical investigations into the effects of fluids and fractures on anisotropic elastic constants, and consequent constraints on lithology that may be obtained from seismic parameters.

Project Description: Seismic anisotropy, now widely recognized as a common feature of most subsurface formations, may lead to significant distortions in conventional seismic processing, such as errors in velocity analysis, mispositioning of reflectors, and misinterpretation of the amplitude variation with offset (AVO) response. Furthermore, geophysical characterization of fractured reservoirs via their elastic anisotropy is an extremely important economical problem, in particular for the continental United States. In tight formations, which can include sandstones, shales, carbonates, and coal, often the only practical means to extract fluids is by exploiting the increased drainage provided by fractures. The practical difficulties that must be overcome before effectively using these fractures include: locating the fracture zones, determining the position, orientation, spatial density, and connectivity of fractures, and characterizing the spatial relationships of fractures to other reservoir heterogeneities which might enhance or inhibit the fluid flow. In this project we are developing theoretical models to describe anisotropy in fractured media. Fluids play an important role in the anisotropy. The presence of fluids is a key interpretation problem for the oil and gas industry, in amplitude-*versus*-offset analysis and in fluid substitution modeling using Gassmann's equations.

Results: During this period we explored two research areas:

Fluid Substitution: Rocks are usually at least slightly anisotropic. The anisotropy comes from alignment of grains and pores, nonhydrostatic effective stress, and aligned macrofractures. Yet, we often apply isotropic methods when analyzing seismic data, because of incomplete information about the complete elastic tensor. What is the error in fluid substitution calculations caused by ignoring anisotropy, and how valuable is the information in the full elastic tensor for estimating pore fluid signatures?

We considered a set of laboratory data from rocks that have transverse isotropic symmetry. We applied two different techniques in the fluid substitution problem; one is Gassmann's fluid substitution, which requires only one P and S velocity data as input, implying that we will ignore the anisotropy. The other approach is Brown and Korringa (B&K) fluid substitution, which is the anisotropic version of Gassmann's technique, using the complete elastic compliance tensor of the TIV material to predict the changes in the elastic tensor. In this way, by comparing both results we can evaluate the assumption of isotropy in the problem of fluid substitution for anisotropic rocks.

For these data, Gassmann fluid substitution predicts an increment of P-wave velocity of 10-15 % for brine saturation at low effective pressures, using the horizontal wave (fast direction) as input. For oil, the increment is ~5%. As the effective pressure increases the increment caused by the fluid substitution decreases to 5% for brine and 1% for oil; that is, the rock becomes stiffer and less sensitive to the

presence of different fluids because of crack closing and soft-porosity reduction. It is interesting that the change in velocity due to fluid substitution is significantly higher when using the vertical P-wave velocity (slow direction) as input, the change at the lower pressure being up to 40 % for brine saturation and 20 % for oil. This means that (as expected) the rock is more sensitive to fluid changes when using in seismic data in the vertical direction, or equivalently, along the normals to the cracks and bedding planes. This result already states the importance of considering anisotropy in the problem of fluid substitution, since a different change on the elastic response of the material will be predicted depending on the orientation of the data available.

The B&K fluid substitution results show the same principal characteristics: higher velocity increment (greater fluid sensitivity) at lower effective pressures, and bigger change when propagating along the vertical propagation. In fact for brine and oil substitution, the difference between saturated and dry velocities is higher for lower pressures and becomes pressure-independent for higher values. More important is the fact that B&K approach always predicts larger velocity changes than Gassmann, for both oil and brine as saturating fluids. The discrepancy between the two predictions is slightly larger for higher effective pressures. Assuming the B&K results to represent the correct response, we can conclude then that applying Gassmann in an anisotropic medium may become a poor approximation as effective pressures increases, although the fluid effect itself decreases with increasing pressure. However, the difference in the velocity change predicted when going from a dry state to brine or oil saturation is not very high for these samples, being as much as 100m/s in the worst case.

Dynamic Equivalent Medium Theory for Layered Media: Previous work in this field has uniformly presupposed that the dynamics of wave propagation in a heterogeneously layered solid medium could be modeled as a homogeneous solid whose stiffness (or compliance) elements were made frequency-dependent to account for the loss of coherent energy due to scattering. A corollary to this point of view is that mass density has always been viewed as a scalar. In this project, we begin by showing that the conventional, Rock-physical way of looking at Backus' Result in terms of Layer Thickness, Compliance, and Mass Density has an exact counterpart in an Experimental Acoustics parameterization involving Travel-time, Impedance (or Admittance), and Slowness. This leads to a demonstration that both Impedance and Slowness will usually be frequency-dependent in ways that force Mass Density also to be frequency-dependent and anisotropic. In turn, this suggests that acoustic measurements of layered rocks should involve both slowness and impedance.

The essence of Backus theory (Backus, 1962) is that it allows a stack of layers to be replaced by a single layer. The new homogeneous equivalent medium has elastic properties (Compliance, Mass Density) identical in the long-wavelength limit to the heterogeneous rock under study, and under certain restrictions (uniform heterogeneity) will have the right travel-time. However, it is a kinematic theory; it is silent on the effect that scattering has on wavelet shape as it propagates through the medium.

An important consequence is that, under certain symmetry conditions, both compliance and mass density must have the same frequency-dependence as that of the slowness, which is known by simple argument to be non-zero, because scattering implies dispersion, implies frequency-dependence. By an extension of this argument, it can be shown that P and S waves will usually have different slowness frequency-dependence, in which case the Mass Density function must be both frequency-dependent and anisotropic.

GRANTEE: Stanford University

Department of Geophysics
Stanford, CA 94305-2115

GRANT: DE-FG03-86ER13601

Porous Rocks with Fluids: Seismic and Transport Properties

A. Nur (650-723-9526; Fax: 650-723-1188; nur@pangea.stanford.edu), M. Helgerud, Y. Keehm, W. Bosl, and T. Mukerji

Objectives: In this study we develop a model to simulate flow-limited diagenetic processes in porous media. In addition, we are measuring and modeling the elastic properties of gas hydrate and sediment that contains gas hydrates.

Project Description: 1. *Flow-Limited Diagenesis and Transport Properties of Porous Media Using the Lattice Boltzmann Method.* We use a model that combines a Lattice-Boltzmann flow simulation with pore filling mechanisms. After investigating the transport properties for each mechanism, we group the mechanisms into related classes and evaluate the results relative to commonly used empirical porosity-permeability relationships.

2. *Measuring and Modeling the Elastic Properties of Gas Hydrate and Sediment Containing Gas Hydrates.* Natural gas hydrates are nonstoichiometric crystalline solids comprised of a hydrogen-bonded water lattice and entrapped “guest” molecules, predominantly methane. Gas hydrate with methane as the guest species is stable at the pressure and temperature conditions present in the sediments beneath most of the world’s continental margins and deep inland seas and also in arctic sediments below the permafrost layer. Enormous amounts of methane are believed to be trapped in nature by hydrates; both in the hydrate crystal structure itself and in sediments beneath hydrate deposits. This large reservoir of natural gas may be a future energy resource and may play a significant role in global climate change. The formation and melting of gas hydrate also has a strong effect on sub-sea slope stability. Unfortunately, all distribution and hydrate-related methane estimates are very inexact because accurate estimates of the amount of methane hydrate *in situ* are not currently available on a regional or site specific basis. A remote sensing technique that can accurately assess the amount and distribution of hydrate in natural deposits is needed to improve these distribution and hydrate-related methane estimates.

The best technique for remotely probing sediments several hundred meters below the surface or beneath deep bodies of water is seismic reflection profiling. Interpreting seismic data to deduce the amount of gas hydrate in place requires a relation between the hydrate fraction in the sediments and the elastic properties of the hydrate-sediment composite.

Results:

1. *Flow-Limited Diagenesis and Transport Properties of Porous Media Using the Lattice Boltzmann Method.* Eight different pore-filling mechanisms related to the fluid flow were calculated during the evolution of pore geometry. After investigating the transport properties in each mechanism, we identified four distinct groups: 1. Grain boundary related; 2. Low-flux related; 3. High-flux related; and 4. Random filling mechanisms. The boundary related mechanism showed very good correlation with empirical relations (Kozeny-Carmen relation and Archie’s law). Because the empirical relations

represent averaged relations of real data and theoretical models, the grain boundary can be regarded as a major factor in the diagenetic process of sedimentary rocks. Low-flux related mechanisms showed very small change in permeability even in latter stages of diagenetic processes. For this case, electric conductivity decreases faster than permeability. High-flux related mechanisms are the most efficient in reducing permeability. Since the pore filling starts in efficient flow paths, the flow simulation in this case is very slow to converge. One of the innovations was to change the iterative Lattice-Boltzmann algorithm of the flow simulation to a sparse matrix form. The matrix method showed better convergence in high flux related diagenetic mechanisms. Random filling showed an intermediate behavior between high-flux related and boundary related mechanisms. At early pore filling stages, the permeability decreases very rapidly, followed by a trend very similar to the boundary-related mechanism. This modeling enables us to efficiently explore the complicated relationship between fluid flow and evolving porosity for ranges of realistically complex pore geometry.

2. Measuring and Modeling the Elastic Properties of Gas Hydrate and Sediment Containing Gas Hydrates. To address the lack of data on the properties of gas hydrates, we first made propane hydrate in the laboratory by bubbling gas through water and water saturated sand in a clear walled pressure vessel. Propane was chosen as the hydrating gas because the pressure conditions were less stringent, making a glass pressure vessel practical. These experiments were all videotaped. They were a great success at demonstrating why there are so few elastic property measurements published in the literature. The reason is that it is relatively easy to make gas hydrate in the laboratory, but it is nearly impossible to create well-characterized, pure samples by bubbling gas through water, the traditional way of making samples. It is very difficult to drive the reaction to completion; so unreacted water and/or gas generally remain in the pressure vessel. With a research group at the SUGS in Menlo Park, we obtained very successful measurements of the compressional and shear wave speeds of pure, compacted, polycrystalline methane hydrate.

Next, we modeled the effect that gas hydrate formation would have on wave speeds through sediments, using theoretical effective-medium modeling. Based on existing models, we know that the effective elastic moduli of sediments strongly depend on the location of pore filling material within the pore space (*i.e.*, grain contact cement or suspended in the pore fluid). We apply three types of models: one in which the hydrate is suspended in the pore fluid, one in which the hydrate becomes a load-bearing component of the sediment framework and one in which the hydrate forms as a grain contact cement. The cementation model is appropriate only for high porosity sands, but the other two models are appropriate for both sands and ocean-bottom sediments. The models are tested against real world data from ODP hole 995 (methane hydrate in clay rich, high porosity ocean bottom sediments) and Northwest Eileen State Well #2 (methane hydrate in onshore, arctic sands beneath permafrost). In both cases, the data strongly suggest that gas hydrate forms as a load-bearing component of the sediment framework.

GRANTEE: Stanford University

Department of Geophysics
Stanford, CA 94305-2115

GRANT: DE-FG03-98ER14904

Rock Physics for Seismic and SAR Characterization and Monitoring of Reservoir Fluids and Their Recovery

A. Nur (650-723-9526; Fax: 650-723-1188; nur@pangea.stanford.edu), H. Xu, J. Dvorkin, and I. Takahashi

Objectives: The future of geophysics includes the potential to track reservoir fluid distribution during the life of a field through the use of periodic geophysical snapshots or time lapse geophysical monitoring. To this end our research focuses on the advanced use of rock physics for interpreting remote measurements for accurate detection and monitoring of subsurface fluids using 2 methods: (a) seismic, both surface and borehole; and (b) differential interferometric synthetic aperture satellite radar (DInSAR) measurements.

Project Description: We are conducting analyses of experimental data to determine the variation in seismic properties as a function of pressure and water saturation. We are also exploring quantitative methods to estimate rock properties from one or more seismic observables. Finally, we are exploring the use of extracting reservoir rock properties from subsidence measurements made using synthetic aperture radar.

Results: *Seismic research: Pore pressure and fluid detection from compressional and shear-wave data.* By analyzing experimental data we show that in many rock-dry rocks, the Poisson's ratio (PR) decreases with differential pressure (confining minus pore pressure). In many liquid-saturated rocks the opposite is true: PR increases with decreasing differential pressure. This means that in gas-saturated rocks, PR decreases with increasing pore pressure and in liquid-saturated rocks it increases with increasing effective pressure. We confirm the generality of the observed effect by theoretically reproducing it via effective medium modeling. This effect can be used as a new tool for seismic pore pressure and pore fluid monitoring during production as well as for overpressure detection from surface seismic, cross-well, sonic logs and measurements ahead of the drill bit.

Quantifying information and uncertainty of rock property estimation from seismic data. We consider quantitative methods to estimate rock properties from one or more seismic observables. We first explore well and laboratory data, as well as rock physics model parameters, and clarify the effects of rock properties on various combinations of seismic attributes. We then introduce statistical formulations of information theory and Bayes decision theory to quantitatively describe the information about rock properties carried by seismic attributes, as well as the estimation uncertainty about the rock properties. We also present a method of combining stochastic simulation and Bayes inversion for quantifying information about rock properties provided by seismic reflectivity. Finally, we explore multi component seismic data and compare how P-S converted wave data can reduce uncertainty about rock properties.

SAR research: Land subsidence over Belridge and Lost Hills oil fields, Southern California, observed by differential SAR interferometry. Land subsidence over the Belridge and Lost Hills oil fields, Southern California in 1995 and 1996, was measured using space borne interferometric synthetic aperture radar (InSAR). The detailed deformation maps clearly show that there are strong correlations

between oil production and surface subsidence. However, the relation between the absolute values of oil production and surface subsidence is not linear, which indicates that besides absolute production volume, reservoir properties such as rock compressibility, permeability, fluid viscosity, are also essential factors in forming the final pattern of surface subsidence. Therefore, it may be possible to infer those reservoir properties when precise surface subsidence measurements are easily available from InSAR techniques.

GRANTEE: Stanford University

Department of Petroleum Engineering
Green Earth Sciences Building
367 Panama Street, Rm. 65
Stanford, CA 94305-2220

GRANT: DE-FG03-99ER14983

Diffusion of CO₂ during Hydrate Formation and Dissolution

F. M. Orr, Jr. (650-723-2750; Fax: 650-725-6566;fmorr@pangea.stanford.edu)

Objectives: The overall goals of this research are to understand and predict rates of CO₂ hydrate formation and dissolution. The specific objectives are as follows: 1) determine the mechanisms of hydrate film growth, 2) measure the rate of hydrate growth, 3) calculate solute diffusivity through the hydrate, and 4) measure hydrate dissolution rates.

Project Description: Disposal of liquid CO₂ in the oceans has been studied as a means of reducing global greenhouse gas emissions to the atmosphere. Understanding and quantifying the transport processes affecting liquid CO₂ dissolution into the seawater will be a primary factor in determining the overall transport from the ocean to the atmosphere.

Formation of a hydrate film complicates the CO₂-seawater dissolution process. Hydrate may grow on the outside of CO₂ droplets, form thin layers on liquid pools, or form a precipitate. In this project, laboratory experiments are being carried out to measure the rate of hydrate film growth as a function of water and CO₂ concentrations in the CO₂ and water phases. These measurements will allow for determination of the hydrate growth mechanism, as well as calculation of solute diffusivity through the hydrate film.

Results: This project was only recently initiated.

GRANTEE: Stanford University

Department of Geological and Environmental Sciences
Stanford, CA 94305-2115

GRANT: DE-FG03-94ER14462

Development of Fracture Networks and Clusters: Their Role in Channelized Flow in Reservoirs and Aquifers

D. D. Pollard (650-723-4679; Fax: 650-725-0979; dpollard@pangea.stanford.edu) and A. Aydin (650-725-8708; Fax: 650-725-0979; aydin@pangea.stanford.edu)

Objectives: Prediction of the spatial distribution of permeability in subsurface aquifers and reservoirs as determined by structural heterogeneities is a challenging problem for water resources and waste management in hydrogeology, and for both exploration and production in the oil and gas industry. To address this problem we are carrying out an integrated plan to map structural heterogeneities (deformation bands, joints, sheared joints, and faults) in an analogue reservoir and developing conceptual models for the evolution of these structures. We are studying the signature of the ancient chemically reactive flow systems within the Aztec Sandstone. The spatial distribution of chemical alteration formed from these reactive fluids reflects their flow pathways, and enables us to infer the *in situ* permeabilities of the structures with which the fluids interacted. This fluid flow also results in diagenetic alteration of the Aztec sandstone. The hypothesis is that the altered sandstone horizons have different fracture/fault populations. If true, an understanding of the fracture distribution in terms of the alteration pattern would be a useful knowledge base for subsurface fracture/fault prediction.

Project Description: We are following a methodology based on detailed field mapping of fractures and faults in the Aztec Sandstone in the Valley Fire State Park, Nevada, and numerical analyses for permeability upscaling and fluid flow modeling using the field data.

Results: (1) *Distinguishing Deformation Style with Petrophysical Characterization:* It has been shown that the fundamental structural elements in sandstone bear differing influence on fluid migration. Knowledge of the presence and relative abundance of a structural element in a given sandstone body is therefore important for accurate consideration of bulk fluid flow properties. In the Valley of Fire, Nevada, we have identified two domains within the Aztec sandstone that have considerably different abundances of structural elements. The Lower domain (red sandstone) has a dominant abundance of opening mode joints; the Upper domain (buff sandstone) has a dominant abundance of deformation bands. These two domains are further distinguished with respect to their petrophysical properties. The Lower domain has lower porosity and higher bulk density and elastic moduli. Likewise, it has been found that P- and S-wave velocities are greater [by as much as 500 m/s] for the Lower domain. These observations will aid in the remote characterization of deformed sandstone bodies at depth.

(2) *Fluid Flow in Fractured Sandstone:* We have two major results to report in this category:

(2.1) *Geometry and Effective Permeability of Deformation Band Sets:* Field investigations in the Aztec sandstone at the Valley of Fire State Park, southern Nevada revealed five characteristic patterns for sets of deformation bands: parallel, anastomosing parallel, conjugate, sigmoidal, and boxwork. The patterns are shown to be continuous on length scales ranging from 1 m to 100 m. Deformation bands within the patterns vary in thickness from 1 mm to 1.5 cm, and the spacing between bands varies from about 1 mm to 2 m. Within the five patterns, there exist only three orientations of deformation bands. Conceptual

models for the formations of these patterns suggest that all three sets of bands and all the patterns were formed due to compression generated by northeast vergent thrusting during the Sevier Orogeny.

Analytical methods and fine-scale finite-difference and finite-element modeling based on homogenization theory were used to calculate upscaled effective permeability tensors for the matrix rock plus the deformation bands. This method is capable of discretely representing the deformation bands. Effective permeability tensors were calculated for each of the deformation band patterns while varying the band permeability/matrix permeability ratio and while varying the thickness and spacing of the deformation bands. It was found that these patterns of deformation bands can reduce the host rock bulk permeability by 2+ orders of magnitude. Likewise, the bands can create permeability anisotropy of up to 2 orders in magnitude.

The bulk permeability reduction and anisotropy caused by the deformation band sets are of the same order of magnitude as those caused by the presence of shale lenses within sandstone. We conclude that these small-scale structural heterogeneities can have equally important effects on permeability and permeability anisotropy as large-scale structural or sedimentological heterogeneities. This result has profound implications for the design and implementation of reservoir and aquifer flow simulations.

(2.2) Upscaling Permeability of Faults developed from shearing across pre-existing joint zones: The structure of strike slip faults resulting from slip along pre-existing joint sets has been described by detailed geologic mapping used to determine their hydrodynamic properties. The resulting fault zone corresponds to a damage zone composed of joints, sheared joints, fault related deformation bands, and fault gouge. A permeability upscaling methodology using quantitative analog data from the faulted Aztec sandstone was used to quantify the permeability properties of blocks around 25 m² comprising parts of the fault zone. Permeability of each fault zone's features and open fracture apertures have been measured or estimated and considered for the upscaling of permeability properties of faults. A numerical procedure for the determination of equivalent grid block permeability tensors for heterogeneous porous media was used; and, in order to determine their upscaled permeability properties, the large blocks were discretized in smaller grid blocks.

Cross-plots of upscaled permeability calculated for each grid block, as well as the permeability tensor characterizing the whole studied block, indicate that faults formed by shearing of joint zones have a strongly anisotropic permeability structures. Fault-parallel permeability may be increased by up to 2 orders of magnitude relative to the host rock. Fault-normal permeability may be reduced by up to 3 orders of magnitude compared to the host rock. These properties are related to the width and continuity of the fault gouge zones as well as the density of deformations bands or small faults within and around the fault. They are also function of the aperture and distribution of orientations of splay fractures as well as the matrix permeability. Principal permeability directions of the upscaled block may correspond to an average direction between mean joint trend and mean fault core direction for a small amount of slip. At larger slip amounts, principal permeability directions get closer to the mean fault core, but can deviate noticeably from this direction.

We have also shown that fault zone permeability varies with slip magnitude. Although increased slip leads to higher density of shear induced joints, the fault-parallel permeability is not necessarily increased because of the dispersion in joint orientations. For the same reason, fault-normal permeability doesn't necessarily decrease when slip increases, although the number and density of low permeability features, such as gouge, sheared joints and deformation bands, increases. As a result, for a given size of block, principal permeability values may decrease as slip increases.

GRANTEE: Stanford University

Department of Geophysics
Stanford, CA 94305-2115

GRANT: DE-FG03-00ER14962.001

Coupled Fluid Deformation Effects in Earthquakes and Energy Extraction

P. Segall (650-725-7241; Fax: 650-725-7344; segall@stanford.edu)

Objectives: A fundamental understanding of the effect of magmatic intrusions on geothermal systems.

Project Description: The focus of the project is Long Valley caldera, an active hydrothermal area east of the Sierra Nevada in California. Long Valley is the site of anomalous seismic activity and ground deformation. One aspect of the project is to assess whether the hydrothermal system is playing an active role in the current activity at Long Valley. Repeated micro-gravity measurements can discriminate between magmatic intrusion on the one hand and, thermal expansion or pressurization of the hydrothermal system on the other. Before gravity changes can be interpreted, however, they must be corrected for the effects of uplift, and changes to the depth of the water table. The second aspect of the project is to investigate the poro-thermo-elastic effects of intrusion on ground uplift and subsidence in volcanic areas.

Results: Precise relative gravity measurements conducted in Long Valley in 1982 and 1998 reveal a decrease in gravity of as much as -107 ± 6 microgal ($1 \text{ gal} = 0.01 \text{ m/s}^2$) centered on the uplifting resurgent dome. A positive residual gravity change of up to 64 ± 15 microgal was found after correcting for the effects of uplift and water table fluctuations. Assuming a point source of intrusion, the density of the intruding material is 2.7 to 4.1 gm/cc at 95% confidence. The gravity results require intrusion of silicate magma, and exclude *in situ* thermal expansion or pressurization of the hydrothermal system as the cause of uplift and seismicity. To improve upon these results, in July 1999 we resurveyed 39 precise gravity stations in Long Valley, as well as 45 leveling monuments using dual-frequency GPS receivers. All sites were occupied at least twice, and data from continuous GPS sites were included in the analysis. Our estimated ellipsoidal heights have standard errors of 1.7 cm. The GPS ellipsoidal heights are converted to orthometric heights using the NGS geoid. The combined gravity change/deformation data set will be used in simultaneous inversions to estimate the magma chamber geometry and average density.

GRANTEE: Temple University

Department of Chemistry
Philadelphia, PA

GRANT: DEFG029ER14644

Surface Chemistry of Pyrite: An Interdisciplinary Approach

D. R. Strongin (215-204-7119; Fax: 215-204-1532; dstrongi@nimbus.ocis.temple.edu) and M. A.A. Schoonen (Department of Geosciences, State University of New York, Stony Brook, NY; 516-632-8007; schoonen@sbmpo4.ess.sunysb.edu)

Objectives: The primary goal of this research program is to understand the microscopic aspects of pyrite oxidation. Determining the charge development on pyrite surfaces and evaluating the interaction of the pyrite surface with an array of simple inorganic and organic molecules are the immediate goals. Through a combination of macroscopic observations and observations at the atomic/molecular level new insights are gained that will lead to a better understanding how pyrite reacts in a range of chemical environments.

Project Description: The charge development, interaction with inorganic and organic constituents, and the reactivity of pyrite are being investigated. Emphasis is placed on integrating macroscopic information from low-temperature techniques such as electrophoresis and microscopic information from modern surface science techniques that are used in the ultra high vacuum (UHV) environment. Using model, atomically clean “as-grown” surfaces of pyrite, electron spectroscopies in UHV are used to understand the atomic composition and the nature of the functional groups on pyrite after exposure to the aqueous solutions. The integration of the UHV and low-temperature studies will provide a complete picture of the type of surface functional groups at the pyrite surface, their acid-base behavior, and interaction with selected aqueous constituents.

Results: *Surface Science Studies of pyrite structure and oxidation.* Photoelectron Spectroscopy was used to investigate the surface structure and reactivity of {100} planes of pyrite that have been prepared by two commonly employed means. Specifically, synchrotron-based photoelectron spectroscopy was used to investigate the structure of two {100} pyrite surfaces. One was prepared by exposing a {100} pyrite growth surface to HCl, and one was produced by mechanical fracture. Results show that acid-washed growth surface (*i.e.*, exposed to HCl) showed a higher concentration of elemental sulfur and/or polysulfide impurities. Perhaps, surprisingly, the surfaces showed similar initial oxidation reactivity under well-controlled H₂O/O₂ gaseous environments. This result implied that the fraction of both surfaces that underwent the initial oxidation reaction were similar in structure. The oxidation activity of these surfaces were, however, were experimentally determined to be significantly less than the initial oxidation activity of an acid-washed {111} growth surface. Photoelectron and ion scattering spectroscopy suggest that a reason for this structure sensitivity may be due to differences in the concentration of Fe in the outermost layer of the different crystallographic planes of pyrite.

Studies of the pyrite-phosphate interaction. Electrophoresis and surface science experiments have been carried out to understand the interaction between phosphate and pyrite. Electrophoresis experiments show that under anoxic conditions only a relatively small fraction (no more than 10 %) of dissolved phosphate irreversibly sorbs onto the pyrite surface. Surface science studies suggest that this irreversibly bound pyrite adsorbs to non-stoichiometric sites on pyrite. Results to date indicate that

phosphate is preferentially bound to sulfur-deficient (possibly Fe^{3+}) defect sites. Research carried out in prior funding cycles suggests that these sites play a critical role in the oxidation of pyrite by dissolved O_2 . Aqueous-based oxidation experiments and experiments carried out in a combined ultra-high vacuum/high pressure apparatus suggest that this relatively small amount of adsorbed phosphate results in a significant oxidation suppression of pyrite. This result emphasizes how minority sites (non-stoichiometric sites) control the oxidation reactivity of pyrite.

GRANTEE: The University Of Tennessee

Institute for Rare Isotope Measurements
10521 Research Drive, #300
Knoxville, TN 37932

GRANT: DE-FG05-95ER14497

Development of Laser-Based Resonance Ionization Techniques for ^{81}Kr and ^{85}Kr in the Geosciences, II

N. Thonnard (865-974-9700; Fax: 423-974-8289; nthonnar@utk.edu), T.C. Labotka and L.D. McKay

Objectives: (1) Bring into operation a new analytical methodology for ^{81}Kr and ^{85}Kr , (2) identify performance limitations and implement improvements in reproducibility, accuracy, throughput and sample size, and (3) initiate research in the geosciences.

Project Description: Cosmogenic ^{81}Kr (2.3×10^5 year half-life; 20,000 to 1,000,000 year dating range) and anthropogenic ^{85}Kr (10.8 year half-life; 0.1 to 40 year dating range) are potentially useful for aiding our understanding of processes in the environment, including dating of polar ice and very old ground water, ocean circulation, and modern water flow patterns. Their chemical inertness should simplify interpretation of results. The only ^{81}Kr measurements from natural samples to date are a handful of results from old groundwater and polar ice using the laser-based analytical technique under development here, although a few measurements of ^{85}Kr from 200-liter water samples using decay counting have been demonstrated. This new technique should permit ^{85}Kr measurements using only 1- to 5-liter samples and ^{81}Kr measurements from 10- to 20-liter samples. It is a multi-step process involving: (1) degassing of the water sample; (2) separating Kr from the recovered gas; (3 & 4) two isotopic enrichments reducing interfering isotopes by $>10^8$; and (5) detecting the rare isotope in a time-of-flight mass spectrometer. The sensitivity, element specificity, and immunity to isobaric interference of resonance ionization (100 ^{85}Kr atom detection limit) are utilized to detect the few thousand analyte atoms remaining in the sample.

Results: During this fiscal year, progress was made on all five steps of the analytical procedure. A new Ph.D. student headed the degassing [step (1)] and Kr separation [step(2)] processes. After much hardware modification, testing, and process optimization, consistent recovery of more than 95% of all dissolved gases in 20-liter water samples was achieved. Tests indicated that less than 0.5% of the original gases were left in the sample. The four-step cryogenic gas separation process was optimized with hardware and procedural changes for samples ranging from 0.1 to 6 liters of air. Although Kr is only ~1 ppm in air, more than 92% of the Kr in the original water sample was recovered with less than 10% of other gases remaining in the sample, while atmospheric contamination is less than 0.1%. Therefore, it should be feasible to extend ^{85}Kr dates to 1960, in which, due to decay and lower atmospheric concentration at that time, the anticipated ^{85}Kr level in the sample would be only 1% of modern. The reproducible and high efficiency of the degassing and Kr separation process makes it feasible to determine recharge temperatures from noble gas solubilities. Utilizing Hall probe field measurement and feedback from a selected stable isotope, plus electrostatic shielding of internal connections in the first enrichment system [step (3)] resulted in better than 20 ppm positional stability (<1% ion current change) after 12 hours of enrichment, in which more than 50% of the separated, desired isotope is collected. Operation of the second enrichment system [step (4)] poles at 400° C has resulted in reduction of sample losses (and hence, memory) by a factor of two, resulting in collection of

60% of the desired isotope. The resonance ionization time-of-flight mass spectrometer [step(5)] came on-line at the end of this period with the detection of Kr and Xe.. Most of the effort went into integration of the new laser system and data acquisition improvements. Processing of the Sturgeon Falls samples is approximately halfway completed.

Collaboration with the University of Memphis Ground Water Institute continues. Three joint grant applications have been submitted for combining emerging environmental tracer measurements, particularly ^{85}Kr , with physical and hydrogeochemical measurements to address non point-source pollution and recharge issues in managing a major groundwater resource. A three-year program has been funded by the American Water Works Association Research Foundation. Researchers at the Danish Geological Service have submitted an application for collaborative research to include ^{85}Kr in an assessment of pesticide contamination to a shallow aquifer.

GRANTEE: Texas A&M University

Center for Tectonophysics, Geology & Geophysics Dept.
College Station, TX 77843-3115

GRANT: DE-FG03-ER14887

Fluid-Assisted Compaction and Deformation of Reservoir Lithologies

A.K. Kronenberg (979-845-0132; Fax: 979-845-6162; a-kronenberg@tamu.edu), F.M. Chester, J.S. Chester, and A. Hajash

Objectives: This research addresses the volumetric creep compaction, chemical reaction processes, and distortional deformation of fine-grained quartz aggregates and quartz-clay mixtures subjected to aqueous fluids at temperatures, effective pressures and stress states representative of diagenetic conditions. Specific goals include 1) determination of the transition from isochemical brittle deformation to fluid-assisted solution-transfer creep, 2) identification of the mechanisms of solution-transfer creep, and 3) evaluation of mechanical and chemical rate laws for clastic reservoir lithologies.

Project Description: The compaction and diagenesis of sandstones that form reservoirs to hydrocarbons depend on mechanical compaction processes, fluid flow at local and regional scales, and chemical processes of dissolution, precipitation and diffusional solution transport. Using an experimental approach, the rates of compaction and distortional deformation of quartz and quartz-clay aggregates exposed to reactive aqueous fluids at varying stress states are under investigation. Pore fluid compositions and reaction rates during deformation are measured and compared with creep rates, and acoustic emissions and microstructures of specimens are used to determine the contributions of mechanical and chemical processes to deformation and pore-structure evolution.

Results: Significant progress has been made towards characterizing critical conditions required for rapid cataclastic compaction of St. Peter sand, and measuring long-term compaction of St. Peter sand and Arkansas novaculite (1) in the absence of a reactive pore fluid, (2) with H₂O vapor present, (3) with liquid H₂O saturating pores under static conditions, and (4) with aqueous fluid slowly percolating (0.12 ml/hr) through the specimens. Room temperature values of Pe^* associated with Hertzian cracking at grain contacts for St. Peter sand (of 80 MPa) are marked by curvature in pressure-volume curves and are well above the effective pressures applied in the long-term experiments. At $Pe = 34.5$ MPa, quartz aggregates are observed to creep at low strain rates. Specimens vented to atmosphere exhibit transient logarithmic creep at rates down to $\sim 3 \times 10^{-10} \text{ s}^{-1}$ and show little grain size sensitivity. Quartz aggregates loaded sequentially while vented, exposed to H₂O vapor, and saturated by liquid H₂O exhibit systematic increases in creep rate (from $\sim 3 \times 10^{-10} \text{ s}^{-1}$ to $\sim 4 \times 10^{-9} \text{ s}^{-1}$ and $\sim 6 \times 10^{-9} \text{ s}^{-1}$, respectively). Strain rates under wet conditions follow logarithmic creep relations of similar form but quantitatively distinct from the relation exhibited under dry conditions. Creep rates of samples with percolating fluid are yet another order of magnitude greater than those measured with static fluids saturating pores.

During closed system, wet experiments, static pore fluids become highly supersaturated (195 ppm) with respect to α -quartz at T and P_p (equilibrium SiO₂ at 160 ppm). During open system, slow-flow experiments, fluids exiting specimens remain supersaturated though at lower levels (~ 170 ppm). We conclude that creep under open-system conditions is limited by the dissolution rate at loaded grain contacts and that rates under closed-system conditions may ultimately be governed by much slower precipitation kinetics.

GRANTEE: University Of Texas

Department of Geological Sciences
P.O. Box 7726, Austin, TX 78713-7726

GRANT NO.: DE-FG03-97ER14812

High-Resolution Temporal Variations in Groundwater Chemistry: Tracing the Links Between Climate, Hydrology, and Element Mobility in the Vadose Zone.

J. L. Banner (512-471-5016; Fax: 512-471-9425; banner@mail.utexas.edu)

Objectives: To evaluate the extent to which radiogenic and stable isotopic and trace element variations in speleothems and modern groundwater from the same aquifer provide a means to reconstruct temporal changes in groundwater geochemistry, flow routes, and corresponding climatic controlling processes.

Project Description: This study is using cave calcite deposits (speleothems) and modern groundwater samples to develop a new approach, integrating Sr, Nd, C, O, H and U-series isotope variations with other geochemical and hydrologic tracing tools, to provide 1) improved sensitivity in reconstructing temporal records of groundwater evolution, and 2) a new perspective on the links between climate variability, hydrology, soil evolution, and groundwater chemistry. An understanding of controls on the modern hydrologic system provides a framework within which to interpret the speleothem record. Groundwater, soils, rainfall, speleothem and aquifer rocks are sampled in selected catchments using low-contamination procedures, and analyzed by mass spectrometry. Two karst aquifers were selected for intensive study to achieve the aims of this project. The results are presented below for each aquifer.

Results: *Barbados, W. I. aquifer:* On Barbados, recharge seasonality is inferred by comparison of groundwater and rainwater oxygen isotope values. This indicates that recharge occurs by rapid infiltration during the wettest 1-3 months of the year. Observed nitrogen leaching from the soil reflects these recharge patterns. Seasonal and interannual variations of Barbados groundwater elemental and isotopic compositions are responses to seawater mixing and the amount of rainfall. Variations in C isotopic composition of two speleothems over the past 4000 years of growth show a consistent two per mil offset. The variations from site to site portray a local control on dripwater chemistry, such as that controlled by specific flow routes feeding the drips. The consistent offset between the sites portrays a larger scale control on chemistry, such as changes in vegetation above the cave.

Edwards aquifer, Texas: High-resolution uranium-series geochronology on speleothems from a regional aquifer in central Texas provides a growth rate record for the past 70,000 years (70 ka). The record shows rapid speleothem growth in this subtropical region between 55 ka and 70 ka and for the last glacial period between 25 ka and 12 ka. Independent climate evidence indicates that central Texas was cooler and wetter during these glacial periods compared to present interglacial conditions. This is consistent with speleothem growth rates providing a proxy for paleo-moisture. Correspondingly, carbon isotope records for the speleothems exhibit increased variability during these glacial periods. These records offer insight into both regional and local effects of climatic variations on aquifer recharge, element mobility, and hydrologic flow regimes.

GRANTEE: University Of Texas

Center for Lithospheric Studies
P.O. Box 830688 (FA31)
Richardson, TX 75083-0688

GRANT: DE-FG03-96ER14596

Integrated 3-D Ground-penetrating Radar, Outcrop, and Borehole Data Applied to Reservoir Characterization and Flow Simulation

G. A. McMechan (972-883-2419; Fax 972-883-2829; mcmec@utdallas.edu), J. Bhattacharya (972-883-2449; Fax: 972-883-2537; janokb@utdallas.edu) and C. Forster (801-581-3864; Fax: 801-581-7065; cforster@mines.utah.edu)

Objectives: 3-D ground-penetrating radar (GPR) is used for characterization of the geometry of a clastic hydrocarbon reservoir analog. Sedimentologic mapping and porosity and permeability measurements from core plugs extracted from cliff-faces and boreholes allow population of the model with realistic flow parameters. The final step is 3-D flow simulation through the model to evaluate the effects of flow barriers and baffles to hydrocarbon production.

Project Description: Existing reservoir models are based on 2-D outcrop studies; their 3-D aspects are inferred from correlation between well data, and so are inadequately constrained for reservoir simulations. Field study sites are in the Cretaceous Ferron Sandstone in Utah. Detailed sedimentary facies maps of cliff faces define the geometry and distribution of reservoir flow units, barriers, and baffles at the outcrop. High-resolution 3-D ground-penetrating radar (GPR) images extend these reservoir characteristics into 3-D, to allow development of realistic 3-D reservoir models. Models use geometrical information from the mapping and the GPR data, petrophysical data from surface and cliff-face outcrops, lab analyses of outcrop and core samples, and petrography. Flow simulation in the final models will illustrate the applicability of reservoir analog studies to well siting and reservoir engineering for maximization of hydrocarbon production.

Results: The focus of activity in this second project year was on completion of data acquisition and on data processing and analysis. New data acquired this year include completion of the measurements of the topography of the surface and cliff faces, digital mapping of the major bounding surfaces of the architectural elements and their internal features, two new stratigraphic and gamma ray profiles, resolution of questions raised by the initial interpretations, completion of Hassler and probe permeameter measurements on the cores and core plugs, and a new series of 2-D GPR data (on a 100 x 150 m grid) to attempt to image individual lateral accretions. Core photography and detailed logging of the four continuous cores acquired in 1998 was also completed. All the data are digital, and are referenced to the same 3-D coordinate frame using GPS. Processing and migration of the 3-D GPR data is in progress.

Preliminary results indicate the existence of four main architectural elements, which, from bottom to top are (1) low-sinuosity bedload dominated fluvial, (2) high-sinuosity tidally influenced fluvial, (3) estuarine, and finally, (4) tidal. The outcrops and 3-D GPR data clearly show a lateral accretion set, channels, and crossbedding, on scales of less than a meter to hundreds of meters. Tying these features to their corresponding permeability distributions will complete the 3-D model and provide the input for 3-D flow simulations in the third project year.

GRANTEE: University Of Texas

Department of Geological Sciences
Austin, Texas 78712-1101 U.S.A.

GRANT: DE-FG03-97ER14772

Thermohaline Convection in the Gulf of Mexico Sedimentary Basin, South Texas

J. M. Sharp, Jr. (512-471-3317 or 512-471-5172; Fax: 512-471-9425; jmsharp@mail.utexas.edu), C. T. Simmons (Co-PI), School of Chemistry, Physics, and Earth Sciences, Flinders University, Adelaide, South Australia; Craig.Simmons@es.flinders.edu.au)

Objectives: The initial three research tasks were: 1.) The selection and development of models of thermohaline convection and cross-formational diffusion; 2.) Evaluation of the evolution thermohaline convection above and within the overpressured zone; and 3.) Modeling the effects of the hydrostratigraphic framework of the Gulf of Mexico Basin and its effects on thermohaline convection scenarios. To these we have added: 4.) Evaluation of the effects of sediment heterogeneity, including fractures on free convection.

Project Description: In order to test the hypotheses posed to address the objectives stated above, we have compiled an extensive data base of fluid pressures, water chemistries, and formation temperatures from industrial data services, state well records, and the published literature; installed these data on a G.I.S. for analysis; analyzed selected drill cores and cuttings for their mineralogy; obtained samples from which we have collected thermal conductivity, radiogenic heat production, and porosity/bulk density data; analyzed several major commercial and governmental computer codes for possible utilization; and written several codes to simulate heat conduction and analyze the propensity for free convection. We are presently continuing to collect thermal property data; validating the temperature and pressure data to infer predevelopment conditions; calculating areal buoyancy gradients; and implementing a 2-D/3-D model to simulate the study area's temperatures and pressures.

Results: We selected the U. S. Geological Survey code SUTRA (and forthcoming versions) as the primary model and created simplified pre- and post-processors for the system and extensions for the graphics. We, particularly Dr. Simmons, the Australian collaborating scientist at Flinders University of South Australia (FUSA) and colleagues, evaluated several models, but SUTRA was, perhaps, the most robust and also allows full access to the code. The initial set of simulations was completed by the end of November 1998. These simulations documented the appropriate ranges of parameters for the processes that create the salinity inversions in the Gulf of Mexico Basin. This upwelling of brines into the permeable rocks creates lateral salinity variations and observed density inversions. These are largely responsible for the instability that creates thermohaline convection.

In the Gulf of Mexico Basin shale permeabilities below the top of overpressures, on geological time and spatial scales, are greater by an order of magnitude or more than above the overpressures. This is created by natural hydraulic fracturing. The salinity inversions do not appear to be maintainable for long ($>10^4$ years) in the extremely overpressured or the hydropressed zones.

The gathering of data on the hydrostratigraphic framework proved unexpectedly difficult. The existing stratigraphic interpretations were far too large in scale to meaningful in our modeling efforts, whereas most salinity data spatial distributions were both spotty and sparse. Shale permeability variations have never been documented, although petrographic data show significant heterogeneity. We resorted to

numerical simulations of high permeability zones caused by either zones of microfracturing or facies changes.

The model simulations show several significant results. These are: a) Traditional Rayleigh Number criteria used to estimate whether or not a system will freely convect are of questionable validity in this setting. The effects of permeability and salinity field heterogeneities may dominate the determination of a system's stability or instability. Hitherto, these parameters have been rarely addressed. In addition, there exists a transition zone between diffusion and convection dominated solute transport. Free convection, at least in this setting, is not a simple "on – off" process. b) The effects of fractures on thermohaline convection were evaluated, and we developed a closed form analytical solution on this process. The calculations suggest that fracture sets with even minimal apertures are enough to dissipate salinity inversions. c) The transition zone, across which there is a large increase in fluid pressures, is sufficient to arrest thermohaline convection in Gulf Coast sediments. d) These results demonstrate the process by which sedimentary basins become density stratified with geologic time. Salinity inversions are rare phenomena (geologically) that dissipate on time scales of 100 to 10^4 years.

GRANTEE: Texas Tech University

Dept. of Chemical Engineering
Lubbock, TX 79409

GRANT: DE FG03-99ER14932

Continuum and Particle Level Modeling of Concentrated Suspension Flows

A. Graham (806-742-3553; agraham@ttacs.ttu.edu), L. Mondy (Sandia National Laboratories), and M. Ingber (University of New Mexico)

Objectives: The purpose of this program is to combine experiments, computations, and theory to make fundamental advances in our ability to predict transport phenomena in concentrated, multiphase, disperse systems, particularly when flowing through geologic media.

Project Description: The proposed research will elucidate the underlying physical principles that govern concentrated multiphase systems in areas essential to continued progress in geosciences. In order to be of use in real world applications, significant enhancements to currently available continuum-level suspension flow models will be required. We will use both experimentation and high performance computing to obtain microstructural information that is necessary to the development and refinement of the continuum models. For example, we expect to use this microstructural information to gain insight into the physics of particle bridge formation and collapse and particle sedimentation, which are particularly important in sand control issues found in petroleum production. Further, we expect that continuum-level modeling could eventually be directly implemented in codes currently used to predict hydraulic fracturing operations in the petroleum industry. The understanding gained about the physics of multiphase flows will, however, have much broader application in geosciences.

Results: The continuum models originally developed by Phillips *et al.* (1992) and Nott and Brady (1994) has been extended to account for normal stress contributions. This allows accurate predictions of suspended particle migration in curvilinear flows. The Phillips-type model currently also allows for non-neutrally buoyant particles and non-Newtonian suspending liquids. Results from the new models, which have been implemented into a general-purpose finite element computer code, show good agreement with experimental measurements based on nuclear magnetic resonance (NMR) imaging. Also, massively parallel computing has allowed particle level simulations, based on the boundary element method (BEM), with up to a thousand particles. These simulations are currently being used to determine the magnitude of the normal stresses developing from particle interactions, as well as to develop more accurate hindered settling functions for particles interacting with other types of particles or in a porous medium. These simulations lead to detailed information on individual particle and fluid motion that is unobtainable through experiments. In addition, a multipole-accelerated boundary element method (BEM) has been developed to simulate many thousands of individual interacting particles. Two-dimensional dynamic simulations show qualitative agreement with (three-dimensional) laboratory experiments, and three-dimensional simulations are now possible for “snapshots” of interacting particles.

GRANTEE: University Of Utah

Department of Geology and Geophysics
135 S. 1460 S.
Salt Lake City, Utah 84112-0101

GRANT: DE-FG03-93ER14313

High Resolution Imaging of Electrical Conductivity using Low-Frequency Electromagnetic Fields

Dr. Alan C. Tripp (801-462-2112 or 801-581-4664; Fax: 801-581-7065; actripp@mines.utah.edu)

Objectives: The project seeks to determine means of increasing the resolution of low frequency electromagnetic techniques by means of an optimal use of *a-priori* information

Project Description: The research concentrates on enhancing the resolution of EM probing without sacrificing depth of investigation through better understanding the nature of the EM response and its relationship with other sources of geological information. This is accomplished through:

1) Improvement of Modeling Algorithms:

Forward and inverse modeling algorithms of increasing power and versatility permit subtle data features to be modelled, thus increasing the amount of resolution provided by a given data set.

2) Knowledge Adaptive EM Survey Design:

EM experimental design should use the known conductivity structure to optimize resolution of the unknown target. Borehole information, baseline data, or hypothesized structure can all be used to optimize source waveforms, array weighting, or array phasing.

3) Solution Space Characterization:

Geophysical targets should be refined as much as possible using independent geological or engineering information.

Results:

1) Improvement of Modeling Algorithms:

Reference [2] demonstrates a numerical optimization for the PML boundary condition, which markedly facilitates reduced grid sizes during modelling. Reference [5] is a discussion of the FDTD method for an electrical engineering audience.

2) Knowledge Adaptive EM Survey Design:

Reference [1] demonstrates the utility of EM amplitude focussing for delineation of a conductor in a highly resistive host. Reference [4] demonstrates EM focussing in delineation of fracture packets in a borehole environment.

3) Solution Space Characterization:

Reference [3] develops conductive models for anisotropic fractures and discusses the use of triaxial EM data in resolving these fracture packets. Reference [6] demonstrates for a suite of anisotropic petrophysical models that triaxial induction logging, while giving increased resolution to that afforded by uniaxial data, needs to be constrained by other data sets for full formation resolution.

References:

- [1] Johnson, D., Cherkaeva, E., Tripp, A.C., and Furse, C., 1999, Cross-borehole delineation of a conductive ore deposit in a resistive host - Experimental Design: accepted by *Geophysics*.
- [2] Johnson, D., Furse, C., and Tripp, A.C., 2000, Application and optimization for the perfectly matched layer boundary condition for geophysical simulations: *Microwave and Optical Technology Letters*, 25, no. 4, p. 253-255.
- [3] Tripp, A.C., Bruhn, R., Jarrard, R.D., and Brown, S., 1999, Inductive detection of fractures in geothermal systems - Petrophysical aspects and geophysical implications: Proceedings of the 1999 Stanford Workshop on Geothermal Reservoir Engineering.
- [4] Cherkaeva, E. and Tripp, A.C., 1999, Inductive source design for inductive fracture detection: Proceedings of the 1999 Stanford Workshop on Geothermal Reservoir Engineering.
- [5] Furse, C., Johnson, D., and Tripp, A.C., 1999, Application of the FDTD method to geophysical simulations: *Advances in Computational Electromagnetics Society Newsletter*, March 1999.
- [6] Jarrard, R.D. and Tripp, A.C., 1999, Triaxial induction logging in anisotropic media - Petrophysical considerations, 1999, with R.D. Jarrard, presented at the 1999 Annual AAPG Meeting

GRANTEE: Utah State University

Department of Geology
Logan, UT 84322-4505

GRANT: DE-FG03-98ER14851

Big Hole Drilling Project: Characterization of Fault Zone Properties from *In-Situ* Analyses

J. P. Evans (801-797-2826; Fax: 801-797-1588; jpevans@cc.usu.edu), Z. K. Shipton (zshipton@cc.usu.edu), and T. E. Lachmar (lachmar@cc.usu.edu)

Objectives: We examine the *in situ* hydraulic properties of faulted sandstones to evaluate the impacts such faults have on the subsurface fluid flow regimes. We use our data to develop stochastic models to predict the spatial distribution of faults, and to establish methods for extrapolation of the permeability architecture of faulted rocks

Project Description: We examine the hydraulic properties of the well-exposed Bighole in central Utah. We drilled five core holes through the fault zone, collected geophysical logs from all core holes, logged the core, and performed mini-permeameter, whole-core and *in-situ* hydraulic tests of rocks in and around the fault zone. We have now done some preliminary interpretation of the tests, and calculated the bulk permeabilities of the faulted regions based on core and test data.

Results: Six water injection tests were conducted, one into each zones above, within, and below the fault zone at the tip region of the fault and at the higher displacement site. Preliminary results of the *in situ* hydraulic tests reveal that the hydraulic characteristics of the fault zone are far more complex than we had originally anticipated. Based on these estimates, it appears that the permeabilities of all three zones associated with the fault zone at the higher displacement site in Big Hole Wash are higher than the permeabilities of the three zones at the tip site. Furthermore, at the high-displacement site, it appears that the zone immediately below the fault in the footwall had the highest permeability, and the zone immediately above the fault in the hanging wall had the lowest permeability. In contrast, at the tip site, the zone in the hanging wall had the highest permeability and the footwall had the lowest permeability.

We have also calculated the bulk permeability of the fault. The transmissibility factor, T , is used in oil-field settings to represent the effects of faults in flow simulations. The value of T is taken to be K_{av}/K_{host} , where K_{av} is the averaged permeability over some interval across the fault. The arithmetic mean considers fault-parallel; the harmonic mean estimates the bulk permeability transverse to the fault. We calculate an inverse power mean, which considers a random system of a log-normal distribution of permeability elements. We use the results of the permeability tests and core analyses for a four-component fault system: the host rock; single deformation bands; the fault core; and the slip surface. Transverse flow yields the lowest K_{av} and transmissibility value, with 9-38 mD as the bulk permeabilities. The low porosity deformation band faults reduce the permeability by up to a factor of 25 for the low confining pressures for the K_H value of 100 mD. The inverse power calculations suggest a range of transmissibility factors of 0.4 to 0.6. The bulk permeability of the system is most sensitive to the thickness of the fault zone, the host rock permeability, and the scale over which the calculation is made.

GRANTEE: Utah State University

Department of Mathematics and Statistics, and
Department of Geology
Logan, UT 84322-4505

GRANT: DE-FG03-95ER14526

Growth of Faults and Scaling of Fault Structure

K. Hestir (801-797-2826; Fax: 801-797-1822; hestir@sunfs.math.usu.edu) and J. P. Evans (801-797-2826; Fax: 801-797-1588; jpevans@cc.usu.edu), in collaboration with S. Martel (University of Hawaii, 808-956-7797; Fax: 808-956-5512; martel@soest.hawaii.edu), and J.C.S. Long (University of Nevada at Reno; 702-784-6987; Fax: 702-784-1766; jcslong@mines.unr.edu)

Objectives: We examine faults up to 10 km long in two localities to determine how fault structure scales, and develop a mechanically based stochastic model of fault growth that appears to represent the structure of faults, when conditioned by the field data and understanding of the three-dimensional mechanics of the faults.

Project description: To achieve these objectives, we documented the geometry and slip distribution of long faults, and compare those attributes to those of small faults to assess how fault geometry and slip distribution scale. We also documented and compared the style and extent of deformation near the ends of strike-slip faults and normal faults that range in length from several meters to several kilometers to assess how fault tip deformation scales. The structure near the ends of small faults resembles the structure where small faults are linked, and we expect information on the structure near the ends of large faults will provide insight into how linkages develop along large faults and how these linkages change with scale. Finally, we develop a model of fault growth based on the work of Martel (Univ of Hawaii).

Results: Structural analyses of two 8-10 km long strike-slip faults help us understand the processes of brittle fault growth, linkage, and termination for 1 - 10 kilometer-long, $M=5-6$ producing faults. The Gemini fault zone is a 9 km-long sinistral fault system composed of four northeast-striking noncoplanar segments joined by left- and right-stepping linkages. Fault segments dip steeply and vary in width from 3 to 10 m, show dominant strike-slip movement. The segments are sharply bounded by sub-parallel fault planes, resembling the structure of much smaller faults, such as Martel's (1990) simple fault zones. Net slip varies between segments from < 1 to 140 m. Where several fault zones converge, adjacent segments have up to 70 m of slip difference. This slip deficit may be accommodated in complex left-stepping zones of faults at 30° to the main faults. Segments differ in strike by $10-15^\circ$ and are connected by right and left-stepping linkages. The Glacier Lakes Fault (GLFZ), is composed of two major fault segments. Slip vectors vary, due to interaction of two fault segments. Fault termination may have occurred by slip on GLF being transferred to splay zone with slightly steeper rakes, and the GPF would be interpreted as an older structure, which may have been a barrier to slip, or slip is transferred to the GPF in a complex left step. The Gemini and GL fault zones resemble a scale-up version of the simple fault zone model developed by Martel (1990). A newly developed stochastic algorithm, now soon to be published, shows how these data can be merged with the results of Martel, to postulate the likely three-dimensional structure of the fault zones. A master-fault-splay fault structure is suggested, with the most abundant splays at the Mode II tips of the fault zones. Thus, maximum slip, and hydraulic, connectivity is predicted at the propagating tips of the faults, with little connectivity in the vertical plane.

GRANTEE: Virginia Polytechnic Institute & State University

Fluids Research Laboratory
Department of Geological Sciences
Blacksburg, Virginia 24061

GRANT: DE-FG05-89ER14065

Experimental Studies in the System H₂O-CH₄-“Petroleum”-Salt Using Synthetic Fluid Inclusions

R. J. Bodnar (540-231-7455; Fax: 540-231-3386; bubbles@vt.edu)

Objectives: The objective of this project is to experimentally determine the pressure-volume-temperature-composition (PVTX) relationships of fluids in the C-O-H-NaCl system over the complete range of PTX conditions encountered in crustal energy, resource, and waste-related environments. These data are used to develop equations of state to predict the behavior of these fluids in crustal rocks and to interpret results obtained from natural fluid inclusions.

Project Description: Volumetric (PVT) data provide the fundamental information needed to understand the physical and chemical behavior of fluids in energy, resource and waste-related environments. Further, these data represent the basis for developing and testing empirical or theoretical equations of state to predict the thermodynamic properties of fluids over crustal PTX conditions. In this study the PVTX properties of fluids in the C-O-H-NaCl system are being experimentally determined using the synthetic fluid inclusion technique. With this technique, fluids of known composition are trapped as inclusions by healing fractures in quartz at known temperatures and pressures. Recent efforts have focused on fluids representing the H₂O-CH₄-NaCl system. Phase relations and P-T locations of isochores in the H₂O-CH₄-NaCl system are obtained by observing the temperatures and modes of homogenization of the synthetic fluid inclusions during subsequent heating and cooling experiments in a fluid inclusion stage mounted on a petrographic microscope.

Results: During FY99 synthetic fluid inclusions containing known compositions in the H₂O-CH₄ system were used to determine the location of the bubble point / dew point curve at PTX conditions appropriate to oil and gas reservoirs. These data were compared with previously published data and recent equations of state for the system H₂O-CH₄.

Data obtained from synthetic fluid inclusions are being used to develop a methodology for obtaining the pressure at homogenization for methane-bearing aqueous fluid inclusions. In research related to hydrocarbon basins, pressure is one of the least understood variables, and information concerning the evolution of pressure with time (and temperature) is critical to the development of accurate models for basin evolution. Preliminary results indicate that techniques developed here provide a reasonable approximation of the pressure associated with the entrapment of methane-bearing fluid inclusions in hydrocarbon basins. This information, combined with temperatures obtained from fluid inclusions and other geothermometers may be used to constrain the burial history and the timing of oil generation and migration during burial history.

Synthetic fluid inclusion data have been used to determine the slopes of lines of constant homogenization temperature (approximating isochores) for the system methane-water. These data represent the most complete dataset for this important chemical system, and include the PTX range

appropriate for understanding hydrocarbon reservoirs. This information will permit a more accurate interpretation of natural methane-bearing fluid inclusions from petroleum reservoirs.

An important technical result of this research is the development of a high temperature, high-pressure flow-through cell that can be used to analyze fluids *in situ* using Raman spectroscopy. This cell is currently being developed to determine the Raman characteristics of H₂O-CH₄ over a wide range of PTX conditions relevant to energy environments. These data will allow the Raman calibration data previously collected in this project to be extrapolated to higher temperatures and pressures.

GRANTEE: University Of Washington

Geophysics Program
Seattle, WA 98195

GRANT: DE EG03-97ER-14781

Electromagnetic Imaging of Fluids in the San Andreas Fault

M. Unsworth (206-543-4980; unsworth@geophys.washington.edu)

Objectives: To obtain high-resolution images of the electrical resistivity of the San Andreas fault (SAF) zone. This will permit the fault zone architecture and fluid distribution to be constrained.

Project description: There is increasing evidence that fluids may play a significant role in the earthquake rupture process. However, the difficulty of directly observing fluids in active fault zones currently limits progress in understanding these processes. Magnetotelluric (MT) data collected in 1994 at Parkfield and Carrizo Plain showed that the fault zone at these locations has very different electrical structure.

To further examine how these differences might be related to fault zone seismicity, a two-phase program of MT data acquisition and interpretation is being undertaken. In the first phase, data will be collected on additional profiles across the SAF at Middle Mountain, Parkfield to obtain a three-dimensional image of the electrical resistivity in this area. In the second phase, a three-dimensional survey of the central creeping section of the SAF near Hollister will be undertaken.

These surveys will allow the distribution of fluids within the fault zone to be determined, and to show how these distributions vary between segments with different seismic behavior.

Results: The second phase of data acquisition had been scheduled for October 1998, but was delayed until the end of FY1999. During this survey magnetotelluric data were collected on two profiles that crossed the creeping section of the San Andreas Fault south of Hollister. Measurements were made every 100 m close to the surface traces of major faults, and at 2-3 km spacing elsewhere. The northern profile crossed both the San Andreas and Calaveras faults near Paicines. The southern profile was located in Bear Valley. Owing to cultural electrical noise, processing of the Hollister time series data is more difficult than it was during fieldwork at Parkfield in 1997. To fully remove local electrical and magnetic noise from the Hollister data, the remote reference data that is simultaneously recorded at Parkfield will be required. Initial inversions of the southern profile have revealed a broad zone of low resistivity that is bounded on the east by the Calaveras Fault. A full comparison with the Parkfield segment will be possible once the careful analysis of the Hollister time series data is completed.

GRANTEE: University Of Wisconsin

Department of Civil and Environmental Engineering
Madison, Wisconsin 53706

GRANT: DE FG02-99ER14995

Resolution and Accuracy of 3-D Electromagnetic Imaging

D. L. Alumbaugh (608-262-3835; alumbaugh@enr.wisc.edu) and G. A. Newman (Sandia National Laboratories)

Objectives: The objective of this research two fold. The first objective is to develop and analyze techniques for quantifying the resolution of, and appraising the accuracy of images produced by 2D and 3D electromagnetic inversion schemes, and to apply these techniques to field data. The second objective is to develop and the implement 3D magnetotelluric (MT) modeling and inversion schemes to demonstrate expected resolution improvements compared to standard, and much faster, 2D data analysis over 3D targets.

Project Description: Non-linear electromagnetic inversion for 2D and 3D subsurface imaging of electromagnetic properties has rapidly evolved over the last decade due to its potential benefit in the areas of contaminant waste site characterization, oil and mineral exploration and delineation, and ground water resource evaluation. However, before we can proceed on inverting field data and interpreting the resulting images with any level of confidence, methods of appraisal and error analysis must be developed. The purpose of this project is to examine established methods for this purpose such as calculating the model covariance and model resolution matrices through direct matrix inversion using Bakus-Gilbert theory, and examine procedures that estimate these resolution parameters without direct matrix inversion; the latter is required when iterative techniques such as Conjugate Gradients are employed within the inversion scheme.

An outstanding problem in the interpretation of 3D magnetotelluric (MT) data sets have been the lack of robust and computationally efficient 3D inversion schemes. Whilst 3D forward modeling can be applied to these types of data sets, it is often too cumbersome to use for trial and error fitting of observed data. To overcome the computational barriers of 3D inversion, we have implemented a preconditioned non-linear conjugate gradient solution on massively parallel computing platforms. Thus, large 3D MT data sets can now be analyzed and it is now possible to study the resolving power of 3D inversion compared to standard 2D data analysis.

Results: Linearized methods have been developed for appraising resolution and parameter accuracy in images generated with two- and three-dimensional (2D and 3D) non-linear electromagnetic inversion schemes. When direct matrix inversion is employed, the model resolution and aposterior model covariance matrices can readily be calculated. Traditionally the main diagonal of the model resolution matrix has been employed to estimate the resolution properties of the inversion process. However, because this parameter alone cannot distinguish how the resolution varies in the different directions, we chose analyzing individual columns the model resolution matrix, which allows the spatial variation of the resolution in the horizontal and vertical to be estimated. Plotting the diagonal of the model covariance matrix provides an estimate of how errors in the inversion process such as data noise and incorrect *a priori* assumptions map into parameter error, and thus provides valuable information about the uniqueness of the resulting image.

Methods were also derived for linearized image appraisal when the iterative conjugate gradient technique is applied to solve the inverse problem rather than direct inversion. This technique must be employed for the 3D problem as direct inversion is computationally too demanding. An iterative statistical method was demonstrated to yield accurate estimates of the model covariance matrix as long as enough iterations are employed. Although determining the entire model resolution matrix in a similar manner is computationally prohibitive, individual columns of this matrix can be determined. Thus, the spatial variation in image resolution can be determined by calculating the columns of this matrix for key points in the image domain, and interpolating between. These linearized image analysis techniques were conducted on 2D and 3D synthetic cross well EM data sets, as well as a field data set collected at the Lost Hills Oil Field in Central California.

Because the above methods are linearized about a final model, there is uncertainty of how realistic an estimate they provide given that we are solving a nonlinear inverse problem. To investigate this aspect of image appraisal, a nonlinear technique for determining estimates of parameter uncertainty was developed for 2D cross-well EM inversion, and the results of this appraisal method compared to those provided by the linearized technique. Here, parameter variance estimates are determined using the same Monte Carlo technique as employed above, except the entire nonlinear inversion rather than just the last iteration is rerun N times. Two oil field examples from California indicate that the linearized approach produces the same general pattern in the uncertainty estimates as the nonlinear estimation process. However, the linearized estimates are smaller in magnitude and show less spatial variation compared to the full nonlinear estimates, and the deviation between the two techniques increases as the contrast between the maximum and minimum parameter values increases within the inversion domain.

Three-dimensional (3D) magnetotelluric (MT) forward and inverse solutions have been implemented and applied in a resolution study for sub-salt imaging of an important target in marine magnetotellurics for oil prospecting. In the forward problem, finite difference methods are used to efficiently compute predicted data and cost functional gradients. A fast preconditioner is introduced at low induction numbers to reduce the time required to solve the forward problem. We demonstrate a reduction of up to two orders of magnitude in the number of Krylov subspace iterations and an order of magnitude reduction in time needed to solve a series of test problems. For the inverse problem, we employ a nonlinear conjugate gradient solution developed on massively parallel computing platforms. Solution stabilization is achieved with Tikhonov regularization. To further improve the image resolution of sub-salt structures, we have also incorporated two additional constraints within the inversion process. The first constraint allows for the preservation of known structural boundaries within the inverted depth sections. This type of constraint is justified for the sub-salt imaging problem because the top of salt is constrained by seismic data. The other constraint employed places variable lower bounds on the electrical conductivity above and below the top of salt. Cross sections of the inversion results over the center of the salt structures indicate that the 3D analysis provides somewhat more accurate images compared to faster 2D analysis, but is computationally much more demanding. On the flanks of the structures, however, 3D analysis is necessary as 2D inversion shows significant image artifacts arising from the 3D nature of the data. We conclude, however, that 3D inversion may not be cost effective for the sub-salt imaging problem. Very fine data sampling along multiple profiles employed in the 3D analysis yielded only a marginal improvement in image resolution compared to 2D analysis along carefully selected data profiles. The study also indicates that in order to provide resolution that is required to accurately define the base of the salt, additional constraints beyond that employed here, need to be incorporated into the 3D inversion process.

GRANTEE: University Of Wisconsin

Department of Geology and Geophysics
Madison, Wisconsin 53706

GRANT: DE-FG02-93ER14328

Comparative Studies of Physiochemically and Biologically Mediated Reactions at Mineral Surfaces

J. F. Banfield (608-265-9528; Fax: 608-262-0693; jill@geology.wisc.edu)

Objectives: The goal of this research is to identify and the ways in which microorganisms impact the rates and mechanisms of weathering reactions at interfaces between organisms and minerals via production of small organic molecules and extracellular polymers. We also aim to understand how mineral precipitation in proximity to cell surfaces impacts the form and distribution of metals in the environment.

Project Description: This work builds on a model for microbe-mineral interactions that was developed through high-resolution characterization of the intact interface between communities of microorganisms (the lichen-rock association) and mineral surfaces. Initial studies defined a series of zones in which distinct processes operate over millimeter to sub-millimeter distances. Research includes experiments designed to quantify phenomena in each of these zones. Firstly, we measured the extent to which microorganisms can modify the pH of their environments and conducted experiments designed to quantify the ways in which organic acids enhance release of ions from minerals. Secondly, the association between microbes, cell surface polymers, and primary and secondary minerals was defined. Dissolution experiments were conducted to measure effects of polymers in association with dissolving minerals. Energy-filtered transmission electron microscopy (EFTEM) and electron energy loss spectroscopic (EELS) imaging were used to map element distribution patterns on the few nanometer scale in order to develop an understanding of how microbial products localize mineral precipitation and control the mineralogy of the secondary phases.

Results: Following completion of dissolution experiments with cells and organic acids last year, we turned to secondary mineral formation in proximity to active cells and mineral surfaces. Experimental data indicated that dissolution reactions lead to accumulation of ions in solution in non-stoichiometric proportions compared to the reacting phase. Direct characterization of microbial surfaces from natural samples verified the importance of extracellular polymers in nucleating secondary minerals, including clays and oxyhydroxide phases. Consequently, we conducted a series of experiments to evaluate the relative roles of specific types of microbial polymers in metal binding and biomineralization. We characterized cells exposed to metals (especially U) under laboratory conditions using field emission energy-filtered transmission electron microscopy. Because uranium is especially strongly bound by organic ligands, we focused on uranium-microbe interactions as a model system for investigation of microbial biomineralization. Metal uptake capacity varied dramatically with both cell type and polymer type. For specific cells, results revealed extremely heterogeneous metal binding, with considerable intracellular uptake of metals. Extensive mineralization of extracellular polysaccharides and intracellular structures, including concentric bodies, was documented. However, the relevance of these results to natural systems is unclear. Consequently, samples of soils, solutions, and microorganisms were collected from a uranium-contaminated field site. Organisms were cultured in solutions containing high uranium concentrations, bacteria were isolated from pH 4 and pH 7 aerobic and anaerobic environments, and

cells identified by DNA-based methods. Initial data indicate biomineralization of cell surfaces, especially by sulfate-reducing bacteria.

GRANTEE: University Of Wisconsin

Department of Materials Science and Engineering
Madison, WI 53706

GRANT: DE-FGO2-98ER14850

Deformation and Fracture of Poorly Consolidated Media

B. C. Haimson (608-262-2563; Fax: 608-262-8353; haimson@enr.wisc.edu)

Objectives: The objective of this research is to investigate the process of hydraulic fracturing and of borehole breakout formation in poorly consolidated granular rock. Specifically we are interested in studying the mechanisms leading to these two types of borehole failure, and establishing whether either or both could be used as *in situ* stress indicators in high porosity weak rocks.

Project description: For borehole breakout studies we employ a specially fabricated biaxial loading cell mounted inside a compression loading machine, which allow us to carry out drilling of axial boreholes (diameters of 14-40 mm) in rock blocks (150x150x230 mm) already subjected to a state of true triaxial *in situ* stress. Berea sandstone of 24-26% porosity, other sandstones, and artificial granular material of similarly high porosity are tested. For hydraulic fracturing experiments we use cylindrical rock specimens (100x150 mm) mounted in a triaxial vessel through which we apply lateral and axial loads, as well as pore pressure and borehole fluid pressure.

Results: Borehole Breakout: We completed a series of laboratory drilling tests in high-porosity Berea sandstone (BSs25). BSs25 is dominated by large quartz grains (0.4 – 0.6 mm) cemented primarily by sutured grain contacts. Drilling into BSs25 prismatic specimens pre-subjected to high true triaxial far-field stresses induced fracture-like borehole breakouts orthogonal to the direction of maximum far-field compression. These fracture-like breakouts originate at the points of highest stress concentration at the borehole wall, along the σ_h springline, and extend in the same direction for distances several times the borehole diameter, depending on the far-field stress condition [Haimson *et al.*, 1999; Haimson, 1999]. Micrographs of breakouts in BSs25 show the development of an apparent *compaction band* just ahead of the breakout tip in the form of a narrow layer within which grains have been compacted normal to σ_H , creating a zone of low porosity. Some grain splitting is evident, a result of loosened grains crowding each other in the σ_H direction. The occurrence of the compaction bands is practically identical to that described in field situations. The mechanism leading to fracture-like breakouts may be directly related to the formation of the compaction band, which is the result of sutured grain contact loosening and grain debonding. This process enables the drilling fluid to flush out the compacted loose grains. As the breakout tip advances, the stress concentration ahead of it persists, extending the compaction band, which in turn leads to breakout lengthening. It is envisaged that in field situations this process may continue for large distances, leading to substantial sand production.

We studied the effects of several variables on the dimensions of fracture-like breakouts in high porosity Berea sandstone. (a) Results show that breakout-fracture length increases with the maximum horizontal far-field stress, when the other two principal stresses are kept constant. The correlation between breakout length and stress indicates the possibility that this dimension could be used to estimate one of the principal *in situ* stresses. (b) Borehole size effect has been tested by drilling using different-diameter bits. It has been shown that larger diameter boreholes produce increasingly longer breakouts for otherwise identical conditions of far-field stress. By extrapolation, we suggest that breakouts may reach

lengths of several meters in typical field wellbores. (c) Tests of drill-bit penetration-rate effect and drilling-fluid flow-rate effect were also performed. For the ranges tested thus far neither of these two factors showed significant effect on breakout shape or size. Perhaps the most remarkable finding was that most fracture-like breakouts had a consistent width of 5-10 grain diameters regardless of test variables. This finding reinforced a suggestion that the fracture-like breakouts are “emptied compaction bands” (which typically are several grain diameters thick).

Hydraulic Fracturing: We carried out several series of hydraulic fracturing (HF) tests in axial holes drilled into cylindrical specimens of two different Berea sandstones, BSs17 (17% porosity) and BSs25 (averaging 25% porosity) and a high porosity (30%) Table Rock sandstone (TR30). Specimens were subjected to confining pressure (simulating the far-field horizontal stress) and a vertical stress inside a pressure vessel that also enables the application of pore pressure P_o . Three hydraulic oils (viscosity μ of 0.04, 0.39 and 3.48 Pa s at 40°C) were used as injection fluids. An acoustic emission recording system was installed for monitoring fracture initiation.

Our initial concern was whether the wellbore pressure in such highly permeable sandstones could be raised sufficiently to induce fracturing. By speeding up the controlled injection-fluid flow rate, we were able to hydrofracture BSs17 specimens using any of the three oils. In BSs25 specimens, fracturing was achieved only when the thickest oil ($\mu = 3.48$ Pa s) was employed.

The first series of HF tests was conducted under drained conditions, *i.e.* the far-field pore pressure and the confining pressure were equal and remained constant during borehole pressurization. Hydraulic fracturing was induced in these tests at breakdown pressures that were proportional to the far-field horizontal stress. The straight line is remarkably well predicted by either the Hubbert-Willis (1957) elastic model, or the Haimson-Fairhurst (1970) poroelastic model.

A major effort was spent on establishing relationships between far-field pore pressure under undrained conditions and the breakdown pressure. Little if any information is found in the literature on this subject. A surprising dichotomy was found between the Berea sandstone and the Table Rock sandstone. Irrespective of the porosity, the breakdown pressure in Berea sandstone decreases as the far-field pore pressure rises (for otherwise identical stress conditions). On the other hand, in Table Rock sandstone the same pressure is proportional to the pore pressure. In terms of effective values, however, the breakdown pressure in both rocks declines with the pore pressure. It is apparent that the two sandstones behave differently mechanically, and that a closer look at the micromechanics of the hydraulic fracturing is called upon.

GRANTEE: University Of Wisconsin

Department of Geology and Geophysics
Madison, Wisconsin 53706

GRANT: DE-FG02-93ER14389

Microanalysis of Stable Isotope Ratios in Low Temperature Rocks

J. W. Valley (608-263-5659; Fax: 608-262-0693; valley@geology.wisc.edu)

Objectives: To further develop microanalytical techniques for stable isotope analysis and to employ them to decipher the complex effects of superimposed hydrothermal events in modern and fossil geothermal systems (Long Valley, Yellowstone, BTIP/Skye, Timber/Yucca Mtn.)

Project Description: This study focuses on samples of altered volcanic rocks from the Long Valley Exploratory Well, CA and other drilling and outcrop samples from Long Valley and Yellowstone, and on hydrothermally altered granites from related rocks from the British Tertiary Igneous Province (BTIP). New techniques allow analysis of stable isotope ratios in ultra-small samples and oxygen isotope ratio can now be contoured across single crystals. Mineral zonation patterns provide new insights into the process of water/rock interaction: mechanisms of exchange, timing, degree of equilibration, variability of fluid fluxes, and fluid sources. Enhanced understanding of these processes is essential for improving computer models of fluid flow through hot rocks.

At the Long Valley caldera and at Yellowstone, these results provide information on the nature of magma chambers at depth, the size of the modern geothermal resource, and the volcanic hazards. On the Isle of Skye, Scotland, samples of granite from beneath an ancient, deeply eroded caldera provide further insights for active systems.

Results: At Long Valley, analysis of samples from additional wells has greatly expanded our coverage and extended our study to the west of the Resurgent Dome. These results document shallow lateral flow of heated meteoric waters radially outwards from the Resurgent Dome due to convection driven by post 500Ka intrusions.

At Yellowstone, 400 analyses of zircons and quartz have been made from 24 units erupted over the past 2Ma. Zircon preserves the best record of primary magmatic composition and some quartz is altered. In common with earlier studies of quartz, extreme depletions of oxygen isotope ratio occur after caldera forming eruptions. In contrast to earlier studies, analysis of zircons reveals periods of extreme disequilibrium in oxygen isotope fractionation that correlate to the periods of isotopic depletion. Some zircons were found to be zoned in oxygen isotope ratio (by air abrasion/ laser analysis and by ion microprobe). The zonation and low oxygen isotope ratios record wholesale melting of hydrothermally altered rocks from the down-dropped cauldron after major eruptions and not assimilation as previously proposed. The shape and depth of these isotopic gradients provides a timescale for the longevity of the melt and rules out rapid or explosive processes.

At BTIP, oxygen isotope analysis of zircons from 22 rock units has shown that most granites formed from isotopically light magmas. These data document a more complex and protracted history of hydrothermal alteration and magmatic interaction than was previously detected by analysis of quartz or feldspar. Samples have been analyzed from four magmatic centers on the Isle of Skye and from other plutons of the BTIP (Arran, Mull) that stitch domains with basement ages from Archean to Phanerozoic.

The evolved oxygen isotope compositions are decoupled from trends seen in Pb or Sr isotopes, and do not correlate to basement and are dominated by processes in the shallow crust.

At Timber Mountain/ Oasis Valley caldera complex, we have collected samples and begun to separate zircons and quartz. Preliminary analysis confirms earlier reports that magmas were low in oxygen isotope ratio. While the amount of isotopic depletion is smaller, the size of the anomalous magmas is suggested to be much larger, up to 1000 cubic km. We plan to test our new model for the genesis of such magmas. One aspect of this study will be investigation of primary magmatic compositions for the wall rocks at the Yucca Mountain site. Knowledge of primary compositions at Yucca Mtn. will provide a boundary condition for estimating the effects of paleohydrothermal alteration.

GRANTEE: University Of Wisconsin

Department of Geology and Geophysics
Madison, Wisconsin 53706

GRANT: DE-FG02-98ER14852

Pore-Scale Simulations of Rock Deformation, Fracture, and Fluid Flow in Three Dimensions

H. F. Wang (608-262-5932; Fax: 608-262-0693; wang@geology.wisc.edu)

Objective: The objective of this project is to develop a numerical percolation model on the geologic scale for two-phase, immiscible fluid displacement in a porous medium.

Project Description: Two-phase displacement in a porous medium occurs in many geologic processes. Although pore scale mechanics can be readily understood in terms of the relevant viscous, capillary, and buoyancy forces, geologic scale, multiphase flows (large and slow) remain beyond the capabilities of current models. Conceptual and computational methods are being developed to separate a geologic-scale percolation model into a series of simulations that capture appropriately the dominant percolation behavior. The product of our research will be an understanding of the controls on the spatial distribution of the non-wetting fluid clusters.

Results: A model for secondary migration of oil has been conceptualized into an initial injection phase, a stringer migration phase, and a trapping phase. During early injection, capillary and/or viscous forces will always dominate over buoyancy forces. When buoyancy forces eventually dominate, the flow takes place in a destabilizing gradient in which fingers preferentially grow in the direction of the gradient without branching or merging. As injection into the reservoir ceases, the nonwetting fluid will continue to migrate upward along the fingering pathways. The configuration of the nonwetting fluid cluster at the base is critical in determining the amount of nonwetting fluid that leaves the cluster before it becomes internally disconnected and flow from the cluster ceases. The implementation of the model is currently underway. Once completed, effects of geologic structure and heterogeneity on migration can be simulated.

GRANTEE: Woods Hole Oceanographic Institution

Department of Marine Chemistry and Geochemistry
Woods Hole, MA 02543

GRANT: DE-FG02-97ER14746

Laboratory Constraints on the Stability of Petroleum at Elevated Temperatures: Implications for the Origin of Natural Gas

Jeffrey Seewald (508-289-2966; Fax: 508-457-2164; jseewald@whoi.edu)

Objectives: Constrain the role of water and minerals during organic transformations responsible for the conversion of oil to natural gas at elevated temperatures and pressures

Project Description: Factors that regulate the generation and composition of natural gas during the thermal maturation of petroleum are poorly understood. The origin of natural gas is being investigated by conducting a series of laboratory heating experiments to constrain the stability of petroleum in the presence of water and minerals at elevated temperatures and pressures. These experiments differ from previous studies by the addition of naturally occurring mineral assemblages that buffer redox conditions and the activity of aqueous sulfur species. Results from these experiments will be used to assess the relative influence of reactions regulated by thermodynamic equilibrium and chemical kinetics. In addition, the contribution of water derived hydrogen and oxygen to the production of methane and carbon dioxide will be determined.

Results: Laboratory experiments conducted during the earlier phases of this investigation examined reactions involving an oil phase floating on liquid water containing iron-bearing mineral buffer assemblages. Results from these experiments were augmented in FY99 by mineral-buffered experiments containing oil or single compounds that were completely dissolved in the liquid water phase. Temporal variations in fluid composition demonstrate that oil dissolved in water decomposes through a series of oxidation reactions that produce alkene, alcohol, ketone, and carboxylic acid reaction intermediaries, the latter of which ultimately reacts to form carbon dioxide and methane. The relative abundances of some reaction intermediaries are regulated by a state of reversible redox dependent metastable thermodynamic equilibrium. Reaction rates and the relative abundance of carbon dioxide and methane are strongly dependent on the redox state of the chemical system and reaction medium. In particular, the presence of an aqueous phase may facilitate reaction pathways involving aqueous organic compounds that are not available to hydrocarbons existing in a hydrocarbon (oil) phase. Aqueous based reactions result in the production of a methane and carbon dioxide-rich natural gas relative to "cracking" reactions that occur in an oil phase. These results provide compelling evidence that the stability of petroleum and generation of natural gas in sedimentary basins are influenced by the presence or absence of water and redox sensitive minerals.

GRANTEE: Woods Hole Oceanographic Institution

Department of Marine Chemistry and Geochemistry
Woods Hole Oceanographic Institution
Woods Hole, Massachusetts 02543

GRANT: DE-FG02-89ER13466

Organic Geochemistry of Outer Continental Margins and Deep-Water Sediments

J.K. Whelan (508-289-2819; Fax: 508-457-2164; jwhelan@whoi.edu)

Objectives: The objective of this program is to develop a better understanding of processes of hydrocarbon generation and migration in coastal and offshore sedimentary basins as an aid in predicting favorable exploration areas for oil and gas.

Project Description: Our current research focuses on utilization of organic compounds in elucidating mechanisms, rates, and consequences of subsurface fluid flow. A particular interest is understanding the role of gas in driving fluid movement in sedimentary basin processes in collaboration with scientists at Cornell University, Louisiana State University and oil companies (Global Basin Research Network); the Geochemical and Environmental Research Group (GERG) at Texas A&M; and U. Mass Boston

Results: Previous work provided evidence for on-going oil and gas injection (termed dynamic migration) into reservoirs of Eugene Island Block 330 (EI330) and areas to the south along the Louisiana Gulf Coast shelf edge and slope. All EI330 oils are derived from the same deep Jurassic or Early Cretaceous marine source rock. EI330 oil generation appears to predate the formation of modern reservoirs. Gases are generated considerably deeper than the oils. The collective geochemical, geological, and geophysical data are consistent with an on-going generation of methane from oil cracking at depths of about 12-14 km. Upward flow of methane builds up sufficient pressure to open a pervasive fracture network allowing gas and entrained oil to flow from deeper source rocks/reservoirs upward into present day reservoirs. This process produces a possibly episodic stream of upward flowing gas which "washes" the reservoired oils resulting in:

- Low concentrations phenols and absence of benzocarbazoles in EI330 oils suggesting a high degree of oil-rock contact and gas washing for these Gulf Coast oils.
- C3 through C14 hydrocarbons distributed through both faults and fractures but not in the mudstone matrix.
- Biomarkers indicative of the degree of oil biodegradation show that producing reservoirs were filled at about their present day depths.
- Preliminary compound-specific isotope analyses indicate that a large toluene anomaly found in one well is isotopically related to other C7 compounds in the whole family of EI330 oils. Therefore, short-term changes (less than 5 years) observed for this compound are related to subsurface migration alteration rather than to a change of oil source or a production contaminant.
- Estimation that residual oil in a continuously subsiding source/reservoir system is sufficient to account for the methane needed to drive oil migration and alteration over geologic time. Globally, less than 2% of generated gas and oil worldwide ever make their way into commercial reservoirs with approximately 44% remaining dispersed in the source rock/migration system and about 54%

leaking out of surface sediments. Thus, dynamic migration systems similar to EI330 could be widespread globally and could occur in any actively subsiding basin, including major river deltas and continental slope areas.

During the past year, this study was expanded to include a north south transect across the Gulf coast shelf and slope. Preliminary results from a large suite of oils and gases show that:

- Based on n-alkane profiles, gas washing of oils to the north and west of EI330 has been much more extensive than for EI330. Thus, on-going gas migration and possibly dynamic migration may be pervasive and long term throughout this area.
- Biomarkers over the entire corridor are remarkably similar. Oil biomarkers indicate some enrichment from siliceous deltaic oil source rocks to the north and carbonate-rich marine source rocks to the south.
- Decreases in some condensed aromatics and benzothiophenes to the north may be consistent with enhanced water or gas washing of oils to the north.

GRANTEE: University Of Wyoming

Department of Geology and Geophysics
Laramie, WY 82071-3006

Grant: DE-FG03-96SF14623/A000

Mineral Dissolution and Precipitation Kinetics: A Combined Atomic-Scale and Macro-Scale Investigation

C. M. Eggleston (307-766-6769; Fax: 307-766-6679; carrick @uwyo.edu), S. R. Higgins (307-766-3318; Fax: 307-766-6679; shiggins@uwyo.edu) and K. G. Knauss (925-422-1372; Fax: 925-422-0209; knauss@s19.es.llnl.gov)

Objectives: Our objectives are to build and test an atomic force microscope (AFM) capable of operation at up to 150°C and 6 atm. pressure, and to apply this AFM to direct, *in-situ*, and real-time observation of step dynamics during dissolution and growth of minerals at elevated temperature and pressure.

Project Description: This project combines atomic-scale and macro-scale approaches to the study of mineral-fluid interaction in order to significantly improve our understanding of, and ability to predict the course of, mineral dissolution and precipitation processes. With the successful construction of a hydrothermal atomic force microscope (HAFM), we can measure rates of dissolution and precipitation, determine activation energies, measure rates of step motion across surfaces (including anisotropy), and investigate step-step interactions that affect rate. Such data can then be used to address many questions concerning the exact forms for rate laws near and far from equilibrium, the microscopic interpretation of these rate laws in terms of dissolution and precipitation mechanisms.

Results: Since the successful construction of the HAFM in late 1997 and initial work on the dissolution of barium sulfate, a material whose dissolution and growth rates are of interest to the petroleum industry because of its occurrence as a scale deposit, we have turned our attention to (1) barite growth, and (2) the dissolution of oxide and silicate minerals.

For barite growth, we found that both single-spiral and double-spiral hillocks were common (for single spirals, a single screw dislocation outcrops at the surface, leading to the formation of a spiral growth hillock; for double spirals, two screw dislocations of opposite sense outcrop near each other, leading to the formation of hillocks with closed-loop steps rather than spirals). Because steps in different crystallographic orientations travel at different velocities, the growth hillocks consist of step segments that alternate between single double-molecular layer height, and two steps of monomolecular layer height. Through observation of step dynamics, it is possible to extract information about such fundamental processes as kink detachment as well as thermodynamic properties such as kink formation energy. We have found that attempts to gain thermodynamic information through critical length measurements by AFM likely lead to overestimates of critical length and thus also to overestimates of step energy.

We investigated the dissolution of albite, labradorite, and anorthite feldspars under both acidic and basic conditions up to 125°C. Universally, under acidic conditions, the feldspars roughen to form a surface layer that can be removed by high-force scanning, but can be imaged with low-force scanning. The ability to make landmarks on the mineral surface by varying the loading force on the HAFM cantilever

makes it possible to (a) measure the rate of thickening of the rough, presumably altered layer, and (b) measure the rate of lateral motion of surface features such as macrosteps relative to a fixed point.

Height differences between successive scan fields of different sizes made in the same location, on the one hand, and the surrounding roughened/altered material on the other, all but vanish with time even though the altered layer can be up to 300 nm thick. The formation of a 300-nm-thick layer on anorthite takes place in (0.01 M HCl at 125°C) less than 2 hours. Such roughened layers take much longer on labradorite, and longer still on albite, under acidic conditions. Nevertheless, surface features such as macrosteps move laterally underneath the roughened, altered layer. In contrast, HAFM imaging of anorthite dissolution at pH 12 does not show pervasive roughening, and indeed suggests that dissolution may occur by step motion. The circumneutral pH regime under which most natural dissolution occurs may thus represent a transitional regime between different dissolution mechanisms.

Finally, we have imaged hematite under acidic conditions up to 143°C. Except in cases where the AFM tip appears to have caused surface alteration due to relatively high scanning forces, we have been unable to detect any step retreat on hematite (001) surfaces even at elevated temperature at pH = 1 (HCl). Our results raise questions about the reactivity of hematite surface at the atomic scale, as well as the role of crystallographic anisotropy in hematite dissolution rates.

Finally, as part of this work, we have studied periclase dissolution in order to gain a better understanding of how mineral surface roughen and dissolve due to surface chemical alteration for a material that reacts more quickly than do feldspars.

GRANTEE: Yale University

Department of Geology and Geophysics
New Haven, Connecticut 06520-8109

GRANT: DE-FG02-95ER14522

A Field Experiment on Plants and Weathering

R. A. Berner (203-432-3183; Fax 203-432-3134; berner@hess.geology.yale.edu)

Objectives: For 1999 our objectives were to: (1) study the effects on rock weathering and the geochemical cycling of elements resulting from experimental deforestation; (2) continue our theoretical calculations of how long-term carbon cycling affects the levels of atmospheric O₂ and CO₂; and (3) Examine the feasibility of using the stomatal density of fossil leaves as an indicator of past levels of atmospheric CO₂.

Project description: (1) Drainage waters, subsequent to the cutdown of pine trees from experimental plots at the Hubbard Brook Experimental Forest Station, were continued to be analyzed and water flow and chemistry, monitored on a weekly basis over the year. (2) Computer modeling of the long-term carbon cycle was continued and it focused on the effects of changes in O₂ on carbon isotope fractionation during photosynthesis. (3) An exciting new technique for deducing paleo-atmospheric CO₂ was initiated. The method utilizes the relationship between CO₂ and stomatal density (as represented by stomatal index) in plants. As CO₂ rises, plants can afford to reduce their stomatal density, thereby restricting water loss while maintaining carbon fixation rates. Likewise, as CO₂ drops, stomatal density increases. Ginkgo leaves from herbarium collections have been studied to calibrate the method and fossil Ginkgo leaves from rocks measured to gain some idea of paleo-CO₂ levels.

Results:

1. Since the pine trees were cut down there has been considerable release of dissolved chloride, which presumably represents earlier root storage during growth of the trees. This release of Cl has continued for over 1.5 years and it shows a release pattern totally different in timing from the release of dissolved nitrate. This indicates that Cl is not a conservative tracer of water flow and that it is stored in the root system in a different manner than the nutrient element N.
2. In three published papers the long-term carbon cycle and how it relates to paleolevels of atmospheric O₂ are discussed. In one paper (Berner *et al.*, 2000, *Science*, v.287, p.1630) the effect of changes in atmospheric O₂ on the fractionation of carbon isotopes during photosynthesis is demonstrated for both land plants and marine plankton. The discovery of O₂-dependent fractionation allows resolution of one of the major problems in modelling the evolution of O₂ over geologic time.
3. The stomatal density for Ginkgo leaves collected over the past 140 years correlates very closely, in an inverse manner, with known atmospheric CO₂ level ($r^2=0.98$; $n=34$). This demonstrates that the stomatal density method is applicable to the fossil leaf record. On this basis, values of paleo-CO₂ have been determined for portions of the Cretaceous, Paleocene and Eocene periods (70-45 Ma).

GRANTEE: Yale University

Department of Geology and Geophysics
P.O. Box 208109
New Haven, Connecticut 06520-8109

GRANT: DE-FG02-90ER14153

Reactive Fluid Flow and Applications to Diagenesis, Mineral Deposits, and Crustal Rocks

D. M. Rye (203-432-3174; Fax 203-432-3134; danny.rye@yale.edu) and E. W. Bolton (203-342-3149)

Objectives: To initiate new: modeling of coupled fluid flow and chemical reactions of geologic environments; experimental and theoretical studies of water-rock reactions; collection and interpretation of stable isotopic and geochemical field data at many spatial scales of systems involving fluid flow and reaction in environments ranging from soils to metamorphic rocks.

Project Description: Theoretical modeling of coupled fluid flow and chemical reactions, involving kinetics, has been employed to understand the differences between equilibrium, steady state, and non-steady-state behavior of the chemical evolution of open fluid-rock systems. The numerical codes developed in this project treat multi-component, finite-rate reactions combined with advective and dispersive transport in multi-dimensions. The code incorporates heat, mass, and isotopic transfer in both porous and fractured media. Experimental work has obtained the kinetic rate laws of pertinent silicate-water reactions and the rates of Sr release during chemical weathering. Ab-initio quantum mechanical techniques to obtain the kinetics and mechanisms of silicate surface reactions. Geochemical field-based studies were carried out on the Wepawaug metamorphic schist, on the Irish base-metal sediment-hosted ore system, in the Dalradian metamorphic complex in Scotland, and on weathering in the Columbia River flood basalts. The geochemical and isotopic field data, and the experimental and theoretical rate data, were used as constraints on the numerical models and to determine the length and timescales relevant to each of the field areas.

Results: Analytical and numerical models were created to elucidate metamorphic processes in the presence of mixed volatiles (CO₂ and water). These models include systems open to heat and fluid flow, and describe the central features of kinetic control of metamorphic reactions. Reactions which occur in these systems may follow temperature / composition pathways quite distinct from what would be expected, and steady states can be maintained that are away from thermodynamic equilibrium. Detailed comparisons of time-integrated fluid flux estimates based on the equilibrium approach with the actual fluxes computed from a kinetic model underscore the crucial role of kinetics, especially near lithologic boundaries and for high flow rates. Of particular interest is the crucial role of metastable reactions because stable reactions can be overstepped. Numerical models also indicate that mass transfer and the observed reaction progress can be driven largely by substantial local diffusion gradients due to differences in fluid composition between adjacent rock types, and/or by fluid flow. Pervasive up-temperature fluid flow is not required to drive reactions as previously thought.

A white light interferometric system directly measured dissolution rates of anorthite, indicating strong spatial variations of dissolution, with etch pits retreating up to an order of magnitude faster than the bulk.

Ab initio methods indicate that a Grotthus type of reaction path is energetically reasonable for hydrogen isotope exchange between water and dissolved silica. Calculated equilibrium values were in good agreement with experiments.

A field study indicated that weathering rates of basalt were about three times those of either diorite or granite. Strontium fluxes were approximately equal in all three rock types, with Sr isotopic ratios similar to the parent rock. Plagioclase dissolution experiments found rates similar to previous estimates. The Sr release during plagioclase weathering is stoichiometric. The $^{87}\text{Sr}/^{86}\text{Sr}$ of the weathering solution was the same as that of the reacting plagioclase.

Subject Index

- Acids, 1, 27, 29, 43, 44, 50, 77, 113, 126, 142, 171, 197
 organic, 43, 44, 190
- Actinides, 72
- Activity coefficients, 28, 44, 119
- Age dating, 10, 25, 26, 27, 32, 33, 34, 42, 76, 139, 149, 173, 176
 exposure ages, 42, 76
- Aluminum, ii, 9, 14, 27, 29, 43, 44, 49, 55, 59, 77, 78, 79, 100, 125, 126
- Amphiboles, 65, 80
- Atomic Force Microscopy, 14, 25, 26, 35, 46, 47, 81, 82, 99, 113, 122, 151, 200, 201
- Bacteria, 11, 42, 51, 77, 122, 190
- Basalt, 6, 10, 11, 12, 24, 26, 33, 71, 76, 90, 115, 203, 204
- Basalts
 MORB, 33, 90
- Beamlines, 92
- Biofilms, 159, 160
- Biominalization, 51, 113, 114, 126, 190
- Bonding, chemical, 56, 94, 159
- Borehole, 5, 6, 7, 55, 65, 152, 158, 165, 181, 182, 192, 193
 stability, 7, 192
- Boron, 68, 69
- Brines, 28, 40, 68, 149, 161, 162, 178
- Brucite, 40, 45
- Cadmium, 44, 66, 81
- Calorimetry, 80
- Capillarity, 17, 62, 91, 101, 147, 154, 196
- Carbon, iv, 10, 11, 16, 23, 31, 33, 42, 43, 46, 53, 56, 65, 83, 85, 118, 144, 156, 176, 197, 202
 carbon cycle, 33, 202
- Carbon dioxide, viii, 6, 9, 10, 12, 13, 33, 38, 39, 42, 43, 45, 53, 62, 65, 75, 99, 101, 147, 155, 167, 202, 203
- Carbonates, 2, 9, 12, 33, 45, 46, 47, 80, 81, 82, 83, 99, 113, 139, 160, 161, 199
 minerals, 46, 99, 113
 calcite, 1, 14, 27, 45, 46, 47, 65, 76, 81, 82, 83, 85, 113, 114, 118, 139, 155, 176
 dolomite, 81, 84, 149
- Cesium, 13, 25
- Chemical potential, 109, 110
- Chromatography, 3, 156
- Chromium, 16, 50, 51, 66, 120, 121, 123, 124, 160
- Clays, 1, 13, 16, 58, 59, 65, 66, 68, 69, 80, 84, 100, 116, 127, 149, 164, 175
 illite, 68, 69, 150
 kaolinite, 59, 80, 85, 99, 118
 smectite, 13, 59, 66, 68, 150
- Climate Change, 10, 56, 144, 163
- Colloids, 17, 18, 72
- Compaction, 7, 12, 53, 56, 85, 117, 118, 127, 144, 145, 146, 175, 192, 193
- Conductivity
 electrical, 5, 23, 24, 31, 58, 65, 127, 189
 hydraulic, 132, 133
 thermal, 178
- Convection, 60, 86, 129, 178, 179, 194
 thermohaline, 86, 178, 179
- Cosmic rays, 36, 76
- Creep, 32, 130, 175, 187
- Defects, 45, 46, 47, 50, 51, 120, 121, 123, 124, 143, 151, 172
- Deforestation, 202
- Diagenesis, 3, 4, 41, 66, 68, 69, 85, 99, 117, 118, 119, 149, 150, 156, 175
- Diamond anvil, 92
- Diffusion, 13, 16, 28, 29, 41, 45, 47, 63, 84, 86, 90, 91, 102, 130, 148, 154, 155, 178, 179, 203
 coefficients, 28, 45, 90, 91, 154
- Dissolution, 1, 22, 24, 25, 26, 27, 29, 34, 35, 43, 46, 47, 48, 77, 78, 79, 82, 85, 90, 111, 113, 116, 118, 119, 122, 125, 151, 154, 167, 175, 190, 200, 201, 203, 204
- Earthquakes, 6, 11, 12, 21, 30, 32, 70, 96, 152, 187
- Elastic Properties, 162, 163, 164
- Electrolytes, 28, 44, 109, 119
- Electron transfer, 51, 121, 124
- Energetic particles, 36
- Energy transport, xiii, 34, 97
- Enthalpy, 80, 125

Entropy, 86
 Epidote, 45
 Equation of state, 29, 49, 109
 Erosion, 26, 34, 85, 111, 117, 118
 rates, 26, 34
 Estuaries, 72
 Fault, ii, vi, vii, viii, ix, 11, 65, 115, 117, 132,
 149, 152, 169, 183, 184, 187
 faults, xii, 70, 85, 96, 97, 115, 116, 117, 118,
 132, 146, 152, 168, 169, 183, 184, 187, 198
 Faults and faulting, 10, 11, 12, 13, 65, 86, 115,
 116, 117, 127, 129, 132, 145, 146, 149, 152,
 168, 169, 183, 184, 187
 gouge, 12, 169
 mechanics, 127
 San Andreas Fault, ix, 11, 65, 187
 Feldspars, 41, 68, 84, 99, 127, 151, 194, 200,
 201
 albite, 151, 200, 201
 anorthite, 26, 151, 200, 201, 203
 orthoclase, 1
 plagioclase, 85, 118, 151, 204
 Fingering, 196
 Fluid flow, iii, xii, 15, 19, 22, 47, 53, 56, 62,
 68, 83, 85, 95, 97, 98, 99, 101, 103, 107,
 111, 112, 116, 117, 118, 144, 147, 149, 154,
 161, 163, 168, 175, 183, 193, 194, 198, 203
 fast flow, 21, 97, 135
 multiphase, 62, 63, 101, 116, 136, 140, 147,
 180, 196
 reactive, 22, 85, 118, 168
 unsaturated, 17, 63
 Fluid inclusions, 41, 149, 185
 Fluid-rock interactions, 2, 40, 41, 42
 Fluorescence, 2, 92, 94, 159
 Fractional derivatives, 132
 Fractionation, 11, 33, 40, 42, 43, 45, 68, 69,
 71, 90, 91, 128, 202
 Fractures, xiii, 2, 7, 10, 17, 19, 21, 22, 63, 85,
 94, 95, 97, 98, 101, 102, 104, 111, 112, 116,
 117, 118, 133, 134, 135, 142, 144, 147, 148,
 153, 161, 168, 169, 171, 179, 181, 182, 192,
 193, 198
 aperture, 17, 22, 97, 101, 135, 147, 169
 mechanics, 144
 systems, 10, 95, 104, 134
 Friction, 12, 18, 70, 96
 Gas
 hydrates, 163, 164
 natural, 38, 128, 156, 163, 197
 noble, 10, 12, 15, 26, 107, 128, 173
 Gassmann technique, 21, 161, 162
 Geomorphology, 26, 106
 Geophysical logging, 183
 Geothermal, xiii, 10, 24, 33, 38, 39, 40, 42, 69,
 83, 84, 170, 182, 194
 Glaciation, 106
 Glass, 7, 24, 25, 33, 42, 86, 101, 103, 125, 126,
 127, 147, 151, 164
 Grain boundaries, 65, 120, 121, 123, 124, 164
 Granite, 12, 84, 115, 146, 194, 204
 Granular flow, 95
 Gravity, 8, 18, 62, 95, 101, 135, 147, 170
 Greenhouse gas, 11, 38, 167
 Ground-penetrating radar, 177
 Groundwater, 5, 12, 15, 85, 107, 118, 128, 173,
 174, 176
 Hydrocarbons, xiii, 15, 16, 21, 38, 53, 68, 69,
 74, 83, 107, 108, 128, 177, 185, 186, 197,
 198
 Hydrology, xi, 117, 132, 168, 176
 Hydrolysis, 43, 44, 50
 Hydrothermal, v, 2, 26, 33, 38, 39, 41, 43, 45,
 69, 72, 83, 84, 92, 94, 127, 149, 150, 170,
 194, 200
 fluids, 69, 72, 92, 94
 processes, 33
 systems, v, 41, 83, 84, 92, 170
 hydroxyl, 78, 82
 Imaging, 5, 6, 22, 30, 58, 64, 88, 120, 121,
 123, 124, 134, 135, 136, 153, 180, 189, 190,
 201
 seismic, 6
 subsurface, xi, 57, 188
 Instability, 61, 116, 129, 130, 146, 178, 179
 Inverse methods, 5, 6, 54, 55, 56, 57, 58, 104,
 113, 158, 165, 188, 189
 Iron, ii, iii, 14, 23, 35, 43, 49, 50, 51, 52, 59,
 72, 77, 81, 83, 93, 122, 142, 171
 oxides, 34, 35, 42, 51, 66, 93

goethite, 35, 49, 50, 52, 77, 119, 159, 160
 hematite, 14, 35, 42, 49, 50, 51, 52, 119,
 149, 201
 magnetite, 42, 43, 44, 50, 51, 119, 149,
 150
 Isotopes, 39, 71
 argon, v, 83, 84
 boron, 68, 69
 carbon, 12, 42, 43, 45, 83, 202
 cosmogenic, 15, 26, 27, 34, 76, 107, 128
 exchange, 42, 45
 fractionation, v, 11, 40, 42, 43, 45, 68, 69,
 71, 90, 91, 194, 202
 helium, 12, 15, 107
 hydrogen, 40, 45, 204
 lead, 139
 noble gas, ix, 173, 174
 oxygen, 10, 12, 41, 42, 43, 45, 83, 84, 176,
 194, 195
 stable isotopes, v, 39, 42, 45, 71, 83, 128,
 173, 194
 strontium, 204
 uranium, 33, 72, 139
 Kerogen, 3, 69, 74, 75
 Kinetics, xiii, 1, 16, 25, 39, 43, 47, 49, 51, 69,
 85, 90, 91, 94, 99, 113, 114, 116, 118, 119,
 127, 151, 175, 197, 203
 Krypton, 15, 173
 Lattice gas models, 60, 97
 Lattice-Boltzman models, 56, 95, 98, 111, 112,
 134, 135
 Lead, 9, 10, 12, 35, 66, 83, 84, 139, 159, 160,
 195
 Lichen, 11, 190
 Magmatism, 9, 11, 32, 33, 84, 86, 87, 90, 128,
 129, 170, 194, 195
 Magnetosphere, 36
 Mantle, 10, 12, 13, 15, 20, 21, 23, 31, 56, 72,
 74, 86, 92, 107, 128, 129, 130, 154
 Marble, 12, 22, 146
 Mass spectrometry, 3, 26, 33, 72, 83, 151, 176
 accelerator mass spectrometry, 26, 27
 ion microprobes, v, 41, 45, 65, 83, 84, 194
 resonance ionization, 173, 174
 time-of-flight, 65, 173, 174
 Mechanics
 micromechanics, 56, 193
 Melts, 24, 71, 76, 86, 129
 Mercury, 44, 66, 125, 160
 Methane, ix, 10, 11, 38, 42, 43, 156, 163, 164,
 185, 197, 198
 Micas, 80, 99, 120, 121, 123, 124
 biotite, 120, 121, 123, 124
 chamosite, 66
 muscovite, 1, 99
 Microorganisms, 35, 42, 52, 94, 122, 159, 190
 microbes, 190
 Minerals
 dissolution, 25, 26, 44, 82, 200
 growth, 1, 45, 99, 113
 solubility, 154
 surface chemistry, 1, 16, 26, 46, 81, 92, 113,
 122, 125, 159, 160, 190, 200, 201
 Molecular dynamics, 13, 49, 50, 59, 110, 129
 Molecular modeling, 58, 59, 78, 125
 NaCl, 25, 28, 38, 40, 42, 44, 185
 Neodymium, 9, 10, 12, 44, 176
 Nitrogen, 38, 39, 128, 176
 Nonlinear, 31, 32
 Nuclear Magnetic Resonance (NMR), 24, 25,
 64, 78, 79, 125, 126, 136, 180
 Oceans, 3, 10, 33, 71, 72, 73, 90, 164, 167, 173
 Olivine, 10, 24, 65, 76, 130
 Oxidation state, 50, 94
 Paleoclimate, 33
 Paleohydrology, 85, 118
 Paleomagnetism, 149
 Peclet number, 101, 148
 Permeability, 13, 17, 21, 22, 24, 38, 54, 56, 60,
 61, 62, 85, 95, 97, 99, 102, 118, 127, 132,
 137, 138, 145, 146, 148, 154, 155, 163, 164,
 166, 168, 169, 177, 178, 179, 183
 measurement, 61, 62, 137
 Perturbation methods, 43
 Petroleum, v, 3, 30, 62, 63, 74, 83, 101, 136,
 147, 152, 156, 180, 186, 197, 200
 pH, 1, 14, 16, 24, 25, 43, 44, 50, 77, 82, 99,
 120, 123, 151, 160, 190, 201
 Phase
 relationships, 38

Plasma instabilities, 35
 Platinum, 45, 72, 73, 154
 Pore structure, 103, 127, 144, 163
 Poroelastic properties, 20, 21, 193
 Porosity, xiii, 2, 7, 8, 10, 21, 22, 24, 53, 56, 85, 87, 99, 116, 117, 118, 127, 140, 141, 144, 146, 151, 155, 162, 163, 164, 168, 177, 178, 183, 192, 193
 Porous media, 17, 24, 56, 60, 86, 99, 111, 129, 163, 169
 Precipitation, 1, 10, 14, 22, 25, 28, 33, 42, 43, 51, 68, 85, 97, 113, 118, 139, 149, 154, 175, 190, 200
 Protonation, 50, 119
 Pyrite, 142, 150, 171
 Pyrolysis, 74
 Quantum mechanics, 47, 50, 109, 125, 126, 203
 Quartz, ii, 14, 26, 27, 41, 65, 68, 99, 116, 119, 127, 155, 175, 185, 192, 194, 195
 Reservoirs
 characterization, 5, 21
 dynamics, 39
 Reynolds
 equation, 63, 101, 102, 147, 148
 Rheology, 86, 116, 117, 129, 130
 Rivers, 199
 Rock mechanics, xi, 55, 56, 144
 Sandstone, 2, 7, 9, 53, 56, 103, 127, 137, 144, 168, 169, 192, 193
 Scaling relationships, 61
 Sedimentology, 2, 16, 51, 85, 99, 117, 118, 150, 163, 164, 178, 203
 Seismology, 6, 30
 computational, 6
 exploration, 54
 Selenium, 16
 Shale, 68, 169, 178
 Shear localization, 146
 Silica, 7, 14, 25, 86, 90, 91, 110, 119, 126, 159, 204
 Silicates, xiii, 7, 25, 50, 65, 66, 69, 71, 86, 90, 119, 120, 123, 125, 127, 170, 200, 203
 Soils, 11, 16, 66, 81, 94, 153, 160, 176, 190, 203
 Solar wind, xiv, 35, 36
 Solid solutions, 29, 80, 81, 83
 Solubility, 10, 15, 28, 43, 44, 60, 91, 107, 125, 128, 154
 Sorption, 1, 14, 16, 47, 48, 49, 59, 65, 77, 78, 93, 119, 120, 121, 123, 124, 151, 159, 160
 Space plasmas, 35
 Speciation, 3, 13, 16, 25, 29, 39, 44, 51, 94, 119, 159, 160
 Spectrometry
 Mössbauer, 51
 Spectroscopy, 1, 3, 14, 16, 25, 65, 78, 79, 92, 99, 100, 120, 123, 142, 151, 159, 160, 171, 186
 electron spectroscopy, 151
 electron spectroscopy
 electron energy loss spectroscopy (EELS), 120, 123, 190
 XANES, ii, 3, 16, 93
 X-ray photoelectron spectroscopy, 121, 124
 Speleothems, 176
 Strontium, 1, 9, 10, 12, 47, 66, 72, 151, 160, 176, 195, 203, 204
 Sulfates, 3, 28, 29, 44, 50, 80, 160, 191, 200
 Sulfides, 4, 125
 Sulfur, 3, 4, 142, 143, 171, 172, 197
 Surface
 charge, 44, 99, 119
 chemistry, 14, 25, 46, 78, 79, 151
 Synchrotron radiation, 1, 92
 Synthetic Aperture Radar (SAR), 165
 Tectonics, 9, 33, 127, 152, 153
 Thermochronometry, v, 83
 Thermodynamics, xiii, 28, 29, 38, 48, 51, 74, 80, 81, 94, 100, 109, 119, 157, 185, 197, 200, 203
 Thorium, 33, 72
 Tomography, 2, 5, 24, 140, 144
 Tortuosity, 22, 97, 102, 148
 Trace elements, 10, 16, 66, 87, 94, 176
 Transmission Electron Microscopy (TEM), 67, 120, 123, 190
 Tuff, 93, 137, 138
 Uranium series, 32, 33, 176
 Viscoelasticity, 21, 130

Volcanoes, 10, 11, 15, 25, 33, 76, 84, 107, 137,
170, 194
Water, ix, 38, 39, 40, 42, 50, 74, 126, 142, 155,
171, 175, 185
Wave equation, 30, 88
Wave propagation, 6, 21, 30, 32, 54, 55, 88,
89, 153, 162

Weathering, 25, 44, 72, 99, 119, 122, 149, 151,
190, 202, 203, 204
 rock varnish, 106
Xenon, 9, 10, 15, 174
X-ray diffraction, 49
Zeolites, 80

Author Index

<u>Contributor</u>	<u>Organization</u>	<u>Page</u>
Aldridge, D. F.	Sandia National Laboratories	54
Alumbaugh, D. L.	University of Wisconsin	188
Amonette, J. E.	Pacific Northwest National Laboratory	46
Anovitz, L. M.	Oak Ridge National Laboratory	38
Aydin, A.	Stanford University	168
Baer, D. R.	Pacific Northwest National Laboratory	46
Ballentine, C. J.	University of Michigan	128
Banfield, J. F.	University of Wisconsin	190
Banner, J. L.	University of Texas	76
Becker, A.	Lawrence Berkeley National Laboratory	5
Bedzyk, M. J.	Northwestern University	1
Bénezeth, P.	Oak Ridge National Laboratory	43
Benson, D.	Desert Research Institute	132
Berge, P. A.	Lawrence Livermore National Laboratory	20
Bernabé, Y.	Université Louie Pasteur, France	127
Berner, R. A.	Yale University	202
Berryman, J. G.	Lawrence Livermore National Laboratory	20
Beveridge, T.	Pacific Northwest National Laboratory	51
Bhattacharya, J.	University of Texas	177
Birn, J.	Los Alamos National Laboratory	36
Blair, S. C.	Lawrence Livermore National Laboratory	19
Blencoe, J. G.	Oak Ridge National Laboratory	38
Bodnar, R. J.	Virginia Polytechnic Inst. & State Univ.	185
Boles, J. R.	University of California, Santa Barbara	85, 118
Bolton, E. W.	Yale University	203
Bonner, B. P.	Lawrence Livermore National Laboratory	22
Bosl, W.	Stanford University	163
Bourcier, W. L.	Lawrence Livermore National Laboratory	22, 24
Brantley, S. L.	The Pennsylvania State University	151
Broecker, W. S.	Columbia University	106
Brown, G. E.	Stanford University	159
Brown, S.R.	New England Research	134
Buseck, P. R.	Arizona State University	66
Caffee, M.	Lawrence Livermore National Laboratory	26, 27, 34, 76
Caprihan, A.	New England Research	134
Carroll, S. A.	Lawrence Livermore National Laboratory	24
Casey, W. H.	University of California, Davis	78, 81
Chester, F. M.	Texas A&M University	175
Chester, J. S.	Texas A&M University	175
Cole, D. R.	Oak Ridge National Laboratory	39, 41, 42, 45
Constable, S.	Scripps Institute of Oceanography, UCSD	158
Cooper, C. A.	Desert Research Institute	60
Cygan, R. T.	Sandia National Laboratories	58
Davis, J.A.	U. S. Geological Survey	14

de Groot-Hedlin, C.	Scripps Institute of Oceanography, UCSD	158
DePaolo, D. J.	Lawrence Berkeley National Laboratory	9
deSouza, A. R.	National Academy of Sciences	131
Dietrich, W. E.	University of California, Berkeley	34, 76
Dixon, D. A.	Pacific Northwest National Laboratory	48
Dove, P. M.	Georgia Institute of Technology	113
Duba, A. G.	Lawrence Livermore National Laboratory	23, 31
Dupuis, M.	Pacific Northwest National Laboratory	48
Durham, W. B.	Lawrence Livermore National Laboratory	22
Dvorkin, J.	Stanford University	165
Eggleston, C. M.	University of Wyoming	25, 200
Elbert, D. C.	Johns Hopkins University	120, 123
Elbring, G. J.	Sandia National Laboratories	54
Elmore, R. D.	University of Oklahoma	149
Engel, M. H.	University of Oklahoma	149
Epstein, S.	California Institute of Technology	71
Evans, B.	Massachusetts Institute of Technology	127
Evans, J. P.	Utah State University	115, 132, 183, 184
Fehler, M.	Los Alamos National Laboratory	30
Felmy, A. R.	Pacific Northwest National Laboratory	48
Feng, H.	Brookhaven National Laboratory	2
Fenter, P.	Argonne National Laboratory	1
Finkel, R. C.	Lawrence Livermore National Laboratory	26, 27, 34, 76
Forster, C.	University of Texas	177
Fredrich, J. T.	Sandia National Laboratories	55, 144
Fredrickson, J. K.	Pacific Northwest National Laboratory	51
Garven, G. T.	Johns Hopkins University	85, 118
Gary, S. P.	Los Alamos National Laboratory	35
Ge, S.	University of Colorado	97
Glass, R. J.	Sandia National Laboratories	60, 62, 101, 147
Goldstein, S. J.	Los Alamos National Laboratory	32
Gorby, Y.	Pacific Northwest National Laboratory	51
Graham, A.	Texas Tech University	63, 136, 180
Grechka, V.	University of Colorado	104
Guyer, R. A.	Los Alamos National Laboratory	31
Haimson, B. C.	University of Wisconsin	7, 192
Hajash, A.	Texas A&M University	175
Halliday, A. N.	University of Michigan	128
Hanson, G. N.	State University of New York, Stony Brook	139
Harrison, T. M.	University of California, Los Angeles	83
Helgerud, M.	Stanford University	163
Helgeson, H. C.	University of California, Berkeley	74
Hersman, L.	Los Alamos National Laboratory	34, 77, 122
Hervig, R. L.	Arizona State University	68
Hess, A.C.	Pacific Northwest National Laboratory	47
Hestir, K.	Utah State University	115, 132, 184
Higgins, S. R.	University of Wyoming	25, 200

Holcomb, D. J.	Sandia National Laboratories	53
Horita, J.	Oak Ridge National Laboratory	39, 42, 45
Ilton, E. S.	Lehigh University	120, 123
Ingber, M.	University of New Mexico	63, 136, 180
Jones, K. W.	Brookhaven National Laboratory	2
Johnson, A.	Purdue University	152
Johnson, L. R.	Lawrence Berkeley National Laboratory	6
Johnson, P. A.	Los Alamos National Laboratory	31
Keehm, Y.	Stanford University	163
Kennedy, B. M.	Lawrence Berkeley National Laboratory	9, 11, 15, 107
Klein, W.	Boston University	70, 96
Knauss, K. G.	Lawrence Livermore National Laboratory	25, 200
Koplik, J.	City College of the City University of NY	95
Kronenberg, A. K.	Texas A&M University	175
Labotka, T. C.	University of Tennessee	173
Lachmar, T. E.	Utah State University	183
Ladd, A. L.	University of Florida	19, 111
Larner, K.	Colorado School of Mines	104
Lee, K. H.	Lawrence Berkeley National Laboratory	5
Liang, J.-J.	Sandia National Laboratories	58
Lindquist, W. B.	State University of New York, Stony Brook	140
Liu, T.	Columbia University	106
Long, J. C. S.	University of Nevada	115, 132, 184
Majer, E. L.	Lawrence Berkeley National Laboratory	6
Mango, F. D.	Rice University	156
Martel, S.	University of Hawaii	115, 132, 184
Mathez, E. A.	American Museum of Natural History	23, 31, 65
Maurice, P.	Kent State University	34, 77, 122
Mavko, G. M.	Stanford University	161
McEvelly, T. V.	Lawrence Berkeley National Laboratory	6
McKay, L. D.	University of Tennessee	173
McMechan, G. A.	University of Texas	177
Meyers, W. J.	State University of New York, Stony Brook	139
Miller, D. G.	Lawrence Livermore National Laboratory	28
Mondy, L.	Sandia National Laboratories	63, 136, 180
Morrison, H. F.	Lawrence Berkeley National Laboratory	5
Muir, F.	Stanford University	161
Mukerji, T.	Stanford University	163
Murrell, M. T.	Los Alamos National Laboratory	32
Myer, L. R.	Lawrence Berkeley National Laboratory	7, 8
Nagy, K. L.	University of Colorado	99
Navrotsky, A.	University of California, Davis	80
Newman, G. A.	Sandia National Laboratories	56, 188
Nicholl, M. J.	Oklahoma State University	62, 101, 147
Nihei, K. T.	Lawrence Berkeley National Laboratory	7, 8
Nishiizumi, K.	University of California, Berkeley	34, 76
Nur, A.	Stanford University	163, 165

Olsson, W. A.	Sandia National Laboratories	53
Orr, F.M.	Stanford University	167
Ortoleva, P. J.	Indiana University	116
Pantano, C.	The Pennsylvania State University	151
Parks, G. A.	Stanford University	159
Phillips, B. L.	University of California, Davis	78
Pili, E.	Departement Analyse et Surveillance de l'Environnement, France	11
Pollard, D. D.	Stanford University	168
Pyrak-Nolte, L. J.	Purdue University	153
Rajaram, H.	University of Colorado	62, 101, 147
Rard, J. A.	Lawrence Livermore National Laboratory	28
Reedy, R.	Los Alamos National Laboratory	34, 76
Reeves, G. D.	Los Alamos National Laboratory	36
Reitmeyer, R.	U. S. Geological Survey	14
Richter, F. M.	University of Chicago	90
Riciputi, L. R.	Oak Ridge National Laboratory	41, 45
Rivers, M. L.	University of Chicago	92
Roberts, J. J.	Lawrence Livermore National Laboratory	23
Rock, P. A.	University of California, Davis	81
Rudnicki, J. W.	Northwestern University	146
Rundle, J. B.	University of Colorado	70, 96
Rustad, J. R.	Pacific Northwest National Laboratory	48
Rye, D. M.	Yale University	203
Ryerson, F. J.	Lawrence Livermore National Laboratory	27
Schiffries, C. M.	National Academy of Sciences	131
Schoonen, M. A. A.	State University of New York, Stony Brook	142, 171
Seewald, J.	Woods Hole Oceanographic Institution	197
Segall, P.	Stanford University	170
Shankland, T. J.	Los Alamos National Laboratory	23, 31
Sharp, J. M.	University of Texas	78
Sherwood-Lollar	University of Toronto, Canada	128
Shipton, Z. K.	Utah State University	183
Shock, E. L.	Washington University	109
Simmons, C. T.	Flinders University, South Australia	78
Singh, J.	Oak Ridge National Laboratory	38
Smith, E.	Los Alamos National Laboratory	31
Spera, F.	University of California, Santa Barbara	86, 129
Spetzler, H.	University of Colorado	103
Sposito, G.	Lawrence Berkeley National Laboratory	13, 34, 77, 122
Stockman, H. W.	Sandia National Laboratories	60, 134
Stolper, E.	California Institute of Technology	71
Strongin, D. R.	Temple University	142, 171
Sturchio, N. C.	Argonne National Laboratory	1
Sverjensky, D. A.	Johns Hopkins University	119
Sutton, S. R.	University of Chicago	92, 94
Takahashi, I.	Stanford University	165

TenCate, J. A.	Los Alamos National Laboratory	31
Thonnard, N.	University of Tennessee	173
Tidwell, V. C.	Sandia National Laboratories	61, 137
Tokunaga, T. K.	Lawrence Berkeley National Laboratory	16, 17
Tompson, A.	Lawrence Livermore National Laboratory	22
Torgerson, T.	University of Connecticut	15, 107
Toksoz, M. N.	Massachusetts Institute of Technology	30
Tossell, J. A.	University of Maryland	125
Tripp, A. C.	University of Utah	181
Tsvankin, I.	Colorado School of Mines	104
Tyler, S. W.	Desert Research Institute	60
Unsworth, M.	University of Washington	187
Vairavamurthy, M. A.	Brookhaven National Laboratory	3
Valley, J. W.	University of Wisconsin	194
Veblen, D. R.	Johns Hopkins University	120, 123
Wan, J.	Lawrence Berkeley National Laboratory	17
Wang, H. F.	University of Wisconsin	19, 196
Wasserburg, G. J.	California Institute of Technology	72
Watson, E. B.	Rensselaer Polytechnic Institute	154
Waychunas, G.A.	Lawrence Berkeley National Laboratory	14
Wesolowski, D. J.	Oak Ridge National Laboratory	39, 42, 43
Whelan, J. K.	Woods Hole Oceanographic Institution	198
Williams, L.	Arizona State University	68
Wilson, J. L.	New Mexico Institute of Mining and Technology	61, 137
Womble, D. E.	Sandia National Laboratories	54
Wong, T.	State University of New York, Stony Brook	55, 144
Wood, R. H.	University of Delaware	109
Wu, R.-S.	University of California, Santa Cruz	30, 88
Xu, H.	Stanford University	165
Yuen, D. A.	University of Minnesota	86, 129
Zachara, J. M.	Pacific Northwest National Laboratory	51

DOE/OBES Geosciences Research: Historical Budget Summary
(Thousands of dollars)

	FY 95	FY 96	FY 97	FY 98	FY 99
Total, on-site	10442	10865	10826	10263	9940
Total, off-site	<u>7937</u>	<u>8815</u>	<u>9705</u>	<u>11226</u>	<u>12851</u>
Total, operating	18379	19680	20531	21489	22791
Equipment	<u>1141</u>	<u>1258</u>	<u>1450</u>	<u>1256</u>	<u>1235</u>
Total GEOSCIENCES	19520	20938	21981	22745	24026
ON-SITE INSTITUTIONS					
Institution	FY 95	FY 96	FY 97	FY 98	FY 99
Argonne National Laboratory	655	600	620	620	740
Brookhaven National Laboratory	460	528	350	425	595
Idaho National Laboratory	119	65	40	40	0
Los Alamos National Laboratory	2241	1960	2096	1509	1260
Lawrence Berkeley National Laboratory	1875	2197	2170	2320	2160
Lawrence Livermore National Laboratory	1921	1940	1915	1421	1445
Oak Ridge Inst for Sci and Ed				85	110
Oak Ridge National Laboratory	1140	1251	1195	1228	1235
Pacific Northwest Laboratory	665	684	600	770	760
Sandia National Laboratory	<u>1345</u>	<u>1616</u>	<u>1725</u>	<u>1845</u>	<u>1635</u>
Total, on-site	10442	10865	10826	10263	9940
OFF-SITE INSTITUTIONS					
Institution	FY 95	FY 96	FY 97	FY 98	FY 99
Am. Mus. Nat'l. Hist. (Mathez)	72	69	85	98	87
Arizona St. (Buseck)	126	132	139		
Arizona St. (Hervig/Williams)	86	59	74	83	70
Boston Univ. (Klein)	71	74	77	123	129
Brown U (Yund)		152			
Cal Tech (Clayton)	55				
Cal Tech. (Stolper)	123	140	142	146	150
Cal Tech. (Wasserburg)	400	400	400	465	400
Calif, Univ. of Berkeley (Helgeson)		185	192	195	197
Calif, Univ. of Berkeley (Nishiizumi)			160	164	160
Calif, Univ of Berkeley (Sposito)			67	70	73
Calif. Univ. of Davis (Casey)		110	108	104	121
Calif, Univ. of Davis (Leshner)	75				
Calif, Univ of Davis (Navrotsky)			150		169
Calif, Univ. of Davis (Rock)		151	134	138	
Calif, Univ. of LA (Harrison)	105	111	119	123	124
Calif, Univ. of LA (McKeegan)		44			
Calif. Univ. of SB (Boles)		20	31	16	

Institution	FY 95	FY 96	FY 97	FY 98	FY 99
Calif. Univ. of SB (Spera)	82	75	76	89	92
Calif, Univ of Santa Cruz (Wu)				278	267
Calif, Univ of San Diego (DeGroot-Hedlin)			49	58	
Carnegie Inst of Wash (Hemley)				37	
Chicago, Univ. of (Richter)			183	141	
Chicago, Univ. of (Sutton/Rivers)		341	418	429	440
Chicago, Univ. of (Sutton)	138	159	131	137	299
Colo, Univ. of (Ge)	179	13	86		120
Colo, Univ of (Nagy)					99
Colo, Univ. of (Rajaram)		79	124		60
Colo, Univ. of (Rundle)	109	114	120	130	136
Colo, Univ. of (Spetzler)	126	132	152	161	168
Col Sch of Mines (Tsvankin)				230	240
Columbia Univ. (Broecker)	131	137	134	154	130
Columbia Univ. (Walker)	113				
Conn. Univ. of (Torgersen)	76	65	68	79	188
Delaware, Univ. of (Wood)	108	109	111	124	236
Desert Res. Inst. (Tyler)		80	148		
Duke Univ (Malin)				44	
Florida, Univ. of (Ladd)				85	70
Geophys. Lab, CIW (Bell)	92				
Georgia Tech (Dove)	91	91	39	86	145
Hawaii, Univ. of (Martel)	81	79	84	130	
Illinois, Univ of (T. Johnson)			138		
I.R.I.S. (Simpson)	211	211			
Indiana, Univ. of (Ortoleva)	100	102	108	141	124
John Hopkins Univ.(Garven)		67	70	77	
Johns Hopkins Univ.(Sverjenski)		118	105	108	110
Johns Hopkins Univ.(Veblen)	156	156	163	110	110
Kent State Univ (Maurice)			33	34	69
Lehigh Univ. (Ilton)	44	44	37	115	115
Lehigh Univ. (Moses)		123			
Maine Science & Tech (Shehata)			340		
Maryland, Univ. of (Tossell)		28	56	47	48
Miami, Univ. of (Eberli)	155				
Michigan, Univ. of (Ballentine)		69	71	69	
Michigan, Univ. of (Halliday)	172	207	226	200	
Minn. Univ of (Yuen)	82	78	76	91	100
MIT (B. Evans)			185	188	198
MIT (Madden)	74				
MIT (Rothman)					134
MIT (Toksoz)	367			150	160
NASA (Blankston)		113	95	113	
NAS/NRC (Schiffries/DeSouza)	100	100	100	100	100
Nevada, Univ of (Long)				106	106
New England Res (S. Brown)				211	372

Institution	FY 95	FY 96	FY 97	FY 98	FY 99
New Mexico Inst. Min. Tech.(Wilson)		30	64		72
New Mexico, Univ of (Ingber)				76	80
New Mexico, Univ. of (Miller)	100	100			
NY, City Univ. of CC (Koplik)	125	98	98	100	99
NY, State Univ. of SB (Hanson)	126	131		155	164
NY, State Univ. of SB (Lindquist)	33	33	35	50	95
NY, State Univ. of SB (Schoonen)		48	51	54	65
NY, State Univ. of SB (Wong)	70	71	99	100	106
Northwestern Univ. (Rudnicki)	85		88	148	91
Notre Dame Univ (Pyrak-Nolte)	65	78	81	83	
Ohio St. Univ (Adler)		43			
Okla, Univ. of (Elmore)	112	158		219	131
Okla Sate (Nicholl)					40
Oregon St. Univ (Egbert)		41			
Penn St. Univ. (Barnes)		81	87	93	
Penn St. Univ. (Brantley)	115	117	107	200	142
Penn St. Univ. (Brantley) conf.		10			
Princeton Univ (Navrotsky)	150	150			
Purdue Univ. of (Johnson)				130	238
Purdue Univ. (Pyrak-Nolte)					180
Renesselaer Polytech. Inst. (Watson)	140	146		181	179
Rice Univ. (Mango)	136	105	109	111	213
Rust Geotech, Inc. (Fukui)	87	87	35		
Rutger Univ (Cheney)			75	75	
Calif. Univ. of So (Aki)		112			
Stanford Univ. (Brown)	210		247	259	268
Stanford Univ. (Harris)	115	120	125		
Stanford Univ. (Liou)	80				
Stanford Univ (Mavko)					115
Stanford Univ. (Nur)	185	193	196	211	219
Stanford Univ. (Nur)				150	150
Stanford Univ (Orr)					136
Standard Univ. (Pollard)	224	232	250	195	199
Stanford Univ. (Segall)	83				93
Stanford Univ. (Zoback)	38				
Temple Univ. (Strongin)		76	49	52	60
Tennessee Univ. of (Thonnard)	100	82	69		
Texas, Univ of (Banner)				152	152
Texas, Univ. of (Hardage)	170	175	175		
Texas, Univ of (Sharp)			61	58	59
Texas, Univ of Dallas (McMechan)		164	124	162	137
Texas, A&M Univ. (Kronenberg)	167			184	350
Texas Tech Univ (Graham)					100
Utah, Univ. of (Tripp)	64	55	57	60	80
Utah St. (Hestir)	99	160	157	73	84
Utah St (Evans)				129	147

Institution	FY 95	FY 96	FY 97	FY 98	FY 99
VPI & SU (Bodnar)	104	100	104	122	118
VPI & SU (Hochella)					161
Washington, Univ. of (Booker)		116			
Washington, Univ of (Booker-conf)				8	
Washington, Univ. of (Unsworth)			96	97	205
Washington Univ, St. Louis (Shock)	53	75	80	106	201
Wisconsin (Alumbaugh)					52
Wisconsin, Univ of (Bahr)	49				
Wisconsin, Univ of (Banfield)		104	139	149	114
Wisconsin, Univ of (Haimson)				125	127
Wisconsin, Univ. of (Valley)	149		148	153	147
Wisconsin, Univ of (Wang)	60			50	95
WHOI (Chave)	91	55			
WHOI (Eglinton)		135			
WHOI (Seewald)			130	79	134
WHOI (Whelan)	191	195	200	205	377
Wyoming, Univ. of (Eggleston)		81	56	56	
Yale Univ. (Berner)	78	91	92	177	197
Yale Univ. (Lasaga)	207	290	295	240	247
Other	<u>87</u>	<u>90</u>	<u>244</u>	<u>222</u>	<u>316</u>
OFF-SITE TOTAL	7937	8815	9705	11226	12851